

**DOSIMETRIC ANALYSIS OF PLANNING TARGET VOLUME MARGINS AND
PRESCRIPTION ISODOSE LEVELS FOR THE TREATMENT PLANNING OF
STEREOTACTIC RADIOSURGERY TREATMENTS FOR SINGLE BRAIN
METASTATIC TUMOR: A PHANTOM-BASED STUDY**

BY

EMMANUEL FIAGBEDZI

(10220240)


**THIS DISSERTATION IS SUBMITTED TO THE UNIVERSITY OF GHANA,
LEGON IN PARTIAL FULFILMENT OF THE REQUIREMENT FOR THE AWARD
OF A DOCTOR OF PHILOSOPHY DEGREE IN MEDICAL PHYSICS**

**COLLEGE OF BASIC AND APPLIED SCIENCES
SCHOOL OF NUCLEAR AND ALLIED SCIENCES
DEPARTMENT OF MEDICAL PHYSICS**

SEPTEMBER 2024

DECLARATION

I, Emmanuel Fiagbedzi (Medical Physics Department, UG-Legon), hereby declare that this thesis was prepared in accordance with the University of Ghana PhD thesis guidelines and is the product of my own original research undertaken under the supervision of Prof. Francis Hasford, Dr. Samuel Nii Adu Tagoe and Prof. Andy Nisbert. No part of this work has been presented for any degree in the University of Ghana or any other University elsewhere.


.....

Date: ...25/09/2025...

Emmanuel Fiagbedzi
(Student)


.....

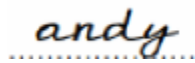
Date: ...30/09/2025

Prof. Francis Hasford
(Principal Supervisor)


.....

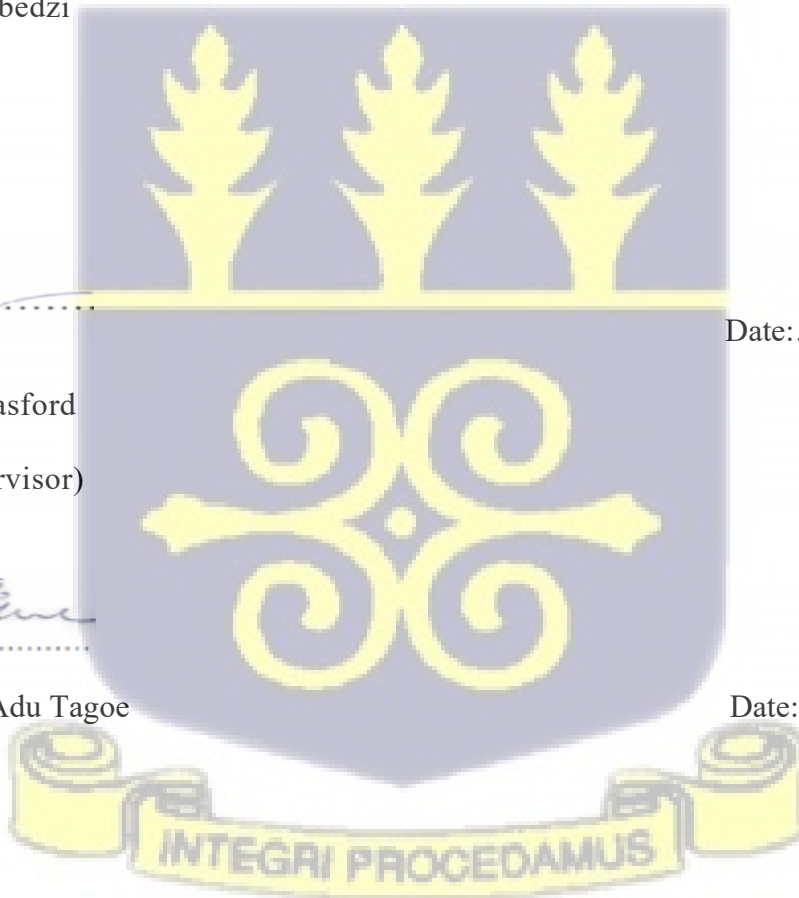
Dr. Samuel Nii Adu Tagoe
(Co-Supervisor)

Date: 01/10/2025....


.....

Prof. Andy Nisbert
(Co-Supervisor)

Date: ...27/09/2025..



LIST OF PUBLICATIONS

A. JOURNAL MANUSCRIPTS

PAPER I (Published)

Fiagbedzi, E., Hasford, F., Tagoe, S.N., Nisbert A (2023). Radiotherapy infrastructure for brain metastasis treatment in Africa: practical guidelines for implementation of a stereotactic radiosurgery (SRS) program. Health Technol. 13, 893–904. <https://doi.org/10.1007/s12553-023-00799-3>

PAPER II (Published)

Fiagbedzi E, Hasford F, Tagoe SN. (2024). Impact of Planning Target Volume Margins in Stereotactic Radiosurgery for Brain Metastasis: A Review. Prog Med Phys.;35(1):1-9. <https://doi:10.14316/pmp.2024.35.1.1>

PAPER III (Published)

Fiagbedzi E., Hasford F., Tagoe SN. (2024). Dose Verification for LINAC-Based Stereotactic Radiosurgery Planned at Different Prescription Isodose Levels Using Delta 4 Phantom+: Global Clinical Engineering Journal, 6(4), 14–22. <https://doi.org/10.31354/globalce.v6i4.198>

PAPER IV (Published)

Fiagbedzi, E., Tagoe, S. N. A., Hasford, F., & Nisbet, A. (2025). Influence of planning target volume margins using various prescription isodoses in gamma knife radiosurgery for single brain metastasis: a phantom study. Journal of Radiotherapy in Practice, 24, e4. [doi:10.1017/S1460396925000019](https://doi.org/10.1017/S1460396925000019)

B. CONFERENCE PROCEEDINGS/ABSTRACT

1. **Fiagbedzi, E.**, Hasford, F., Tagoe, S.N., Nisbert A (2024) Impact of planning target volume margins with different prescription isodose in gamma knife radiosurgery for brain metastasis: A phantom study: ePoster Presenter at the United Kingdom Imaging and Oncology Congress, June2023,Liverpool,UK.

https://pure.ulster.ac.uk/ws/portalfiles/portal/139174499/Abstracts-Book-2023_UKIO_2023.pdf page 74

2. **Fiagbedzi, E.**, Hasford, F., Tagoe, S.N., Nisbert A (2023). Impact of Planning Target Volume Margins on Organ sparing in Gamma Knife Stereotactic Radiosurgery for Single Brain Metastasis: A Phantom Study: ePoster presenter at the 2023 International conference on Radiation Research, August 27-30, 2023 in Montréal, Canada.

<https://www.radres.org/mpage/2023LBabstracts>

3. **Fiagbedzi, E.**, Hasford, F., Tagoe, S.N., Nisbert A (2024). Radiotherapy infrastructure for brain metastasis treatment in Africa: practical guidelines for implementation of a stereotactic radiosurgery (SRS) program: ePoster presenter at the 16th International Stereotactic Radiosurgery Society Congress in New York City, May 12-15,2024.

<https://isrscongress.org/eposters-displayed/>



ABSTRACT

The purpose of this study was to evaluate the influence of the choice of planning target volume margins and prescription isodose levels on the dosimetry indices used to assess the quality of treatment plans of stereotactic radiosurgery treatments for single brain metastatic tumor on both the Gamma Knife and LINAC-based Systems SRS, respectively using the STEEV Phantom. The research aim was further developed into five specific objectives.

Computed Tomography scan images of the STEEV anthropomorphic phantom were transferred into the GAMMA PLAN Treatment planning System at Queen Square Gamma Knife Unit of the University College London Hospital, UK. A target measuring 4.9 cm^3 was contoured centrally with organs at risk. Plans without a planning target volume margin for five prescription isodose levels from 50% to 70% at 5% increments were created. Afterwards, the Planning target volume margin was adjusted to 0.5, 1, 1.5, and 2mm, and identical plans having the same prescription isodose levels as the previous ones were generated. Adjustments were made to each plan to achieve same target coverage. One-way ANOVA test was used to analyse the influence of planning target volume margins on the plan quality dosimetric indices whilst organs at risk were evaluated in terms of maximum and minimum doses. The CT images of the STEEV Phantom with contours were later transferred into the Eclipse treatment planning system at the Centro riferimento di Oncologico (CRO), in Aviano-Italy where the impact of a set of prescription isodose levels (50, 55, 60, 65, 70, and 80%) were assessed using commonly used planning target margins (0, 1, and 2 mm) in SRS planning of brain metastasis and compared against constraints used at CRO. The accuracy of this set of plans was further evaluated using the new wireless delta 4 phantom+ with a gamma-index passing rate of 2 mm/2% (distance to agreement/dose deviation). The opinions of planning medical physicists with experience in SRS treatment planning on margin additions in the SRS treatment of single brain metastasis were also collected through a simple

survey made up of five questions. The last objective was done by exploring the geographical distribution of radiotherapy machines for brain metastasis treatment in Africa from the DIRAC database and relevant literature and some guidelines/models for the implementations of the SRS program developed. The findings indicated that, increases in PTV margins target expansion for Gamma knife radiosurgery though a relatively novel concept, it influences all dosimetric parameters as well as organs at risk. The PTV margin of 2.0 mm exhibited the highest mean selectivity of (0.93 ± 0.00), PCI (0.92 ± 0.01), GI (2.50 ± 0.04), V12 (16.17 ± 0.38) and treatment time (118.32 ± 2.91 min). The 0.0 mm PTV margin had the lowest mean value for all the parameters except for the treatment time (105.58 ± 3.48 min) which was slightly higher compared to the 0.5 mm PTV margin ($M = 86.36 \pm 4.13$ min). LINAC-based SRS planning reveals that using prescription isodose levels at 50 and 55% with 0 mm margins and 70 and 80% for higher margins like 1 mm or 2 mm can minimize dose to organs at risk while maintaining adequate tumour coverage. The 2 mm margin leads to increased exposure across all structures, particularly the brain stem and optic nerves at SRS80. This larger margin results in less sparing of critical structures. The calculated treatment planning system (TPS) dose and the measurement with the Delta4 phantom were in excellent agreement. The minimum gamma pass rate was 99.6% and the maximum 100%. The gamma passing rate above 95% for all plans and dose goals were achieved. In the survey, the response rate to whether or not to use margins in SRS, which was the most critical question, was 50%, thereby making no consensus to be achieved. In all of Africa, only two Gamma Knife machines were found. Two Cyberknives; one in Egypt and one in Kenya and 432 other megavoltage units (366 LINAC s, 66 cobalt-60) distributed across the continent can be used for the treatment of brain metastasis although the level of cancer burden was found to be increasing. The GDP per capita of a nation was a significant predictor of the availability of these machines in countries, but it did not account for the heterogeneity in number.

Based on the results of this study, planning target volume margins beyond 0 mm should not be used with the Gamma Knife, as they increase all dosimetric metrics associated with radionecrosis. For LINAC-based SRS, higher prescription isodose levels may be combined with larger margin sizes, but this approach requires careful evaluation. The expansion of radiotherapy through the use of linear accelerators suggests a promising future for the continent in enhancing its stereotactic radiosurgery treatment centres by adopting LINAC-based SRS in accordance with appropriate guidelines. This will assist in delivering thorough care to individuals and enhance their overall well-being.



DEDICATION

I want to dedicate this research to the memory of my late Dad, Mr. Padmore Fiagbedzi. This piece is a celebration of his great influence in my foundation years in life. This work is also dedicated to my entire family especially my dear spouse, Sedina Fiagbedzi and daughter Giovanna Aseye Fiagbedzi for their prayers and unflagging support throughout this PhD Journey.



ACKNOWLEDGMENTS

I want to convey my sincere gratitude to God Almighty for giving me life, the fortitude, determination, and commitment to start and finish my Ph.D. journey. My heartfelt appreciation goes to my supervisors, Prof. Francis Hasford, Dr. Samuel Nii Adu Tagoe, both from the University of Ghana and Prof. Andrew Nisbert of the University College in London for their invaluable input, constructive comments, thoughtful criticism, and guidance throughout the entire study. Their expertise and mentorship have significantly shaped the direction and quality of this research work. I am incredibly thankful to the Commonwealth Scholarship Secretariat, United Kingdom and the Ghana Education Trust Fund (GETFUND), Ghana for their financial support, which enabled me to do this research. Special thanks go to Prof Giovanna Sartor, Head of the Medical Physics Department, and Paola Chiovati, Senior Medical Physicist at the Centro Riferimento Oncologico (CRO), Aviano-Italy, who allowed me to carry part of this work at their Centre. Other thanks go to Ian Paddick and Diana Grischuk, the expert Medical Physicists at the Queen Square Gamma Knife Centre of the University College London Hospital who trained me in Gamma Knife treatment planning and assisted me in the data collection process which served as a pivotal role in the success of this study. To everyone who contributed to this research work, directly or indirectly, your support has been invaluable and deeply appreciated.

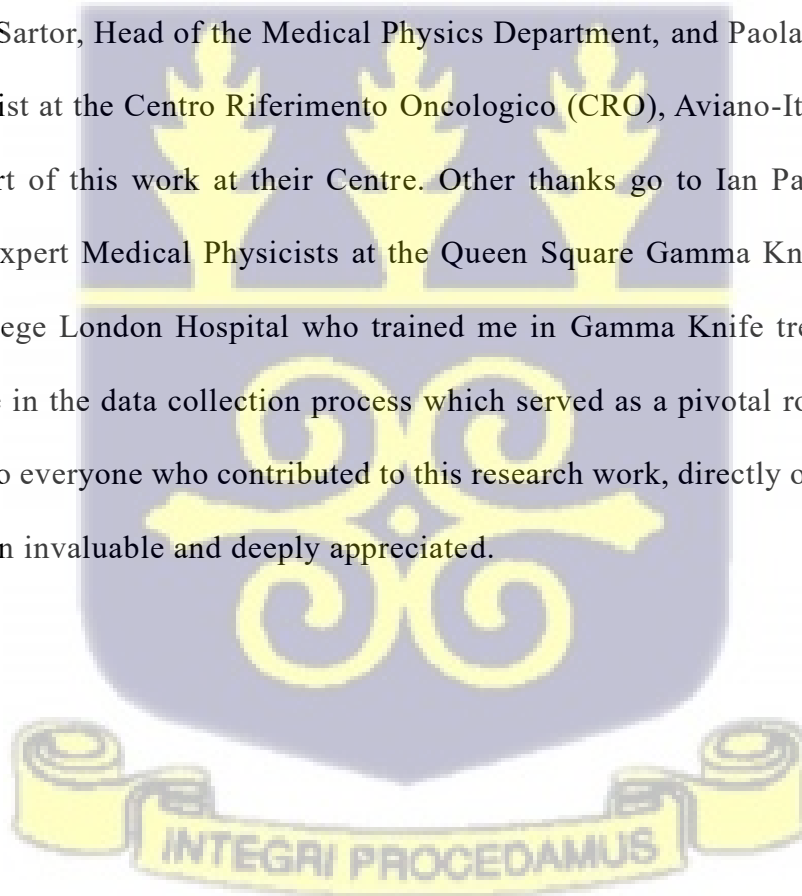


TABLE OF CONTENTS

DECLARATION	II
LIST OF PUBLICATIONS	III
ABSTRACT.....	V
DEDICATION.....	VIII
ACKNOWLEDGMENTS	IX
LIST OF FIGURES	XVII
LIST OF TABLES	XX
LIST OF ABBREVIATIONS	XXI
CHAPTER ONE.....	1
INTRODUCTION.....	1
1.0 Background	1
1.1 Introduction to Brain Metastasis	1
1.1.1 Causes and Risk Factors	2
1.1.1.1 Causes of Brain Metastasis	2
1.1.1.2 Risk Factors for Brain Metastasis	3
1.1.2 Pathophysiology.....	4
1.1.3 Symptoms and Diagnosis	6
1.1.4 Treatment Options.....	7
1.1.5 Impact on Quality of Life	9
1.2 Stereotactic Radiosurgery.....	11

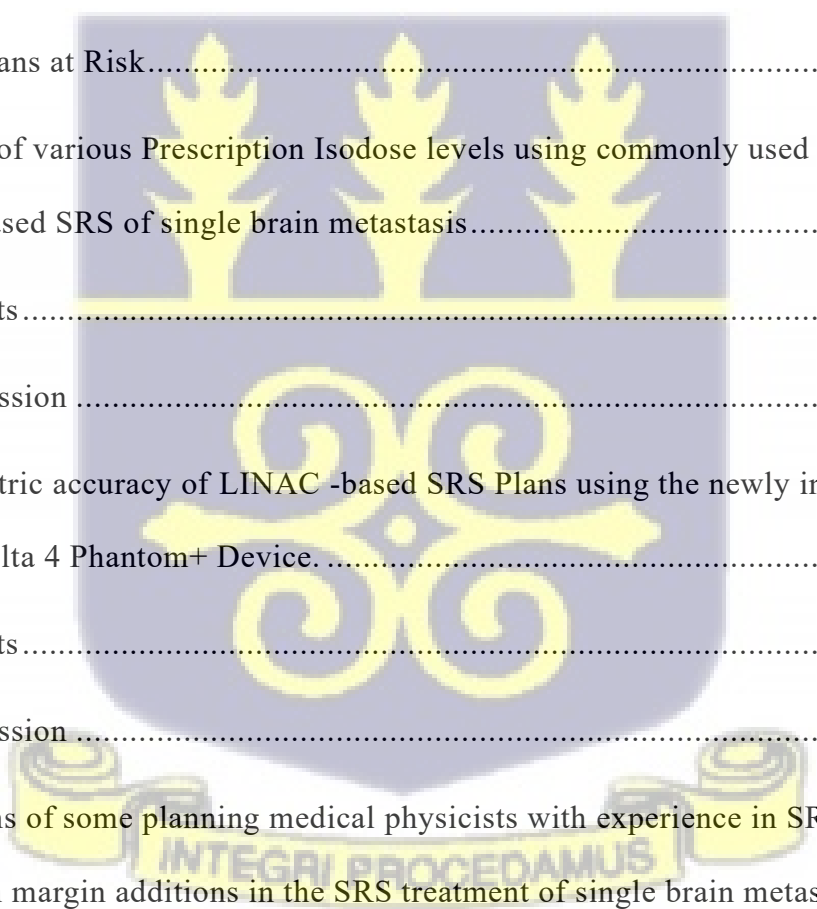
1.2.1 Indications for Stereotactic Radiosurgery.....	14
1.2.2 Key benefits SRS has over other treatment	15
1.3 Planning Target Volume Margins and Prescription Isodose in Radiosurgery	18
1.3.1 PTV Margins in LINAC -based Radiosurgery	19
1.3.2 PTV Margins in Gamma Knife Radiosurgery	20
1.3.3 Factors Influencing PTV Margin.....	22
1.3.4 Prescription Isodose in Radiosurgery	24
1.3.5 Clinical Considerations	25
1.4 Aim of the Study	26
1.5 Specific Objectives	26
1.6 Statement of problem and justification.....	27
1.7 Significance of the Study	30
1.8 Organization of the Thesis.....	31
CHAPTER TWO	33
LITERATURE REVIEW.....	33
2.0 Introduction	33
2.1 History of Stereotactic Radiosurgery: Global Perspective and Its Development in Africa.....	33
2.2 Margin determination in Radiotherapy.....	36
2.3 Margin in SRS	43
2.4 The SRS Process	45
2.4.3 Delivery Modalities.....	45

2.4.3.1 LINAC-based Systems	48
2.4.3.2 Tomotherapy	49
2.4.3.3 Cyber Knife	50
2.4.3.4 Gamma Knife.....	51
2.4.3.5 The Zap-X System.....	52
2.4.4 Treatment Planning	53
2.4.4.1 Localization and imaging	53
2.4.4.2 Image import and Contouring	54
2.4.4.3 Prescription and Planning	54
2.4.5 Patient Specific QA.....	56
2.4.6 Patient Positioning and Plan delivery.....	56
2.5 PTV Margins in Gamma Knife Stereotactic Radiosurgery for Single Brain Metastasis.....	57
2.6 Prescription Isodose Levels in Gamma Knife SRS and Their Impact on Dose Distribution	58
2.7 Interplay Between PTV Margins and Prescription Isodose Levels in Tumor Control and Toxicity.....	61
2.8 Technological Advances and Clinical Implications for PTV Margins and Prescription Isodose Levels in Gamma Knife SRS	64
2.9 LINAC -Based SRS and Prescription Isodose Levels	66
2.10 Impact of Higher Prescription Isodose Levels on Dose Conformity and Tumor Control	69

2.11 Comparative Analysis of Lower Prescription Isodose Levels and Clinical Trade-offs.....	71
2.12 The Role of PTV Margins in LINAC -Based SRS	74
2.13 Clinical Implications and Decision-Making in LINAC -Based SRS for Brain Metastasis.....	75
2.14 Quality Assurance in SRS.....	76
2.15 Patient-Specific QA Devices for Stereotactic Radiosurgery (SRS).....	76
2.16 Artificial intelligence (AI) in Stereotactic Radiosurgery (SRS) Treatment Planning	81
CHAPTER THREE	83
MATERIALS AND METHODS	83
3.0 Introduction	83
3.1 Materials.....	83
3.1.1. The Stereotactic End-to-End Verification (STEEV) phantom.....	83
3.1.2. The Delta 4 Phantom+.....	85
3.1.3. The Gamma Plan treatment planning system for Gamma Knife	87
3.1.4. The TrueBeam Linear Accelerator	89
3.1.5. Eclipse Treatment Planning System	91
3.1.6 The DIRAC Database.....	94
3.2 Methods.....	95

3.2.1 Influence of different planning target volume (PTV) margins with different prescription isodose levels for stereotactic radiosurgery (SRS) of a single brain metastasis on the Gamma Knife Treatment Planning System.....	95
3.2.1.1 Gamma Knife Treatment Planning	95
.....	98
3.2.1.2 Data Analysis	98
3.2.2 Impact of various Prescription Isodose levels using commonly used margins in the LINAC -Based SRS of single brain metastasis	99
3.2.2.1 Eclipse Treatment Planning	99
3.2.2.2 Data Analysis	102
3.2.3 Dosimetric accuracy of LINAC -based SRS Plans using the newly introduced wireless Delta 4 Phantom+ Device.	103
3.2.3.1 Procedure.....	103
3.2.3.2 Data Analysis	105
3.2.4 Opinions of some planning medical physicists with experience in SRS treatment planning on margin additions in the SRS treatment of single brain metastasis.	106
3.2.4.1 Justification of sample size.....	106
3.2.4.2 Data Analysis	106
3.2.5 Geographical distribution of SRS Systems for brain metastasis treatment in Africa and develop guidelines for the implementations of SRS program in Africa. ..	107
3.2.5.1 Procedure.....	107
3.2.5.2 Data Analysis	108
3.3 Ethical clearance sought for the study.....	108

CHAPTER FOUR	109
RESULTS AND DISCUSSION	109
4.0 Introduction	109
4.1 Influence of different planning target volume (PTV) margins with different prescription isodose levels for stereotactic radiosurgery (SRS) of a single brain metastasis on the Gamma Knife Treatment Planning System.....	109
4.1.1 Results.....	109
4.1.2 Discussion	115
4.1.2.1 Dosimetric Parameters.....	115
4.1.2.2 Organs at Risk.....	119
4.2 Impact of various Prescription Isodose levels using commonly used margins in the LINAC -Based SRS of single brain metastasis.....	121
4.2.1 Results	121
4.2.2 Discussion	137
4.3 Dosimetric accuracy of LINAC -based SRS Plans using the newly introduced wireless Delta 4 Phantom+ Device.	141
4.3.1 Results	141
4.3.2 Discussion	143
4.4 Opinions of some planning medical physicists with experience in SRS treatment planning on margin additions in the SRS treatment of single brain metastasis.	146
4.4.1 Results.....	146
4.4.2 Discussion	148



4.5 Geographical distribution of SRS Systems for brain metastasis treatment in Africa and develop guidelines for the implementations of SRS program in Africa.....	150
4.5.1 Results.....	150
4.5.2 Discussion	158
4.5.2.1 Guidelines for the Implementation of SRS Programs in Africa	161
CHAPTER FIVE.....	167
CONCLUSION AND RECOMMENDATIONS	167
Introduction.....	167
5.1 Conclusion.....	167
5.2 Limitations	169
5.3 Novel Contributions and Extension of this Thesis	170
5.3.1 Novel Contributions.....	170
5.3.2 Extension of this Thesis	172
5.4 Recommendations.....	173
REFERENCES.....	175
APPENDICES.....	224
Appendix I.....	224
Survey Questionnaire.....	224
Appendix II (Ethics approval letters).....	227
Appendix III (PUBLICATIONS FROM THE THESIS)	230
Appendix IV (Supplementary LINAC Data)	209

LIST OF FIGURES

Figure 1: A CT radiograph depicting 3 brain metastasis (3 small white circles) 2

Figure 2: A pictorial presentation of the steps associated with brain metastases development from primary tumors. 6

Figure 3: A brain metastasis been managed with stereotactic radiosurgery. 17

Figure 4: A multiple brain metastasis from a breast cancer patient before and after treatment with radiosurgery..... 17

Figure 5: PTV margin addition with isodose levels in a single brain metastasis in a LINAC -based SRS..... 20

Figure 6: Margin addition in Gamma Knife treatment planning for single brain metastasis 22

Figure 7: Illustration of margin expansion in standard radiation therapy 37

Figure 8: Immobilization Devices (a) Illustration of a relocatable head frame with the stereotactic localizer box attached. (b) Gill-Thomas-Cosman frame. (c) Thermoplastic mask 46

Figure 9: CT (a), MRI (b) and DSA (c) 47

Figure 10: LINAC -based System for SRS 49

Figure 11: A Tomotherapy Machine for SRS 50

Figure 12: A Cyberknife System 51

Figure 13: Image of the Gamma Knife System for SRS 52

Figure 14: The Zap-X System 53

Figure 15: Image of the SRS MapCHECK 77

Figure 16: Image of the myQA SRS 78

Figure 17: Image of the Arc CHECK 78

Figure 18: Image of the StereoPHAN..... 79

Figure 19: Image of a 3D Printed Patient-Specific Phantoms	80
Figure 20: Image of a microdiamond detector	81
Figure 21: Image of the STEEV Phantom.....	85
Figure 22: The image of the wireless Delta4 Phantom+	86
Figure 23: The interface of the Gamma Plan Treatment Planning System.....	89
Figure 24: The Truebeam Varian LINAC	91
Figure 25: The Eclipse Planning system in Use	94
Figure 26: DVH and the volume analysis tools from Planning System	97
Figure 27: The phantom through sagittal, coronal and axial planes with the target insert (a) inside the cavity (b) Target delineation in Gamma Plan TPS (c) Dose distribution in the target in the treatment planning system.....	98
Figure 28: The interface of the Eclipse treatment planning system during planning	100
Figure 29: The optimization interface during planning	102
Figure 30: The Wireless Delta 4Phantom+ during measurement	104
Figure 31: Truebeam LINAC monitor interface during measurement.....	105
Figure 32: PTV margin and Selectivity with all Prescription Isodose	113
Figure 33: PTV margin and PCI with all Prescription Isodose	113
Figure 34: PTV margin and GI with all Prescription Isodose	114
Figure 35: PTV margin and V12Gy (cc) with all Prescription Isodose	114
Figure 36: PTV margin and Beam-On-Time (min) with all Prescription Isodose.	115
Figure 37: Distribution of the impact of prescription isodose on organs at risk at margin 0 mm	125
Figure 38: Distribution of the impact of prescription isodose on treatment metrics at margin 0mm	126

Figure 39: Distribution of the impact of prescription isodose on organs at risk at margin 1mm 130

Figure 40: Distribution of the impact of prescription isodose on treatment metrics (GI and CI) at margin 1mm 131

Figure 41: Distribution of the impact of prescription isodose on organs at risk at margin 2 mm 136

Figure 42: Distribution of the impact of prescription isodose on treatment metrics at margin 2 mm 137

Figure 43: The Delta4 phantom+ software displaying the result. The absolute dosage is shown in two diode arrays in three dimensions on the top panel, with colour coding used to indicate the dose..... 143

Figure 44: The Delta4 phantom+ software displaying three histograms: distance to agreement, dose deviation and gamma index..... 143

Figure 45: The graphical response of respondents for four of the questions..... 147

Figure 46: A bar graph distributions of respondents answer to the fifth question: what should be the maximum and optimal PTV Margin to be used accepted and applied in SRS treatment 148

Figure 47: Current number of radiation therapy machines across the African continent.. 155

Figure 48: Scatter plot illustrating the total quantity of machines in relation to the anticipated number of brain metastases, categorised by GDP per capita (\$) across African nations. . 156

Figure 49: A bar graph showing the total number of machines per country in Africa

Figure 50: Model of guidines for implementation of SRS 166

LIST OF TABLES

Table 1: Constraint for optimization in TPS 101

Table 2: One-way ANOVA test for planning dosimetric parameters and PTV margins in the study 111

Table 3: Dose distribution across the different margins with the various prescriptions isodose levels 117

Table 4: Distribution of one sample t-test at margin 0 mm for organs at risk 122

Table 5: Distribution of one sample t-test at margin 0 mm for treatment metrics 124

Table 6: Distribution of treatment time for margin 0 mm 127

Table 7: One sample t-test of margin 1 mm for organs at risk 127

Table 8: One sample t-test of margin 1 mm for treatment metrics (GI and CI) 129

Table 9: Distribution of treatment time for margin 1 mm 131

Table 10: Distribution of sample t-test for margin 2 mm 132

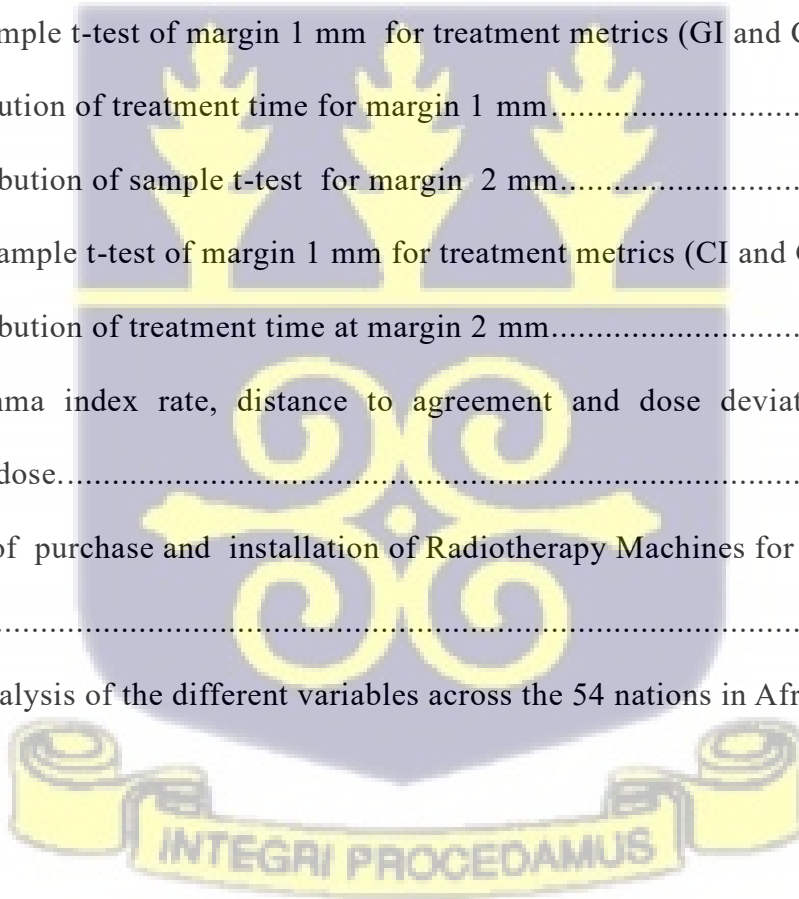
Table 11: One sample t-test of margin 1 mm for treatment metrics (CI and GI) 134

Table 12: Distribution of treatment time at margin 2 mm 135

Table 13: Gamma index rate, distance to agreement and dose deviation of different prescription isodose 142

Table 14: Cost of purchase and installation of Radiotherapy Machines for Brain Metastasis Treatment 151

Table 15: An analysis of the different variables across the 54 nations in Africa 152



LIST OF ABBREVIATIONS

PCI	Paddick Conformal Index
CT	Computed Tomography
TPS	Treatment Planning System
Co60	Cobalt-60
DD	Dose Difference
FFF	Flattening Filter Free
S	Selectivity
IMRT	Intensity-modulated radiation therapy
GK	Gamma Knife
WBRT	Whole Brain Radiotherapy
SRT	Stereotactic Radiotherapy
IAEA	International Atomic Energy Agency
CRO	Centro Riferimento di Oncologico
UCL	University College London
DCA	Dynamic Conformal Arcs
ILGKS	International Leksell Gamma Knife Society
LB	Linear Accelerator-Based
GI	Gamma Index
STEEV	The Stereotactic End-to-End Verification
CK	CyberKnife
MRI	Magnetic Resonance Imaging
LINAC	Linear Accelerator
CBCT	Cone Beam Computed Tomography
NC	Non-Coplanar



SRS	Stereotactic Radiosurgery
DTA	Distance-To-Agreement
Tt	Treatment time
BED	Biologically Effective Dose
CI	Conformal Index
ON	Optic Nerve
QA	Quality Assurance
SBRT	Stereotactic Body Radiotherapy
GI	Gradient Index
AI	Artificial intelligence
MLC	Multi-Leaf Collimator
SD	Standard Deviation
OAR	Organ At Risk
RTOG	Radiation Therapy Oncology Group
PTV	Planning Target Volume
MD	Mean Difference
VMAT	Volumetric Modulated Arc Therapy
ANOVA	Analysis of variance
VHMF	Van Herk Margin Formula
AAPM	American Association of Physicists in Medicine
DIRAC	Directory of Radiotherapy Centres



CHAPTER ONE

INTRODUCTION

1.0 Background

This chapter serves as an introductory section for the research, establishing the foundation of the study. It begins with the background on brain metastasis, covering causes, risk factors, clinical indications, pathophysiology, treatment options, and quality of life and then explores stereotactic radiosurgery, highlighting its benefits over other treatments as well as the planning target volume margins and prescription isodose levels used in Gamma Knife and LINAC-based systems, respectively. With a focus on the study's scope, five specific objectives were outlined. The chapter concludes with a summary of the structure of the thesis.

1.1 Introduction to Brain Metastasis

Brain metastasis is the most common brain tumor in adult patients, with an incidence of 9-14 per 100,000 annually (Habbous *et al.*, 2021). Given moderate improvements in survival for many systemic malignancies since the early 1980s, a corresponding increase in the incidence of brain metastasis from 8 to 13% has been identified in this period. Cancers with the greatest propensity to spread to the brain are those arising from the lung, breast, kidney, skin (particularly melanomas), and colon (Kuksis *et al.*, 2021; Mitchell *et al.*, 2022). Brain metastases are a major source of morbidity in these patients, often causing severe headaches, focal motor/sensory deficits, altered mental status, and gait/coordination impairment (Cagney *et al.*, 2017; Liu *et al.*, 2022; Murrell *et al.*, 2016; Tabouret *et al.*, 2012). Despite aggressive treatment, median patient survival from the diagnosis of brain metastases remains short, on the order of months; only 35% of patients with brain metastases survive one year after treatment, and a dismal 11% remain alive at the two-year mark (Jin *et al.*, 2018). On Computed Tomography, brain metastases often appear as multiple, well-circumscribed

lesions at the gray–white matter junction, surrounded by vasogenic edema, and enhancing after contrast, often ring-shaped as shown in Figure 1 (Arnaout *et al.*, 2024)

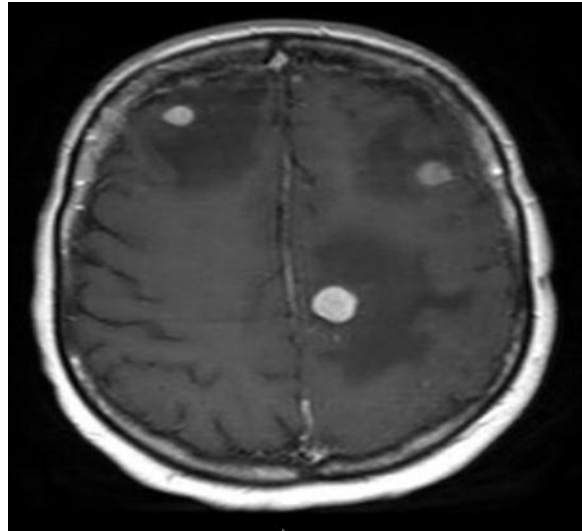


Figure 1: A CT radiograph depicting 3 brain metastasis (3 small white circles)(Arnaout *et al.*, 2024; Tabouret *et al.*, 2012)

1.1.1 Causes and Risk Factors

Understanding the causes and risk factors related to brain metastasis is crucial for early detection, treatment, and improving patient outcomes. An in-depth look at the causes and risk factors is the follows:

1.1.1.1 Causes of Brain Metastasis

1. Metastatic Spread from Primary Tumors

Brain metastases are primarily caused by the spread of cancer cells through the bloodstream or lymphatic system. The primary cancers most frequently associated with brain metastases are: Habbous *et al.* (2021) conducted a population-level analysis and reported that lung cancer accounts for approximately 60 % of all brain metastases, followed by breast cancer at 11 %, melanoma at 6 %, colorectal cancer at 4 %, and renal cell carcinoma (kidney cancer) at 3 %. Brain metastases commonly arise from systemic spread via the bloodstream or lymphatic system, with lung cancer responsible for approximately 60 % of cases, followed

by breast cancer (~11 %), melanoma (~6 %), colorectal cancer (~4 %), and renal cell carcinoma (~3 %) (Habbous *et al.*, 2021).

2. Tumor Characteristics

A comprehensive study found that in primary melanoma, a higher mitotic rate is strongly associated with decreased survival. Mitotic rate was the second most powerful independent predictor of survival after tumor thickness with statistical significance ($\chi^2 = 67.0$; $P < .001$) (Thompson *et al.*, 2011).

3. Duration of Cancer

The longer a person has cancer, the higher the risk that it will metastasise to other organs, including the brain (Lauko *et al.*, 2020).

1.1.1.2 Risk Factors for Brain Metastasis

1. Age

The risk of developing brain metastases increases with age, particularly in individuals over 45 years old. Older patients often have more advanced cancers, which increases their likelihood of metastasis (Valiente *et al.*, 2018).

2. Gender

Some studies suggest that men may be at a higher risk for developing brain metastases compared to women, although this can vary based on the type of primary cancer (Fecci *et al.*, 2019; Lauko *et al.*, 2020) .

3. Type of Primary Cancer

Certain cancers are more likely to result in brain metastases: Lung cancer (especially non-small cell lung cancer) has a high incidence rate of brain metastasis. Breast cancer, particularly in its advanced stages, frequently spreads to the brain. Melanoma is known for its aggressive nature and tendency to metastasize.(Fecci *et al.*, 2019)

4. Presence of Other Metastases

Patients with existing metastases in other organs (like bone or liver) are more likely to develop brain metastases (H. Lee *et al.*, 2016).

5. Genetic Factors

Genetic predispositions can increase susceptibility to tumors that may spread to the brain. Conditions like neurofibromatosis type 1 (NF1) are linked with a higher risk of developing various tumors, including those that can metastasize (Boire *et al.*, 2020).

6. Weakened Immune System

People with weakened immune systems, such as those affected by HIV/AIDS or undergoing immunosuppressive treatments, may face an increased likelihood of developing metastatic tumors (Goncalves *et al.*, 2016).

7. Radiation Exposure

Previous exposure to radiation therapy, particularly to the head, can increase the risk of developing secondary brain tumors later in life (Suh *et al.*, 2020).

8. Family History

A family history of certain cancers may increase an individual's risk of developing metastatic disease (Lauko *et al.*, 2020).

9. Lifestyle Factors

Smoking and other lifestyle choices may contribute to increased risks for certain types of cancers that can lead to brain metastasis. (Gutschenritter *et al.*, 2021)

1.1.2 Pathophysiology

The process of tumor metastasis is intricate and requires several steps. After invading and extending through surrounding tissues, a subpopulation of tumor cells must follow the flow

of fluids and circulating elements to leave the primary lesion. They then use blood vessels as the primary means of dissemination, leading to the formation of brain metastasis. However, non-vascular spaces can also contribute to the establishment of metastasis in certain cancers. Only a small percentage of circulating tumor cells can form metastasis in the brain, as well as other organs. The brain itself presents unique challenges for successful colonisation by tumor cells (Dou *et al.*, 2021; Rajput, Kumar Sharma, and Malviya, 2023). One of the accepted hypotheses for the pathogenesis of brain metastases is the “seed and soil” hypothesis by Paget (Qiang Liu *et al.*, 2017; Mazzola *et al.*, 2019). The successful development of metastases for certain tumors depends on the interaction of the cancer cells (seeds) and their affinity for the various target organs (soil). Thus, the cancer cells must migrate from the primary tumor into the blood vessels, survive the high pressures of circulation and eventually exit the vasculature and implant on the target organs (soil) (Phadke *et al.*, 2022). The tumor cells in the primary sites undergo proliferation and initiate angiogenesis thus forming new blood vessels. These cells then initiate an invasion process into the host stroma, thereby gaining entrance into the circulation system. The tumor cells then escape through the microvasculature of the host circulation system and deposit on the target organs (soil) and survive (Mazzola *et al.*, 2019).

A great number of brain metastases are mostly identified in the cerebrum with a special affinity for the frontal and parietal lobes (Khalsa *et al.*, 2013). This is due to the low cerebral arterial blood pressure at the watershed of the brain which favours the emboli process of the tumor cells (Qiang Liu *et al.*, 2017). Therefore, it is crucial to gain a deeper understanding of the specific factors that lead to the colonization and growth of metastatic cells in the brain. This understanding will help in the development of personalized and more effective therapeutic strategies, which can be used alone or in combination with other treatments for

the removal of malignant cells. Figure 2 below presents a pictorial view of how cancer metastases from primary tumors to the brain.

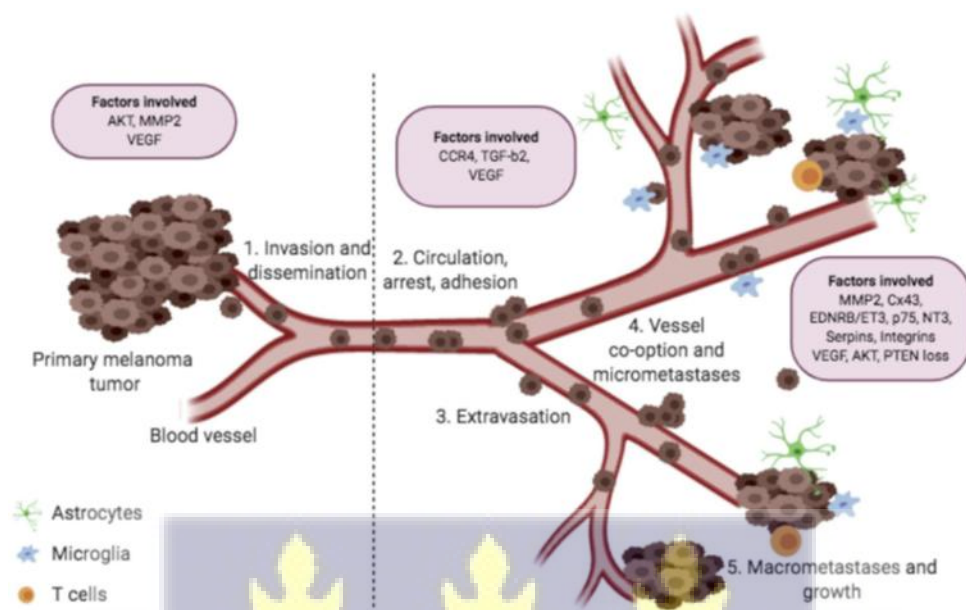


Figure 2: A pictorial presentation of the steps associated with brain metastases development from primary tumors (Phadke *et al.*, 2022)

1.1.3 Symptoms and Diagnosis

Diagnosis of a brain tumor, typically involves taking patient's medical history and conducting thorough neurological examination. This examination typically includes assessing reflexes, muscle strength, eye and mouth movements, coordination, and alertness. They would also evaluate the patient's mental state, personality, and memory. To visualize the tumor, a Magnetic Resonance Imaging with gadolinium contrast or a computed tomography scan is usually necessary. In some cases, additional diagnostic methods, such as a biopsy to remove a sample of tumor tissue, may be required. When a patient with known cancer in another part of their body presents symptoms of a brain tumor and has nodules in the brain with similar receptors, it is referred to as brain metastasis. However, it should be noted that extensive local disease is not considered brain metastasis. Interestingly, a secondary brain tumor may

actually be the initial sign of the disease, as the primary lesion may not have been identified at the stage of the brain metastasis diagnosis (Garcia *et al.*, 2018; Zou, Dong, and Kevin Teo, 2018).

The commonest symptoms of metastatic brain tumors are headaches and seizures, which are usually complex partial seizures or partial complex seizures. Other symptoms such as nausea, vomiting, and drowsiness can also occur (Leone and Leone, 2015; Tabouret *et al.*, 2012). It is worth noting that these symptoms can also be present in a patient with primary brain cancer. Seizures typically occur when the tumor compresses the cerebral cortex or the blood vessels that supply it, a condition known as the mass effect. In some cases, brain tumors can push the brain against the skull, creating pressure that leads to seizures. Additionally, seizures can sometimes serve as an early warning sign, prompting the individual to seek medical attention and discover the tumor before it becomes very large (Lin and Avila, 2017).

1.1.4 Treatment Options

Treatment has become increasingly complex with the need to manage both intracranial and systemic disease, and although new therapeutic strategies are developing, their systemic toxicity may limit the life of many patients who have a limited life expectancy (Suh *et al.*, 2020).

The current guidelines provided by the National Comprehensive Cancer Network (NCCN) offer several treatment options for individuals who have between one and three metastases. Specifically, for those with a single metastasis, surgery followed by radiation is recommended. However, it is important to note that this option is only appropriate for individuals with a good Eastern Cooperative Oncology Group (ECOG) performance status or Karnofsky Performance Status (KPS) and longer life expectancies. For individuals who have up to four metastases and are unable to undergo surgical resection, stereotactic radiation

therapy is considered the preferred treatment, as long as their tumors are no larger than 4 cm. Additionally, the NCCN guidelines state that some individuals with oligometastatic disease may benefit from using stereotactic radiation targeted solely at the metastatic region (Arvold *et al.*, 2016; Jung *et al.*, 2020).

In cases where other factors deem it necessary, whole brain radiation therapy is commonly used (Mizuno *et al.*, 2019). However, when there is a possibility of recurrence, SRS may be utilized for individuals who have previously received whole brain radiation therapy. In certain cases, surgical resection of the metastasis is often one of the most effective treatments, leading to higher rates of survival compared to other therapies. The timing of metastasis removal depends on factors such as the size and location of the metastasis, the type and stage of the original tumor, the presence of multiple metastases, as well as the age and overall health of the individual (Eaton, Lee, and Paddick, 2018; Jairam *et al.*, 2013; Mazzola *et al.*, 2019). Recent advancements in microsurgery and neurosurgery, along with improved safety precautions, indicate that surgery may now be more successful in removing metastasis than in the past (Niedermeyer *et al.*, 2024).

Furthermore, radiation therapy, in various forms such as whole-brain radiotherapy, and stereotactic radiosurgery, is mostly used to address metastasis. For individuals with multiple metastases who are not suitable candidates for surgery, whole-brain radiation is typically recommended. Whole-brain radiation therapy is directed to the skull, where many of the tumors are located. X-rays are used, and two large beams are para-opposed to the patient's skull. This is done to homogenise the dose distribution to the brain volume and try to spare normal tissue. The most common treatment schedule for brain metastasis using whole-brain radiotherapy is 30 Grays (Gy) given in 10 fractions.

Stereotactic radiosurgery techniques like Gamma Knife, CyberKnife, and others offer non-invasive methods of delivering high doses of radiation specifically to tumors, while

minimising exposure to healthy brain tissue. Usually, treatment is given either in a single session or over multiple fractions spanning a few days to a few weeks (Fecci *et al.*, 2019; Gutzmer *et al.*, 2020; Knisely and Apuzzo, 2019; Lippitz *et al.*, 2014; Tong, and Wang, 2019). Chemotherapy has been believed to be ineffective for patients with brain involvement. Historically, there was a failure to demonstrate meaningful responses. For some years, chemotherapy has played second fiddle to radiation and surgery for parenchymal spreading. Chemotherapy is widely used for the treatment of systemic tumors. In the case of brain tumors, the blood-brain barrier (BBB) prevents penetration by useful drugs, and the rapid development of resistance may also limit efficacy (Anand *et al.*, 2023). At present, chemotherapy for secondary brain tumors is only used to treat systemic metastatic cancer when the patient is too weak for surgery or when the general condition of the primary site has improved. Better cooperation between oncologists and neurosurgeons is needed to safely and effectively deliver chemotherapy to patients. Some chemotherapy drugs have been recommended for treating systemic tumors associated with secondary brain tumors (Anand *et al.*, 2023; Suh *et al.*, 2020). Epirubicin in particular has been reported to have significant effects in cases of breast cancer, and an increasing number of reports have been published advocating the use of trastuzumab in combination with radiotherapy. However, currently there is insufficient evidence (Ormrod *et al.*, 1999).

1.1.5 Impact on Quality of Life

In patients with good survival, quality of life becomes an important issue as it can be impacted both by gastrointestinal or bladder symptoms related to the primary cancer and psychological factors, such as depression or despair due to the diagnosis of an incurable stage of cancer and the challenge of managing advanced technology with relatively limited resources. Until now, there have not been many systematic studies focusing on the effects of

brain metastasis on psychological status and quality of life, although multiple studies have been reported that are generally observational and contain fewer patients (Papadopoulou *et al.*, 2022; Youyang Wang and Feng, 2022). Management of short-term effects of brain metastasis on patients includes treatment such as radiation therapy or surgery, which are recognised as standard; and management of long-term effects of brain metastasis eventually leads to improving functional status and quality of life. Other reported items are relatively consistent with the aspects of the clinical syndrome for which brain metastasis patients complain in daily life (Kocher *et al.*, 2014; Mazzola *et al.*, 2019).

Brain metastasis from solid tumors has generally been associated with poor survival. Most reports have not been segregated by primary tumors, but rather there have been several of them on mixed histologies (Badiyan *et al.*, 2016; Simpson *et al.*, 2006; Traylor *et al.*, 2019; Valiente *et al.*, 2018). However, the advancement in the understanding of cancer biology and improvement in brain imaging leading to the detection of a relatively larger number of brain metastasis at an early stage of the disease could change this notion. In the current era of routine magnetic resonance imaging (MRI) screening, especially in patients with certain solid tumors, it is possible that patients diagnosed with brain metastasis could live for several years. However, this is not true in patients with some solid tumors arising from melanoma and with kidney cancer, as they are known to be particularly aggressive (Putz *et al.*, 2020). Since the aforementioned primary cancers are more common in life, a reasonable percentage of cancer patients with brain metastasis could have good survival as well. Of the almost 1.59 million cancer cases reported in the United States, 400,000 of the patients were confirmed to have brain metastasis. This large number represents an increase in detection due to using advanced imaging and a possible increase in life expectancy (Brain Tumor Facts, 2022). Unfortunately, this cannot be said of Africa where there is no continental data on the number of confirmed brain metastasis.

1.2 Stereotactic Radiosurgery

Stereotactic radiosurgery is a form of external beam radiotherapy which is minimally invasive or non-invasive, which operates behind the principle of using a focal technique to deliver high radiation doses with the help of multiple convergent beams of high-energy photons to a distinct target volume while sparing healthy surrounding tissues (Jairam *et al.*, 2013). Stereotactic radiosurgery is a potent treatment for patients with minimal brain metastases and has high local tumor control as compared to whole-brain radiotherapy (Ebner *et al.*, 2015).

The objective of stereotactic radiosurgery is to provide a substantial ablative dosage to the tumor with high precision and conformity, therefore reducing the exposure to adjacent healthy tissues. To achieve this objective, numerous fundamental prerequisites for stereotactic radiosurgery must be fulfilled, including precise localisation, mechanical accuracy, patient safety and optimum dose distribution (Choi *et al.*, 2012; Lupattelli *et al.*, 2020; Meeks *et al.*, 2011). Various groups, including the Radiation Therapy Oncology Group (RTOG) and the American Association of Physicists in Medicine (AAPM Report No. 54), have published their SRS guidelines (Buatti *et al.*, 2000; Schell *et al.*, 1995). The term stereotactic was first employed and the technique was explored by the teams of Robert H. Clarke and Victor A. H. Horsley in the early 1900s, even though the invention of SRS was attributed to Lars Leksell (Knisely and Apuzzo, 2019).

Stereotactic radiosurgery (SRS) which involves a single fraction of high dose radiation precisely focused on sharply circumscribed intracranial targets, is a less invasive option to surgery. It is also a well-established treatment for the management of metastatic intracranial disease (Qi Liu, Tong, and Wang, 2019; Skourou *et al.*, 2021; Vergalasova *et al.*, 2019). The rapid dose fall-off and high degree of conformity to spare normal tissues are the key

advantages of SRS. However, as radiation is delivered in a single fraction, normal tissue toxicities limit the dose of radiation delivered, and the size of target treated (Dimitriadis and Paddick, 2018). The usual “4 Rs” of radiation therapy (repair, repopulation, redistribution, and reoxygenation) do not strictly apply to SRS but rather, the effect of early and late responding tissues is of higher consideration. The intracranial target may be either early (high α/β ratio) or late responding, but the surrounding normal intracranial structures are always late responding tissues (low α/β ratio). It has been argued that one fraction SRS results in a suboptimal therapeutic ratio between tumor control and late effects on normal tissues (Korytko *et al.*, 2006). One of the main criticisms of SRS is the delivery of radiation in a single dose, which corresponds to a smaller α/β ratio of late reacting tissues relative to that of the target and early responding tissues. A second issue with single dose fractionation is tumor hypoxia, as existing hypoxic cells in the target would not be easy to eradicate in a single treatment. Thirdly, single treatment does not take advantage of the cell cycle redistribution of the tumor, lessening the impact of radioresistance of the S-phase cells (Kirkpatrick *et al.*, 2017; Shibamoto & Iwata, 2020). Lastly, due to the single fraction nature of SRS, there is an inverse dependence of dose administered to the treated volume, limiting the dose to ensure normal tissue complications are at an acceptable level (Nakazawa *et al.*, 2014; Shibamoto and Iwata, 2020). Specifically for brain metastases, SRS is usually directed at patients with tumors less than 4 cm in maximum diameter. This setback for SRS is associated to the risk of radiation necrosis, a late effect of radiosurgery (Chao *et al.*, 2018). Korytko *et al.* demonstrated that the volume receiving 12 Gy (V12) serves as a predictor for radiation necrosis in intracranial tumors, with a substantial increase in risk when V12 exceeds 10 cm³, irrespective of plan conformance. This is a crucial clinical concern when establishing and incorporating safety margins for intracranial targets (Korytko *et al.*, 2006).

SRS is commonly prescribed and delivered using a Gamma Knife planning and treatment system (Meeks *et al.*, 2011). The Gamma Knife (Leksell Gamma Unit, Elekta Radiosurgery Inc, Atlanta, GA) prototype was developed in 1968 by Lars Leksell (Skourou *et al.*, 2021) . The availability of modern technologies has made it possible for SRS to be delivered using CyberKnife, Tomotherapy as well as LINAC-based systems with specialized treatment planning systems (TPS). This is now accessible to most linacs (Skourou *et al.*, 2021). With the introduction of these new techniques in the radiosurgery community, clinical studies have shown a survival advantage in SRS therapy for 1-4 metastases that would have previously warranted immediate referral for Whole-Body Radiotherapy (WBRT) (Eaton, Lee, and Paddick, 2018). These days, prognostic characteristics unique to each patient and illness are taken into consideration while choosing a course of therapy. A more targeted strategy using SRS alone, backed by data from randomised controlled trials, has replaced the widely used upfront WBRT for patients whose longer-term survival is anticipated. This approach is for patients with 1-4 brain metastases and favourable prognostic characteristics (Kirkpatrick *et al.*, 2017; Vogelbaum *et al.*, 2022). For patients with a greater number of brain metastases (>4), the approach is also changing. Retrospective and single-institution prospective studies indicate that SRS is both effective and safe without WBRT (Chao *et al.*, 2018; Mizuno *et al.*, 2019). Although the maximum volume and/or number of metastases best treated with SRS are unclear, total tumor volume seems to be a more useful measure for prognostication than the absolute number of metastases. Randomized trials and some of the studies are looking at treating up to 20 metastases.(Chao *et al.*, 2018; Choi *et al.*, 2012). Ongoing management with radiosurgery is widely used, whereby newly identified metastases on follow-up imaging are aggressively treated as they arise, while whole-brain radiotherapy is reserved only for palliation or leptomeningeal illness(El Shafie *et al.*, 2020).

1.2.1 Indications for Stereotactic Radiosurgery

There are contraindications to the use of SRS. Although there is widespread use of SRS in developed countries to manage patients with a variety of brain tumors, the rapidly expanding nature of symptoms caused by some malignant tumors signals a more progressive and unstoppable process precluding SRS (patients with very small, accessible recurrence or metastasis might be successfully treated with SRS even for those nascent lesions arising from a very malignant primary cancer). Similarly, medical illness might render a patient noncompetitive for or intolerant of a neuro-navigation procedure (Badiyan, Regine, and Mehta, 2016).

The high precision and localization achieved with stereotactic radiosurgery (SRS) allow for the safe delivery of high doses of radiation with minimal tissue toxicity to a small, precisely defined target volume in the brain. Historically, it was proposed that SRS would be principally useful in patients with small, relatively accessible deep-seated abnormalities, but considerable progress has shown that SRS has wide and expanding applications in patients with benign and malignant neoplasms, functional disorders, and in selected patients with vascular malformations and other functional disorders (Badiyan, Regine, and Mehta, 2016; Soliman *et al.*, 2016; Yamamoto *et al.*, 2014). Given its widespread ability to treat selected patients with uncomplicated or minimally complicated disorders, and since SRS is an office or clinic-based, non-invasive (in comparison with the alternative invasive or surgical) procedure, a most important consideration for its use by those not dedicated to using radiosurgery is choosing what conditions or patients will benefit from treatment. Some of the common indications for stereotactic radiosurgery include brain metastases, gliomas and glioblastomas, pituitary adenomas, meningiomas: acoustic neuromas (vestibular schwannomas), craniopharyngiomas, chordomas, Arteriovenous malformations (AVMs),

cavernous angiomas, trigeminal neuralgia, certain behavioural disorders (Fecci *et al.* 2019; Gilbo, Zhang, and Knisely, 2017; Kraft *et al.*, 2019).

1.2.2 Key Benefits SRS has over Other Treatment

Stereotactic radiotherapy/radiosurgery has changed the standard of treatment of brain metastases. Key benefits over other treatment techniques used in the management of brain metastases include;

- **Gradual elimination of surgical resection for the treatment of brain metastases**

Both surgical resection and radiosurgery are used in the treatment of metastases of <30.0 mm. However, radiosurgery has the capability to deliver doses to tumors without any invasion. Its non-invasiveness and the likelihood to treat multiple lesions simultaneously make it a preferred technique to surgery. Sometimes, radiosurgery is used post-operatively to treat the tumor cavity thereby decreasing the risk of local reoccurrence (Badiyan, Regine, and Mehta, 2016).

- **Serving as an adjuvant treatment to whole-brain radiotherapy (WBRT)**

Stereotactic radiosurgery has shown to be highly effective for lesions <30.0 mm with a local tumor control of about 80-95%. The inclusion of stereotactic radiosurgery to whole-brain radiotherapy as a boost will help increase survival rates in patients with single metastases as radiosurgery has an effective local tumor control and local tumor cavity reoccurrence will be decreased (Khalsa *et al.*, 2013).

- **High radiation conformity**

Radiosurgery uses the focal technique to deliver high radiation doses to distinct target volume. Unlike WBRT, radiosurgery ensures that radiation dose is delivered to only

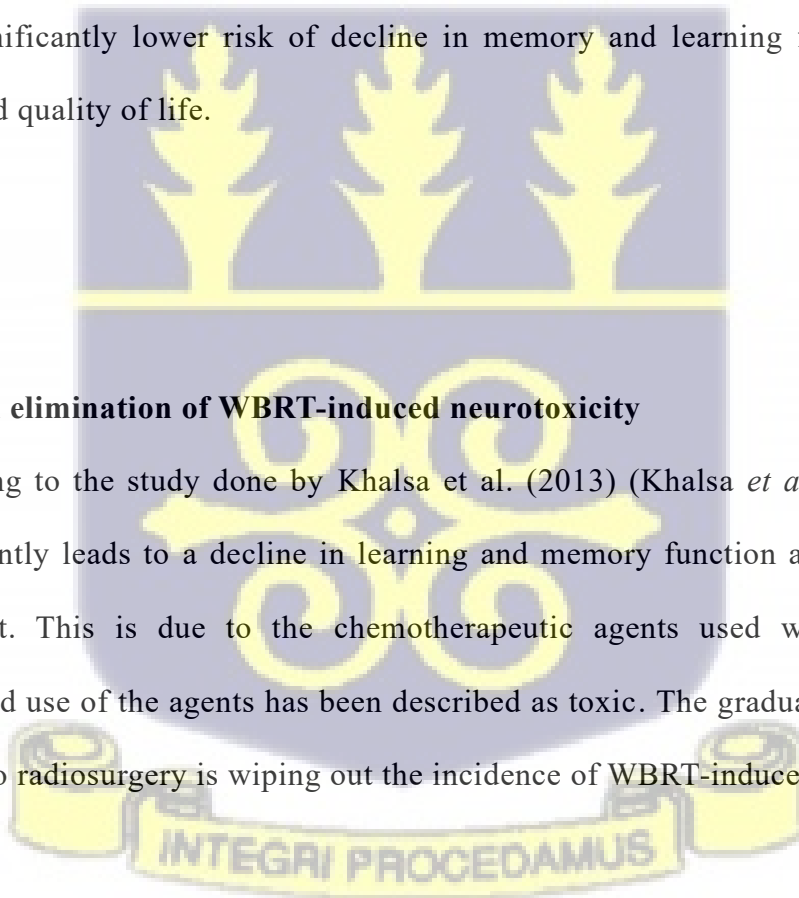
the gross tumor targeted while sparing the surrounding healthy cells (Lippitz *et al.*, 2014).

- **Serving as a monotherapy with high clinical efficacy**

Radiosurgery has proven to be efficient with high local tumor control and in the management of oligometastases (1-4 lesions) in the brain (Kocher *et al.*, 2014). Though the combining power improves survival rates, radiosurgery as a monotherapy has proven to be efficient and reliable with increased survival rates, high local tumor control and decreased local tumor cavity recurrence. According to the study by Lippitz *et al.* (2014) (Lippitz *et al.*, 2014) patients receiving radiosurgery alone were at a significantly lower risk of decline in memory and learning function with an improved quality of life.

- **Gradual elimination of WBRT-induced neurotoxicity**

According to the study done by Khalsa *et al.* (2013) (Khalsa *et al.*, 2013), WBRT significantly leads to a decline in learning and memory function after 4 months of treatment. This is due to the chemotherapeutic agents used with WBRT. The prolonged use of the agents has been described as toxic. The gradual transition from WBRT to radiosurgery is wiping out the incidence of WBRT-induced neurotoxicity.



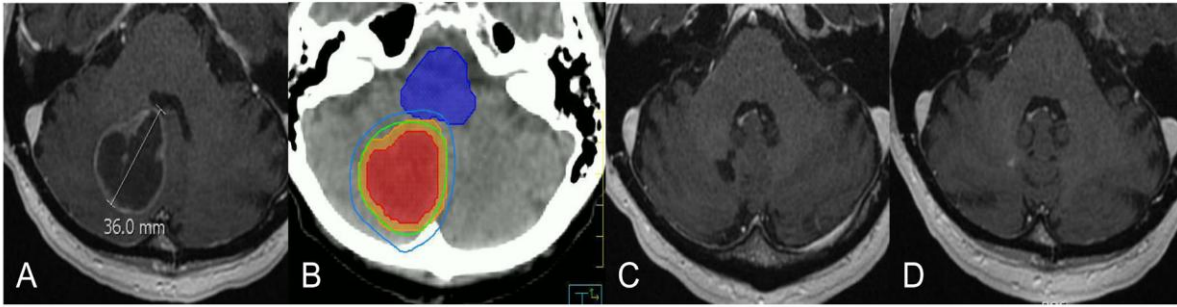


Figure 3: A brain metastasis being managed with stereotactic radiosurgery.

Image A represents an MRI of the cerebellar of the brain with a metastasis measuring 36.0mm (3.6 cm) in diameter. Image B represents a treatment planning around the gross tumor (red colour) and planning target volume (orange colour) with the brain stem (blue colour) been spared from irradiation. Image C represents MRI after months of irradiation of the tumor. Image D represents a complete resolution and damage to the tumor after a year of irradiation. (Soliman *et al.*, 2016)

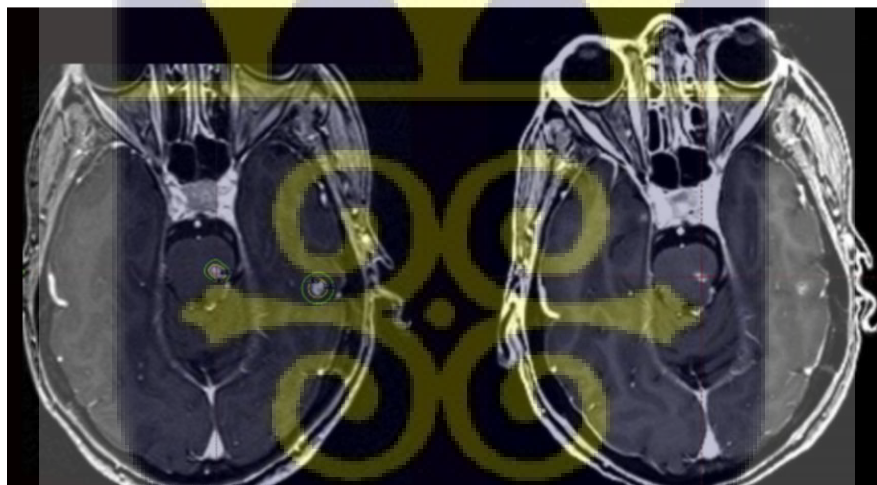


Figure 4: A multiple brain metastasis from a breast cancer patient before and after treatment with radiosurgery. First Image shows metastases from the breast cancer with diameter <math>< 30.0\text{ mm}</math> (3.0 cm). Second Image shows years after the radiosurgery treatment of the metastases (Lippitz *et al.*, 2014)

1.3 Planning Target Volume Margins and Prescription Isodose in Radiosurgery

One of the key challenges in using radiosurgery for the treatment of brain metastasis is determining the optimal planning target volume (PTV) margins and prescription isodoses. The PTV margins refer to the additional space around the target tumor that needs to be treated to ensure that all cancer cells are effectively targeted, while the prescription isodoses specify the radiation dose that will be delivered to the tumor (Leszczyńska *et al.*, 2017; Ma *et al.*, 2014). The debate surrounding the optimal PTV margins and prescription isodoses for radiosurgery in the treatment of single brain metastasis centers around the balance between maximizing the effectiveness of the treatment and minimising the risk of damaging healthy brain tissue. Some experts argue for larger PTV margins and higher prescription isodoses to ensure that all cancer cells are destroyed, while others advocate for smaller margins and lower doses to reduce the risk of side effects. Ultimately, the decision on the optimal PTV margins and prescription isodoses for radiosurgery in the treatment of a single brain metastasis must be made, taking into account factors such as the size and location of the tumor, the patient's overall health, and the risk of complications (Stojkovski, Krstevska, and Smichkoska, 2017; Youssoufi *et al.*, 2021; Zhao *et al.*, 2014).

Furthermore, when treating multiple metastases, a 2018 benchmark of SRS centres in England found that most Cyberknife centres and all Gamma Knife centres do not use a GTV-PTV margin, but the majority of LINAC centres use a 1-mm margin. The use of surgically attached frames to the skull may contribute to the Gamma Knife's zero margin. Also, the prescriptions isodose used varies across centres. The non-invasive nature of frameless thermoplastic face masks has led to their progressive replacement of frames in patient immobilization. It is unclear whether the no margin approach can be applied to these newer therapies. There is a strong association between the risk of radiation necrosis and normal brain V12 Gy doses; thus, a margin may be added to treatments to guarantee adequate dose

coverage to metastases. Using no margin, however, may lower the risk of brain necrosis (Eaton, Lee, and Paddick, 2018).

1.3.1 PTV Margins in LINA -based Radiosurgery

The advent of LINAC-based stereotactic radiosurgery has transformed the field of oncology, offering a non-invasive treatment option for patients with brain metastasis. This innovative technique combines the precision of stereotactic localization methods with the power of a linear accelerator (LINAC), enabling many centres to implement radiosurgery. Despite its numerous advantages, one of the critical challenges in LINAC-based stereotactic radiosurgery is the determination of appropriate planning target volume (PTV) margins (Bayman *et al.*, 2010; Gill *et al.*, 2015; Jhaveri *et al.*, 2019).

The PTV margin is a crucial factor that must be determined for appropriate LINAC-based radiosurgery treatment planning. In general, LINAC-based radiosurgery is limited to between 3 and 6 fractions. Treatments with a small number of large fractions are more susceptible to delivery errors, which may compromise the prescribed dose distribution and damage the surrounding organs. In radiotherapy and radiosurgery practice, PTV margins are individualised to accommodate a range of uncertainties based on setup systems, target motion, and cases. Since smaller internal target volume (ITV) margins result in a more conformal dose to the target, a margin reduction necessitates an optimization of the prescribed isodose volume (Kirkpatrick *et al.*, 2015). Adding PTV margins allows the effects of organ motion and setup uncertainties to be reduced and to increase the total dose to the tumor. Figure 5 below presents the PTV margins with the isodose levels in a single brain metastases. The sum of CTV and PTV makes the volume obtained large by creating a large exposure to radiation of the normal tissue around the tumor. In principle, it is aimed to increase the total dose to the tumor by giving this large dose to the tumor. However, this clinically makes it

difficult to increase the percentage of tumor control if a high radiation dose is also given to the organ at risk (Grishchuk *et al.*, 2023; The Royal Australian and New Zealand College of Radiologists, 2022).

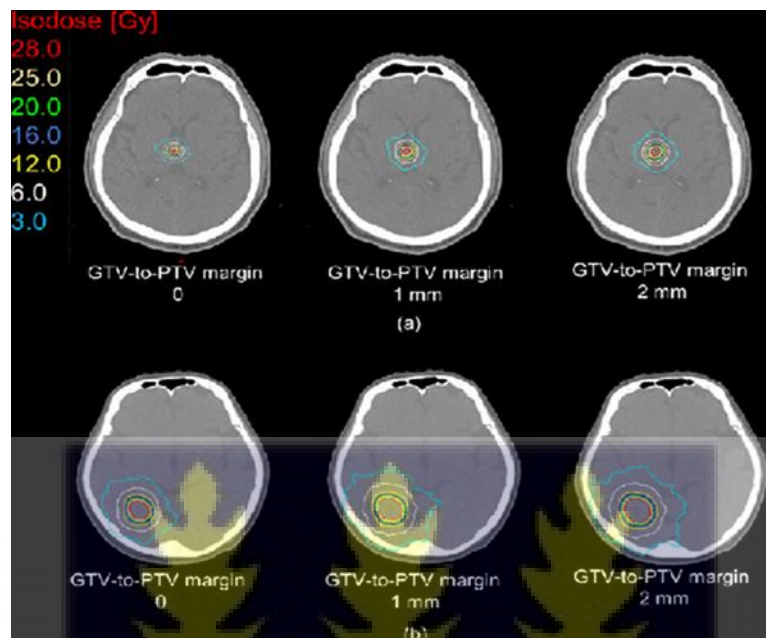


Figure 5: PTV margin addition with isodose levels in a single brain metastasis in a LINAC-based SRS (Ueda *et al.*, 2019)

1.3.2 PTV Margins in Gamma Knife Radiosurgery

Traditionally, radiosurgery treatments have been delivered with a Gamma Knife. It is a common practice in conventional radiotherapy to place a margin around the clinical target volume (CTV) to form a planning target volume (PTV). The PTV compensates for the inaccuracies intrinsic to the process of radiotherapy, including patient alignment, geometrical setup uncertainties, and patient intra-treatment motion. If the dose to the PTV is set too low or too high, the margin will not be enough, and the benefits of modern high-precision radiotherapy techniques cannot be successfully harnessed. Defining an excessive amount of volume as part of PTV can lead to higher chances of injury to the surrounding critical organs receiving collateral high doses (International Commission on Radiation Units and

Measurements, 1999; Kron, 2008; The Royal Australian and New Zealand College of Radiologists, 2022).

A Gamma Knife (GK) radiosurgery system uses small arcs of cobalt-60 sources to deliver high dose precision local radiation. The GK system is equipped with a treatment planning system (TPS) (Schmitt *et al.*, 2020; Skourou *et al.*, 2021). It is an uncommon practice in planning Gamma Knife radiosurgery to place an additional planning margin around the target volume to compensate for treatment uncertainties from patient head motion during treatment or beam collimation uncertainties or both. Some studies suggest that planning target volume (PTV) margins can vary significantly for small targets and fractionated treatment compared to conventionally fractionated treatments (Duggar *et al.*, 2022a, 2022b). The Leksell stereotactic coordinate system, which revolutionized radiosurgery delivery capabilities through multiple platforms, has raised the need to redefine margin addition (Grishchuk *et al.*, 2023).

Planning target volume (PTV) margins are important components in establishing acceptance and delivery appropriateness of external beam therapies including Gamma Knife radiosurgery (GKRS). They are added to the CTV to provide for uncertainties in the localization, contouring of the target volume and for uncertainties in the planning and delivery of the treatment (Fiagbedzi, Hasford, and Tagoe, 2024). For intracranial targets including brain metastases (BM), the magnitude of the added PTV margin might vary significantly across different GK models and treatment settings such as single session verse hypofractionation, based on the GK radiation delivery geometry and commissioning methods (Agazaryan *et al.*, 2021; Mesko *et al.*, 2020). Most importantly, choosing appropriate PTV margins and adding margin additions are essential in preventing marginal recurrence. Figure 6 below presents the margin and its addition in Gamma Knife treatment planning for single brain metastases. The choice is based on understanding that a CTV is delineating the

radioresistant tumor during brain imaging examinations. However, treatment takes place in a rapidly altering headspace environment and advancing technologies offer new detailed insights to allow for better approaches in radionecrotic risk estimation (Bernstein *et al.*, 2021; Duggar *et al.*, 2022a, 2022b; SABR UK Consortium 2015). The traditional method of rigid immobilization fixation for a single fraction GK SRS utilizes the convention of a 0 mm PTV, analogous to surgical excision of brain targets. Planning target volume (PTV) margins are important when performing Gamma Knife radiosurgery (Kutuk *et al.*, 2022)

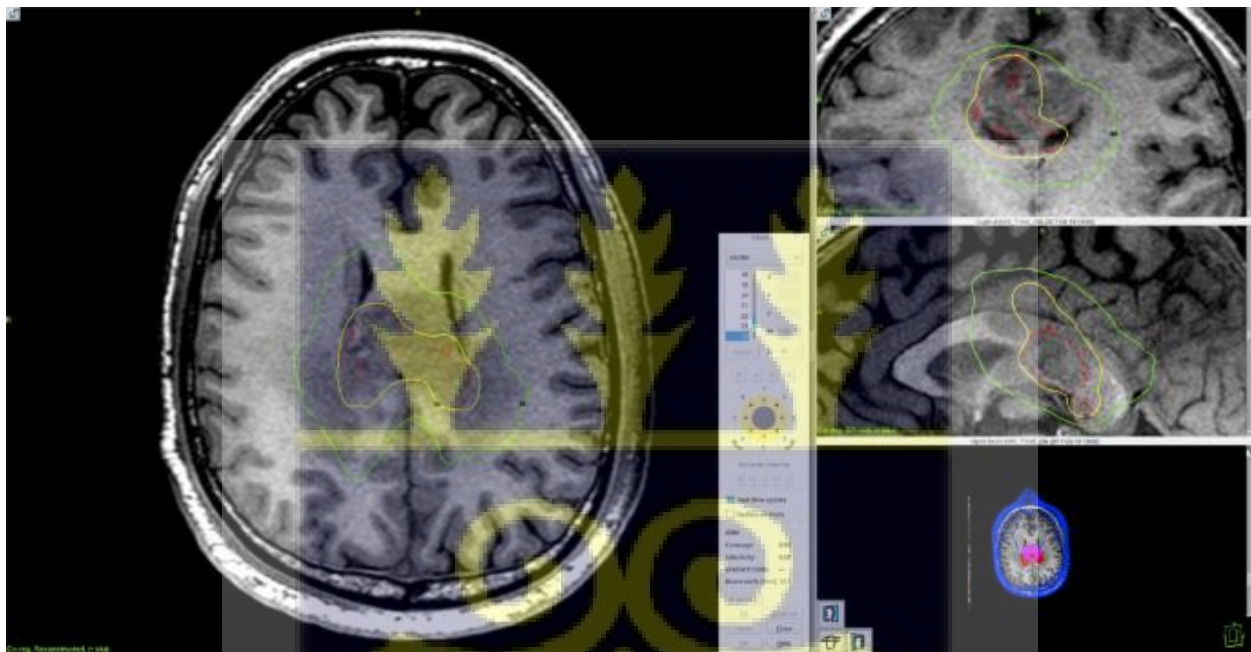


Figure 6: Margin addition in Gamma Knife treatment planning for single brain metastasis

1.3.3 Factors Influencing PTV Margin

Several factors could influence the choice of the optimal PTV margin, which can be roughly divided into clinical, stereotactic, and more purely physical parameters. The first aspect is based on pathoanatomical and dosimetric considerations that are specific for different pathologies. This is mainly true in the so-called multi-metastatic procedures (Kirkpatrick *et al.*, 2015). Other clinical parameters depend on patient tolerability, which is indeed related

not only to individual anatomic and dosimetric factors, but also to the technical details of the planning, including isocentre coordinates in the LINAC frame. In particular, it is important to consider a fixed or individually specified factor. However, neglecting further pathoanatomical considerations, a possible scenario for optimization in the choice of the PTV margin might be to link the PTV margin to the extremely small volume of the target, further attenuating wherever possible the dose reduction by prescribing the lower isodose available. In a radiosurgical context, prescribing a dose lower than the critical threshold for the single lesion could mean that the tumor can remain finally untouched even at follow-up imaging, which is generally rejected in the international community of radio-neurosurgeons (Bayman *et al.*, 2010; Noël *et al.*, 2003).

The most stereotactic aspect depends on functional parameters, such as distance from critical structures, admittance of off-isocentre non-coplanar beams, reproducibility of patient positioning and setup. The most purely stereotactic factors include those based on the length of the path, the type of collimator, the definition of the isocentre on which it is possible to reconstruct the three oblique projections for radiological targeting. In summary these factors can be classified as follows:

- **Tumor Size and Location:** The size of the tumor significantly influences the margin applied. For smaller tumors (less than 1 cm), higher doses (22–25 Gy) can be prescribed, while larger tumors (2.5–3 cm) may receive lower doses (under 18 Gy) due to increased risk of toxicity (Combs *et al.*, 2021).
- **Treatment Technique:** The choice of treatment modality (e.g., Gamma Knife vs. LINAC-based systems) can affect margin decisions. Some institutions may apply a 1-2 mm margin when using LINAC systems, while others might opt for no margin at all in specific scenarios (Fiagbedzi, Hasford, and Tagoe, 2024).

- **Clinical Protocols:** Different clinical protocols and studies have suggested various margin use. For instance, the Van Herk Margin Formula (VHMF) has been identified as effective for maintaining normal tissue tolerances while ensuring target coverage, generally translating to a margin of just over 1 mm (Duggar *et al.*, 2022a).

1.3.4 Prescription Isodose in Radiosurgery

The prescription isodose refers to the percentage of maximum dose (D_{max}) in a three-dimensional treatment plan which sets the exact dose of radiation that will be delivered to the lesion or affected area (Xuyao *et al.*, 2020). According to the American Association of Physicists in Medicine (AAPM) TG-101 report, prescription isodose in radiosurgery is termed as the prescription dose isodose and is described as the percentage of maximum dose that is prescribed to a target. Other technical terms closely related to the prescription isodose include the hottest permitted isodose line and the maximum peripheral dose (Dai *et al.*, 2021). The prescription isodose lies between 50% and 100%, and a lower value is more frequently reported, which suggests a steep dose fall-off at the target periphery. In LINAC - based radiosurgery (LBRS), the prescription isodose is often chosen between 50% and 80% in order to spare organs at risk (OAR) and achieve good dose conformity, defined as the volume covered by the prescription dose divided by the volume of the planning target volume (PTV). There are dosimetric image analytic vectors centred on the dose-volume histogram (DVH) that can be used to predict response and toxicity. These may add weight to a decision about the suitability of a particular isodose line that may be patient specific when the tumor volume and location are considered. Thus, it is possible to optimize for both tumor volume

and critical structure avoidance volume as the prescription isodose line varies (Romano *et al.*, 2017; Zhao *et al.*, 2014).

The planning target volume (PTV) represents the volume of the tumor plus a margin for dosimetric uncertainty intended to ensure that 95% of the prescribed dose covers at least 99% of the tumor volume (Frederick *et al.*, 2022). The volume of the PTV is increased above the clinical target volume (CTV) mostly because of inter-fractional movements in combination with positioning uncertainties in the treatment plan for very small target volume with steep dose gradients. Since it is obvious that the PTV size cannot be smaller than the CTV size, the size of the CTV is of interest when aiming at reducing the planning target volume. The volume enclosed by this isodose's surface is called prescription target, and it is the planning target volume (PTV). This percentage is usually based on clinical guidelines and published data to maintain a favourable therapeutic profile with the objective of protecting the surrounding critical structures. The choice of the prescription should be a trade-off of taking into consideration the biological response of tumor and surrounding normal tissues (Sikdar *et al.*, 2024; Youssoufi *et al.*, 2021).

1.3.5 Clinical Considerations

The prescription isodose is typically selected empirically, based on the clinician's judgment of the desired treatment effect and the normal tissue tolerance at the margin of the target. It considers the physical, dosimetric, radiobiological, and treatment planning considerations. Practical constraints for prescription isodose include standardized local protocols in the treatment planning computer systems (Hellerbach *et al.*, 2022).

In practice, the prescription isodose is also a compromise influenced by elements such as clinical experience, lesion site, target volume size, previous irradiation, presence of surrounding critical structures and organs at risk (OAR), the importance of sparing them, the

active constraints in treatment margins, as well as treatment times for each patient (Zhao *et al.*, 2014).

1.4 Aim of the Study

To evaluate the influence of planning target volume margins and prescription isodose levels on the treatment planning of stereotactic radiosurgery treatments for single brain metastatic tumor on both the Gamma Knife and LINAC-based Systems respectively using the STEEV Phantom.

1.5 Specific Objectives

1. To determine dosimetrically the influence of different planning target volume (PTV) margins with various prescription isodose levels for stereotactic radiosurgery (SRS) of a single brain metastasis on the Gamma Knife Treatment Planning System.
2. To evaluate the impact of various Prescription Isodose levels using commonly used planning target volume margins in LINAC-Based SRS of single brain metastasis.
3. To validate the dosimetric accuracy of LINAC-based SRS Plans using the newly introduced wireless Delta 4 Phantom+ Device.
4. To undertake a survey to ascertain the opinions of some planning medical physicists with experience in SRS treatment planning on margin additions in the SRS treatment of single brain metastasis.
5. To determine the geographical distribution of radiotherapy machines for brain metastasis treatment in Africa and develop guidelines for the implementations of SRS program.

1.6 Statement of problem.

Brain metastasis is one of the most common intracranial tumors among cancer patients, occurring in 20-40% of cases during the course of their disease (Lauko *et al.*, 2020). In Africa, the second-largest and most populous continent with approximately 16% of the global population (Hasford *et al.*, 2020), the number of patients with metastatic brain cancer is projected to rise to more than 450,000 by 2030 (Hamdi *et al.*, 2021). A preliminary survey at the oncology department of Komfo Anokye Teaching Hospital in 2020 also revealed a high incidence of cancer and brain metastasis cases. The burden on patients is substantial, as symptomatic lesions cause headaches, seizures, sensory and visual disturbances, speech difficulty, and limb ataxia, with survival ranging from 2–3 months to over two years depending on clinical and treatment factors (Enrique *et al.*, 2019).

Currently, surgery and radiotherapy are the main treatment options for brain metastases. Radiotherapy may be delivered as whole-brain radiotherapy (WBRT), stereotactic radiosurgery (SRS), or both. In many African countries, including Ghana, only WBRT and surgery are commonly available (Ekpene *et al.*, 2018). Although WBRT enhances local control, it does not prolong overall survival (Velten *et al.*, 2021), and it is associated with significant neurocognitive sequelae. As a result, SRS has emerged as an alternative treatment paradigm, offering a single high-dose fraction of radiation targeted precisely at the lesion (Badiyan *et al.*, 2016; Hartgerink *et al.*, 2019). While Gamma Knife technology is considered the gold standard for SRS, its high cost, limits availability in low-resource settings. Recent advancements, however, allow SRS delivery using linear accelerators (LINACs), making the technique more feasible in low- and middle-income countries (Scobioala *et al.*, 2019; Vergalasova *et al.*, 2019).

Despite these advances, the optimal planning target volume (PTV) margin size and prescription isodose level in SRS for single brain metastases remain undefined. Gamma

Knife systems traditionally use no PTV margin, but there is considerable variation in margin selection and prescription isodose levels across treatment centres worldwide. PTV margins are critical for ensuring adequate tumor coverage while minimizing exposure to healthy tissues, as excessive margins increase toxicity and insufficient margins risk treatment failure (Grishchuk *et al.*, 2023; Kocher *et al.*, 2014). Similarly, prescription isodose levels strongly influence conformity, gradient, and sparing of adjacent structures (Zhao *et al.*, 2014). While Gamma Knife is often preferred for small lesion accuracy (Alongi *et al.*, 2016), modern LINAC systems employing advanced techniques such as volumetric modulated arc therapy (VMAT) are increasingly capable of comparable precision (Palmisciano *et al.*, 2022).

There is, however, a lack of comprehensive studies that systematically evaluate the impact of PTV margins and prescription isodose levels on treatment quality and outcomes for single brain metastasis, particularly in African contexts. Existing evidence in international literature is limited and inconclusive, and there is no consensus among experts or professional societies on the optimal parameters to maximize efficacy while minimizing toxicity. This gap underscores the urgent need for further investigation into the influence of PTV margins and prescription isodose levels in SRS. Addressing this problem will guide clinical decision-making, optimize treatment planning protocols, and support the safe implementation of SRS programs in resource-limited African settings.

1.6.1 Justification

Brain metastases represent a major clinical challenge due to their high incidence, significant morbidity, and limited survival outcomes. In Africa, the growing cancer burden coupled with restricted access to advanced treatment technologies heightens the need for optimized and resource-appropriate therapeutic strategies (Hamdi *et al.*, 2021; Hasford *et al.*, 2020). While stereotactic radiosurgery (SRS) has emerged as a superior alternative to whole-brain

radiotherapy (WBRT) in terms of local control and reduced neurocognitive sequelae (Badiyan *et al.*, 2016; Hartgerink *et al.*, 2019), its implementation across low- and middle-income countries remains limited. The introduction of linear accelerator (LINAC)–based SRS provides a cost-effective pathway for wider adoption in Africa, yet optimisation of planning parameters such as planning target volume (PTV) margins and prescription isodose levels is essential to ensure safe and effective treatment. Currently, there is no consensus on the optimal PTV margin or prescription isodose level for single brain metastasis treatment using SRS. Overly generous margins increase normal tissue exposure and the risk of radionecrosis, while insufficient margins risk undertreatment and local failure (Hellerbach *et al.*, 2022; Kocher *et al.*, 2014). Likewise, inappropriate selection of prescription isodose levels may compromise conformity and gradient indices, reducing both tumor control and normal tissue sparing. Given the variability in practice across Gamma Knife and LINAC-based systems (Alongi *et al.*, 2016; Palmisciano *et al.*, 2022), evidence-based guidance tailored to diverse resource settings is urgently required. This study is justified on three key grounds. First, it addresses an urgent clinical need by seeking to optimise dosimetric parameters that directly impact treatment efficacy and toxicity in patients with brain metastases. Second, it provides context-specific relevance by generating data that can inform SRS implementation protocols in Ghana and other African countries, where LINAC-based systems are more feasible than Gamma Knife. Third, it contributes to global knowledge by clarifying the influence of PTV margins and prescription isodose levels on treatment quality for single brain metastasis, thereby filling a critical gap in the international literature. By systematically evaluating these parameters, the study will offer practical recommendations for improving radiosurgery planning and delivery, with the potential to enhance therapeutic outcomes, reduce treatment-related toxicities, and guide safe adoption of SRS programs in resource-limited settings. This not only supports evidence-based clinical decision-making

but also aligns with broader global health efforts to reduce disparities in access to advanced cancer care.

1.7 Significance of the Study

Stereotactic radiosurgery (SRS) has revolutionised the management of brain metastases, offering a non-invasive form of treatment that delivers very high focused radiation to tumors while sparing surrounding healthy tissue. With brain metastases affecting a substantial portion of cancer patients, the ability to optimize treatment planning through precise and efficient delivery of radiation is critical for improving patient outcomes. However, despite the widespread adoption of SRS, some factors that directly influence treatment efficacy, such as planning target volume (PTV) margins and prescription isodose levels, remain areas of ongoing debate and investigation. This study seeks to fill key gaps in the understanding of these factors and their role in the treatment of single brain metastases, with a focus on Gamma Knife and LINAC-based systems.

Firstly, one of the study's aims is to assess the impact of different PTV margins and prescription isodose levels using both the Gamma Knife and LINAC-based systems. By doing so, it will address a significant clinical question: "How do variations in these parameters impact the precision and effectiveness of radiosurgery for a single brain metastasis"? Currently, there is limited data on how different approaches to margin and prescription dose selection affect treatment outcomes, and this research will provide essential evidence to guide medical physicists in optimizing treatment plans, reducing complications, and enhancing tumor control.

The introduction of advanced technologies such as the new Delta 4 Phantom+ device for dosimetric validation further emphasizes the study's significance. Accurate dose delivery is a cornerstone of radiosurgery, and the validation of LINAC-based plans with cutting-edge

equipment will enhance the credibility and reliability of treatment protocols. This will support the clinical adoption of more accurate and reliable LINAC-based treatments, complementing the established benefits of Gamma Knife systems. Moreover, this study will contribute by providing insights from experienced medical physicists on the role of margin additions in SRS planning. These expert opinions are critical for understanding real-world challenges and developing protocols that are both scientifically sound and clinically practical. Beyond the technical aspects, the study will explore the geographical distribution and use of SRS systems in Africa, a continent where access to advanced cancer treatment technologies remains limited. By examining the availability and utilization of SRS systems for brain metastasis treatment, this research will help identify disparities in access to care and provide a foundation for the development of guidelines aimed at expanding SRS programs across Africa. This has far-reaching implications, as it addresses not only the technical optimization of radiosurgery but also the global health challenge of equitable access to cancer care.

In a nutshell, the findings will have a direct impact on improving patient outcomes, enhancing treatment precision, and addressing disparities in access to life-saving technologies, making it a significant contribution to the field of radiosurgery and cancer treatment.

1.8 Organization of the Thesis

This thesis was arranged into five (5) chapters. Chapter One served as an introduction, providing the background of the research, including a clear statement of the research problem, significance, aim and specific objectives, scope.

In Chapter Two, a comprehensive literature review was conducted, encompassing relevant studies related to the research topic and objectives, such as brain metastasis, radiosurgery,

planning target volume margins, prescription isodose levels, the African situation with SRS, quality assurance for SRS, and finally introducing the new concept of artificial intelligence for SRS. Chapter Three focused on the materials and methods utilised, describing in detail each of the key materials and procedures used in the study. The fourth chapter was dedicated to the results and discussions, covering all aspects of the objectives outlined for this study. Finally, Chapter Five encompassed the conclusion and recommendations drawn from the research findings. References and appendices are presented after the last chapter. The references section presents the list of all the sources cited throughout the thesis, formatted and arranged according to the APA citation style.



CHAPTER TWO

LITERATURE REVIEW

2.0 Introduction

This chapter is centered on a thorough review of previous studies connected to the research topic and objectives.

2.1 History of Stereotactic Radiosurgery: Global Perspective and Its Development in Africa

Stereotactic radiosurgery (SRS) is a highly precise, non-invasive medical procedure that uses focused radiation beams to treat abnormalities in the brain. It was developed to provide an alternative to traditional surgical methods by targeting tumors and other disorders without the need for incisions. This innovation stems from advances in both neurosurgery and radiation therapy, allowing for the treatment of complex conditions such as brain tumors, arteriovenous malformations (AVMs), and functional disorders like trigeminal neuralgia (Guckenberger *et al.*, 2020).

SRS was first envisioned in 1949 by the Swedish neurosurgeon Lars Leksell, who introduced the term “radiosurgery”. Leksell's idea was to leverage imaging technologies combined with precise radiation to treat brain conditions with minimal invasiveness. He developed a stereotactic frame that enabled three-dimensional targeting of brain regions. This approach laid the foundation for the Gamma Knife system, which Leksell, together with physicist Börje Larsson, developed in the late 1960s. The Gamma Knife utilizes cobalt-60 radiation sources to treat intracranial disorders with unparalleled accuracy, revolutionizing how certain brain conditions are managed (Trifiletti *et al.*, 2023).

By the 1980s, the benefits of SRS had become evident, and its use spread beyond Sweden to North America, Europe, and Japan. This expansion was facilitated by advancements in medical imaging techniques such as MRI and CT scans, which improved the ability to visualize and target tumors accurately. The introduction of linear accelerator (LINAC-based)

systems in the late 1980s provided a significant alternative to the Gamma Knife, allowing for more flexibility in treating not only brain tumors but also extracranial tumors in other parts of the body. LINAC-based systems increased the global appeal of SRS, as they could be adapted for a wider range of conditions (Grishchuk *et al.*, 2023; McDonald *et al.*, 2023). While SRS became a standard treatment in many high-income nations, its adoption in low- and middle-income countries (LMICs), including those in Africa, has lagged behind. Several challenges have slowed this progress, including the high cost of the required medical equipment, limited access to specialized training for healthcare professionals, and underfunded healthcare systems. Despite these barriers, there has been a recent surge of interest and investment in advanced cancer care, including SRS, across Africa (Ordinario *et al.*, 2024).

South Africa has been a pioneer in implementing SRS on the African continent. Major cities like Johannesburg and Cape Town have installed Gamma Knife and LINAC -based systems, providing treatment to both local and international patients. These centers have demonstrated the potential of SRS in improving outcomes for brain tumors, especially in cases where conventional surgery is too risky (Fiagbedzi *et al.*, 2023).

Despite some efforts made by some countries, access to SRS in Africa remains highly centralized in a few urban centres. Patients in rural or underserved areas continue to face significant challenges in accessing advanced cancer treatments, including SRS. The cost of maintaining expensive equipment, ensuring stable power supplies, and recruiting specialized medical personnel with training in SRS delivery remain significant obstacles (Omotoso *et al.*, 2023).

Efforts to decentralize and expand access to radiotherapy across Africa are ongoing. International partnerships between African medical centres and institutions in Europe and North America have facilitated the training of healthcare professionals in advanced

radiotherapy techniques including SRS. These collaborations, along with charitable organizations and global health initiatives, are instrumental in setting up cancer treatment centres equipped with advanced radiation technology. African governments have also begun implementing healthcare policies aimed at improving cancer treatment infrastructure and training programs.

In Ghana, cancer treatment has seen improvements over recent years, but access to advanced therapies such as SRS is still limited. Although Ghana has invested in improving oncology services, most treatments remain concentrated in urban areas like Accra and Kumasi. The lack of specialized equipment and training, as well as high costs associated with establishing SRS centres, has hindered widespread implementation (van Heerden *et al.*, 2023). However, there is hope that through regional collaboration and international support, Ghana could eventually integrate SRS into its healthcare system. Organizations such as the Ghana Cancer Board, Ghana Atomic Energy Commission and international bodies like the International Atomic Energy Agency (IAEA), Mayo Clinic, and City Cancer Challenge Foundation are working towards improving cancer treatment access across the country.

Globally, SRS is now considered a gold standard for treating specific brain conditions, and its applications are expanding to include extracranial tumors. In high-income countries, the availability of advanced medical imaging, skilled personnel, and cutting-edge technology has allowed SRS to become a routine treatment for many cancer patients. However, the global disparity in access to SRS is stark, particularly in LMICs. There is a pressing need for continued international cooperation, investment in healthcare infrastructure, and training to ensure that life-saving technologies like SRS become more accessible to underserved populations worldwide (Trifiletti *et al.*, 2017).

In a nutshell, SRS has a rich history, beginning with its development in Sweden, and has become a vital tool in the treatment of complex medical conditions globally. While its

adoption in Africa, particularly in countries like South Africa and Egypt, marks a significant step forward, there is still much work to be done to improve access to SRS across the continent. The case of Ghana highlights the ongoing challenges faced by many African nations in adopting this advanced medical technology. However, with continued investment in healthcare infrastructure, training, and international partnerships, SRS has the potential to become a widely accessible treatment option across Africa, providing hope for patients with brain tumors and other serious conditions.

2.2 Margin Determination in Radiotherapy

Radiotherapy relies on two key principles: ensuring effective coverage of the target area while reducing radiation to nearby organs-at-risk (OARs). These goals often conflict when designing margins, where the aim is to deliver the intended radiation dose to the tumor while reducing the impact on healthy tissues. Achieving the right balance between these priorities helps limit side effects in normal tissues. However, geometric uncertainties during the treatment process pose challenges to delivering radiation with precision (Goldberg, Langer, and Shtern, 2024; Tsz and Li, 2014).

The clinical target volume (CTV) is determined by expanding the gross tumor volume (GTV), as identified through physician-led fusion and delineation techniques (refer to Figure 7) The planning target volume (PTV), in turn, is derived from the CTV, representing an additional geometric expansion. Determining the appropriate margin from the CTV to the PTV is critical, too large a margin risks unnecessary irradiation of healthy tissues, while too small a margin may result in inadequate dosing of the CTV. Consequently, researchers have developed margin formulas to estimate the safest expansion required (Grierson *et al.*, 2023).

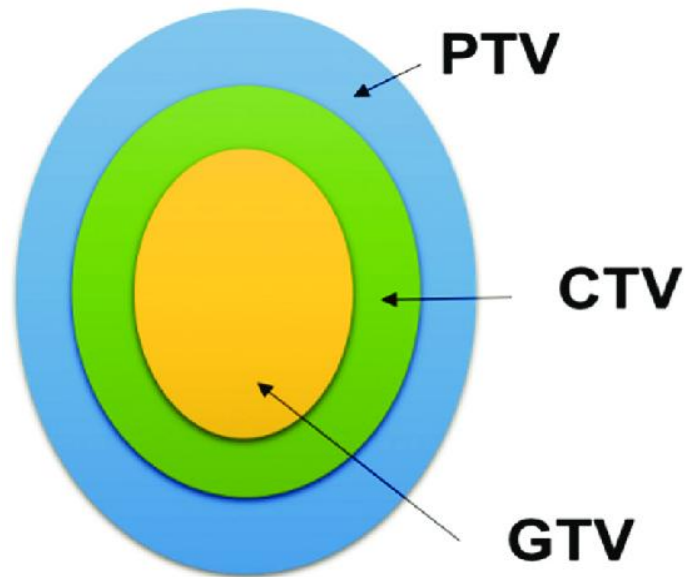


Figure 7: Illustration of margin expansion in standard radiation therapy. The gross tumor volume (GTV) is outlined by the radiation oncologist. The clinical target volume (CTV) accounts for sub-clinical disease and potential microscopic spread, while the planning target volume (PTV) compensates for geometric uncertainties during treatment delivery (Grierson *et al.*, 2023).

Conventional methodologies for calculating the planning target volume (PTV) margin (MPTV) assume that both systematic and random uncertainties are normally distributed and independent of each other. Random errors, or execution uncertainties, encompass inter-fractional variations such as daily shifts in patient setup or equipment alignment and intra-fractional variations, which include patient motion or movement of the gross tumor volume (GTV) or clinical target volume (CTV) during a single fraction. Systematic uncertainties arise during treatment preparation and include errors in patient positioning, organ motion during CT simulation, contouring inaccuracies, and equipment calibration errors (Robert *et al.*, 2023).

These uncertainties are typically modelled using a Gaussian distribution, a statistical tool for describing random variables that cluster around a central mean. This modelling approach is

grounded in the central limit theorem, which asserts that the sum of numerous random variables tends to approximate a normal distribution under mild conditions. Researchers widely agree that the cumulative effect of systematic and random uncertainties should be combined in quadrature (Dileep *et al.*, 2023).

Pioneering work by Bel *et al.* and Antolak *et al.* focused on deriving formulas to account for random uncertainties (denoted as σ) in margin expansion. These authors analysed the shrinkage of the high-dose region typically the 95% isodose line caused by random deviations. Their respective formulas for the PTV margin were $MPTV = 0.7\sigma$ (Bel *et al.*, 1996) and $MPTV = 1.65\sigma$ (Antolak & Rosen, 1999), where σ represents one standard deviation of random error. The Bel's (1996) approach aimed to ensure that 95% of the CTV receives the prescribed dose, though it may not guarantee uniform coverage across complex geometries. The margin of Antolak and Rosen (1999) being more expansive, ensures that the CTV edge resides within the PTV about 95% of the time, thus incorporating a larger dosimetric buffer. Both approaches assumed that systematic errors were negligible due to mitigation via quality assurance protocols and offline image-guided radiation therapy (IGRT) techniques. However, the exclusion of systematic uncertainties could result in an underestimation of required margins, particularly in intracranial targets where systematic deviations can displace the entire dose distribution (Antolak & Rosen, 1999).

Van Herk *et al.* (2000) advanced the field by segregating geometric uncertainties into their random (σ) and systematic (Σ) components in their widely adopted margin formula. The van Herk formula, expressed as $MPTV = 2.5\Sigma + 0.7\sigma$ remains a cornerstone in radiation oncology (Van Herk *et al.*, 2000). It provides a framework to systematically integrate both types of uncertainties into a single margin calculation. This formulation is based on probability density histograms and is frequently cited for its robustness in clinical

applications, ensuring that the entire CTV is covered with high probability while maintaining the desired dose conformity (Rojo-Santiago *et al.*, 2023).

In contemporary radiotherapy, precision in defining PTV margins is critical for ensuring optimal dose coverage of the CTV while minimizing the risk of radiation-induced toxicity to surrounding healthy tissues. The accurate determination of these margins is inherently linked to a deeper understanding of both random and systematic uncertainties.

Random uncertainties (σ) encompass unpredictable variations that can fluctuate daily, such as patient positioning or intra-fractional motion. These variations tend to be transient and non-cumulative. Systematic uncertainties (Σ), however, are persistent and consistent throughout the entire course of treatment. These include factors like initial errors in imaging or patient positioning during the planning phase. The weight assigned to systematic uncertainties in margin formulas is higher because their effects pervade each fraction, potentially shifting the entire dose distribution over the course of treatment (van Reenen *et al.*, 2023).

The use of quadrature to combine systematic and random uncertainties remains a fundamental approach in radiotherapy margin design. Systematic errors tend to shift the entire treatment volume, while random errors create variability in coverage across multiple fractions. By incorporating both sources of error using quadrature, modern margin formulas provide a more comprehensive estimate of the spatial buffer required to account for all treatment uncertainties (Sikdar *et al.*, 2024). The margin formula of Van Herk *et al.* (2000), $MPTV = 2.5\Sigma + 0.7\sigma$, has become the gold standard in margin calculation, particularly for high-precision techniques like volumetric modulated arc therapy (VMAT) and intensity-modulated radiation therapy (IMRT). This formula acknowledges that systematic uncertainties have a more profound impact on dose distribution than random uncertainties, justifying the 2.5 multiplier. The formula is widely utilized due to its proven efficacy in

ensuring CTV coverage, particularly in anatomical regions where high precision is required, such as in head-and-neck and brain tumors (Dileep *et al.*, 2023; Hurkmans *et al.*, 2001).

With the integration of advanced imaging modalities like 4D CT, cone-beam CT (CBCT), and MRI-guided radiotherapy, clinicians can now achieve real-time verification of patient anatomy and tumor positioning. This has significantly enhanced the ability to account for both intra- and inter-fractional variations. For instance, adaptive radiotherapy (ART) allows for the dynamic modification of treatment plans based on changes in tumor morphology and patient anatomy, potentially reducing the PTV margins without compromising tumor control probability (TCP) (Herrmann *et al.*, 2019). Image-guided radiation therapy (IGRT) has revolutionized the concept of margin design. Real-time imaging during treatment enables clinicians to track and correct for positional deviations, reducing the reliance on large PTV margins. Additionally, ART offers the potential for margin adaptation, where treatment plans are recalculated based on daily or even intra-fractional anatomical changes. These techniques hold particular promise for reducing radiation-induced toxicity, especially in sensitive structures such as the spinal cord, optic chiasm, or parotid glands (De Crevoisier *et al.*, 2022). In high-resource settings, where IGRT, ART, and stereotactic techniques like stereotactic body radiotherapy (SBRT) and stereotactic radiosurgery (SRS) are common, margin reduction is a key focus. These technologies enable smaller, more precise PTV margins by correcting for uncertainties in real-time. In low- and middle-income countries (LMICs), where access to advanced radiotherapy technologies is limited, more traditional approaches, like the Bel *et al.* (1996) and Antolak and Rosen (1999) formulas, might still be in use (Antolak & Rosen, 1999; Bel *et al.*, 1996). These formulas provide a conservative margin estimation to compensate for larger uncertainties in patient setup, imaging, and equipment calibration.

The calculation of cumulative dose distributions across patient populations, commonly known as dose-population histograms, plays a critical role in understanding the effects of systematic and random geometric deviations on the cumulative dose delivered to the clinical target volume (CTV). The margin formula used to expand the CTV to the planning target volume (PTV) heavily relies on the accuracy of the convolution method. However, this margin recipe is accompanied by a significant number of assumptions. These include the exclusion of biological parameters, the assumption of an infinite number of treatment fractions, its validity for only spherical targets, and the neglect of tumor distortions and shape changes. It also assumes that all uncertainties can be described as translational errors, that the patient population is homogeneous, and that the radiotherapy beam has a conformal penumbra. Furthermore, perfect concordance of the dose distribution with the target is presumed, which is rarely achievable in real-world clinical settings (Faruqi *et al.*, 2020; Zeng *et al.*, 2020).

When applied to intracranial targets, some of these assumptions hold, particularly for brain metastases. Brain metastases are generally spherical in shape, and the doses delivered during stereotactic radiation therapy (SRT) are highly conformal, providing near-perfect alignment between the dose and the target. However, stereotactic radiosurgery (SRS), which is often administered in a single fraction, challenges the conventional assumptions used in margin formulas. With advances in frameless immobilization devices, larger tumors are now treated using three-fraction regimens, further complicating the assumptions that underpin population-based margins over numerous fractions. The assumption of an infinite number of fractions becomes less applicable in hypo-fractionated treatments like SRS, which demands more refined margin models. These refined models must consider both systematic and random errors to properly address the uncertainties inherent in fewer treatment fractions (Lupattelli *et al.*, 2020; Miura *et al.*, 2023).

Stroom *et al.* (2003) developed an empirical margin formula that accounts for both systematic and random uncertainties: $MPTV = 2\Sigma + 0.7\sigma$ (Stroom *et al.*, 2002) This formula is similar to the one analytically derived by van Herk but focuses more on separating the effects of systematic and random errors on the probability of adequate coverage of the CTV. The formula of Stroom *et al.* (2002) is designed to ensure that 95% of the CTV receives the prescribed dose with 99% confidence. However, for small targets, particularly those with diameters less than two standard deviations of the deviation distribution, the margin formula becomes less effective. This issue is common in SRT, where smaller target volumes often result in a higher probability of the CTV extending beyond the PTV. Geometric uncertainties also cause significant “blurring” in narrow CTV regions, further complicating dose delivery. Nonetheless, the formula ensures 95% dose coverage for 99% of the CTV, with only minor variations compared to the original formula of van Herk’s (Bernstein *et al.*, 2021; Gupta *et al.*, 2014; Leszczyńska *et al.*, 2017).

McKenzie *et al.* (2002) sought to clarify the margin formula of van Herk’s by focusing on the contribution of random errors. In their investigation, they determined that the original formula ($1.64 \times (\sigma - \sigma_p)$) did not fully account for random setup errors or organ motion uncertainties during treatment, particularly in multi-beam configurations. Multi-beam setups, such as those used in volumetric modulated arc therapy (VMAT) or intensity-modulated radiation therapy (IMRT), tend to reduce the blurring effect at the target edges, which in turn reduces the margin size required to account for geometric uncertainties. To address this, McKenzie and colleagues introduced a coefficient (β) to quantify the extent of dose blurring, a value that was found to be relatively insensitive to the target shape (McKenzie *et al.*, 2002). However, even this revised formula allowed for some degree of imperfect conformity between the dose and the target. This issue is particularly relevant in SRS for brain metastases, where beam arrangements and dose conformity require further

investigation. SRS treatments often use numerous cobalt-60 beamlets, as seen in the Gamma Knife, which delivers a highly conformal dose with a sharp drop-off. The challenge lies in ensuring that the margin formula accurately reflects these unique treatment parameters while maintaining precise dose delivery to minimize damage to surrounding healthy tissue (Ludmir, Grosshans, and Woodhouse, 2018).

Parker et al. (2002) developed a margin formula for stereotactic treatment over 14 fractions using the GTC frame based on Monte Carlo simulations for a single patient. The margin recipe they derived, $MPTV = \Sigma + \sqrt{(\sigma^2 + \Sigma^2)}$, was specifically for intracranial lesions and was designed to ensure, with 99% confidence, that the clinical target volume (CTV) receives 95% of the prescribed PTV dose. The formula was applicable to both 5 and 30-fraction treatment regimens. However, since the simulation was performed on only one patient, the margin requires further validation before being generalized to other patients (Parker, 2002; Youssoufi *et al.*, 2021).

2.3 Margin in SRS

There has been a growing interest in refining planning target volume (PTV) margins for stereotactic radiosurgery (SRS) and stereotactic radiation therapy (SRT). Traditional fractionation formulas may not be suitable for single or hypo-fractionated treatment schedules because the impacts of systematic and random setup errors differ from those observed in conventional treatment schedules. Zhang *et al.* (2016) aimed to establish PTV margins specifically for single fraction SRS cases. They observed that, in a single fraction treatment, both systematic and random errors affect the dose distribution similarly (Zhang *et al.*, 2016). Their estimates assumed a non-zero mean for the errors, incorporating machine-specific systematic uncertainties. The derived formula was developed mathematically, utilizing polynomial functions to calculate coefficients. However, without incorporating

patient-specific data, assessing the formula's validity is challenging. Additionally, the applicability of this formula is limited, as it was only validated for the specific machines used in their study. Herschtal *et al.* (2013) defined hypo-fractionated treatment as consisting of five or fewer treatment fractions and proposed an algorithm to calculate lower limit PTV margins for such regimens. The upper limit was determined using the previously validated Van Herk formula (Herschtal *et al.*, 2013). They utilized Monte Carlo simulations to create artificial displacement data for 10,000 hypothetical patients, establishing dose population histograms based on various systematic and random uncertainties. This formula relies on four key parameters: random error, systematic error, penumbral width, and the number of fractions. However, since the simulations did not include actual patient data or dose distributions and the algorithm assumed perfectly spherical treatment targets, its applicability may be constrained due to variations in target shapes and distributions among real patients. In conclusion, while conventional radiotherapy PTV margin formulas are available in the literature, the methods and criteria used to derive them are not directly applicable to SRS or hypo-fractionated SRT. Recent attempts to optimize margin formulas for the SRS/SRT population do have limitations and may not be widely applicable. This is understandable, considering that the concept of margins is relatively new for SRS, which has traditionally been performed without PTV margins to accommodate patient positioning errors or intrafraction motion. Empirically derived margins of 1 mm and 2 mm have been noted in the literature, although these carry the risks of missing the target or inadvertently overdosing surrounding organs at risk (Mesko *et al.*, 2020; Yoda, 2017). In the context of frameless fractionated treatments, SRT planning must take movement effects into account. Given that the risk to adjacent critical structures is higher with SRT, an ideal margin formula should recognize the importance of both target coverage and the avoidance of critical structures (Schmitt *et al.*, 2020).

2.4 The SRS Process

2.4.1 Immobilization and Localization

The goal of stereotactic radiosurgery is to deliver higher dose, maintain accuracy and precision while ensuring that the patient is stabilized during the treatment. Two basic conditions are required for this procedure: i) immobilization of the patient and ii) verification of the exact position of the tumor. In order to achieve these conditions, a trained physician can use either a conventional technique which is a fixed frame or an image-based frame. (Minniti *et al.*, 2015). The use of a frame also solves two important issues: first, it eliminates the chance of head movement, and second, it sets up an external reference point that coordinates the internal structures of the brain (Leybovich, 2002).

Before an imaging procedure is performed, a localization box, which is made of N-shaped fiducial rods, is attached to the head frame. This allows the physician to determine the coordinates of the internal structures of the patient. Stereotactic frames are very accurate and reliable for treating intracranial tumors, but they are not practical for patients if treatment is carried with longer fractionated regime as in SBRT (Solberg *et al.*, 2008). Due to the recent advancements in image guidance systems, a new approach known as frameless stereotactic mask (SRS) has been used in many clinics. This method involves the use of a non-invasive mask to immobilize a patient. With this method, the uncertainty in the patient's movement within the mask can be reduced by up to 1 mm (Park, Choi, and Jang, 2021). In order to visualize the tumor in the isocentre, in-room imaging techniques are used. These techniques are performed by taking images of the patient and comparing them with 6 digital reconstructions of the same image. The Digitally Reconstructed Radiographs (DRRs) are used to reference the images of the patient in the planned position (Dimitriadis and Paddick, 2018). In comparison with conventional such as the use of immobilization devices (figure 8)

as techniques, frameless SRS is more convenient to the patients and is able to deliver similar accuracy (Belcher *et al.*, 2017; Hartgerink *et al.*, 2019).

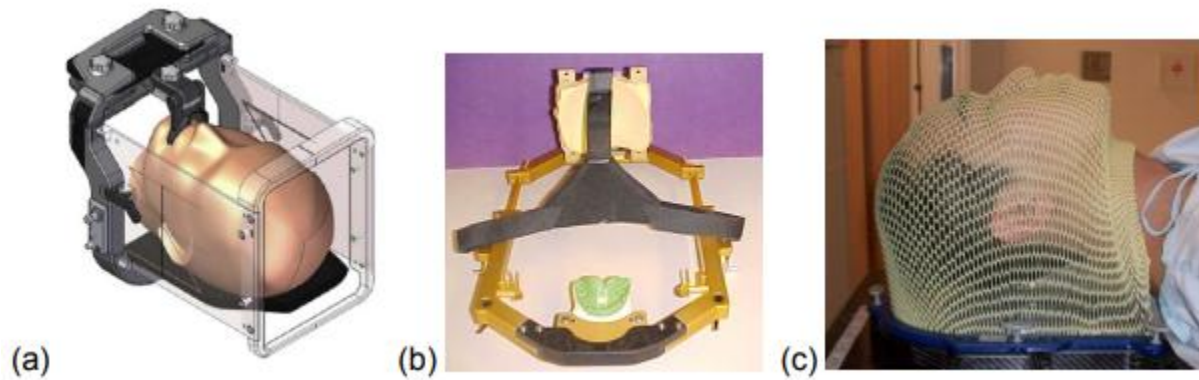


Figure 8: Immobilization Devices (a) Illustration of a relocatable head frame with the stereotactic localizer box attached. (b) Gill-Thomas-Cosman frame. (c) Thermoplastic mask (Lupattelli *et al.*, 2020).

2.4.2 Imaging for Stereotactic Radiosurgery Planning

Imaging modalities mostly used in stereotactic radiosurgery are (a) computed tomography (CT), (b) magnetic resonance imaging (MRI) and (c) digital subtraction angiography (DSA)

(a) CT

CT offers detailed images of a patient by adjusting various slice thicknesses. A localization box equipped with CT fiducial rods is utilized to ascertain the coordinates of a tumor. The process of acquiring CT images relies on the principle that various structures exhibit distinct attenuation coefficients when exposed to an incident low-energy X-ray beam. A CT scan not only reveals the internal anatomy but also offers insights into the electron density of various imaged tissues. This information may be utilized to implement the necessary corrections for heterogeneity in dose calculations (Brook *et al.*, 2015). A CT scan can effectively

differentiate between bony structures and healthy brain tissue, but it offers limited contrast when distinguishing between normal tissue and a tumor, as both exhibit similar attenuation properties. However, MRI and DSA demonstrate excellent tissue anatomy with DSA providing demonstration of vessel involvement in imaging tumor (Zhang *et al.*, 2021).

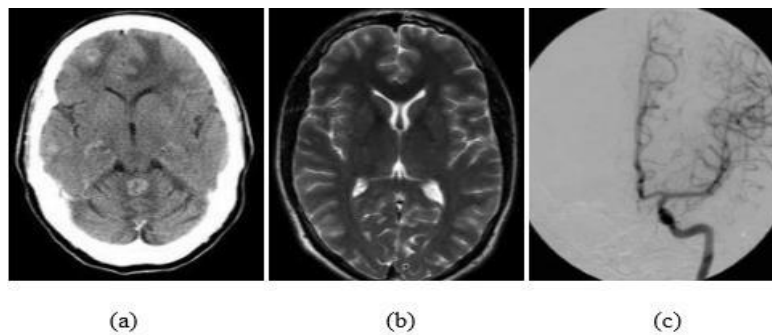


Figure 9: CT (a), MRI (b) and DSA (c) (Zhang *et al.*, 2021).

(b)MRI

The MRI technique leverages the nuclear spin characteristics of numerous hydrogen atoms found within the human body to generate an image. MRI generally provides enhanced differentiation between tumors and adjacent healthy tissues compared to CT scans. (Putz *et al.*, 2020). The MRI technique presents several technical challenges, including a relatively lengthy image acquisition time of approximately 30 minutes, and it lacks the ability to provide information regarding electron density (Patel *et al.*, 2011).

2.4.3 Delivery Modalities

Three distinct forms of ionising radiation or particles are utilised in SRS treatment: gamma rays, megavoltage x-rays, and charged particles (Skourou *et al.*, 2021). Stereotactic radiosurgery (SRS) employs various modalities, each with distinct advantages tailored to specific clinical situations. These modalities include Gamma Knife, linear accelerator

(LINAC-based) systems, tomotherapy, cyberknife proton beam therapy, and heavy ion therapy (carbon ion therapy).

2.4.3.1 LINAC -based Systems

LINAC-based stereotactic radiosurgery (SRS) systems utilize linear accelerators (LINACs) to deliver precise, high doses of radiation to tumors, particularly in the brain. These systems have become increasingly popular due to their versatility, precision, and ability to treat a variety of conditions without the need for invasive procedures. LINAC-based SRS systems offer high precision in targeting tumors, utilizing advanced imaging techniques and treatment planning software. These systems often incorporate advanced beam-shaping technologies such as multi-leaf collimators (MLCs) and circular cones. MLCs allow for dynamic shaping of the radiation beam to conform closely to the tumor's shape, enhancing dose delivery. Unlike traditional methods that require rigid head frames for patient immobilization, many modern LINAC-based SRS systems offer frameless options. This approach improves patient comfort and reduces setup time while maintaining treatment accuracy. Advanced imaging capabilities such as cone-beam computed tomography (CBCT) are integrated into these systems, allowing for real-time verification of patient positioning before and during treatment. Various manufacturers have developed distinct systems utilizing LINAC technology for stereotactic radiosurgery, including Novalis from BrainLab in Heimstetten, Germany, Trilogy, Truebeam, Edge from Varian in Palo Alto, CA, USA, X-knife from Radionics in Burlington, MA, USA, and Elekta HD Versa, all of which are currently in clinical use (Knisely and Apuzzo, 2019; Skourou *et al.*, 2021). Figure 10 below shows a LINAC-based system.



Figure 10: LINAC -based System for SRS (Skourou *et al.*, 2021)

2.4.3.2 Tomotherapy

This combines the principles of computed tomography (CT) with intensity-modulated radiation therapy (IMRT). This innovative technique allows for correct tumor targeting. Tomotherapy utilizes a helical delivery method, where a thin radiation beam is modulated as it rotates around the patient. This continuous motion allows for the treatment of large volumes without the need for field abutting, resulting in a more even distribution of the dose. Tomotherapy can be used for SRS and for conventional radiotherapy. The treatment field's length can be adjusted using collimator jaws, allowing for both small and large treatment areas to be targeted effectively (Saw *et al.*, 2018). Figure 11 below presents a picture of a tomotherapy machine for SRS.

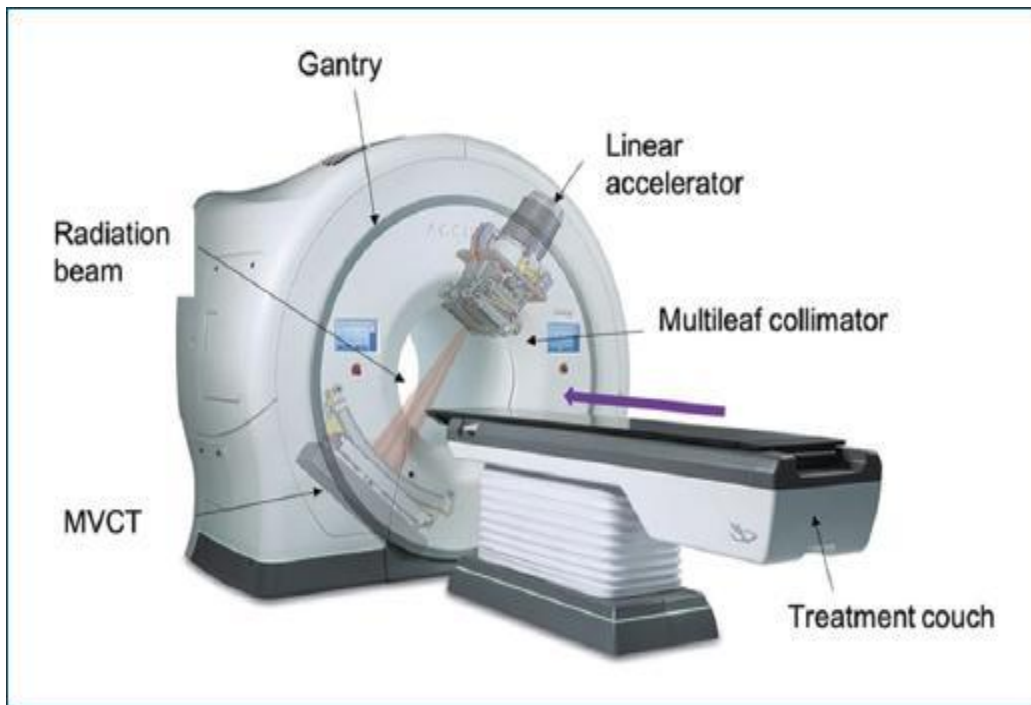


Figure 11: A Tomotherapy Machine for SRS (Skourou *et al.*, 2021)

2.4.3.3 Cyber Knife

The Cyber Knife system is a state-of-the-art robotic radiation therapy system designed for the precise delivery of high-dose radiation. It is made up of a lightweight linear accelerator affixed on a robotic arm, allowing for flexible positioning and treatment angles. This design enables it to reach tumors in hard-to-access areas. CyberKnife utilizes real-time imaging technology to track tumor movement during treatment. This capability ensures that radiation beams are correctly aligned with the tumor, accommodating any patient movement, such as breathing (Schmitt *et al.*, 2020; Skourou *et al.*, 2021). Figure 12 below presents the image of the CyberKnife system





Figure 12: A Cyberknife System (Skourou *et al.*, 2021)

2.4.3.4 Gamma Knife

The Gamma Knife modality uses 60 Co sources. These devices typically address just intracranial lesions and may use either fixed or spinning sources. This device employs 201 60Co sources configured in a half hemisphere around the patient's head to provide a volume of radiation to the targeted region. The individual sources are stationary, and their distinct “beamlets” simultaneously irradiate the tumor; thus, instead of generating a dose volume through a series of sequential exposures as a LINAC-based system does, the GK administers its dose as a continuous volume throughout the entire treatment (Duggar *et al.*, 2022a). The outside of the treatment unit has 43 cm of cast iron for the external shielding of the 60Co sources. Each source comprises 20 60Co pellets encased inside a capsule constructed of double-walled stainless steel. Each capsule is inserted into a numerically indexed aluminium bushing, and the cap is affixed by screwing it on. The bushings are introduced through the machines outside shell and positioned at the outermost end of the principal collimating channels. The final collimators include circular apertures that generate discrete beams with full width at half maximum dimensions of 4, 8, 14, or 18 mm at the mechanical iso-centre of

the GK unit. The configuration of 201 distinct beamlets produces a singular dosage distribution. Imagining a full spherical shell of uniformly dispersed sources would provide a dosage volume that forms a sphere at the iso-centre of the shell. Utilizing a single hemisphere of sources would provide a dosage distribution in the shape of a hemisphere (Skourou *et al.*, 2021). Figure 13 below shows the image of a Gamma Knife system for SRS.

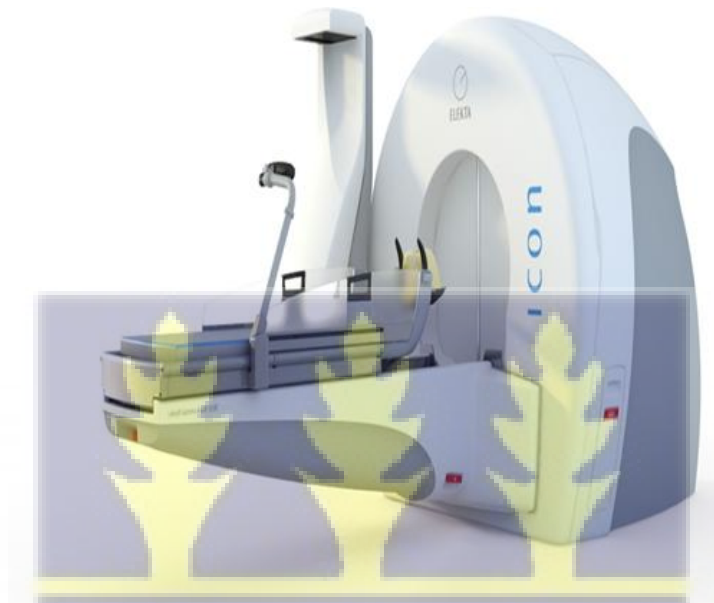


Figure 13: Image of the Gamma Knife System for SRS (Skourou *et al.*, 2021)

2.4.3.5 The Zap-X System

Zap-X is an innovative radiosurgery system designed for the precise treatment of tumors and other abnormalities in the brain and body. It combines advanced imaging technology with a compact design to deliver high doses of radiation with exceptional accuracy utilizes a robotic arm to deliver radiation therapy, allowing for flexible positioning and precise targeting of tumors. This robotic capability enhances the system's ability to adapt to patient movements during treatment. The system integrates advanced imaging modalities, to provide real-time visualization of the tumor and surrounding tissues. This capability ensures accurate targeting

and alignment throughout the treatment process. Unlike traditional linear accelerators that require large treatment rooms, Zap-X features a compact design that can fit into smaller clinical spaces, making it accessible for various healthcare facilities (The ZAP-X® Gyroscopic Radiosurgery System, 2022). Figure 14 below presents the image of the Zap-X System.



Figure 14: The Zap-X System (The ZAP-X® Gyroscopic Radiosurgery System, 2022.)

2.4.4 Treatment Planning

The main requirement of SRS treatment planning is to deliver the highest dose to the tumor while minimizing the dose to the surrounding healthy tissues (Clark *et al.*, 2012). Some of the common treatment planning systems include Monaco, Accuray's CyberKnife System, Eclipse, Element, and GammaPlan.

Several stages are involved in the planning of SRS treatment, as outlined below:

2.4.4.1 Localization and imaging

The initial phase of SRS treatment involves identifying the coordinates of the tumor in relation to an external frame of reference. Upon arrival at the clinic, a skilled physician

carefully affixes a stereotactic head frame to the patient's skull. A localization box is utilized to ascertain the coordinates of the tumor in relation to the reference frame established by the head frame. Subsequently, the individual proceeds with the imaging procedure (CT/MRI/DSA) (Scobioala *et al.*, 2019).

2.4.4.2 Image Import and Contouring

Upon completion of the imaging, data is sent to a treatment planning station (TPS). In the TPS, all CT image slices are localized, indicating that the fiducials of the localizer box are identified to establish the coordinate system used for planning. Image fusion is conducted to use other imaging modalities, such as MRI. The subsequent phase involves contouring, during which a physician delineates the target and the organs at risk (OAR) structures on the imaging slices (Velten *et al.*, 2021). The Gamma Knife treatment procedure typically involves administering a mild sedative to ensure the patient remains comfortable and relaxed during the process, along with local anaesthesia applied at the sites where the head pins are placed. During the application of the frame, attention is focused on positioning the specific region of the brain intended for treatment at the centre. This procedure is implemented to reduce the likelihood of needing to detach and subsequently reattach the head frame, as the treatment position may not be attainable within the limits of the GK helmet. During frameless LINAC-based planning, the patient receives CT simulation a few days before treatment, and a custom mask is created. Plans based on LINAC necessitate a CT, thus the patient's previous MRI must be integrated with the simulation CT (Han *et al.*, 2020).

2.4.4.3 Prescription and Planning

After delineating the target and organs at risk, a radiosurgery plan can be created. The prescribed dose for solitary brain metastases is primarily based on the size of the target.

Typically, the doses are 24 Gy for lesions under 20 mm in diameter, 18 Gy for those between 21-30 mm, 15 Gy for lesions ranging from 31-41 mm, and 12 Gy for lesions smaller than 10 mm, as recommended by the RTOG.(Simon *et al.*, 2022; Y. Xu *et al.*, 2019).

Techniques utilizing LINAC with circular collimators generate spherical dose distributions. A multiple iso-centre technique should be employed for irregularly shaped tumors, where spherical distributions are combined or arranged to encompass the target effectively. The outcome of sphere packing leads to an elevated maximum dose as a result of the overlap in spherical distributions. Consequently, in these instances, the prescribed isodose line typically represents 50% of the maximum dosage. LINAC's that are outfitted with MLCs can effectively address irregular targets using a single iso-centre, typically delivering a dose that is around 80% of the maximum dose prescribed. After the physician prescribes the dosage, a treatment plan can be formulated. Treatment strategies can be approached through two distinct methodologies: planning or inverse planning. In forward planning, the planner establishes the necessary parameters, including beam size, beam arrangement and beam weights. The planner subsequently engages in a systematic process of refining the initially established parameters to enhance the dose distribution. The effectiveness of forward planning is significantly influenced by the user's experience in planning. In inverse planning, treatment objectives are established, and an optimization algorithm computes the various parameters (such as beam intensity modulation and field size) necessary to achieve the defined planning objectives as closely as possible. Currently, the majority of planning systems incorporate algorithms designed for inverse planning (Eaton *et al.*, 2018). In the case of the Gamma Knife, it is observed that when single-shot dose plans are implemented, the peripheral dose tends to be positioned at a higher isodose line compared to multiple-shot dose plans. It is crucial to emphasize that this does not inherently indicate that the dose reduction is more pronounced for a single-shot plan compared to a multiple shot plan. This

phenomenon arises from the normalization of the dose to the maximum level, where multiple shot plans create a concentrated area in regions of overlapping shots, leading to a reduced isodose line at the edges. A single shot exhibits the most pronounced dose decline in three dimensions at an isodose level ranging from 50 to 70%. (Xu *et al.*, 2019).

2.4.5 Patient Specific QA

Unlike Gamma Knife systems, which do not necessitate any patient-specific quality assurance before the delivery of an approved treatment plan, LINAC-based systems do require patient-specific quality assurances. This procedure may require significant effort and attention to detail. This can be accomplished using various patient specific QA tools.

2.4.6 Patient Positioning and Plan Delivery

After the appropriate treatment plan is chosen and authorized, the subsequent step is to administer care to the patient. Proper positioning of the patient is essential for the effectiveness of SRS treatment. There are two distinct methods to achieve the required positional accuracy in SRS treatment: 1) Employing stereotactic frames or 2) Utilizing frameless SRS. In a standard SRS procedure, a stereotactic frame is utilized for the precise positioning of the patient. The coordinates of the individual's internal anatomy established during the imaging process are utilised for positioning the patient (Tanaka *et al.*, 2020). The coordinates of the tumor are utilized to align its location with the machine's iso-centre. The individual is secured to the treatment table, and printouts from the treatment planning system indicating the position of the iso-centre are obtained. The printouts are securely attached to the frame/localizer, and the patient is positioned in alignment with the isocentre indicated on the printouts. In frameless SRS treatments, various imaging techniques such as planar orthogonal images, stereoscopic in-room x-ray images, and cone-beam CT are employed for

precise patient positioning. Once the individual is positioned on the treatment couch with mask immobilization, images are captured using on-board imaging techniques and matched with previously generated images from a treatment planning system. Computer algorithms automatically overlay the images and determine any necessary adjustments in patient positioning. During the treatment process with GK, verification is not conducted. In upcoming GK models, a cone-beam computed tomography (CBCT) system is incorporated to ensure accurate patient positioning verification (Bolten *et al.*, 2023).

2.5 PTV Margins in Gamma Knife Stereotactic Radiosurgery for Single Brain Metastasis

In stereotactic radiosurgery (SRS), planning target volume (PTV) margins play a critical role in accounting for uncertainties, such as patient movement, setup errors, and variations in tumor delineation. This is especially true in systems like Gamma Knife, known for its sub-millimeter precision and the rigid immobilization it provides via a stereotactic head frame. The Gamma Knife's precision allows clinicians to apply very small, or in some cases, zero-millimeter PTV margins. However, these small margins become crucial in determining the dose distribution to both the tumor and adjacent healthy tissues. According to Juloori *et al.* (2023) even minor deviations from the planned target can impact the efficacy of dose delivery and possibly compromise surrounding healthy tissue (Juloori *et al.*, 2023). This precision is paramount in Gamma Knife radiosurgery, where many small radiation beams converge on a target with high spatial accuracy (Kutuk *et al.*, 2022).

What sets Gamma Knife apart from other radiotherapy systems is the lack of internal organ movement, such as breathing, which can complicate dose delivery. Instead, the head frame provides robust immobilization, reducing the need for larger PTV margins. This distinguishes Gamma Knife SRS from systems like LINAC-based treatments, where intrafraction motion and setup errors are more prominent (Callens *et al.*, 2024). However, despite these

advantages, minimizing PTV margins introduces dosimetric challenges, particularly in irregularly shaped lesions or those near critical structures. Belcher *et al.* (2017) observed that using minimal PTV margins can sometimes lead to underdosing at the tumor's periphery, particularly if the prescription isodose level is not properly optimized. This issue is critical when small or irregular tumors require precision in dose delivery (Belcher *et al.*, 2017). The PTV margin's primary role is to compensate for geometric uncertainties between planned and delivered doses. These uncertainties could arise from minor variations in tumor delineation, patient setup, or even microscopic tumor extensions not easily detectable through imaging (Sadeghi *et al.*, 2021). However, the rigid immobilization and advanced imaging technology associated with Gamma Knife SRS mitigate many of these uncertainties, enabling the use of small or zero-millimeter PTV margins. Nonetheless, this precision is contingent on the prescription isodose level applied during the treatment.

2.6 Prescription Isodose Levels in Gamma Knife SRS and Their Impact on Dose Distribution

The prescription isodose level in Gamma Knife SRS is a key parameter that defines how the radiation dose is distributed within the tumor and its surrounding tissues. This parameter is essentially the percentage of the maximum radiation dose that is delivered to the edge of the tumor volume. In most brain metastasis treatments using Gamma Knife, common prescription isodose levels range between 50 and 70% (Shiue *et al.*, 2014). This means that the tumor receives the prescribed dose at an isodose line representing 50-70% of the maximum dose delivered by the Gamma Knife system. The remainder of the dose, the maximum, is concentrated at the centre of the tumor. Lower isodose levels, such as 50%, allow for steeper dose gradients and tighter confinement of radiation to the target, sparing more of the surrounding healthy brain tissue. Higher levels, such as 70%, result in a more

gradual fall-off of dose, distributing more radiation across a larger volume, which can be advantageous in ensuring full tumor coverage but risks exposing more healthy tissue to radiation (Biasi *et al.*, 2018).

Gamma Knife's ability to deliver highly focused radiation with sub-millimeter accuracy allows for very precise control over how and where the radiation is deposited. This precision is especially vital when treating tumors found close to critical organs, such as the optic nerves or brainstem, as it minimizes the chances of radiation-induced damage to these vital areas. The choice of the prescription isodose level is a balance between providing an effective dose to the entire tumor while minimizing radiation exposure to healthy tissue (Ruschin *et al.*, 2020).

Lower isodose levels, such as 50%, create a steep dose gradient, meaning that radiation levels drop rapidly outside the target volume. This steep gradient is particularly advantageous in situations where the tumor is adjacent to critical structures such as the optic chiasm, brainstem, or other organs-at-risk (OARs). This steep gradient ensures that these structures receive minimal radiation exposure. The high level of dose conformity associated with lower isodose levels is one of the defining advantages of Gamma Knife SRS, especially when precision is paramount (Palorini *et al.*, 2019).

However, there are challenges associated with using such steep gradients. Palorini *et al.* (2019) point out that when small PTV margins are combined with lower prescription isodose levels, there is an increased risk of underdosing the tumor's periphery (Palorini *et al.*, 2019). This can be particularly problematic in the case of irregularly shaped tumors or tumors that have microscopic extensions not easily captured in imaging. In such scenarios, the sharp dose fall-off could mean that some parts of the tumor might not receive the full therapeutic dose, leading to potential treatment failure or tumor recurrence. This is why treatment

planning with lower isodose levels must be carefully optimized to ensure comprehensive tumor coverage, particularly for lesions near critical brain structures (Gevaert *et al.*, 2017). Higher prescription isodose levels, such as 70%, spread the radiation dose more evenly across a larger volume. This results in a less steep dose fall-off outside the tumor, meaning that more surrounding tissue is exposed to radiation but with reduced intensity. This can help prevent underdosing at the tumor's edge, particularly for tumors with irregular shapes or for cases where precision targeting may be more challenging. For instance, if a tumor has multiple lobes or an asymmetric structure, a higher isodose level may ensure that all parts of the tumor receive an adequate therapeutic dose (Piedade, 2019).

The selection of the prescription isodose level in Gamma Knife SRS is influenced by several factors, including the tumor's location, shape, size, and closeness to critical structures. For tumors near sensitive organs like the brainstem, optic apparatus, or other OARs, lower isodose levels with minimal PTV margins are often preferred. This combination allows for a steep dose gradient that minimizes the radiation delivered to these critical areas while still concentrating the maximum dose on the tumor itself (Romano *et al.*, 2017).

On the other hand, for tumors located in areas of the brain that are less critical or distant from OARs, clinicians may opt for higher prescription isodose levels. These cases allow for more generous PTV margins to ensure comprehensive tumor coverage without the same level of concern for sparing critical structures. The key is to tailor the treatment plan to the specific needs of the patient, the characteristics of the tumor, and the surrounding anatomy (Pagett *et al.*, 2022). Studies, such as those conducted by Cilla *et al.* (2022) show that a flexible approach that adjusts the isodose level and PTV margins based on the clinical context is crucial to optimizing both tumor control and patient safety (Cilla *et al.*, 2022).

This approach emphasizes the importance of individualized treatment planning in Gamma Knife SRS. The ability to adjust the prescription isodose level and PTV margins allows

clinicians to precisely control the dose distribution, optimizing the therapeutic efficacy while minimizing the risk of complications. It also highlights the need for close partnerships between radiation oncologists, medical physicists, radiation therapists, and neurosurgeons in the planning and delivery of SRS treatments. In summary, the prescription isodose level is a critical factor that shapes the overall success of Gamma Knife SRS treatments. Lower isodose levels provide tighter dose control, which is crucial for protecting sensitive structures, while higher levels ensure better tumor coverage, particularly for irregularly shaped tumors. However, both approaches have associated risks, including potential underdosing of the tumor periphery with lower isodose levels or increased exposure of healthy tissue with higher levels. The careful selection of the prescription isodose level, combined with appropriate PTV margins, is essential to achieving the optimal balance between maximizing the therapeutic dose to the tumor and minimizing the risk to adjacent healthy tissues. Clinicians must evaluate each case individually, considering both the tumor's characteristics and its anatomical context within the brain. By doing so, they can ensure that the patient receives the most effective and safe treatment possible. This flexible, patient-specific approach underscores the precision and versatility of Gamma Knife SRS, which has become a standard of care for treating brain metastases and other complex intracranial lesions.

2.7 Interplay Between PTV Margins and Prescription Isodose Levels in Tumor Control and Toxicity

The interplay between PTV (planning target volume) margins and prescription isodose levels in SRS (stereotactic radiosurgery) is crucial for achieving the delicate balance between effective tumor control and minimizing radiation-induced side effects (Piedade, 2019). PTV margins define the buffer area around the tumor to account for uncertainties in tumor

positioning, while the prescription isodose level defines the percentage of the maximum dose delivered to the tumor's edge (Wilson, 2013). In Gamma Knife SRS, the steep dose gradients allow for precise irradiation of the tumor, but this precision comes with a challenge. Small margins and high dose conformity are beneficial for protecting surrounding healthy tissues, but they may also result in underdosing the tumor periphery, especially for irregularly shaped tumors or those with diffuse borders (Topkan *et al.*, 2021). This underdosing compromises local tumor control, as regions of the tumor may not receive sufficient radiation. Conversely, expanding the margins too much to avoid underdosing can expose healthy brain tissues to higher doses, increasing the risk of side effects like radionecrosis (radiation-induced tissue death) or cognitive impairments. These opposing effects necessitate careful planning to ensure the best outcome (El Shafie *et al.*, 2020). Sahgal *et al.* (2017) conducted an in-depth analysis of how varying PTV margins affect the dosimetric outcomes in Gamma Knife SRS. Their study highlighted that smaller margins combined with lower prescription isodose levels, such as 50%, result in high conformity indices. A conformity index measures how the radiation dose closely conforms to the shape of the tumor. While high conformity ensures that most of the dose is concentrated within the tumor, the potential downside is underdosing the tumor edges, especially when the tumor has an irregular geometry (Sahgal *et al.*, 2017). This is a common concern in SRS, where the precision of targeting is paramount, but positional uncertainties cannot be entirely eliminated. Even with the sub-millimeter accuracy of the Gamma Knife system, irregular tumor shapes or slight shifts in patient positioning can result in parts of the tumor being missed, particularly at the margins. The gradient index (GI) and conformity index (CI) are critical metrics used to assess the quality of an SRS treatment plan.

The GI measures how quickly the radiation dose falls off outside the target area, and the CI evaluates how well the radiation dose conforms to the tumor's shape. In plans where smaller

PTV margins are used with lower prescription isodose levels, the resulting treatment often shows a higher CI, meaning the dose is tightly confined to the tumor with minimal exposure to surrounding healthy tissue. However, this also results in steeper dose gradients, which can increase the risk of marginal misses especially in cases where there are uncertainties in target positioning or when dealing with tumors that have complex or irregular shapes (Simon *et al.*, 2022). A study observed that higher prescription isodose levels offer a more gradual dose fall-off, leading to lower GI values. While this reduces the risk of underdosing the tumor's periphery, it can also compromise the conformity of the dose to the target if the margins are not appropriately adjusted. This trade-off between GI and CI is a central challenge in SRS planning, requiring careful consideration of each patient's tumor characteristics and anatomical context. In clinical practice, the decision-making process surrounding PTV margins, isodose levels, conformity, and gradient indices is complex and must be individualized (Patel *et al.*, 2020). Several factors influence these choices, including the tumor's size, location, shape, and proximity to critical structures. Additionally, patient-specific factors, such as prior radiation treatments and overall brain health, are also important considerations. For example, a patient with prior brain radiation may have more limited tolerance for additional radiation exposure to healthy tissues, necessitating tighter margins and lower isodose levels (Milano *et al.*, 2021). As SRS technologies continue to advance, the ability to fine-tune dosimetric variables like the GI and CI will improve. Innovations in imaging, treatment delivery, and patient positioning are all expected to contribute to more precise and personalized treatment plans, allowing clinicians to optimize the balance between tumor control and minimizing toxicity. These advancements highlight the importance of continual research and refinement in the field of stereotactic radiosurgery, as more precise, targeted therapies will further improve patient outcomes while reducing the risks of adverse effects (Patel *et al.*, 2020).

2.8 Technological Advances and Clinical Implications for PTV Margins and Prescription Isodose Levels in Gamma Knife SRS

Technological advancements in Gamma Knife SRS have greatly enhanced the precision of treatments, particularly through improvements in imaging and treatment planning. High-resolution imaging technologies, like computed tomography (CT) and magnetic resonance imaging (MRI) have reformed the ability to precisely delineate tumor boundaries. This enhanced precision has a direct impact on PTV margins, which are typically used as a buffer to account for uncertainties in target localization. Previously, larger PTV margins were necessary to ensure the entire tumor was irradiated, especially in cases of irregularly shaped or hard-to-define tumors ((Safain *et al.*, 2014). However, with modern high-resolution imaging, the accuracy of tumor identification has significantly improved, reducing the need for large margins. This reduction allows for more targeted treatments that focus radiation on the tumor while sparing surrounding healthy tissues. Additionally, advancements in treatment planning algorithms have further improved the ability to model dose distributions with a high level of accuracy. These sophisticated algorithms enable the creation of highly conformal treatment plans, allowing clinicians to achieve a delicate balance between delivering an effective dose to the tumor and minimizing radiation exposure to nearby critical structures (Beaton *et al.*, 2019).

In addition to advances in imaging and treatment planning, the integration of automated quality assurance (QA) systems and real-time imaging during Gamma Knife procedures has significantly improved the precision of treatment delivery. For example, systems like the Gamma Knife Icon incorporate on-board cone-beam CT imaging, which provides real-time verification of patient positioning during treatment. This real-time feedback allows clinicians to monitor and adjust patient positioning to ensure that the tumor remains precisely targeted

throughout the procedure, even accounting for slight movements or positional shifts (Manna, 2023). This ability to perform real-time verification has been instrumental in further reducing the need for large PTV margins, as uncertainties related to patient movement are minimized. These systems have contributed to the development of more consistent and reliable treatment protocols, providing clinicians with the confidence to use smaller PTV margins without compromising the accuracy or efficacy of the treatment (Han *et al.*, 2020). Furthermore, these technological advancements have offered greater flexibility in selecting the appropriate prescription isodose levels based on individual clinical scenarios, allowing for a more tailored approach to treatment planning. The clinical implications of optimizing PTV margins and prescription isodose levels are profound, particularly in terms of reducing the side effects associated with Gamma Knife SRS while maintaining or improving tumor control. By minimizing the radiation exposure to healthy brain tissue, the risk of adverse effects, such as cognitive impairments, radionecrosis, and neuroendocrine dysfunction, is significantly reduced. Cognitive impairment, in particular, is a common concern in brain radiosurgery, as radiation exposure to critical brain structures can result in long-term neurocognitive deficits (Rahman *et al.*, 2020). Similarly, radionecrosis, which is the radiation-induced death of healthy brain tissue, can cause serious complications if too much surrounding tissue is exposed to high doses of radiation. Optimizing treatment plans to minimize PTV margins and use appropriate prescription isodose levels help reduce these risks, allowing for a more favourable therapeutic ratio. Additionally, ensuring that the entire tumor receives adequate radiation doses improves local control rates, which is critical for preventing tumor recurrence and improving overall survival outcomes, particularly in patients with a single brain metastasis (Dimitriadis and Paddick, 2018).

As research and technological advancements in Gamma Knife SRS continue to evolve, the focus remains on maximizing the therapeutic ratio achieving the highest possible tumor

control while minimizing the risk of toxicity. The ability to fine-tune PTV margins and prescription isodose levels based on the individual characteristics of the tumor and patient anatomy has become a cornerstone of modern radiosurgical treatment planning (Soliman *et al.*, 2016). This approach allows clinicians to tailor treatments to each patient's unique clinical situation, improving outcomes while minimizing the risk of side effects. Continued research into the dosimetric nuances of Gamma Knife SRS, particularly in terms of optimizing the gradient and conformity indices, will further enhance the ability to deliver highly personalized and effective treatments for brain metastases and other intracranial lesions. These ongoing advancements promise to improve both the safety and efficacy of Gamma Knife SRS, ensuring that patients get the best possible care with minimal risk of complications. These advancements are reshaping the clinical landscape for Gamma Knife radiosurgery, offering new opportunities to refine and personalize treatment, ultimately aiming to improve patient outcomes by maintaining effective tumor control and reducing treatment-related toxicity (Cheok *et al.*, 2023).

2.9 LINAC -Based SRS and Prescription Isodose Levels

LINAC-based stereotactic radiosurgery (SRS) is a crucial modality in the management of brain metastases, offering precise, high-dose radiation delivery in a single or limited number of fractions. This modality is characterized by its ability to deliver a highly conformal dose to the target while minimizing exposure to surrounding healthy tissue. The flexibility inherent in LINAC-based systems allows clinicians to adjust key parameters, such as the prescription isodose level, enabling customization of treatment to suit specific clinical requirements. Prescription isodose levels define the percentage of the maximum dose delivered to the tumor boundary, influencing both the dose conformity and the sparing of adjacent critical structures (Hartgerink *et al.*, 2019).

The prescription isodose level plays a critical role in determining the distribution of radiation within the tumor and the surrounding tissue, particularly the dose gradient, which refers to how quickly the radiation dose decreases outside the tumor. A higher prescription isodose level, such as 90%, ensures that the prescribed therapeutic dose is delivered at the tumor's boundary while concentrating the maximum dose in the tumor's core (Sung and Choi, 2018). This distribution creates a steep dose fall-off beyond the tumor's edge, which is essential for protecting nearby healthy tissues and critical structures, such as the brainstem, optic chiasm, or other radiosensitive organs. The steeper the dose gradient, the more abruptly the radiation decreases, which is crucial when tumors are located near sensitive areas (Stojkovski *et al.*, 2017). Pacelli *et al.* (2019) emphasize the benefits of this approach for small, regularly shaped tumors located in critical regions where excessive radiation exposure could lead to severe side effects. By ensuring that only the tumor receives high doses of radiation while sparing adjacent tissues, the steep dose gradient enhances tumor control and reduces the risk of collateral damage, making it a preferred strategy in radiosurgery for tumors near vital structures (Pacelli *et al.*, 2019).

In addition to the ability to manipulate prescription isodose levels, LINAC-based SRS offers clinical flexibility, particularly through its use of frameless immobilization systems. Traditional systems, such as Gamma Knife, often rely on rigid, frame-based immobilization, which can be uncomfortable for patients and increases the complexity of the setup (Alongi *et al.*, 2016). In contrast, frameless systems simplify the treatment process while maintaining a high level of positional accuracy. These systems use advanced imaging techniques, such as cone-beam CT, to ensure that the patient remains in the correct position throughout the procedure, without the need for invasive head frames. This reduction in setup complexity makes LINAC-based SRS more patient-friendly, allowing for easier treatment planning and execution while preserving the precision necessary for effective radiosurgery. This flexibility

makes LINAC-based systems an attractive option for patients with tumors in challenging or sensitive locations, as it minimizes patient discomfort while ensuring accurate treatment delivery (Seravalli *et al.*, 2015).

Despite the flexibility and advancements of LINAC-based SRS, challenges remain, particularly in balancing dose conformity with the management of setup uncertainties and intrafraction motion (movement that occurs during the treatment session) (Romanelli and Beltramo, 2022). Dose conformity refers to how well the radiation dose matches the shape and size of the tumor. While a high degree of conformity is desirable to avoid irradiating healthy tissues, any misalignment or motion during treatment can lead to underdosing or overdosing certain areas. This is especially problematic for irregularly shaped tumors or tumors located in regions prone to movement. Underdosing the tumor can result in poor tumor control, while overdosing healthy tissues can cause unnecessary side effects. Continuous advancements in motion management techniques are crucial for ensuring that the radiation is delivered accurately. Modern motion management strategies often incorporate real-time imaging, such as cone-beam computed tomography (CBCT) and optical surface monitoring, which track the patient's position during treatment. These technologies allow for adjustments to be made in real-time, reducing the risk of treatment errors caused by patient motion.

The integration of real-time imaging systems, such as CBCT and optical surface monitoring, has greatly enhanced the accuracy of treatment delivery in LINAC -based SRS. These imaging technologies allow clinicians to monitor the patient's position and adjust during the treatment session to account for any movement, ensuring that the radiation is accurately targeted at the tumor throughout the procedure (Paoletti *et al.*, 2022). Elbanna *et al.* (2021) highlight that such advancements are key to maintaining a high therapeutic ratio, where the benefits of tumor control outweigh the risks of toxicity. The use of real-time imaging not

only helps mitigate the effects of intrafraction motion but also improves the overall reliability of SRS treatments. By integrating these technologies into routine practice, clinicians can ensure that even the most challenging cases, such as tumors near radiosensitive areas or irregularly shaped tumors, are treated with precision and care. As these technologies continue to evolve, the ability to deliver highly conformal, safe, and effective treatments will improve, further advancing the field of stereotactic radiosurgery (Elbanna *et al.*, 2021).

2.10 Impact of Higher Prescription Isodose Levels on Dose Conformity and Tumor Control

The utilization of higher prescription isodose levels, typically ranging from 80 to 90%, in LINAC-based stereotactic radiosurgery (SRS) has garnered significant attention due to its profound impact on dose conformity, tumor control, and sparing of surrounding healthy brain tissue. The prescription isodose level determines the percentage of the maximum dose delivered to the edge of the planning target volume (PTV), influencing how radiation is distributed both within and beyond the tumor (Zhao *et al.*, 2014). Higher isodose levels concentrate the prescribed dose tightly around the tumor, leading to sharper dose gradients and improved conformity, which is crucial when treating small, well-defined brain metastases. This heightened conformity has been found to reduce the volume of healthy brain tissue exposed to intermediate radiation doses, thereby lowering the risk of radiation-induced toxicities such as radionecrosis, cognitive decline, and other long-term neurological deficits (Scaringi *et al.*, 2018).

Hanna *et al.* highlighted that employing a prescription isodose level of 90% in LINAC-based SRS produces highly conformal dose distributions, meaning the high-dose region closely follows the shape of the tumor, with minimal spillage into adjacent normal tissues. This characteristic is particularly advantageous in cases where the metastasis is located near

critical structures, such as the brainstem or optic nerves, as the steep dose fall-off helps minimize radiation exposure to these radiosensitive areas (Hanna *et al.*, 2019).

Moreover, the conformity index (CI), which quantifies how well the radiation dose conforms to the target volume, is significantly improved when higher isodose levels are used. Uchinami *et al.* reported that the CI is notably higher with a 90% prescription isodose level compared to lower levels such as 70% (Uchinami *et al.*, 2021). Improved conformity not only enhances tumor control but also reduces the incidence of complications related to the irradiation of surrounding normal brain tissue, particularly in patients with small, spherical metastases (Chambrelant *et al.*, 2023). One of the primary advantages of higher prescription isodose levels is their ability to improve local tumor control. By concentrating the dose more effectively within the target, higher isodose levels ensure that the tumor receives a sufficiently high dose, which is crucial for achieving long-term local control. The increased dose conformity ensures that the tumor margins receive the prescribed therapeutic dose, which is vital for preventing tumor recurrence or progression. Higher prescription isodose levels are especially beneficial when treating metastases located in radiosensitive regions of the brain, as they limit the dose delivered to surrounding healthy tissues while maintaining the therapeutic efficacy at the tumor site (Soltys *et al.*, 2021).

Despite the clear benefits of higher prescription isodose levels in terms of conformity and tumor control, there are inherent challenges associated with their use, particularly in cases involving irregularly shaped metastases or when there are uncertainties related to tumor positioning and patient setup. One of the key concerns is the steep dose fall-off associated with higher isodose levels. While this steep gradient is beneficial for sparing healthy tissue, it can also be a double-edged sword, as it increases the risk of underdosing at the tumor periphery. This is particularly problematic in cases of irregularly shaped metastases, where the tumor margins may not receive an adequate dose if the plan is too conformal. This issue

was highlighted by Tsz *et al.* (2014) who emphasized that the sharp dose gradient associated with higher isodose levels may be less forgiving of small deviations in tumor positioning, such as those caused by intrafraction motion or setup variability (Tsz and Li, 2014).

In frameless SRS setups, which are commonly used in LINAC-based systems, intrafraction motion and setup inaccuracies can introduce uncertainties in the precise location of the tumor during treatment. Frameless systems rely on image-guided radiotherapy (IGRT) for patient positioning, but small movements during treatment may still occur, leading to a misalignment between the planned and actual target positions. When higher prescription isodose levels are used, these uncertainties become more critical, as the steep dose fall-off may result in marginal misses, where parts of the tumor receive suboptimal doses. This is particularly concerning for tumors with irregular boundaries or diffuse edges, where the prescribed dose may not fully cover the tumor margin, potentially compromising local control.

The choice of prescription isodose level must therefore be carefully tailored to the specific clinical context. While higher isodose levels offer superior dose conformity and tumor control, they may not be appropriate in all cases, particularly for patients with irregularly shaped tumors or those with a higher risk of motion during treatment. In such cases, a lower isodose level with a more gradual dose fall-off may provide more robust coverage of the tumor margins, reducing the risk of marginal underdosing. Clinicians must weigh the benefits of enhanced conformity against the risks of marginal misses and consider factors such as tumor geometry, patient anatomy, and the likelihood of intrafraction motion when selecting the optimal prescription isodose level (Hellerbach *et al.*, 2022; Shiue *et al.*, 2014).

2.11 Comparative Analysis of Lower Prescription Isodose Levels and Clinical Trade-offs

Lower prescription isodose levels, such as 60 or 70%, result in a broader distribution of radiation, which creates a more gradual dose fall-off from the tumor to the surrounding tissue.

This wider spread ensures that the tumor, especially its periphery, receives sufficient radiation, reducing the risk of missing parts of the tumor, known as marginal misses. While this approach enhances tumor coverage, the broader dose distribution comes at the cost of reduced conformity. In other words, the radiation dose does not conform as tightly to the tumor's shape, meaning that a larger volume of normal tissue is exposed to radiation. This trade-off is particularly concerning for patients with larger brain metastases or multiple lesions, where the cumulative dose to healthy brain tissue can lead to significant side effects. Such side effects include cognitive decline, neuroendocrine dysfunction, or radionecrosis (Saenz *et al.*, 2020). In larger metastases, the delicate balance between tumor control and minimizing damage to surrounding tissues becomes even more crucial; choosing isodose level a critical decision in treatment planning (Mukherji, 2018).

Vergalaso *et al.* (2019) conducted a comparative study on the effects of using 60 versus 90% prescription isodose levels in LINAC-based SRS. Their findings revealed that lower isodose levels, like 60%, provided broader tumor coverage but at the expense of lower dose conformity. In practical terms, this means that while the radiation is more likely to cover the entire tumor, including areas that might otherwise be underdosed, it also irradiates a larger volume of healthy tissue. This broader dose distribution can be advantageous for tumors with irregular shapes or diffuse borders, where precise targeting might be more difficult. However, the downside is the exposure of non-target tissues to radiation, which can lead to increased side effects. The study of Vergalaso *et al.* (2019) showed that the gradient index (GI), which reflects how quickly the dose decreases beyond the tumor, was higher for lower isodose levels. A higher GI indicates that the dose fall-off is more gradual, meaning that surrounding tissues receive more radiation than they would with higher isodose levels. This makes lower isodose levels particularly useful when there are concerns about positional

uncertainties during treatment, ensuring that the entire tumor is adequately treated even if there is some movement (Vergalasova *et al.*, 2019).

Despite the challenges associated with lower isodose levels, there are clinical scenarios where they can be beneficial. Specifically, when brain metastases are located away from critical structures, such as the optic nerves and brainstem, clinicians can afford to adopt a more aggressive treatment approach without risking significant damage to these vital areas. In such cases, the gradual dose fall-off associated with lower isodose levels can provide robust tumor coverage while minimizing the risk of missing parts of the tumor. For instance, in tumors with irregular shapes or where precise targeting is difficult, using a lower isodose level allows for a broader safety margin in terms of dose delivery. This ensures that the tumor is effectively irradiated, even if there are slight deviations in targeting during the treatment process. However, the increased radiation exposure to normal brain tissue raises the likelihood of long-term complications, especially in patients who are expected to survive longer or who may require additional radiation therapy in the future (Minniti *et al.*, 2021).

The decision to use lower prescription isodose levels in SRS must be carefully considered, based on both the potential benefits and risks. While lower isodose levels may improve tumor coverage, particularly for irregularly shaped lesions, they also increase the risk of irradiating normal tissues, leading to late-onset complications such as neurocognitive decline or radionecrosis. Risks are particularly pronounced in patients with longer life expectancies or those undergoing multiple radiation treatments. The increased exposure to radiation can result in delayed side effects that may not become apparent until months or even years after treatment. Therefore, patient-specific factors such as the size, shape, and location of the tumor, as well as the patient's overall health and prior treatment history, must be carefully weighed when selecting the appropriate isodose level. In cases where the tumor is located near critical structures or in patients with long-term survival prospects, higher isodose levels

with tighter conformity might be preferred to minimize the risk of side effects (Chan *et al.*, 2018; Jhaveri *et al.*, 2019).

2.12 The Role of PTV Margins in LINAC -Based SRS

Planning target volume (PTV) margins are an essential consideration in LINAC-based SRS, as they account for uncertainties related to patient positioning, tumor motion, and setup variability. In contrast to Gamma Knife SRS, which uses rigid stereotactic immobilization, LINAC -based SRS often employs frameless systems, making PTV margins critical for ensuring that the prescribed dose adequately covers the tumor. The flexibility of LINAC-based systems allows for the adjustment of both PTV margins and prescription isodose levels, enabling personalized treatment planning (Duan *et al.*, 2019).

Faruqi *et al.* (2020) emphasized that higher prescription isodose levels, such as 90%, necessitate the use of larger PTV margins to ensure robust tumor coverage. This is because the steep dose gradient associated with higher isodose levels makes the plan more sensitive to small positional uncertainties or intrafraction motion. For instance, even slight shifts in the patient's position during treatment can result in portions of the tumor receiving less than the prescribed dose, potentially compromising local control. Therefore, when using higher isodose levels, it is often necessary to expand the PTV margin to provide a buffer against these uncertainties, ensuring that the entire tumor is adequately covered (Faruqi *et al.*, 2020). Conversely, lower prescription isodose levels produce a more gradual dose fall-off, which allows for the use of smaller PTV margins without risking tumor underdosing. This broader dose distribution is less sensitive to positional uncertainties, making lower isodose levels more appropriate for tumors with irregular shapes or in cases where setup variability is a concern. As highlighted smaller PTV margins help to reduce the volume of healthy brain tissue exposed to intermediate doses of radiation, thus minimizing the risk of radiation-

induced complications. However, the trade-off is a less conformal dose distribution, which may result in higher doses being delivered to normal tissues surrounding the tumor. The decision on PTV margin size should be guided by a combination of clinical factors, including tumor characteristics, patient anatomy, and the specific goals of treatment (Navarria *et al.*, 2018). As Minniti *et al.* (2020) noted, larger margins are generally recommended for tumors located near critical structures, as they provide additional coverage to account for setup uncertainties. On the other hand, smaller margins may be preferred in cases where minimizing radiation exposure to healthy tissue is a priority, particularly for patients with longer life expectancies or those who have previously received radiation therapy (Minniti *et al.*, 2020; Navarria *et al.*, 2018).

2.13 Clinical Implications and Decision-Making in LINAC-Based SRS for Brain Metastasis

The choice of prescription isodose levels and PTV margins in LINAC -based SRS is a highly individualized decision that must consider both the technical capabilities of the treatment system and the specific clinical scenario. As highlighted by Faruqi *et al.* (2020) higher isodose levels provide superior conformity and reduce the risk of radiation-induced toxicity to normal tissues, but they also require careful attention to PTV margins and setup accuracy. In contrast, lower isodose levels offer greater flexibility in terms of tumor coverage and positional uncertainties but may increase the risk of side effects due to the irradiation of larger volumes of normal brain tissue (Faruqi *et al.*, 2020).

Recent advances in image-guided radiotherapy (IGRT) and adaptive radiotherapy have further improved the precision of LINAC-based SRS, allowing for real-time adjustments to the treatment plan based on tumor motion or changes in patient anatomy (Hotca & Goodman, 2023). The integration of cone-beam CT (CBCT) and optical surface monitoring systems

enables more accurate positioning of the patient, reducing the need for large PTV margins and allowing for more aggressive treatment plans. These technologies are particularly useful for treating irregularly shaped tumors or tumors located near critical structures, as they provide real-time feedback on the tumor's position during treatment. Ultimately, the goal of LINAC-based SRS for brain metastasis is to maximize local control while minimizing the risk of radiation-induced complications. The choice of prescription isodose levels and PTV margins should be guided by the specific clinical scenario, with the aim of balancing dose conformity, tumor coverage, and the protection of healthy tissues. As research in this field continues to evolve, the development of more sophisticated treatment planning algorithms and real-time monitoring technologies will likely enable even greater precision in the delivery of high-dose radiation to brain metastases (Badloe *et al.*, 2021; Beaton *et al.*, 2019).

2.14 Quality Assurance in SRS

Routine quality assurance (QA) is essential for ensuring the accurate and safe delivery of radiotherapy, particularly when utilizing advanced techniques such as stereotactic radiosurgery (SRS) (Das *et al.*, 2022). The integration of patient-specific QA tools has become increasingly vital in this context, as these tools allow for meticulous customization of treatments based on individual patient characteristics and anatomical specifics.

2.15 Patient-Specific QA Devices for Stereotactic Radiosurgery (SRS)

Here are some key devices and methods used in patient-specific QA for SRS:

1. SRS MapCHECK

This device is a 2D diode array specifically designed for patient-specific QA in SRS and stereotactic body radiation therapy (SBRT). It Provides fast, film-less QA, eliminating the subjectivity associated with traditional film dosimetry. It is capable of measuring multiple

targets in one setup, enhancing efficiency. SRS MapCHECK offers high-resolution measurements that align closely with clinical treatment plans (Al-Basheer, *et al.*, 2023; Lee and Kim, 2021). Figure 15 below presents the image of SRS MapCHECK.



Figure 15: Image of the SRS MapCHECK (Lee and Kim, 2021)

2. *myQA SRS*

myOA SRS is a digital solution that combines the accuracy of film dosimetry with the efficiency of a digital detector array. It is fully compliant with TG-218 guidelines for SRS/SBRT. It supports QA in native plan geometry, including adjustments for non-coplanar beams. Integrates seamlessly with various treatment machines like Varian Halcyon and CyberKnife (James, Al-Basheer, *et al.*, 2023). Figure 16 below presents the image of the myOA SRS device.





Figure 16: Image of the myQA SRS(Al-Basheer, et al., 2023).

3. Arc CHECK

Arc CHECK is a 3D diode array used for comprehensive QA in SRS and SBRT treatments. The ArcCHECK can be compared with other devices, like SRS MapCHECK evaluate their effectiveness in patient-specific QA. While the Arc CHECK is used for QA in SRS and SBRT SRS MapCHECK, is usually the preferred choice in some clinical settings due to the relatively high average gamma passing rates (James, Al-Basheer, et al., 2023). Figure 17 below shows the image of the Arc CHECK.



Figure 17: Image of the Arc CHECK (Al-Basheer *et al.*, 2023)

4. StereoPHAN

This phantom is designed for end-to-end testing and QA in stereotactic procedures. It allows for easy setup across various tests without the need for tools, working with multiple detectors such as ion chambers and films (Sadowski *et al.*, 2022). Figure 18 below presents the image of the StereoPHAN phantom.

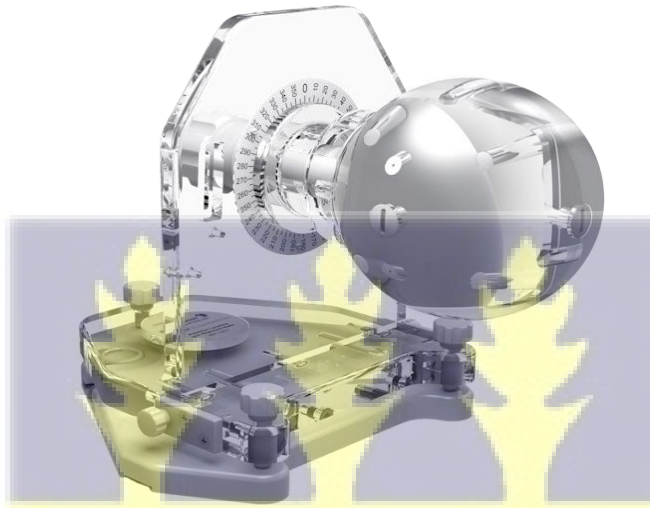


Figure 18: Image of the StereoPHAN (Sadowski *et al.*, 2022).

5. 3D Printed Patient-Specific Phantoms

Advances in 3D printing technology enable the creation of anatomically accurate phantoms based on individual patient CT data. These phantoms can be used alongside polymer gel dosimetry to provide a comprehensive evaluation of dose distributions tailored to each patient's anatomy (Makris *et al.*, 2019). Figure 19 presents Image of a 3D Printed Patient-Specific Phantom.



Figure 19: Image of a 3D Printed Patient-Specific Phantom (Makris *et al.*, 2019)

6. Dosimetry Detectors

These detectors are often placed within phantoms that simulate the patient's head to perform accurate dose measurements.

- Commonly used detectors include:
 - Small-volume ionization chambers
 - Dosimetry diodes
 - Microdiamond detectors
 - Electronic portal imaging devices (EPIDs) (Y. C. Lee & Kim, 2021)

Figure 20 below presents Image of a microdiamond detector.

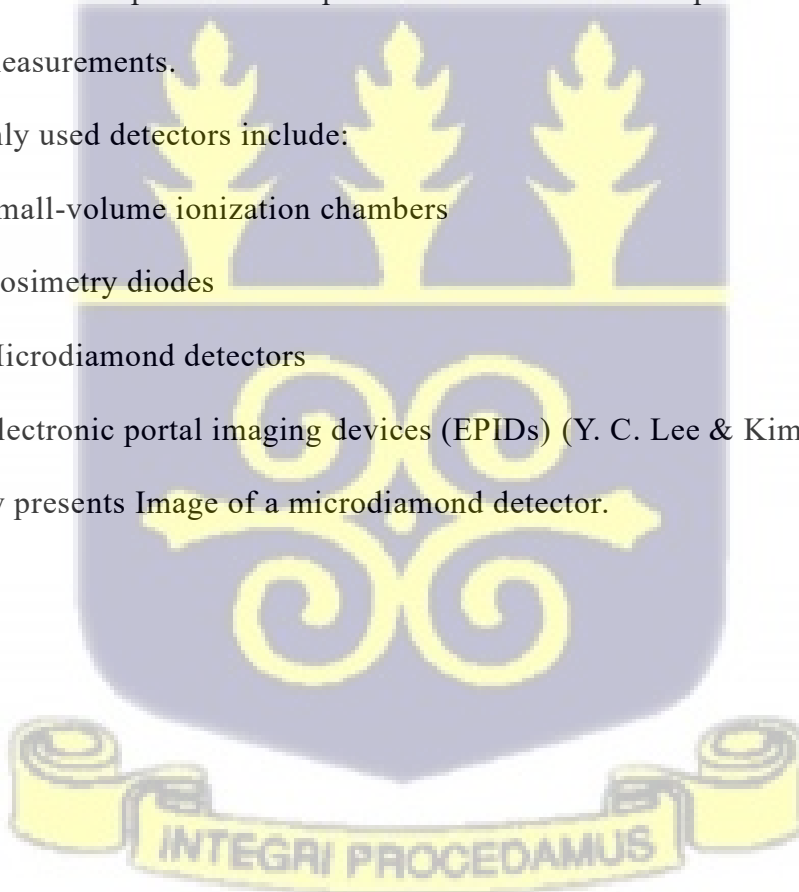


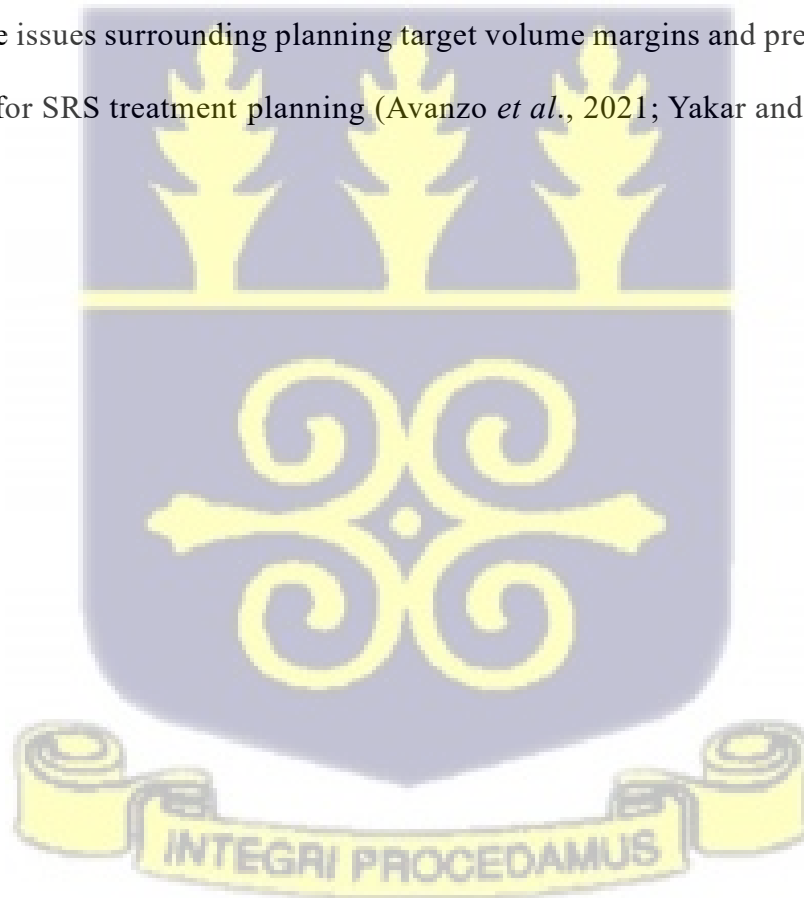


Figure 20: Image of a microdiamond detector (Lee and Kim, 2021)

2.16 Artificial intelligence (AI) in Stereotactic Radiosurgery (SRS) Treatment Planning

Artificial intelligence (AI) is transforming the landscape of stereotactic radiosurgery (SRS) by enhancing treatment planning processes, improving accuracy, and optimizing workflows. AI algorithms, particularly convolutional neural networks (CNNs), are being developed to automate the segmentation of tumors and organs at risk. This reduces the time needed for manual contouring and improves accuracy, as studies show that AI-assisted segmentation can enhance inter-reader agreement and contouring precision, especially for less experienced clinicians (Avanzo *et al.*, 2021; Huynh *et al.*, 2020). AI can significantly reduce treatment planning times, transforming what traditionally took days into processes that can be completed in minutes or even seconds. For instance, automated planning systems can generate treatment plans based on historical data and patient-specific anatomy, leading to quicker decision-making. Machine learning techniques are employed to create knowledge-based treatment plans that are comparable to those generated by human planners. This approach not only standardizes treatment quality but also minimizes variability among different clinicians (Rattan *et al.*, 2019).

AI can assist in quality assurance by continuously monitoring treatment delivery and comparing it against planned parameters. This ensures that any deviations are promptly addressed, enhancing patient safety. AI tools can analyse large datasets to predict treatment outcomes, helping clinicians find which patients are most suitable to benefit from SRS based on their specific characteristics and tumor profiles. The integration of AI into clinical workflows facilitates smoother transitions between different stages of the treatment process, from imaging to planning to delivery. This automation helps reduce human error and improve overall efficiency. AI technologies enable adaptive radiotherapy approaches that adjust treatment plans centred on real-time patient data, such as changes in tumor size or patient positioning during treatment sessions. With this breakthrough, AI might be instrumental in helping mitigate issues surrounding planning target volume margins and prescription isodose level selection for SRS treatment planning (Avanzo *et al.*, 2021; Yakar and Etiz, 2021).



CHAPTER THREE

MATERIALS AND METHODS

3.0 Introduction

This chapter describes the key research materials, data collection procedures, and analytical techniques used in this study. The method sections describe into details procedures with data collection relating to each specific objective.

3.1 Materials

The following are the list of materials that were employed in the research;

3.11 The Stereotactic End-to-End Verification (STEEV) Phantom

The Stereotactic End-to-End Verification (STEEV) phantom developed by CIRS, is an advanced anthropomorphic device designed for comprehensive Quality Assurance (QA) in stereotactic radiosurgery (SRS). The phantom provides a realistic simulation of human anatomy, which is crucial for testing and verifying the accuracy of SRS systems used in cancer treatment. The STEEV phantom represents a significant advancement in the field of radiation oncology, providing medical physicists with the tools necessary to enhance the safety and efficacy of SRS treatments. Its detailed anatomical simulation and versatile QA capabilities make it an essential component in ensuring high-quality patient care in stereotactic radiosurgery (Dimitriadis *et al.*, 2017). The phantom was modified to accommodate a solitary; asymmetrical target positioned 10 mm in front of the brainstem. The design of the phantom facilitates the use of replaceable cuboid inserts for imaging and irradiating the brain's central region. Additionally, it allows for the insertion of radiation detectors via two parallel cylindrical access cavities.

Key Features and Functionality STEEV Phantom

1. *Tissue-Equivalent Materials:*

The STEEV phantom is constructed from proprietary materials that closely mimic the linear attenuation properties of actual human tissues, ensuring that the simulation results are highly accurate. The materials used have linear attenuations within 1% of real soft tissue and bone across a range of energies from 50 keV to 15 MeV.

2. *Anthropomorphic Design:*

Its anthropomorphic exterior includes detailed internal structures such as cortical and trabecular bone, brain, spinal cord, and other anatomical features. This design allows for the evaluation of complex intra- and extra-cranial anatomies, making it suitable for various clinical applications.

3. *Versatile QA Applications:*

The phantom accommodates multiple interchangeable inserts for dosimetry and imaging, allowing for end-to-end testing of SRS systems. It supports various imaging modalities, including CT, MRI, and PET, facilitating comprehensive QA processes from diagnostic imaging to treatment plan verification.

4. *Independent Auditing:*

The STEEV phantom is also utilized in independent auditing of SRS programs, ensuring that treatment centres maintain high standards of accuracy in target localization and dose delivery. This is critical, as even minor errors in SRS can lead to significant clinical complications, such as under-treatment or overdose of surrounding healthy tissues.

5. *End-to-End Testing Capabilities:*

It is designed to meet the requirements set forth by the AAPM TG-101 guidelines for SRS commissioning and QA. This includes verifying patient positioning, treatment

planning accuracy, and conducting geometric machine QA tests. (Anthropomorphic STEEV phantom underpins independent auditing of SRS programmes, 2022). Figure 21 below presents image of the STEEV Phantom

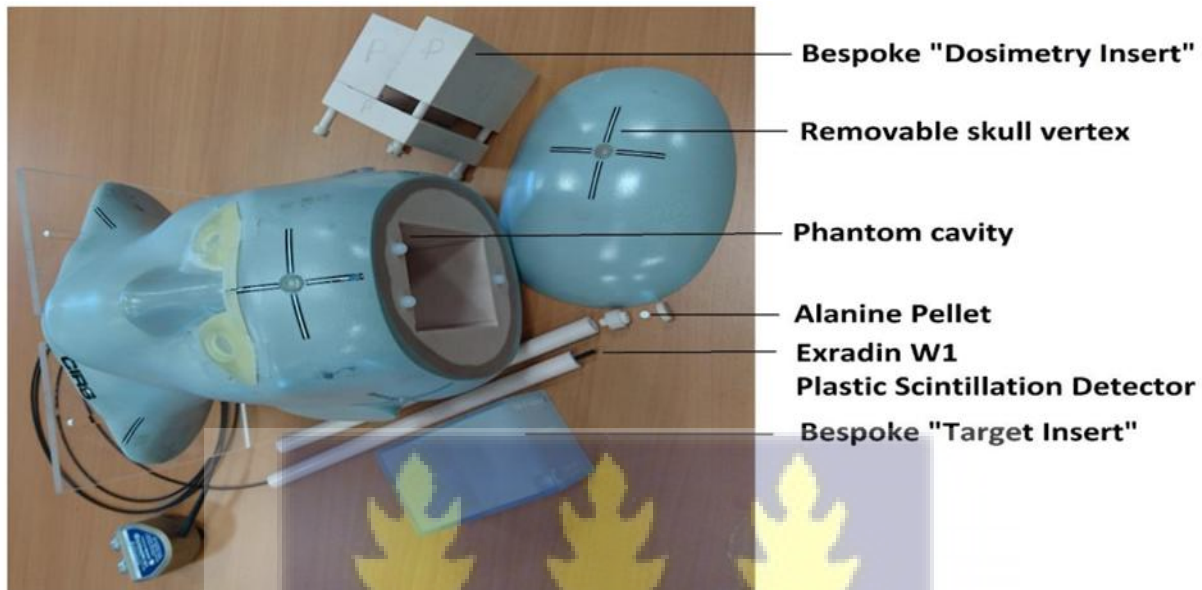


Figure 21: Image of the STEEV Phantom (Phantom Patient for Stereotactic End-to-End Verification-CIRS, 2022).

3.1.2 The Delta 4 Phantom+

The Delta4 Phantom+ is a new wireless system that allows for highly accurate patient-specific quality assurance (QA) of advanced radiotherapy techniques like VMAT, IMRT, SRS, Halcyon and TomoTherapy. It uses a three dimensional (3D) detector array with 1069 detectors to assess the full dose distribution in the isocentric region, rather than just a single planar measurement (The Delta4 Phantom+ wireless Phantom, 2020).

The Delta4 Phantom+ is completely wireless, eliminating the need for power, trigger, and data cables. This makes the setup faster, safer, and more convenient. It uses Wi-Fi communication and is battery-powered. The phantom has two orthogonal detector planes that provide isocentric measurements in the target region. It can merge large fields up to 38 cm longitudinally and 20 cm transversally/sagittally. The detectors have a high resolution of 5

mm at isocentre, which can be increased to 2.5 mm by merging. The Delta4 Phantom+ can be easily transferred to the treatment couch using the ergonomic Delta4 Trolley, eliminating the need for manual lifting. Alignment is quick and accurate, with clear markers on the phantom allowing positioning in 6 dimensions. The system provides quick and accurate absolute dose verification. It can also perform ion chamber measurements in the same phantom. The Delta4 software is integrated into the clinical workflow, allowing easy import of treatment plans and TPS dose. It provides automatic pass/fail analysis as soon as the dose is delivered. The software offers powerful analysis tools, including dose deviation, distance to agreement (DTA), and gamma index.

The Delta4 DVH suite provides unique analyses to determine the clinical significance of deviations, even for structures outside the measured detector plane. The Delta4 Phantom+ represents a significant advancement in radiation therapy QA, offering fast, accurate, and comprehensive verification of complex treatment plans while minimizing setup time and complexity (Srivastava & De Wagter, 2019; *The Delta4 Phantom+ Wireless Phantom*, 2020.).

Figure 22 below presents the image of the wireless Delta4 Phantom+



Figure 22: The image of the wireless Delta4 Phantom+(The Delta4 Phantom+ wireless Phantom, 2020).

3.1.3. The Gamma Plan Treatment Planning System for Gamma Knife

The Leksell GammaPlan (LGP) is a dedicated treatment planning system used specifically for the Gamma Knife, a device designed for stereotactic radiosurgery. It is a sophisticated tool that enhances the precision and efficiency of Gamma Knife radiosurgery, providing clinicians with the capabilities to deliver effective and targeted radiation therapy for complex intracranial conditions (Fallows *et al.*, 2019; Kutuk *et al.*, 2022). Here are features and functionalities of the GammaPlan system:

1. Treatment Planning:

LGP facilitates the planning of Gamma Knife treatments by allowing clinicians to create precise treatment plans for intracranial lesions. It utilizes multiple non-coplanar photon beams produced by cobalt-60 sources to deliver targeted radiation.

2. Inverse Planning Module:

The system includes an inverse planning module that automates the process of shot placement and optimization. This module uses an auto-fill function to populate the target volume with radiation shots and an optimization function to adjust parameters for optimal dose distribution. This capability is particularly beneficial for inexperienced planners, as it standardizes the planning process and improves efficiency.

3. Dose Calculation Algorithms:

LGP offers two primary dose calculation algorithms:

- **TMR10 Algorithm:** This algorithm, grounded in ray tracing and pre-calculated off-axis ratios, is extensively utilized and has a solid foundation of clinical experience.

- Convolution Algorithm: This method employs collapsed cone convolution techniques for precise dose estimation, especially in regions with tissue inhomogeneities. However, it requires more calculation times and a full CT scan of the patient, which has limited its routine use in practice.

4. Optimization Parameters:

The system allows users to define optimization parameters such as coverage, selectivity, and gradient index, which can significantly influence treatment outcomes. A standardized method for using these parameters has been developed to enhance treatment consistency and reduce planning times.

5. Clinical Application:

LGP has been shown to produce clinically acceptable plans with high coverage and conformity indices. Studies have demonstrated that plans generated using the inverse planning module can match or exceed the quality of manually created plans, potentially shortening treatment times (Fallows *et al.*, 2019).

6. User Interface and Workflow Integration:

The Gamma Plan system is designed to integrate seamlessly into clinical workflows, enabling easy import of treatment plans and facilitating real-time adjustments centred on patient-specific anatomy and treatment goals (Guo, 2018).

Figure 23 below presents the image of the Gamma plan treatment planning system.



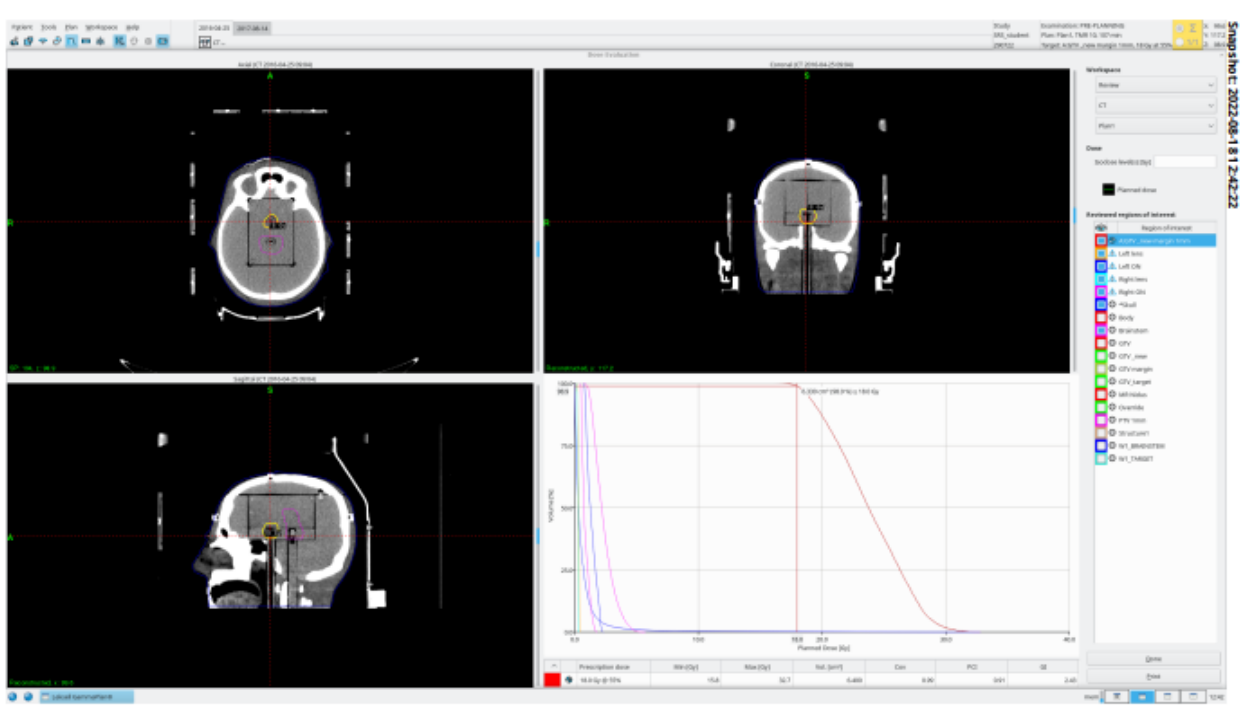


Figure 23: The interface of the Gamma Plan Treatment Planning System

3.1.4. The TrueBeam Linear Accelerator

The TrueBeam Linear Accelerator, manufactured by Varian Medical Systems, is a state-of-the-art radiotherapy system designed to deliver precise cancer treatments. It integrates advanced imaging, beam delivery, and motion management technologies to enhance the accuracy and efficiency of radiation therapy. TrueBeam Linear Accelerator represents a significant stride in cancer treatment technology, offering high precision, speed, and versatility in radiotherapy, making it a crucial tool in modern oncology. Figure 24 below presents the Truebeam Varian LINAC

Key Features and capabilities of the TrueBeam Linear Accelerator

1. *Advanced Imaging:*

The TrueBeam system employs high-resolution imaging techniques, including cone-beam computed tomography (CBCT), to visualize tumors in real-time. It can generate

3D images every 10 seconds, allowing for precise adjustments during treatment to account for patient movement, such as breathing.

2. Precision Targeting:

Utilizing respiratory gating technology, the TrueBeam delivers radiation only when the tumor is optimally positioned, significantly improving targeting accuracy. This capability reduces the risk of damaging surrounding healthy tissues.

3. High Dose Rates:

TrueBeam can administer radiation doses at rates up to 2400 monitor units (MU) per minute, which is twice as fast as many standard systems. This rapid delivery reduces overall treatment time, often allowing procedures to be completed in under two minutes.

4. Versatile Treatment Options:

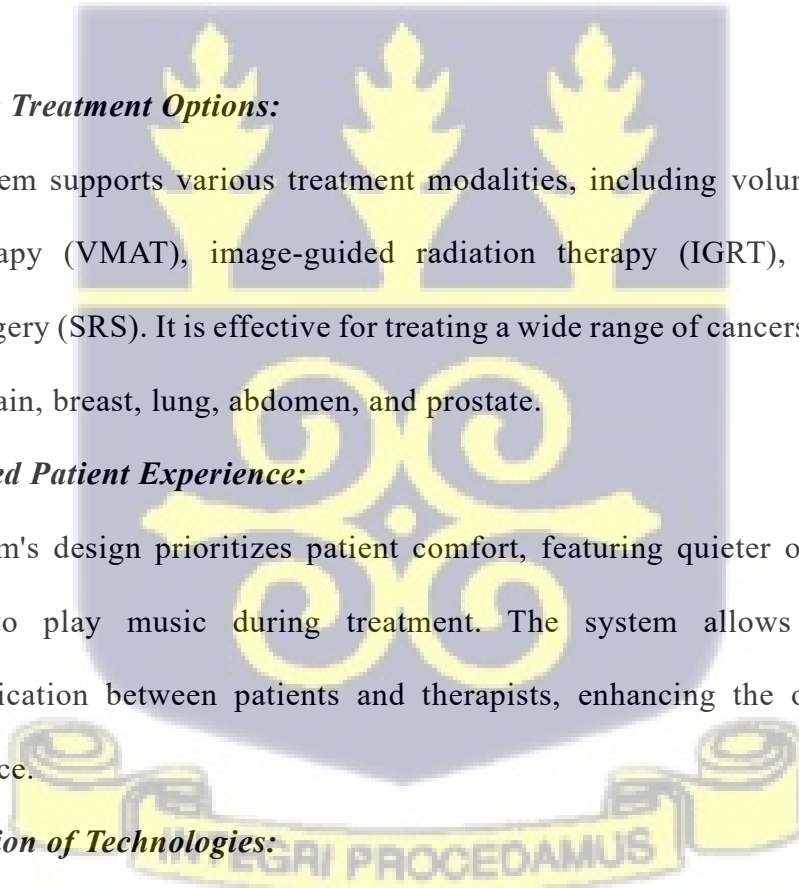
The system supports various treatment modalities, including volumetric modulated arc therapy (VMAT), image-guided radiation therapy (IGRT), and stereotactic radiosurgery (SRS). It is effective for treating a wide range of cancers, including those in the brain, breast, lung, abdomen, and prostate.

5. Enhanced Patient Experience:

TrueBeam's design prioritizes patient comfort, featuring quieter operation and the option to play music during treatment. The system allows for continuous communication between patients and therapists, enhancing the overall treatment experience.

6. Integration of Technologies:

TrueBeam combines multiple functionalities, such as imaging, radiation beam shaping, and patient positioning, into a single platform. This integration streamlines workflows and enhances treatment planning and delivery.



7. *Safety and Calibration:*

The system is equipped with advanced safety features, including Laser Guard II and a capacitive collision detection system, ensuring safe operation. Calibration can further enhance accuracy, achieving error rates as low as 0.5% for both electron and photon beams (TrueBeam, 2024).



Figure 24: The Truebeam Varian LINAC

3.1.5. *Eclipse Treatment Planning System*

The **Eclipse Treatment Planning System**, developed by Varian Medical Systems, is a comprehensive and versatile software solution designed for planning radiation therapy. It supports a wide range of treatment modalities, like external beam radiation therapy (EBRT) using photon, electron, and proton beams, as well as brachytherapy. This system facilitates the creation of high-quality treatment plans while integrating seamlessly into clinical workflows. Its advanced features and user-friendly design make it a preferred choice for

radiation oncology professionals (Saw *et al.*, 2018). Figure 25 presents image of the Eclipse planning system in use.

Features and functionalities

1. Open Architecture:

Eclipse utilizes an open DICOM RT architecture, allowing seamless integration with various imaging devices and treatment platforms. This feature enables users to import treatment plans from other systems and create new or summation plans, enhancing flexibility and accessibility.

2. Advanced Planning Tools:

The system includes a robust set of planning tools for generating:

- a. Conformal radiation therapy plans
- b. Treatment plans for electron beam therapy
- c. Volumetric-modulated arc therapy (VMAT) plans
- d. Intensity-modulated radiation therapy (IMRT) plans
- e. Proton therapy plans, including specialized algorithms for ocular proton treatment

3. User-Friendly Interface:

Eclipse is designed with an intuitive Microsoft Windows-based interface that simplifies the treatment planning process. Features such as drag-and-drop functionality and consistent icons across different workspaces help users navigate the system efficiently.

4. Optimization and Dose Calculation:

Eclipse offers modern optimization algorithms and multiple dose calculation options, enabling precise dose distribution modelling. Users can implement their own optimization algorithms, enhancing treatment personalization.

5. *Integration with Clinical Workflows:*

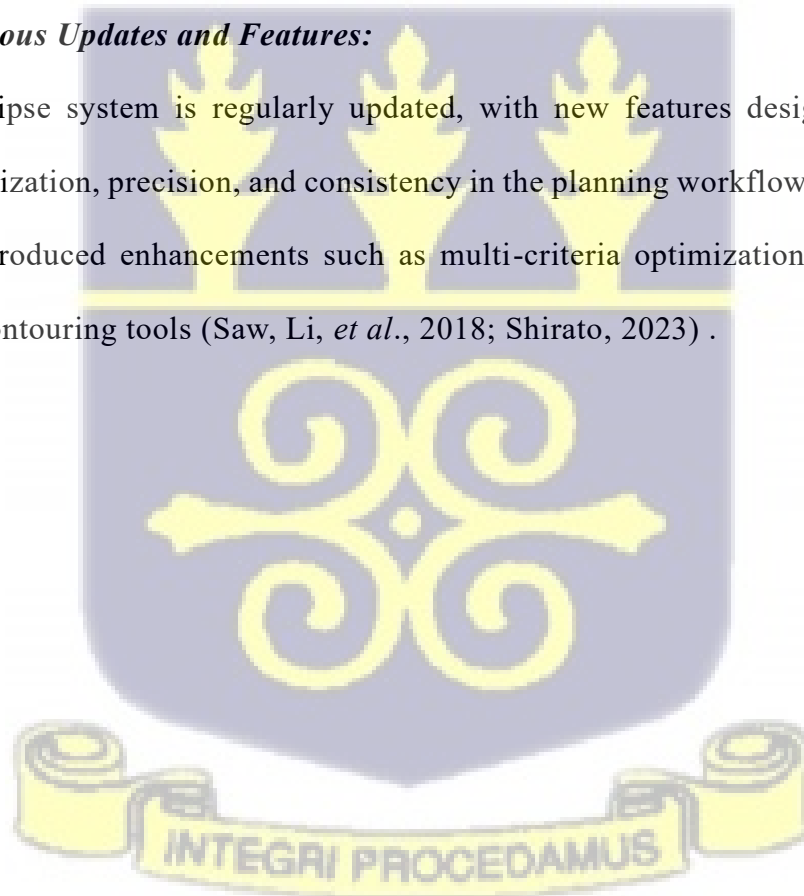
The system integrates with Varian’s ARIA oncology information system, allowing for streamlined data management and minimizing the risk of errors during the planning process. It also supports automated structure delineation and quality assurance checks.

6. *Scripting API:*

The Eclipse Scripting Application Programming Interface (API) allows users to customize and extend the functionality of the planning system. This feature enables the creation of bespoke tools and automated workflows, enhancing efficiency and reproducibility in treatment planning.

7. *Continuous Updates and Features:*

The Eclipse system is regularly updated, with new features designed to improve personalization, precision, and consistency in the planning workflow. Recent versions have introduced enhancements such as multi-criteria optimization (MCO) and AI-based contouring tools (Saw, Li, *et al.*, 2018; Shirato, 2023) .



metrics pertinent to radiotherapy services. Evaluations derived from DIRAC data can promote fairness in the availability of cancer treatment, enhance healthcare facilities, assess radiotherapy assets, and bolster scholarly research. The DIRAC database serves as a collaborative platform, offering essential data analysis insights and interactive mapping features. The DIRAC database is therefore a crucial resource for understanding the global landscape of radiotherapy resources and informing efforts to improve access to cancer treatment worldwide (IAEA-DIRAC, 2024).

3.2 Methods

Treatment planning and measurement were carried out in two centres, namely the Queen Square Gamma Knife Centre of the University College London Hospital in London, United Kingdom for Gamma Knife measurements and Centro di Riferimento di Oncologico (CRO) in Aviano, Italy for LINAC-based SRS measurements.

3.2.1 Influence of Different Planning Target Volume (PTV) Margins with Different Prescription Isodose Levels for Stereotactic Radiosurgery (SRS) of a Single Brain Metastasis on the Gamma Knife Treatment Planning System.

3.2.1.1 Gamma Knife Treatment Planning

The Stereotactic End-to-End Verification (STEEV) head anthropomorphic phantom, manufactured by CIRS in Norfolk, VI, USA, was used for this study. The phantom was modified to accommodate a solitary; asymmetrical target positioned 10 mm in front of the brainstem. The phantom underwent a treatment planning computed tomography (CT) scan, using a Philips Brilliance CT scanner (Philips HealthCare, Best, Netherlands) with a big bore and slice thickness of 2 mm.

The CT images were imported into the Gamma Plan Treatment Planning System, version 11.3.1. As shown in Figure 3, the centre of the internal rectangular part which was the target insert in the phantom was delineated with the gross tumor volume (GTV) with the help of an experienced radiation oncologist and a medical physicist. A target volume measuring 4.9 cc was centrally manually contoured as well as organs at risk (brain, brain stem, right and left optic nerve and lens). Clinical acceptable plans with a 0 mm margin at five prescription isodose levels from 50 to 70% at 5% increment with same tumor coverage were created. Planning target volumes (PTVs) were then regenerated by GTV external expansion of 0.5, 1, 1.5, and 2 mm isotropically, resulting in volumes of 5.6, 6.4, 7.8, and 8.7 cc respectively. These were recalculated at five different prescription isodose levels (50, 55, 60, 65, 70). Manual adjustment with the shots were made when necessary to achieve the same coverage for all plans. A dose of 18Gy in single fraction was used. The dosimetric parameters values were generated at the end of the dose calculation for each plan. PCI, GI and S values were based on Equation 1, 2, and 3 respectively. Obtained values of PCI, GI and S were compared to ideal values set out by the International Leksell Gamma Knife Society Standardization Committee.

$$PCI = \frac{TV \times PIV}{PIV \times TV} \quad (1)$$

where PIV is prescribed isodose volume, TV is the target volume, and TVP_{IV} is the TV receiving the prescription dose. Paddick's conformity index considers the spatial correlation between the prescribed volume and the TV. An optimal value for the PCI conformity should be < 1.18 (Tham *et al.*, 2023; Torrens *et al.*, 2014). The TV, TVP_{IV}, and PIV, for each treatment plan, were obtained from the dose volume histogram (DVH).

The gradient index (GI) is calculated as the ratio of the volume contained by half of the prescribed isodose to the volume of the prescribed isodose itself. This is sometimes referred

to as the 25/50 proportion. An optimal value for the gradient index might be less than 3.0 (Torrens et al., 2014).

$$GI = \frac{PIV50}{PIV} \quad (2)$$

Selectivity index refers to the extent to which normal tissue around the target is preserved. This is calculated by dividing the target volume covered by the prescribed isodose by the total volume of the prescribed isodose. A measure of the selectivity may be needed if a compound conformity index is not applied. An optimal value for selectivity could be > 0.9 (Fallows et al., 2019; Torrens et al., 2014). Figure 27 below presents DVH and the volume analysis tools from Planning System.

$$S = \frac{TVPIV}{PIV} \quad (3)$$

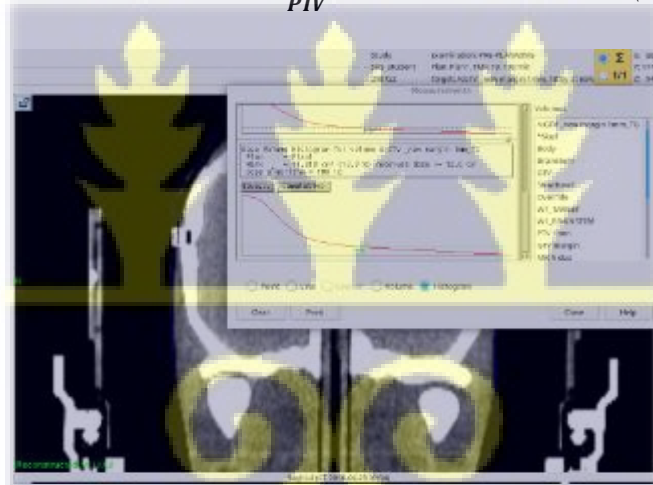


Figure 26: DVH and the volume analysis tools from Planning System



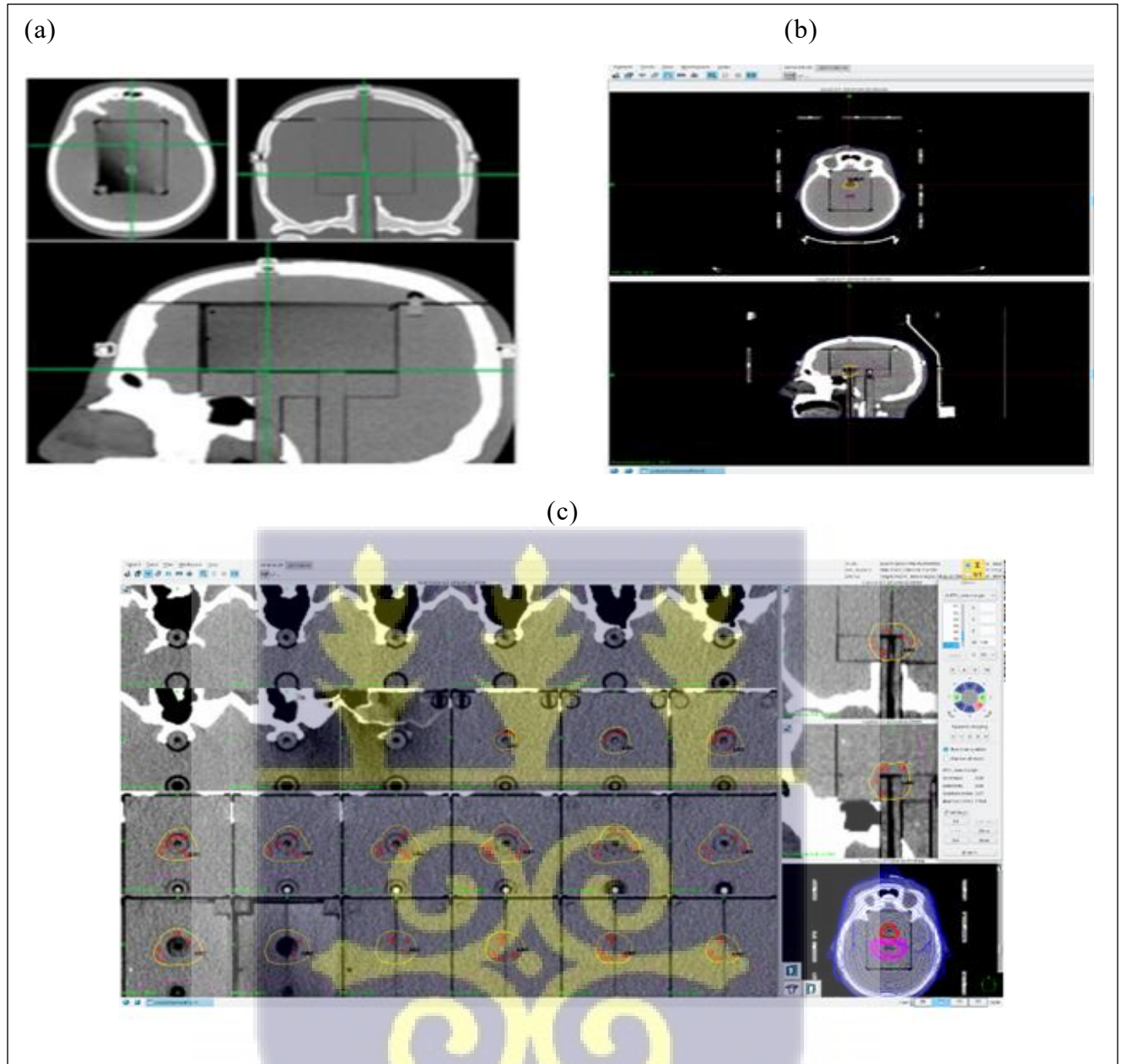


Figure 27: The phantom through sagittal, coronal and axial planes with the target insert (a) inside the cavity (b) Target delineation in Gamma Plan TPS (c) Dose distribution in the target in the treatment planning system

3.2.1.2 Data Analysis

The Statistical Package for the Social Sciences, SPSS software (version 26, IBM Corp., USA), was used to analyze the data. One-way ANOVA test was used to analyze the influence

of planning target volume margins with the various prescription isodoses used on parameters such as Selectivity [S], Gradient index [GI], V12, Paddicks conformal index [PCI] and treatment time [TI]. Statistical significance was set at an alpha value of $p < 0.05$. The organs at risk were evaluated in terms of maximum and minimum doses.

3.2.2 Impact of various Prescription Isodose Levels using Commonly used Margins in the LINAC-Based SRS of Single Brain Metastasis

3.2.2.1 Eclipse Treatment Planning

The CT images of the STEEV phantom with contoured target and organs at risk used for the Gamma Knife was copied onto a secured pen drive and transferred to the Eclipse treatment planning system version 15.0 used in CRO, Italy.

A series of plans were developed with Planning target volume margin of 0, 1, and 2 mm at six levels of prescription isodose level but with similar coverage. The tumor volume according to the margins used were 5.0, 7.7, and 9.4 cm³ respectively. All plans were made with single iso-centre VMAT technique using 6 MV, FFF, five non-coplanar beams normalized such that 95% of target volume receives the prescription dose (PD). The prescribed dose was 18 Gy in single fraction. Couch angle separation was usually between 30 and 40 degrees, with no opposing arcs. Typically, an arc covered 120-140 degrees. The collimator angle was also set at zero degrees to optimize treatment delivery. The treatment plans were optimized using the UK 2022 Consensus on Normal Tissue Dose-Volume Constraints for single brain metastasis (Diez *et al.*, 2022). Gradient index and conformity index were calculated. Treatment time was derived from the summary treatment plan, a feature in the eclipse treatment planning system. Dose to organs at risks were also evaluated.

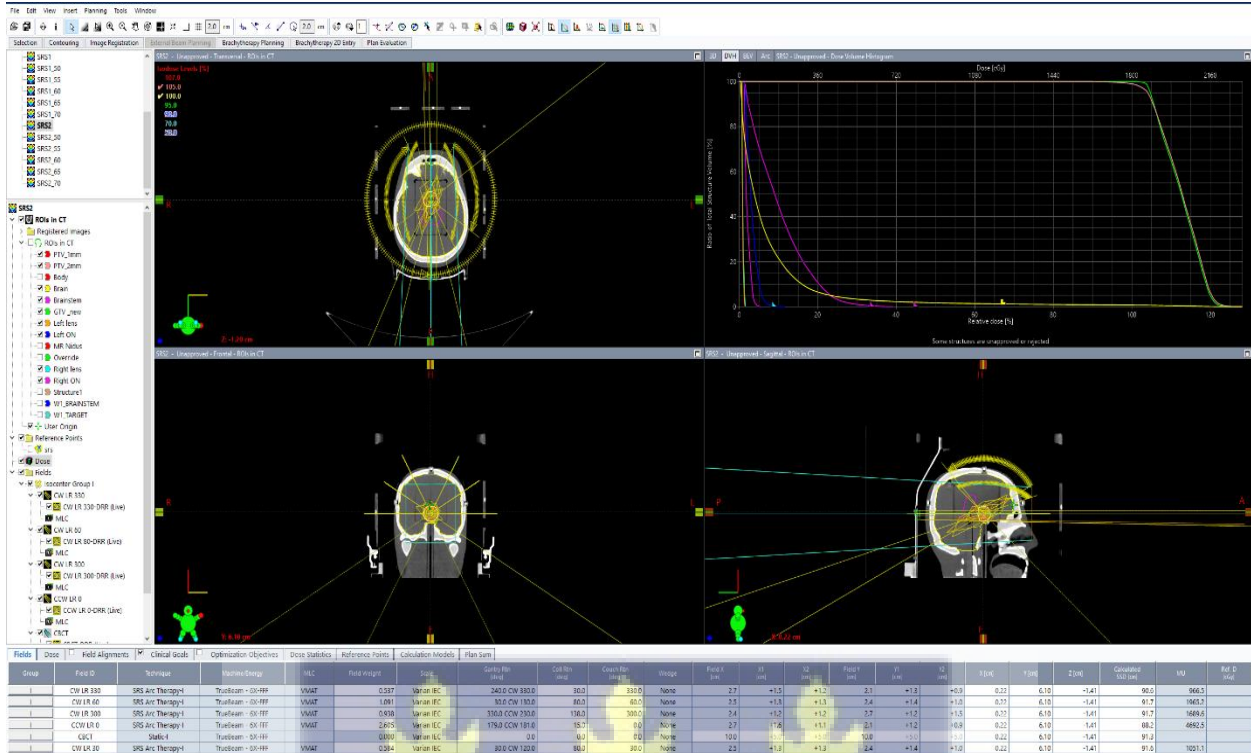


Figure 28: The interface of the Eclipse treatment planning system during planning

The prescription isodose line (PIDL) is defined as the ratio of the prescribed dose to the maximal dose, consistent with previous research and Radiation Therapy Oncology Group (RTOG) 90-05 standards. Figure 29 shows the image of the interface of the Eclipse treatment planning system during planning. The gradient index was defined as:

$$GI = \frac{V_{50}}{PIV} \quad (4)$$

where V_{50} is the volume that receives 50% of the prescription dose and PIV is the volume receiving the prescription dose (Patro *et al.*, 2022). At CRO, the gradient index is accepted at 0.6 mm whiles conformity index at 1

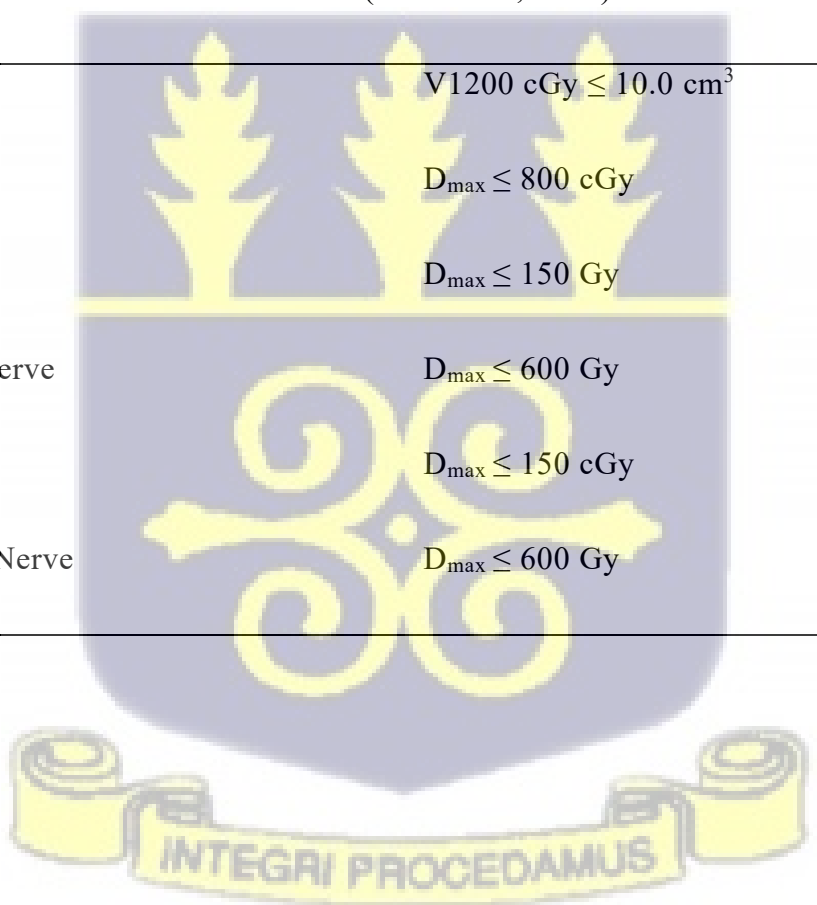
The conformity index (CI) was also calculated using definitions defined by RTOG. The RTOG definition is:

$$CI = \frac{VPD}{TV} \quad (5)$$

where TV is the target volume, VPD is the volume that is covered by the prescription isodose. CI = 1 signifies optimal dose coverage of the target; CI > 1 suggests that the irradiated volume surpasses the target volume, affecting some healthy tissue and CI < 1 suggests that the target volume has not received complete radiation exposure (Zhao *et al.*, 2014). Table 1 below presents the constraints for optimization in TPS.

Table 1: Constraint for optimization in TPS

UK 2022 Consensus on Normal Tissue Dose-Volume Constraints for Single brain metastasis (Diez <i>et al.</i>, 2022)	
Brain	$V_{1200 \text{ cGy}} \leq 10.0 \text{ cm}^3$
Brain Stem	$D_{\text{max}} \leq 800 \text{ cGy}$
Left lens	$D_{\text{max}} \leq 150 \text{ Gy}$
Left Optical Nerve	$D_{\text{max}} \leq 600 \text{ Gy}$
Right lens	$D_{\text{max}} \leq 150 \text{ cGy}$
Right Optical Nerve	$D_{\text{max}} \leq 600 \text{ Gy}$



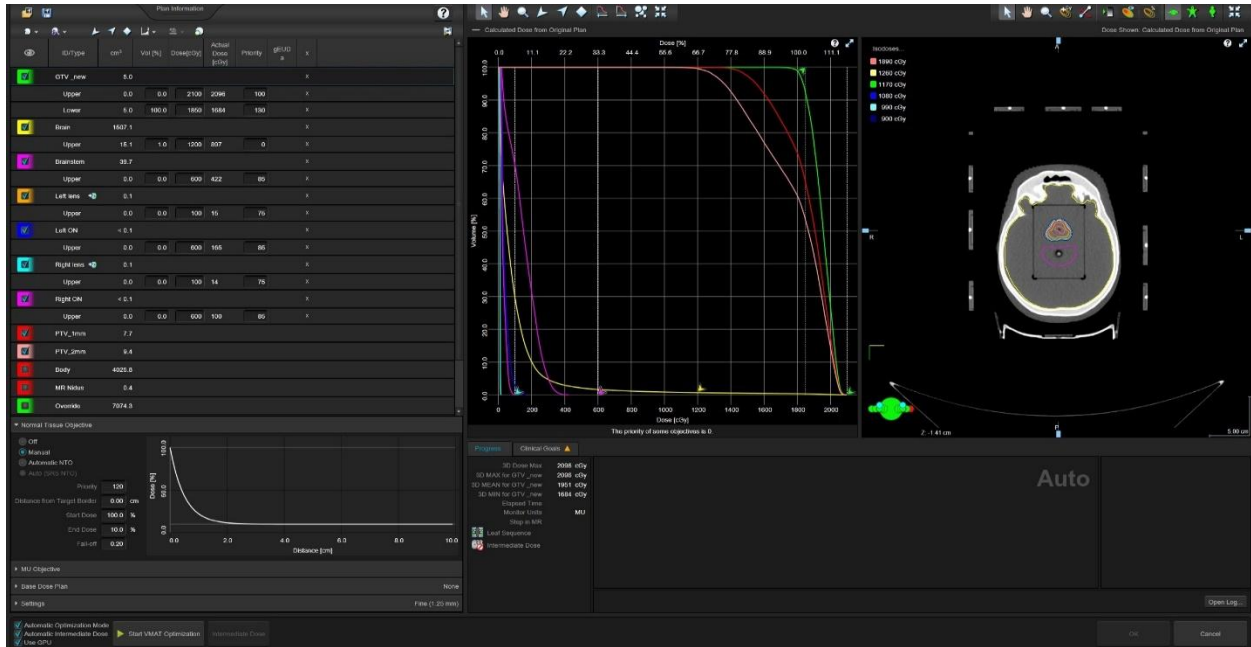


Figure 29: The optimization interface during planning

The plans parameters such as GI, CI, and organs were compared to that used in CRO and analyzed. The treatment time of all plans derived from planning summary report of the planning systems were also compared. Figure 30 below shows the optimization interface during planning.

3.2.2.2 Data analysis

Microsoft excel and IBM SPSS Statistics version 26.0 was used to analyze the data. One sample t-test was performed to compare the means of the different parameters (CI, GI) across the various prescription isodoses. This test assesses whether the mean of a single group differs significantly from a known. Along with the t-test, confidence intervals for the mean differences were calculated. The p-values associated with the t-tests were examined to determine statistical significance. A p-value less than 0.05 was considered statistically significant. The parameters were grouped into organs at risk (brain, brain stem, right lens, right optical nerve) and Treatment metrics (gradient index, conformity index, treatment

time). The organs at risk and treatment metrics were displayed on graphs to compare the impact of prescription isodoses on the target organs and treatment metrics in each margin.

3.2.3 Dosimetric accuracy of LINAC-based SRS Plans using the newly introduced wireless Delta 4 Phantom+ Device.

3.2.3.1 Procedure

All treatment planning and phantom measurements were carried out at the Centro riferimento di Oncologico (CRO), Aviano-Italy. The measurements were done on Varian TrueBeam linear accelerator and with the new wireless Delta 4 Phantom+ (Figure 31). The treatment plans were generated using Varian Eclipse 15.0 treatment planning system (TPS). Clinically accepted VMAT SRS plans made with computed tomography (CT) images of the Stereotactic End-to-End Verification (STEEV) anthropomorphic phantom with six different prescription isodose level (50, 55, 60, 65, 70 and 80), a prescribed dose of 18 Gy in single fraction and using 6 MV flattening filter free (FFF) beam were created. The treatment plans were done with five arcs and three different planning target volume margins (0 mm, 1 mm, 2 mm).

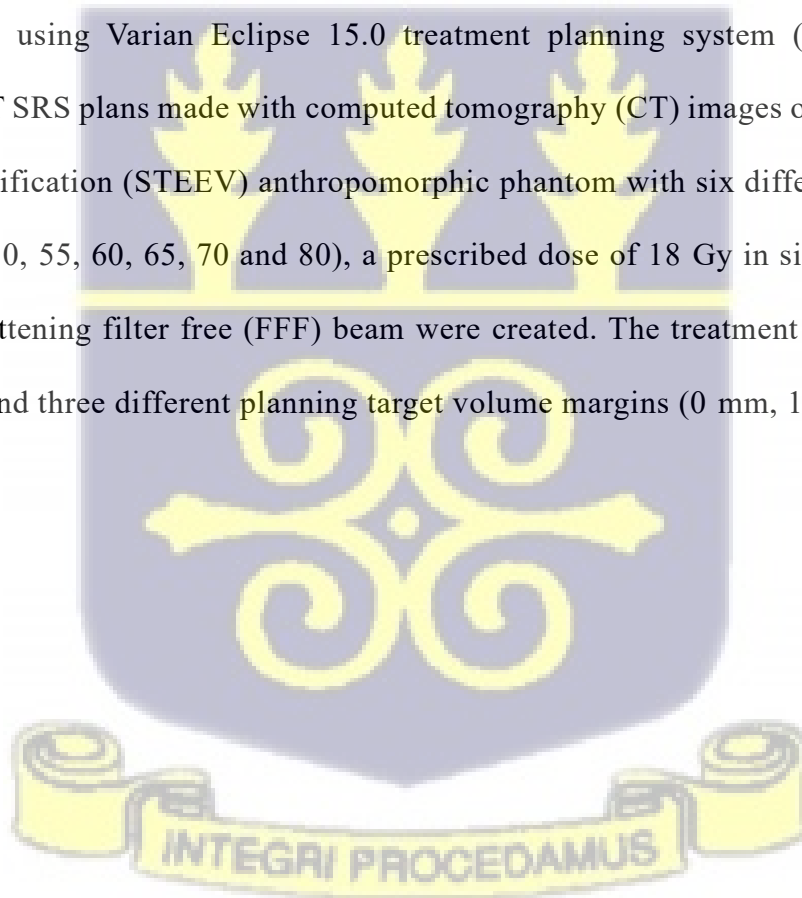




Figure 30: The Wireless Delta 4Phantom+ during measurement

The treatment plans were modelled onto the Delta 4 phantom+ CT scan within the TPS for dose calculation. The dose distribution was recalculated and the planning data, including the beam parameters from the original plan were the same. These plans were then transferred to the True Beam LINAC and delivered. The Delta 4 Phantom+ software offers a range of tools to effectively analyze the disparities between measurement and calculated TPS dose. An analysis was conducted for the key parameters distance to agreement (DTA), dose agreement (DA) and the gamma pass rate.

The concept of gamma pass rate analysis was initially proposed by Low (2010) as a means to quantitatively compare dose distributions that have been calculated and measured (Low, 2010). This utilizes the physical distance and dose difference, which are then normalized based on the criteria of acceptability (Song *et al.*, 2015).

3.2.3.2 Data Analysis

The distance to agreement (DTA), dose deviation (DD) and gamma index passing rates were all calculated by the software of the Delta4 (Low, 2010). The criteria for acceptance used in this centre was DTA of 3 mm, dose difference of 3% and the gamma-index passing rate of 95 and 90% for IMRT and VMAT SRS, respectively, based on the AAPM TG-218 action limit (Xia *et al.*, 2020). In this study a 2% dose difference, 2 mm DTA and the gamma index passing rate of 95% were used. Iso-centric set up position was used for the Delta4+ phantom in measurement. A four field box technique with field size of $10 \times 10 \text{ cm}^2$ was measured for the correction factor (Delta4 Phantom+:The Fastest and most accurate 4D verification system, 2022). Figure 31 presents Truebeam LINAC monitor interface during measurement



Figure 31: Interface LINAC monitor interface during measurement.

3.2.4 Opinions of some planning medical physicists with experience in SRS treatment planning on margin additions in the SRS treatment of single brain metastasis.

A questionnaire consisting of five questions was developed to address specific sections regarding the addition of margins in the treatment of brain metastases with SRS. It was successfully concluded by ten medical physicists who have experience in the planning of SRS treatment.

3.2.4.1 Justification of Sample Size.

Stereotactic radiosurgery (SRS) is a highly specialized treatment available only in facilities equipped with the appropriate technology, and not all medical physicists are trained or actively practicing in this area. As a result, the sample size of 10 reflects the limited pool of professionals with the relevant expertise in brain metastasis treatment using SRS. The study intentionally focuses on medical physicists who are either currently practicing or have direct experience with SRS, ensuring that the data is gathered from a highly knowledgeable group rather than from a general population. This approach justifies the relatively small sample size, as the participants share a homogeneity in their expertise, reducing variability in responses. Additionally, logistical constraints such as the limited number of facilities with the necessary equipment and qualified staff make the sample size of 10 a practical and realistic representation of the available population.

3.2.4.2 Data Analysis

Simple bar graphs and descriptive statistics were employed to analyze the results using IBM SPSS Statistics version 26.0.

3.2.5 Geographical Distribution of Radiotherapy Systems for Brain Metastasis Treatment in Africa and Develop Guidelines for the Implementations of SRS Program in Africa.

3.2.5.1 Procedure

A comprehensive database encompassing the 54 African nations has been established utilizing open-source information. Factors such as population size, gross domestic product (GDP) per capita, cancer incidence, and the availability of radiotherapy equipment were taken into account as variable elements. Estimates for GDP per capita were sourced from the world economics database. This was defined as the total economic output adjusted to a common currency using relative purchasing power and divided by the overall population. The population data by country was sourced from the worldometer database, while information regarding cancer incidence at the country level was obtained from the GLOBOCAN 2022 database.

The IAEA's Division of Human Health's Directory for Radiotherapy Centres (DIRAC) is an electronic, regularly updated, and centralized directory of radiation facilities. It served as the principal source for the distribution of radiotherapy equipment across Africa (Fiagbedzi *et al.*, 2023). Data on radiotherapy equipment availability in African countries was collected in April 2023. A comprehensive literature search was conducted in PubMed to investigate the availability of specialized equipment for the treatment of brain metastases, along with the distribution of linear accelerators across Africa.

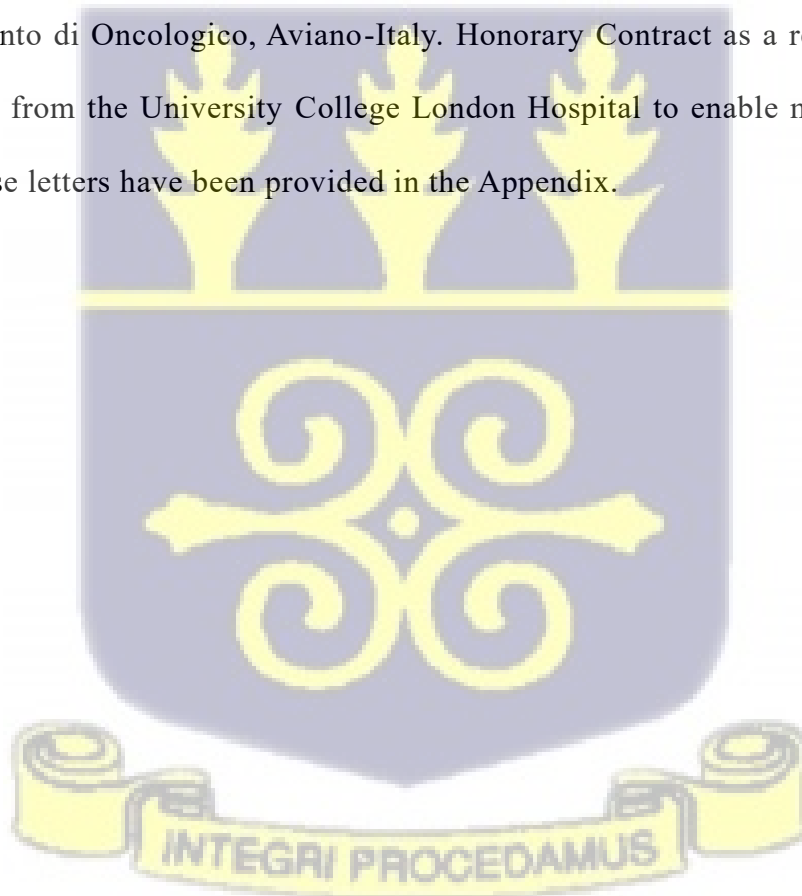
Approximately 20 to 40 percent of cancer cases may potentially progress to brain metastasis (Enrique *et al.*, 2019). Based on the GLOBOCAN 2022 data regarding cancer cases across various African nations, we estimated the incidence of brain metastasis by applying an assumption that thirty percent of the total cancer cases in each country are represented.

3.2.5.2 Data Analysis

Data entry and analysis were conducted utilizing Microsoft Excel and IBM Statistical Package for Social Science (SPSS) version 26. A straightforward linear regression was employed to connect the number of installed equipment with the anticipated number of brain metastases relative to GDP per capita in each nation.

3.3 Ethical Clearance Sought for the Study

Ethical clearance was obtained from the University of Ghana Ethics Committee for Basic and Applied Sciences (ECBAS 077/20-21). An approval letter was also gotten from the Centro riferimento di Oncologico, Aviano-Italy. Honorary Contract as a research physicist was also sorted from the University College London Hospital to enable me carry out data collection. These letters have been provided in the Appendix.



CHAPTER FOUR

RESULTS AND DISCUSSION

4.0 Introduction

The chapter presents data in a clear and organized manner, and the findings are then interpreted in the context of the research objectives. This critical analysis elucidates the implications and significance of the results while addressing the departure of the results from the literature.

4.1 Influence of Different Planning Target Volume (PTV) Margins with Different Prescription Isodose Levels for Stereotactic Radiosurgery (SRS) of a Single Brain Metastasis on the Gamma Knife Treatment Planning System.

4.1.1 Results

The results reported demonstrate that the values of selectivity, gradient index, and paddick conformity index (PCI) across all planning target volume (PTV) margins and prescription isodose levels fell within the ideal range recommended by the International Leksell Gamma Knife Society (ILGKS) Standardization Committee. This finding is significant because it validates the overall quality of the treatment plans, showing that even with incremental changes in PTV margin size (0.0-2.0 mm) and prescription isodose levels (50–70%), the dosimetric indices remained consistent with international benchmarks. Selectivity values within acceptable limits indicate that radiation was highly confined to the target volume, minimizing dose spillage to surrounding tissues. Similarly, conformity values reflect precise alignment between the prescription isodose and the target shape, underscoring the accuracy of tumor coverage. The gradient index, which measures how rapidly the dose falls off outside the target, also remained favourable, suggesting optimal protection of normal brain tissue.

Collectively, these results highlight the robustness of the Gamma Knife planning system in maintaining high dosimetric quality across a range of planning parameters, thereby reinforcing the clinical safety and efficacy of stereotactic radiosurgery for single brain metastasis.

Table 2 show the ANOVA test of the distribution of planning dosimetric parameters values across different PTV margins with the prescription isodoses levels in the study. Similarly, figures 33-37 also presented the graphic representation of the PTV margins for the various planning dosimetric parameters.

The overall mean for selectivity for the 0.0, 0.5, 1.0, 1.5, and 2.0 mm were 0.88, 0.90, 0.91, 0.93, and 0.93. This increases monotonically with increase in margin size but remain fairly steady as the prescription isodose levels increase from within the same margin size, with a statistically significant p-value of < 0.001 . This trend suggests that larger PTV margins enhance the confinement of the radiation dose within the target volume, potentially increasing treatment effectiveness.

Similarly, the paddick conformity index (PCI) shows a positive correlation with PTV margin, also significant at $p = < 0.001$. The PCI increases from 0.87 at a 0.0 mm margin to 0.92 at a 2.0 mm margin. A higher PCI indicates improved conformity of the dose distribution to the target volume, which is critical for minimizing radiation exposure to surrounding healthy tissues.

However, the gradient index (GI) displays a less consistent pattern across the PTV margins, despite remaining statistically significant ($p = < 0.001$). Although there is a slight overall increase, the GI fluctuates between 2.44 and 2.50, without a clear trend, indicating that the sharpness of dose fall-off does not uniformly improve with larger PTV margins. The 2.0 mm, 1.5 mm and 0.5 mm PTV margins had the highest and same GI value of 2.50. The PTV margins of 1.0 mm and 0.0 mm had the least GI value of 2.44.

Beam-on time also varies significantly across different PTV margins, with a p-value of < 0.001. It starts at 105.58 minutes for a 0.0 mm margin, decreases to 86.36 min at 0.5 mm, and then increases to 118.32 min at 2.0 mm. The increase in beam-on time with larger PTV margins may result from the need for more extensive radiation delivery to cover the larger volume, potentially affecting treatment efficiency.

Finally, the V12 Gy (cc) which is an important parameter in SRS shows the volume (V12) receiving 12 Gy and is a prognosticator for radiation necrosis (Gondi *et al.*, 2022). The V12 Gy increases steadily with the PTV margin, also with statistical significance at $p = < 0.001$. V12 Gy rises from 9.45 cc at 0.0 mm to 16.17 cc at 2.0 mm. This trend suggests that while larger margins may enhance selectivity and PCI, they also lead to a greater volume of surrounding tissue being exposed to potentially harmful radiation doses. Across all the margins sizes the highest V12 values were recorded with the 70% prescription isodose.

Table 2: One-way ANOVA test for planning dosimetric parameters and PTV margins in the study.

Parameter	PTV margin (mm)	Prescription Isodose					M	SD	95% CI		p
		50	55	60	65	70			Lower	Upper	
Selectivity	0.0	0.88	0.90	0.87	0.87	0.88	0.88	0.01	0.865	0.895	0.000
	0.5	0.89	0.90	0.90	0.90	0.90	0.90	0.00	0.892	0.904	
	1.0	0.92	0.92	0.91	0.92	0.90	0.91	0.01	0.903	0.925	
	1.5	0.93	0.95	0.93	0.93	0.93	0.93	0.01	0.923	0.945	
	2.0	0.93	0.93	0.93	0.93	0.92	0.93	0.00	0.922	0.934	

PCI	0.0	0.87	0.89	0.87	0.86	0.87	0.87	0.01	0.858	0.886	0.000
	0.5	0.89	0.89	0.89	0.89	0.89	0.89	0.00	0.890	0.890	
	1.0	0.91	0.91	0.90	0.91	0.89	0.90	0.01	0.893	0.915	
	1.5	0.93	0.93	0.93	0.92	0.92	0.93	0.01	0.919	0.933	
	2.0	0.92	0.92	0.93	0.92	0.91	0.92	0.01	0.911	0.929	
GI	0.0	2.41	2.42	2.42	2.46	2.51	2.44	0.04	2.392	2.496	0.011
	0.5	2.46	2.47	2.49	2.51	2.55	2.50	0.04	2.452	2.540	
	1.0	2.46	2.43	2.41	2.42	2.46	2.44	0.02	2.407	2.465	
	1.5	2.49	2.49	2.49	2.54	2.48	2.50	0.02	2.468	2.528	
	2.0	2.48	2.48	2.47	2.49	2.57	2.50	0.04	2.447	2.549	
Beam On	0.0	107.20	103.00	110.90	102.60	104.20	105.58	3.48	101.262	109.898	
Time											0.000
(min)	0.5	84.50	82.80	86.30	84.80	93.40	86.36	4.13	81.236	91.484	
	1.0	107.70	107.30	107.40	108.10	112.20	108.54	2.07	105.970	111.110	
	1.5	103.60	100.70	108.60	107.50	113.60	106.80	4.94	100.672	112.928	
	2.0	113.60	119.50	121.30	117.80	119.40	118.32	2.91	114.701	121.939	
V12Gy	0.0	9.27	9.10	9.40	9.70	9.77	9.45	0.28	9.096	9.800	
(cc)											0.000
	0.5	10.73	10.72	10.81	10.86	11.10	10.84	0.15	10.652	11.034	
	1.0	11.74	11.70	11.83	11.82	12.26	11.87	0.22	11.591	12.146	
	1.5	14.16	13.90	14.19	14.57	14.74	14.31	0.34	13.895	14.730	
	2.0	15.99	15.93	15.93	16.17	16.83	16.17	0.38	15.694	16.644	



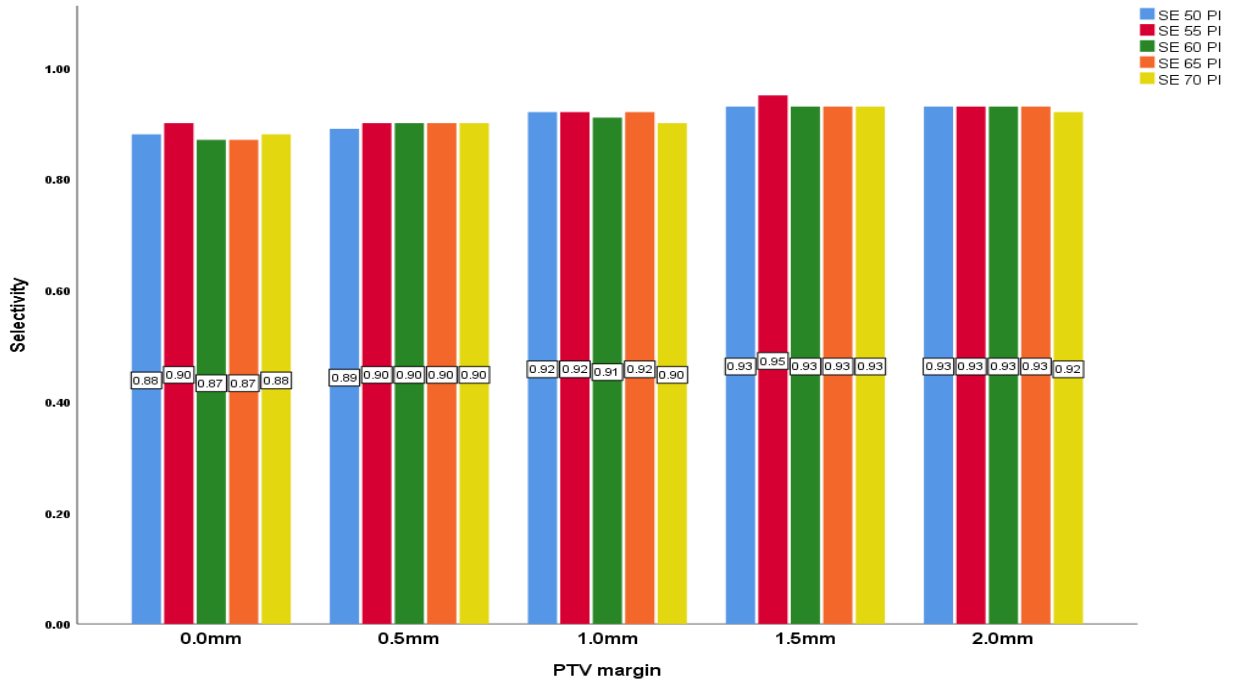


Figure 32: PTV margin and Selectivity with all Prescription Isodose



Figure 33: PTV margin and PCI with all Prescription Isodose

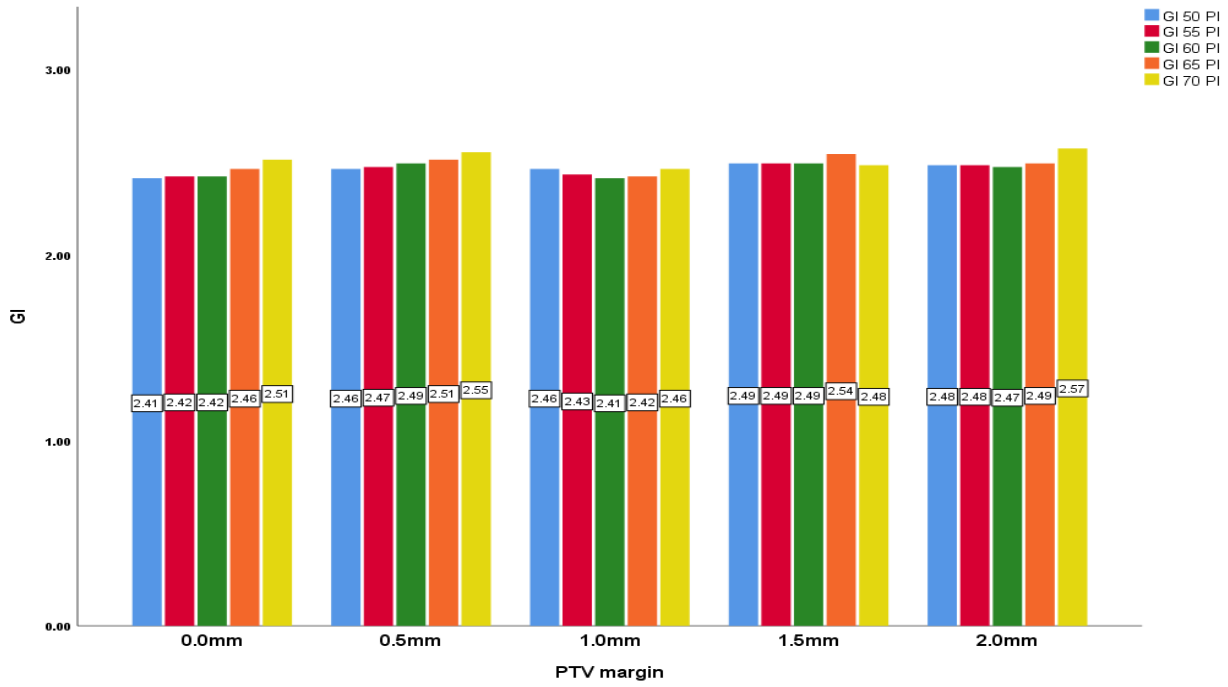


Figure 34: PTV margin and GI with all Prescription Isodose

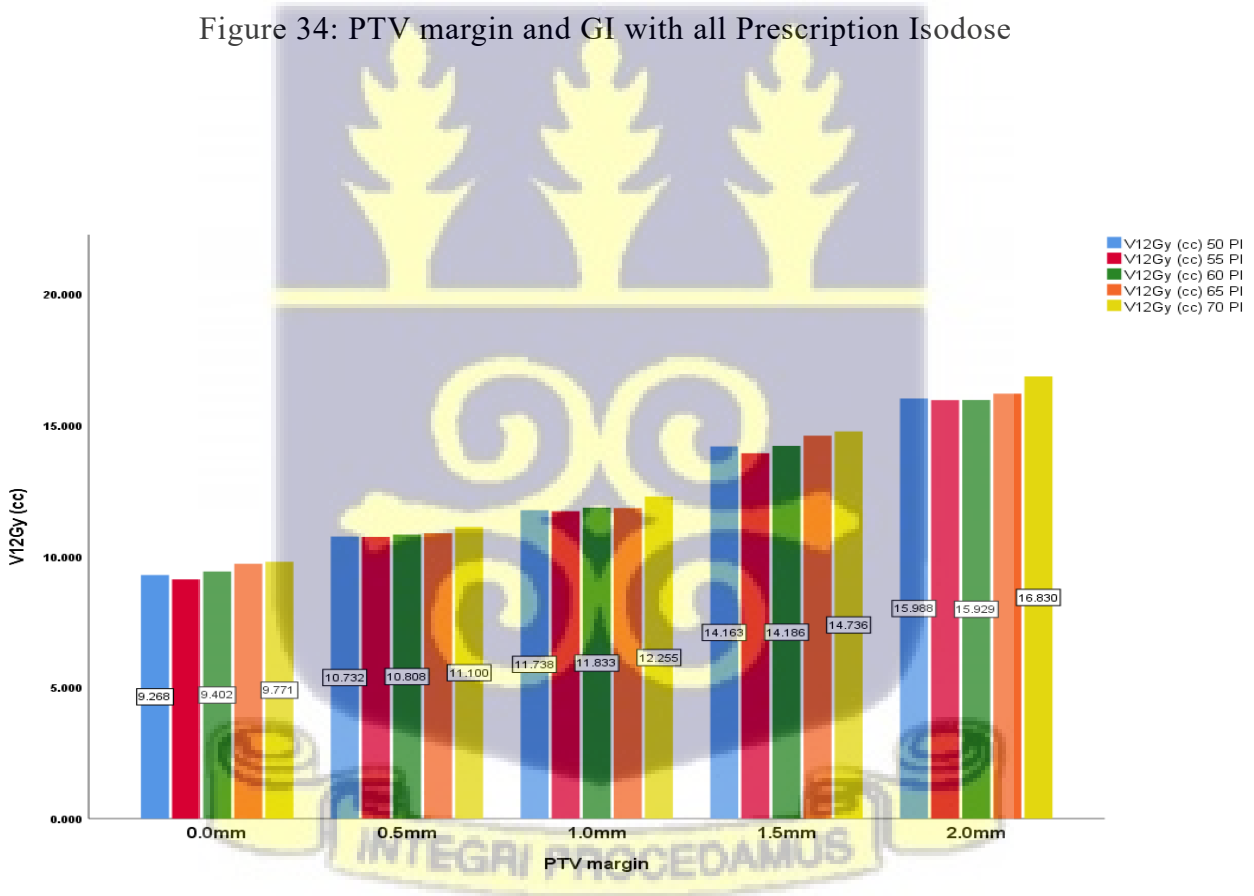


Figure 35: PTV margin and V12Gy (cc) with all Prescription Isodose

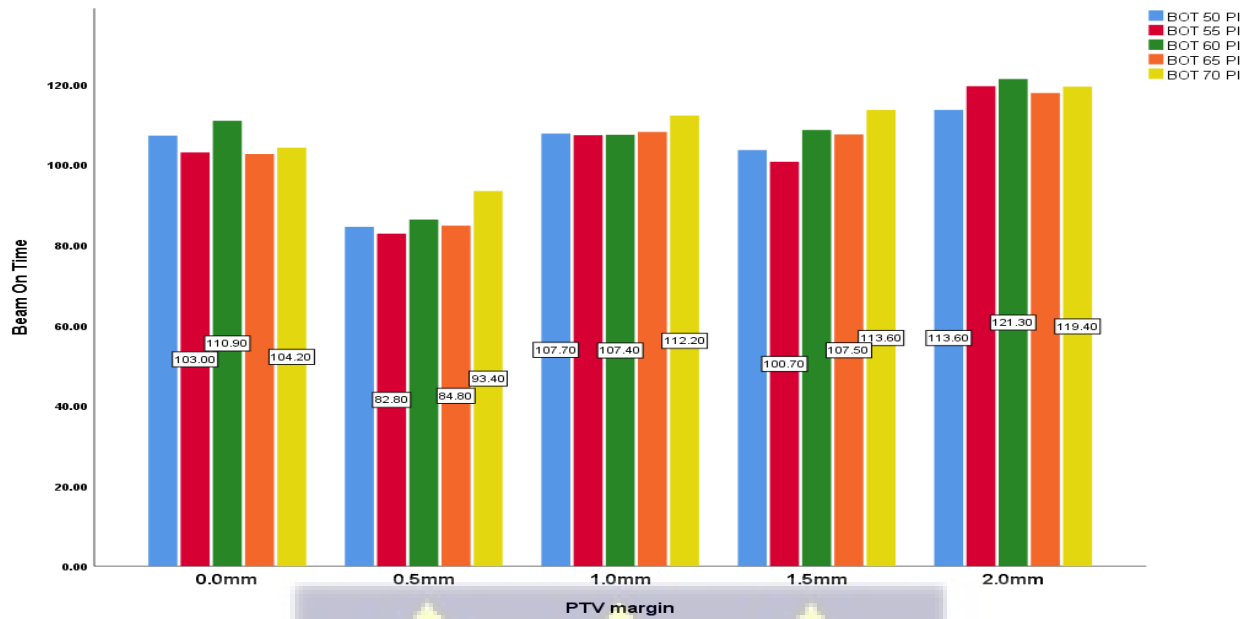


Figure 36: PTV margin and Beam-On-Time (min) with all Prescription Isodose.

4.1.2 Discussion

In this study, we explore the impact of planning target volume margins using various prescription isodose levels on plan parameters such as selectivity[S], gradient index [GI], V12, Paddicks conformal index [PCI], treatment time [TI] and organs at risk in the Gamma Knife Treatment Planning System.

4.1.2.1 Dosimetric Parameters

Values for selectivity, gradient and PCI for all margin sizes with the various prescription isodoses agreed with the ideal values set out by the International Leksell Gamma Knife Society Standardisation Committee. In the clinical setting, manual modification of the plans may be required if the ideal values are not met. The addition of margins to the GTV with the

various prescription isodose levels significantly influences all parameters. The treatment time and V12 were much higher in the 2-mm margin than 0-mm margin. It was also realized and not surprising that when a margin is added to the GTV, the treated volume increases (Xu *et al.*, 2021). The PTV margin addition to volume can be quantified in a linear relationship. The size increase may have detrimental consequences on surrounding healthy brain tissues and organs at risk (Lawrence *et al.*, 2010; Ma *et al.*, 2014). For instance, the addition of 1 mm margin and 2 mm margins resulted in a volume increase of 31% and 76% respectively as reported in table 2 above. Empirical effects of PTV margins used in SRS have been observed in the literature: Noel *et al.* (2003) selected a PTV margin of 1 mm for SRS and this improved local control, but toxicity rates were not influenced (Noël *et al.*, 2003). Nataf *et al.* (2008) found adding a PTV margin of 2 mm to single fraction SRS resulted in an increase of 12.5% in complications (Nataf *et al.*, 2008); Choi *et al.* (2012) found adding a 2 mm margin around the post-surgical cavity of brain metastasis for SRS improved local control without increasing toxicity when compared to using no margin (Choi *et al.*, 2012). Should higher margin be used, strategies such as fractionation should be considered to reduce treatment-related toxicities to the patient. This enables an adequate dose to be prescribed to the target, while limiting late side effects (Xu *et al.*, 2021).

For each PTV margin, prescribing to the 70% isodose line increased treatment delivery time and V12, with minimum impact on selectivity, gradient and Paddicks conformal indices although they increase as the prescription isodose increases from 50 to 70% as reported in table 2. The increase in gradient index has been demonstrated by Paddick and Lippitz (2006) (Paddick and Lippitz, 2006). Lower GIs (<3.0) show an appropriately positioned isocentre and a steep dose gradient. GI is reliant on the size and form of the target and affects the dose that healthy brain tissue receives (Jayaprakash *et al.*, 2022). Lowering the isodose prescription to 50% would decrease dose to normal tissues immediately outside the target

volume. This was in contrast to Brown *et al.* (2023) who found out that toxicity correlated with tumor size but not prescription isodose line (Brown *et al.*, 2023). This should be evaluated and considered in the clinical setting, especially when targets are close to sensitive organs at risk. Treatment time is one other important factor to consider for GK Inverse planning. Prolonged treatment led to patient inconvenience, distress and more treatment uncertainties (Fallows *et al.*, 2019). We also found a significant increase in treatment time when the prescription isodose level and margin increased except for the mean treatment time of the 0.5 mm margin found to be higher than the 0 mm. This might be due to lower throughput from the smaller collimation (Figure 37). This was in agreement with a study carried by Xu *et al.* (2021) who found out that at 30 and 70% prescription isodose level, the treatment time was 21.9% ($p = 0.001$) and 11.7% ($p = 0.009$) longer than at 50% prescription isodose level, respectively for a larger tumors (Xu *et al.*, 2021). In all, the largest impact of changing the isodose prescription was time saving. Such decrease in treatment times also decrease the peripheral scatter dose. Decisions on various parameters should be considered based on all facets that impact on coverage and peripheral dose.

Table 3: Dose distribution across the different margins with the various prescriptions isodose levels

Prescription		50		55		60		65		70	
Organ at Risk	PTV margin	Min (Gy)	Max (Gy)	Min (Gy)	Max (Gy)	Min (Gy)	Max (Gy)	Min (Gy)	Max (Gy)	Min (Gy)	Max (Gy)
Left Lens	0 mm	0.2	0.3	0.2	0.3	0.2	0.3	0.2	0.3	0.2	0.3
	0.5 mm	0.2	0.3	0.2	0.3	0.2	0.3	0.2	0.3	0.2	0.3
	1.0 mm	0.2	0.4	0.2	0.4	0.2	0.4	0.2	0.3	0.3	0.4

	1.5 mm	0.3	0.4	0.3	0.3	0.3	0.3	0.2	0.4	0.3	0.4
	2.0 mm	0.3	0.4	0.3	0.4	0.3	0.4	0.3	0.4	0.3	0.4
Left optic nerve	0 mm	0.7	2.2	0.6	1.8	0.6	1.9	0.7	2.1	0.8	2.2
	0.5 mm	0.7	2.1	0.7	2.1	0.7	2.1	0.7	2.0	0.8	2.3
	1.0 mm	0.8	2.3	0.8	2.3	0.8	2.3	0.7	2.1	0.8	2.3
	1.5 mm	0.8	2.3	0.9	2.2	0.9	2.1	0.7	2.1	0.9	2.4
	2.0 mm	0.9	2.4	0.9	2.4	0.9	2.5	0.9	2.5	0.9	2.1
Right lens	0 mm	0.1	0.3	0.2	0.3	0.2	0.3	0.2	0.3	0.2	0.3
	0.5 mm	0.2	0.3	0.2	0.3	0.2	0.3	0.2	0.3	0.3	0.3
	1.0 mm	0.2	0.3	0.2	0.3	0.2	0.3	0.2	0.3	0.2	0.3
	1.5 mm	0.2	0.4	0.3	0.4	0.3	0.3	0.2	0.5	0.3	0.4
	2.0 mm	0.3	0.4	0.3	0.5	0.3	0.4	0.3	0.4	0.3	0.4
Right optic nerve	0 mm	0.4	1.6	0.4	1.7	0.4	1.5	0.5	1.6	0.5	1.7
	0.5 mm	0.5	1.7	0.5	1.7	0.6	2.0	0.5	1.9	0.6	2.0
	1.0 mm	0.5	1.8	0.5	1.8	0.5	1.8	0.5	1.8	0.6	2.1
	1.5 mm	0.6	2.0	0.7	2.3	0.7	2.0	0.5	2.9	0.8	2.6
	2.0 mm	0.7	2.6	0.8	2.6	0.8	2.7	0.8	2.5	0.7	2.4
Brainstem	0 mm	0.4	5.4	0.4	4.9	0.4	5.0	0.4	4.8	0.3	4.9
	0.5 mm	0.5	4.9	0.5	5.0	0.5	5.1	0.5	5.1	0.4	5.3
	1.0 mm	0.5	5.5	0.5	5.7	0.5	5.8	0.6	5.7	0.5	5.7
	1.5 mm	0.6	6.0	0.6	6.1	0.6	5.1	0.5	6.9	0.7	6.7
	2.0 mm	0.7	6.9	0.7	6.7	0.8	6.8	0.7	7.1	0.6	6.8
Skull	0 mm	0	36	0	32.7	0	30	0	27.7	0	25.7

0.5 mm	0	36	0	32.7	0	30	0	27.7	0	25.7
1.0 mm	0	36	0	32.7	0	30	0	27.7	0	25.7
1.5 mm	0	36	0	32.7	0	30	0	27.7	0	25.7
2.0 mm	0	36	0	32.7	0	30	0	27.7	0	25.7

4.1.2.2 Organs at Risk

Careful management of radiation doses to organs at risk (OARs) is critical in all aspect of radiotherapy including SRS, particularly to minimize the potential for radiation-induced side effects. Table 3 presents result on the radiation dose distribution for each OAR, at different prescribed iso-doses and varying PTV margins.

The result shows that the left lens received a maximum dose of 0.4 Gy. The right lens received similar doses to the left lens, with maximum exposures between 0.3 and 0.4 Gy which is well below the threshold for cataract formation. Protecting both lenses should be a high priority, especially in cases where the eyes may be near the treatment field. This consistent dose-sparing across all prescribed isodoses (50-70 Gy) and planning target volume (PTV) margins (0–2.0 mm) highlights the effectiveness of the SRS in protecting the lens. While the dose recorded is well below the threshold, accumulation of even small doses of radiation can induce cataracts over time, thus maintaining this level of dose reduction is clinically significant. Studies have demonstrated that strategies such as using multi-leaf collimators (MLC) and optimized beam angles can effectively reduce lens exposure (Van Schelt, 2021). The left lens is known to be highly susceptible to radiation-induced cataracts, a common late effect in radiotherapy. A review of a study conducted by Hamada (2023) has shown that doses as low as 0.5 to 2 Gy can increase the risk of cataract formation, with the threshold for lens damage generally noted at 1 Gy (Hamada, 2023). The optic nerve is also another highly radiosensitive structure, with studies suggesting that doses

exceeding 50 Gy can lead to optic neuropathy and vision loss. Additionally, even doses as low as 10 Gy can pose a risk depending on the treatment fractionation schedule (Kinaci-Tas *et al.*, 2023). The results indicate that as the PTV margin increases, the dose to the left optic nerve also rises, reaching a maximum of 2.5 Gy at a 2.0-mm margin. While this is well below the 50-Gy neuropathy threshold, cumulative exposure over multiple treatment sessions must be managed cautiously. The optic nerve's radio-sensitivity is especially critical in patients with pre-existing conditions, such as diabetes, or those receiving concurrent chemotherapy, which can heighten the risk of optic neuropathy (Yongping Wang *et al.*, 2023). Hence, stereotactic radiosurgery (SRS) has shown potential for better sparing of the optic nerve, especially in delicate cases where standard treatments may increase the risk.

As with the left optic nerve, the right optic nerve is also vulnerable to radiation-induced neuropathy. Long-term studies have found that optic neuropathy may occur months or years after radiation, particularly if higher doses are delivered (Yongping Wang *et al.*, 2023). The right optic nerve, at a 2.0-mm PTV margin and 70-Gy prescription isodose, receives a slightly higher maximum dose of 2.7 Gy, compared to the left. While this remains below neuropathy thresholds, the dose variability underscores the importance of symmetrical and precise treatment planning with the Gamma Knife. The brainstem is also known to be vulnerable to radiation and it is imperative to protect it even with a low tolerance for radiation. Studies indicate that doses beyond 54 Gy significantly raise the risk of brainstem necrosis, which can be life-threatening (Handeland *et al.*, 2023). The brainstem receives the highest doses, with a maximum of 7.1 Gy at a 2.0-mm PTV margin and 70-Gy prescription. While this dose remains below the 54 Gy threshold, the cumulative dose should be closely monitored. The skull, being a bony structure, absorbs a significant portion of the radiation. While the skull is relatively radioresistant, the bone marrow it contains remains a concern, particularly in younger patients or those with hematologic conditions (Wolden *et al.*, 2008). The skull

receives a maximum dose of 36 Gy at a 50-Gy prescription isodose, which decreases to 25.7 Gy at a 70-Gy prescription isodose. This inverse relationship suggests that higher prescription isodoses concentrate more energy deeper within the tissues, sparing the superficial skull to some degree.

Effective management of radiation doses to organs at risk (OARs) is essential for optimizing patient outcomes while minimizing the risk of radiation-induced complications. The data from this study underscore the importance of SRS for precise dose delivery to critical structures like the optic nerves, brainstem, and lenses. Although the skull and lenses are relatively radioresistant, continued monitoring is necessary, especially for patients with pre-existing conditions or those undergoing concurrent therapies.

4.2 Impact of Various Prescription Isodose Levels using Used Margins in the LINAC-Based SRS of Single Brain Metastasis

4.2.1 Results

Across all prescription isodose and margins, the mean GI ranges from 0.42 to 0.49, with a mean of 0.46. While the CI, with values ranging from 1.06 to 1.23, with a mean of 1.12 as reported in table 2. The treatment time ranges from 4.29 to 8.22 minutes with a mean of recorded is 6.24 minutes, while there are no explicit international standards for treatment duration in SRS, shorter treatment times are desirable for patient comfort and clinical workflow efficiency. All the organs at risk were able to meet constraint set for optimization with lower values.

The maximum dose (D_{max}) to the brain, ranging from 10.58-18.03 cGy, is significantly lower than the UK 2022 guidelines. The guidelines suggest that the volume receiving 1200 cGy (V_{1200}) should not exceed 10.0 cm³ (Table 2). In this analysis, the doses received by the brain are well within these limits. The brainstem, a critical neurological structure,

demonstrates a Dmax of ranging from 420.97-706.67 cGy. These values are well below the 800 cGy limit set (Diez *et al.*, 2022).

The Dmax for the left lens ranges from 15.31–38.16 cGy, and for the right lens, 12.05-30.90 cGy as reported in table 3. Both are significantly lower than the recommended maximum of 150 cGy for lens exposure. For the left optic nerve (ON), the Dmax ranges from 145.47-247.78 cGy, while the right optic nerve has a Dmax range of 61.33–102.46 cGy (Table 3). These doses are far below the critical threshold of 600 cGy recommended by the guidelines (Diez *et al.*, 2022).

Table 4: Distribution of one sample t-test at margin 0 mm for target organs

Organs At Risk	Prescription Isodose	Mean	Standard	95% CI		P-value
		Difference	Deviation	Lower	Upper	
Brain	SRS50	100.31	175.87	-47.72	235.16	0.156
	SRS55	94.89	169.35	-63.77	261.53	0.187
	SRS60	90.95	151.67	-61.73	251.51	0.189
	SRS65	100.62	162.78	-49.33	231.24	0.164
	SRS70	96.48	153.45	-49.94	251.18	0.153
	SRS80	93.72	152.93	-45.43	238.41	0.147
Brain Stem	SRS50	-489.69	175.87	-853.77	-528.47	0.001
	SRS55	-495.11	169.35	-851.73	-538.49	0.001
	SRS60	-499.05	151.69	-839.33	-558.76	0.001
	SRS65	-489.37	162.79	-839.94	-538.82	0.001
	SRS70	-493.51	153.45	-835.43	-551.59	0.001
	SRS80	-496.27	152.93	-837.72	-554.84	0.001
Left Lens	SRS50	-39.69	175.87	-203.77	121.53	0.559
	SRS55	-45.11	169.35	-201.73	111.51	0.507

	SRS60	-49.05	151.69	-189.33	91.24	0.425
	SRS65	-39.37	162.79	-189.94	111.18	0.546
	SRS70	-43.51	153.45	-185.43	98.41	0.481
	SRS80	-46.28	152.93	-187.72	95.16	0.454
Left ON	SRS50	-489.69	175.86	-653.77	-328.47	0.001
	SRS55	-495.11	169.37	-651.73	-338.49	0.001
	SRS60	-499.05	151.69	-639.33	-358.76	0.001
	SRS65	-489.37	162.80	-639.94	-338.82	0.001
	SRS70	-493.51	153.45	-635.43	-351.59	0.001
	SRS80	-496.28	152.93	-637.72	-354.84	0.001
Right Lens	SRS50	-39.69	175.86	-203.77	121.53	0.559
	SRS55	-45.11	169.37	-201.73	111.51	0.507
	SRS60	-49.05	151.69	-189.33	91.24	0.425
	SRS65	-39.37	162.80	189.94	111.18	0.546
	SRS70	-43.51	153.45	-185.43	98.41	0.481
	SRS80	-46.28	152.93	-187.72	95.16	0.454
Right ON	SRS50	-489.69	175.86	-653.77	-328.43	0.001
	SRS55	-495.11	169.37	-651.73	-338.49	0.001
	SRS60	-499.05	151.69	-639.33	-358.76	0.001
	SRS65	-489.37	162.80	-639.94	-338.82	0.001
	SRS70	-493.51	153.45	-635.43	-351.59	0.001
	SRS80	-496.28	152.93	-637.72	-354.84	0.001

At a 0 mm margin, the mean differences for the brain across various prescription isodoses (SRS50 to SRS80) indicate a relatively high dose concentration, with SRS50 showing a mean difference of 100.31 and SRS80 at 93.72 as reported in table 4. This suggests that while lower isodoses may provide better conformity, they also risk underdosing the tumor.

The brain stem experiences significant exposure, particularly at higher isodoses, with p-values indicating strong statistical significance ($p=0.001$). This raises concerns about potential toxicity, as even slight increases in dose can lead to severe complications.

The left and right lenses, as well as the left and right ONs, show increased mean differences with higher isodoses, indicating a higher risk of radiation-induced damage. The variability in dose delivery (SD) suggests that treatment planning must account for individual anatomical differences.

Table 5: Distribution of one sample t-test at margin 0 mm for treatment metrics

Treatment Metrics	Prescription Isodose	MD	SD	95% CI		P-value
				Lower	Upper	
Conformity Index	SRS50	95.67	167.78	-44.60	235.94	0.151
	SRS55	90.93	161.01	-43.68	225.54	0.154
	SRS60	87.47	144.79	-33.57	208.53	0.131
	SRS65	95.94	155.61	-34.14	226.03	0.125
	SRS70	92.31	146.87	-30.46	215.10	0.119
	SRS80	89.90	146.16	-32.29	212.09	0.125
Gradient Index	SRS50	109.70	175.87	-54.37	270.93	0.154
	SRS55	104.29	169.35	-52.33	260.93	0.154
	SRS60	100.35	151.69	-39.93	240.64	0.131
	SRS65	110.02	162.79	-40.54	260.58	0.124
	SRS70	105.89	153.45	-36.03	247.81	0.118
	SRS80	103.12	152.93	-38.32	244.56	0.125

The CI at 0 mm is generally favourable for lower isodoses, indicating that the radiation is well-conformed to the tumor. However, as the isodose increases, the CI may decrease, suggesting a trade-off between tumor coverage and healthy tissue sparing.

The GI reflects the steepness of the dose fall-off outside the target area. At 0 mm, lower isodoses tend to have a steeper gradient, which is beneficial for protecting surrounding tissues. Table 5 above presents the report of the distribution of one sample t-test at margin 0 mm for treatment metrics

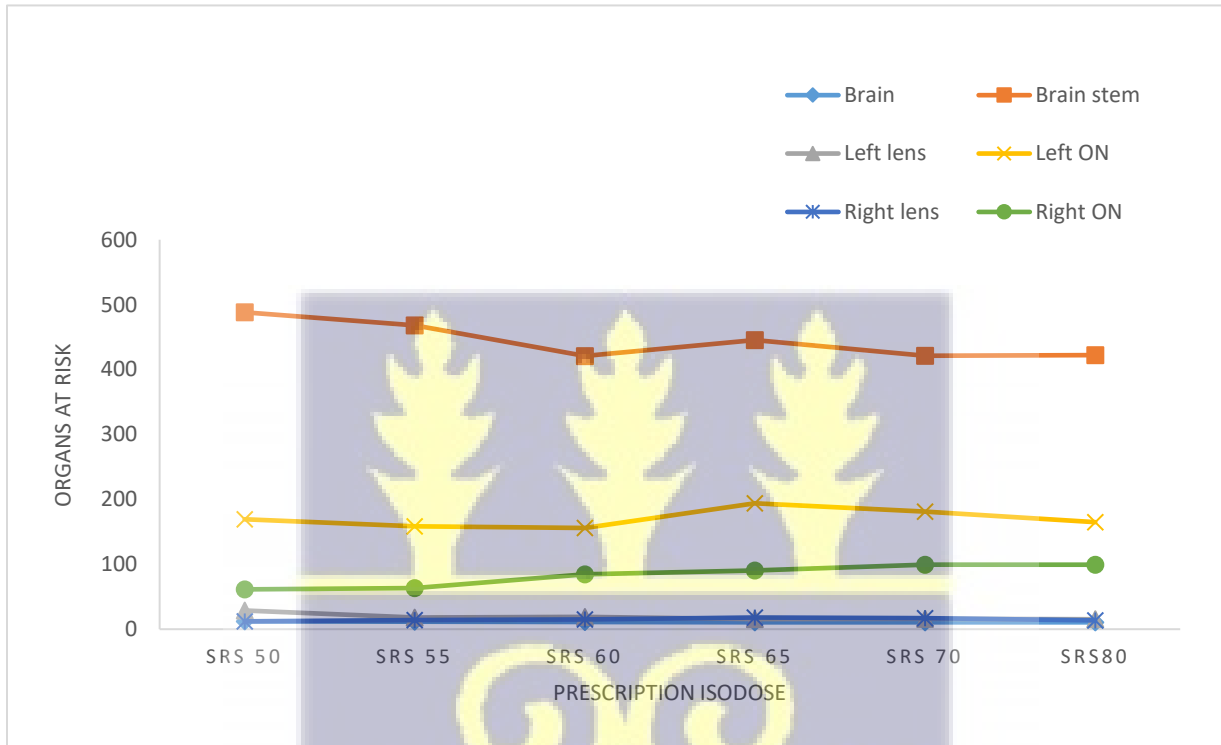


Figure 37: Distribution of the impact of prescription isodose on organs at risk at margin 0 mm

The figure 37 plots the impact of different prescription isodose levels (SRS50, SRS55, SRS60, SRS65, SRS70, SRS80) on various organs at risk such as the brain, brain stem, left lens, left optic nerve (ON), right lens, and right ON at a 0 mm margin. For the brain, the influence fluctuates slightly, across the prescription isodose, indicating that these isodose levels generally might result in slightly more dose delivery to the brain. The brain stem shows

the highest impact at SRS50 and SRS55, with decreasing doses for other levels. Both the left and right lenses show moderate values across all prescription isodoses. The optic nerves (left and right) show increasing exposure with rising isodose levels.

Higher prescription isodose levels correlate with greater exposure to the optic nerves, while the lenses show less variability. This reflects a trade-off between treating the tumor and sparing nearby sensitive structures.

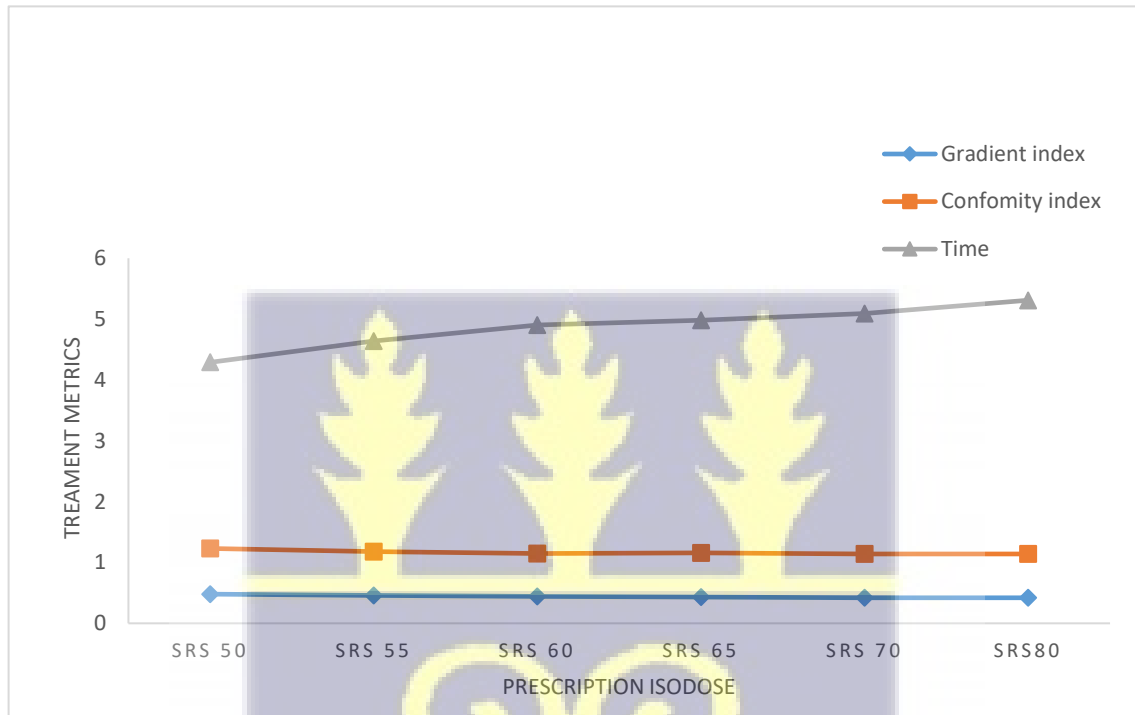


Figure 38: Distribution of the impact of prescription isodose on treatment metrics at margin 0 mm

Figure 38 assesses how different prescription isodose levels affect treatment metrics such as the gradient index, conformity index (CI), and time taken for treatment at 0 mm margin. The gradient index values remain stable across all isodose levels, showing that the tumor is consistently treated regardless of the specific isodose level. The conformity index is highest at SRS50 and decreases slightly at higher isodose levels, indicating a slight reduction as isodose levels increase. Treatment time is shorter at SRS50 and gradually increases at higher

levels (SRS65, SRS70) as reported in table 5. Lower prescription isodose levels (SRS50) are associated with better conformity and shorter treatment times, while higher levels may reduce CI and increase time without substantially altering the effect on gradient index.

Table 6: Distribution of treatment time for margin 0 mm

	SRS50	SRS55	SRS60	SRS65	SRS70	SRS80
Time(Min)	4.29	4.64	4.90	4.98	5.09	5.31

There is a clear upward trend in treatment time as the prescription isodose increases (table 6). This suggests that higher isodoses require more time to deliver the prescribed radiation dose effectively. The increments in treatment time between each isodose level are relatively small but consistent. For instance, the time increases from 4.29 at SRS50 to 5.31 min at SRS80, with each step showing a gradual increase. This pattern indicates that as the dose escalates, the complexity of the treatment delivery also increases, necessitating more time for precise administration.

Table 7: One sample t-test of margin 1 mm for organs at risk

Organs At Risk	Prescription Isodose	MD	SD	95% CI		P-value
				Lower	Upper	
Brain	SRS50	111.08	186.86	-61.74	283.89	0.167
	SRS55	121.44	195.47	-59.34	302.22	0.151
	SRS60	120.95	193.31	-57.83	299.72	0.149
	SRS65	114.38	192.50	-63.65	292.41	0.167
	SRS70	118.75	206.93	-72.63	310.12	0.180
	SRS80	118.75	206.93	-72.63	310.12	0.180
Brain Stem	SRS50	-678.92	186.86	-851.74	-506.10	0.001
	SRS55	-668.56	195.47	-849.34	-481.78	0.001

	SRS60	-669.05	193.31	-847.83	-490.28	0.001
	SRS65	-675.62	192.50	-853.65	-497.59	0.001
	SRS70	-671.25	206.93	-862.63	-479.90	0.001
	SRS80	-671.25	206.93	-862.63	-479.90	0.001
Left Lens	SRS50	-28.92	186.86	-201.74	143.89	0.696
	SRS55	-18.56	195.47	-199.34	162.22	0.810
	SRS60	-19.05	193.31	-197.83	159.73	0.803
	SRS65	-25.62	192.50	-203.65	152.40	0.737
	SRS70	-21.25	206.93	-212.63	170.12	0.795
	SRS80	-21.25	206.93	-212.63	170.12	0.795
Left ON	SRS50	-478.92	186.86	-651.74	-306.10	0.001
	SRS55	-468.56	195.47	-649.34	-287.78	0.001
	SRS60	-469.05	193.31	-647.83	-290.27	0.001
	SRS65	-475.62	192.50	-653.65	-297.59	0.001
	SRS70	-471.25	206.93	-662.63	-279.88	0.001
	SRS80	-471.25	206.93	-662.63	-279.87	0.001
Right Lens	SRS50	-28.92	186.86	-201.74	143.89	0.696
	SRS55	-18.56	195.47	-199.34	162.22	0.810
	SRS60	-19.05	193.31	-197.83	159.73	0.803
	SRS65	-25.62	192.50	-203.65	152.40	0.737
	SRS70	-21.25	206.93	-212.63	170.12	0.795
	SRS80	-21.25	206.93	-212.63	170.12	0.795
Right ON	SRS50	-478.92	186.86	-651.74	-306.10	0.001
	SRS55	-468.56	195.47	-649.34	-287.78	0.001
	SRS60	-469.05	193.31	-647.83	-290.27	0.001
	SRS65	-475.62	192.50	-653.65	-297.59	0.001
	SRS70	-471.25	206.93	-662.63	-279.88	0.001
	SRS80	-471.25	206.93	-662.63	-279.88	0.001

At a 1 mm margin, the mean differences for the brain show a slight increase compared to the 0 mm margin, indicating that the additional margin may lead to increased exposure to healthy

tissues (Table 7). For example, the mean difference for SRS50 is 111.08, which is higher than at 0 mm. The brain stem continues to show significant exposure, with p-values remaining low, indicating that the risk of toxicity persists. The additional margin may not sufficiently mitigate this risk. The mean differences for the lenses and ONs at 1 mm are also elevated, suggesting that the added margin does not significantly reduce the risk of radiation exposure to these critical structures.

Table 8: One sample t-test of margin 1 mm for treatment metrics (GI and CI)

Treatment Metrics	Prescription Isodose	MD	SD	95% CI		P-value
				Lower	Upper	
Conformity Index	SRS50	105.08	178.12	-43.83	254.00	0.139
	SRS55	114.14	186.74	-41.97	270.26	0.127
	SRS60	113.71	184.76	-40.74	268.17	0.125
	SRS65	107.96	183.47	-45.41	261.35	0.140
	SRS70	111.79	196.82	-52.75	276.33	0.152
	SRS80	111.79	196.82	-52.75	276.33	0.152
Gradient Index	SRS50	120.48	186.86	-52.34	293.29	0.139
	SRS55	130.84	195.47	-49.94	311.62	0.127
	SRS60	130.35	193.31	-48.43	309.12	0.125
	SRS65	123.78	192.50	-54.25	301.81	0.140
	SRS70	128.15	206.93	-63.23	319.52	0.152
	SRS80	128.65	206.93	-63.23	319.52	0.152

The CI may improve slightly at 1 mm compared to 0 mm, as the additional margin allows for better targeting of the tumor while potentially reducing exposure to surrounding tissues.

The GI show a less steep fall-off compared to 0 mm (tables 7&8), indicating a broader area of exposure, which could increase the risk of damage to adjacent healthy tissues.

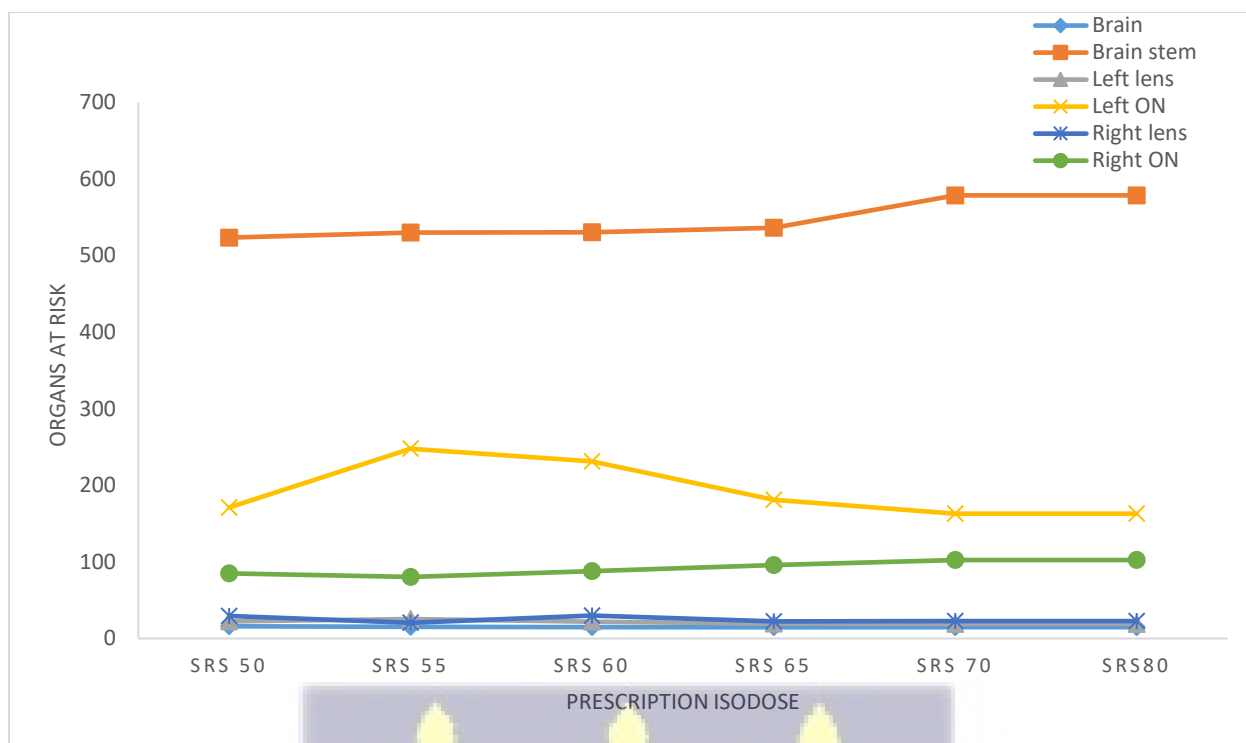


Figure 39: Distribution of the impact of prescription isodose on organs at risk at margin 1 mm

Figure 39 analyses the effects of prescription isodose levels on the brain, brain stem, lenses, and optic nerves at a 1 mm margin. The brain receives slightly increased exposure compared to the 0 mm margin, with the highest impact at SRS55. The Brain Stem again shows its highest exposure at SRS50, with values decreasing at higher levels. The lenses, particularly the left lens, receive increased exposure at this margin, particularly at SRS55. Both optic nerves (left and right) show increased exposure at higher isodose levels, with the right ON receiving more at SRS55 and SRS60. Increasing the margin from 0 mm to 1 mm slightly increases the exposure to critical structures, especially the optic nerves and lenses, while the Brain Stem shows some protection at higher isodose levels.

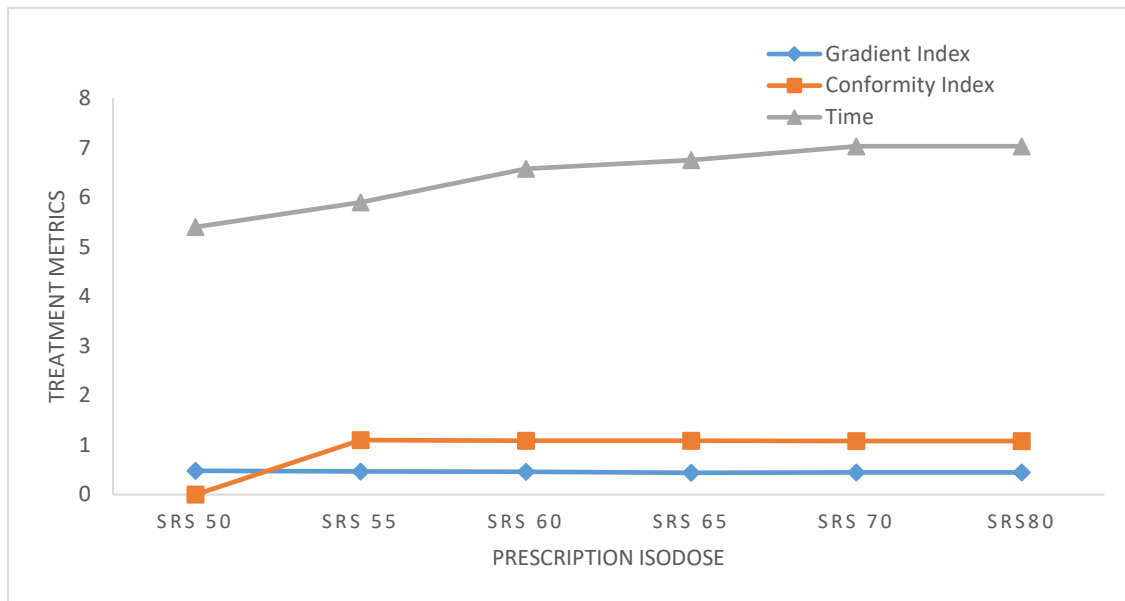


Figure 40: Distribution of the impact of prescription isodose on treatment metrics (GI and CI) at margin 1 mm

Figure 40 also plots gradient index, conformity index, and treatment time, but at a 1 mm margin. The gradient values remain consistent across all isodose levels, similar to the 0-mm margin. The conformity index shows a slight reduction compared to the 0-mm margin, particularly at SRS55, indicating treatment time increases slightly, with higher values seen at SRS70 and SRS80. This trend indicates that higher isodoses require more time for delivery. While gradient is stable, the 1-mm margin leads to reduced (CI) and longer treatment times, especially at higher prescription levels.

Table 9: Distribution of treatment time for margin 1 mm

	SRS50	SRS55	SRS60	SRS65	SRS70	SRS80
Time(Min)	5.40	5.90	6.58	6.75	7.03	7.03

The data table 9 shows a consistent increase in treatment time as the prescription isodose increases. Starting from 5.40 min at SRS50, the time rises to 7.03 min at both SRS70 and SRS80. likely due to the need for more complex radiation delivery techniques to ensure accurate targeting.

Table 10: Distribution of sample t-test for margin 2 mm

Organs At Risk	Prescription Isodose	MD	SD	95% CI		P-value
				Lower	Upper	
Brain	SRS50	116.31	189.33	-57.36	292.85	0.151
	SRS55	115.83	197.75	-63.68	302.09	0.162
	SRS60	125.10	203.93	-65.22	311.98	0.161
	SRS65	128.75	211.28	-68.75	322.06	0.164
	SRS70	121.91	215.69	-79.34	319.63	0.191
	SRS80	145.21	253.55	-89.02	379.97	0.180
Brain Stem	SRS50	-473.69	189.33	-649.18	-298.20	0.001
	SRS55	-474.17	197.75	-658.23	-290.12	0.001
	SRS60	-464.90	203.93	-652.95	-276.84	0.001
	SRS65	-461.25	211.28	-656.33	-266.18	0.001
	SRS70	-468.09	215.69	-667.58	-268.60	0.001
	SRS80	-444.79	253.55	-679.58	-209.99	0.004
Left Lens	SRS50	-23.69	189.33	-199.18	157.80	0.752
	SRS55	-24.17	197.75	-208.23	159.88	0.759
	SRS60	-14.90	203.93	-202.95	173.16	0.853
	SRS65	-11.25	211.28	-206.33	183.82	0.892
	SRS70	-18.09	215.69	-217.58	181.41	0.832
	SRS80	-5.21	253.55	-229.59	240.00	0.958

Left ON	SRS50	-473.69	189.33	-647.36	-297.15	0.001
	SRS55	-474.17	197.75	-653.68	-287.91	0.001
	SRS60	-464.90	203.93	-655.22	-278.02	0.001
	SRS65	-461.25	211.28	-658.75	-267.94	0.001
	SRS70	-468.09	215.69	-669.34	-270.37	0.001
	SRS80	-444.79	253.55	-679.02	-210.03	0.004
Right Lens	SRS50	-23.69	189.33	-199.18	157.80	0.752
	SRS55	-24.17	197.75	-208.23	159.88	0.759
	SRS60	-14.90	203.93	-202.95	173.16	0.853
	SRS65	-11.25	211.28	-206.33	183.82	0.892
	SRS70	-18.09	215.69	-217.58	181.41	0.832
	SRS80	-5.21	253.55	-229.59	240.00	0.958
Right ON	SRS50	-473.69	189.33	-199.18	157.80	0.752
	SRS55	-474.17	197.75	-208.23	159.88	0.759
	SRS60	-464.90	203.93	-202.95	173.16	0.853
	SRS65	-461.25	211.28	-206.33	183.82	0.892
	SRS70	-468.09	215.69	-217.58	181.41	0.832
	SRS80	-444.79	253.55	-229.59	240.00	0.958

At a 2 mm margin, the mean differences for the brain are further elevated, indicating a significant increase in radiation exposure as reported in table 10. For instance, the mean difference for SRS50 is 103.12, which reflects a concerning trend of increasing dose to healthy tissues as the margin widens.

The risk to the brain stem remains high, with significant mean differences and low p-values reported in table 10 indicating that the additional margin does not adequately protect this critical structure from radiation exposure.

The mean differences for the lenses and ONs at 2 mm are concerning, as they indicate a continued risk of radiation-induced damage. The increase in margin does not appear to provide sufficient protection for these sensitive areas.

Table 11: One sample t-test of margin 2 mm for treatment metrics (CI and GI)

Treatment Metrics	Prescription Isodose	MD	SD	95% CI		P-value
				Lower	Upper	
Conformity Index	SRS50	109.65	178.12	-43.83	254.00	0.139
	SRS55	109.23	186.74	-41.97	270.26	0.127
	SRS60	117.34	184.76	-40.74	268.17	0.125
	SRS65	120.54	183.47	-45.41	261.35	0.140
	SRS70	114.55	196.82	-52.75	276.33	0.152
	SRS80	134.94	196.82	-52.75	276.33	0.152
Gradient Index	SRS50	125.71	181.16	-41.80	261.11	0.131
	SRS55	125.23	189.45	-49.15	267.62	0.147
	SRS60	134.50	194.12	-44.94	279.64	0.131
	SRS65	138.15	201.25	-47.71	288.79	0.134
	SRS70	131.31	204.99	-56.82	285.93	0.158
	SRS80	154.61	241.27	-66.76	336.65	0.158

The CI decreased at 2 mm in table 11, suggesting that while the tumor may receive a higher dose, the risk of surrounding healthy tissue exposure increases, complicating treatment outcomes.

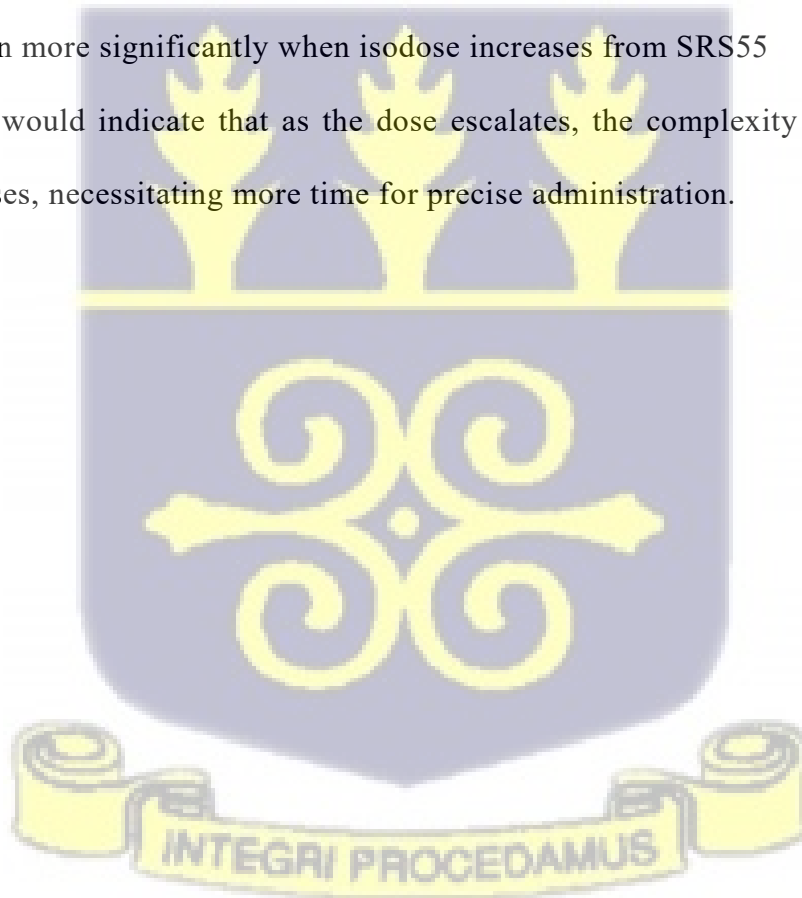
The GI at 2 mm may show a flatter dose distribution, indicating a broader area of exposure, which could lead to increased toxicity risks for adjacent healthy tissues.

Table 12: Distribution of treatment time at margin 2 mm

	SRS50	SRS55	SRS60	SRS65	SRS70	SRS80
Time(Min)	6.29	7.06	7.77	8.22	7.83	7.4

The data in table 12 show an increase in treatment time as the prescription isodose increases. This trend is consistent with findings from the 1 mm margin, where higher isodoses necessitate more complex radiation delivery techniques, leading to longer treatment durations.

The increments in treatment time between each isodose level although small, is very important. For instance, if the time increases when the isodose increases from SRS50 to SRS55, and then more significantly when isodose increases from SRS55 to SRS60, this would indicate that as the dose escalates, the complexity of the treatment delivery increases, necessitating more time for precise administration.



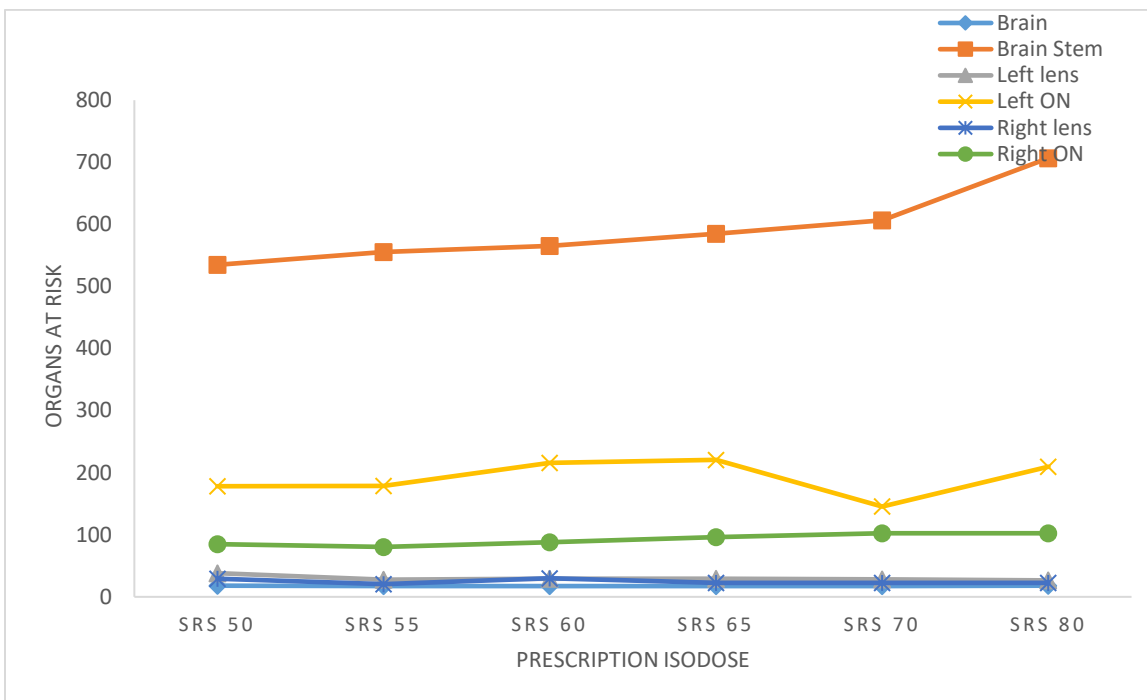


Figure 41: Distribution of the impact of prescription isodose on organs at risk at margin 2

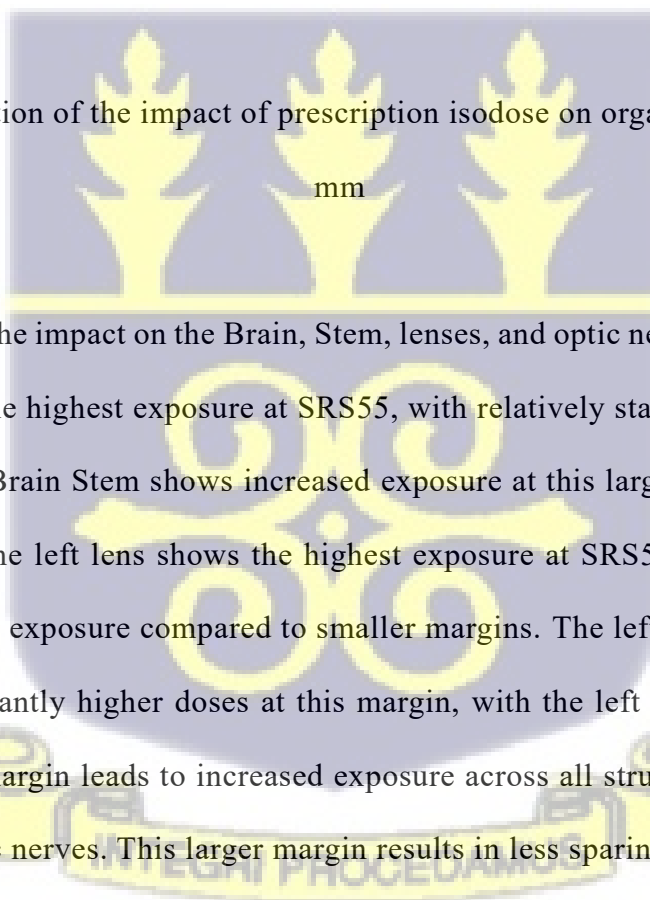


Figure 41 examines the impact on the Brain, Stem, lenses, and optic nerves at a 2 mm margin. The brain receives the highest exposure at SRS55, with relatively stable values across other isodose levels. The Brain Stem shows increased exposure at this larger margin, with values peaking at SRS80. The left lens shows the highest exposure at SRS55, while the right lens also shows increased exposure compared to smaller margins. The left and right optic nerves both receive significantly higher doses at this margin, with the left ON showing a peak at SRS65. The 2 mm margin leads to increased exposure across all structures, particularly the Brain Stem and optic nerves. This larger margin results in less sparing of critical structures.

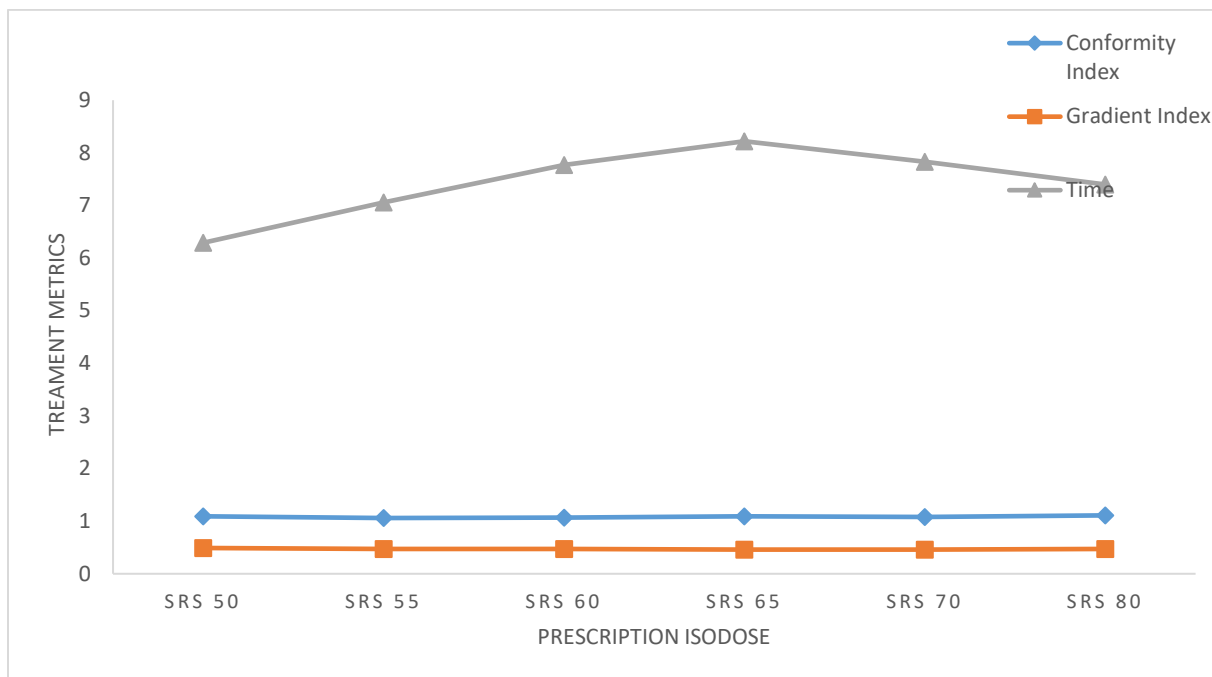


Figure 42: Distribution of the impact of prescription isodose on treatment metrics at margin

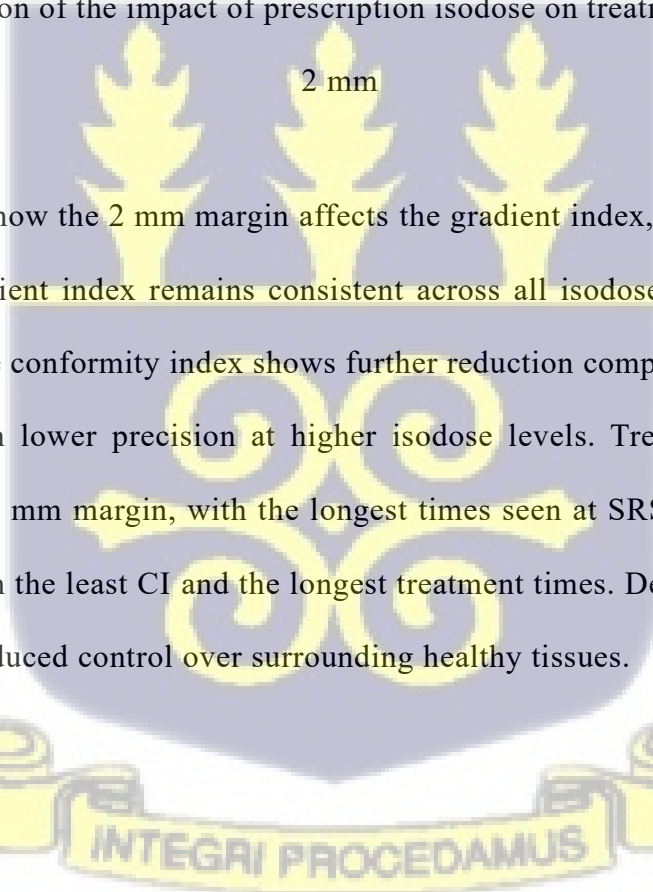


Figure 42 evaluates how the 2 mm margin affects the gradient index, conformity index, and treatment time. gradient index remains consistent across all isodose levels, similar to the smaller margins. The conformity index shows further reduction compared to both 0 mm and 1 mm margins, with lower precision at higher isodose levels. Treatment time increases significantly at the 2 mm margin, with the longest times seen at SRS65 and SRS70. The 2 mm margin results in the least CI and the longest treatment times. Despite consistent tumor targeting, there is reduced control over surrounding healthy tissues.

4.2.2 Discussions

The gradient index and conformity index are two important and integral dose metrics used in the evaluation of LINAC -based SRS plans. gradient index (GI) was developed for stereotactic radiosurgery (SRS) treatment modalities in which a sharp dose gradient is

required. The gradient index definition has been expanded for SBRT treatment of extracranial small lesions using hypo-fractionated plans (Simon *et al.*, 2022). Because of the small volume target in SRS, a strong dose gradient is readily desired, leading in improved CI. In the event of greater volume, GI has a low value, but it is still a viable option to consider when evaluating plans (G. Patel *et al.*, 2020). As the target volume gets larger, the PIDL also becomes higher. The range of prescription isodose level evaluated in the LINAC-based system was from 50 to 80% with margin addition (0 mm, 1 mm and 2 mm) to the GTV. It is not advisable to choose a PIDL less than 50% because of large heterogeneity in dose distribution (Zhao *et al.*, 2014). In fact, differences in PIDL for targets with margin addition of 0 mm, 1 mm and 2 mm was seen. GI is very sensitive to the shape, the location of the target and the beam settings.

Prescribing to a lower isodose line (50, 55, 60, and 65%) resulted in a steeper dose gradient, leading to a lower GI but enhances CI. This sharp fall-off helps protect adjacent critical structures from high radiation doses, reducing the risk of complications such as radiation necrosis. Conversely, higher PIDLs (70 and 80%) lead to a broader distribution of radiation dose around the target. This results in an increased GI (p-value = 0.158) indicating a less steep dose gradient and potentially higher volumes of normal tissue receiving significant doses.

When comparing SRS80 to other isodose levels, such as SRS70 and SRS65, it is evident that SRS80 offers a higher dose to the tumor but at the cost of increased exposure to surrounding healthy tissues across all the margins used but especially with 2 mm. SRS80 may lead to even greater risks of toxicity similar to study by Zhang *et al.* (2014) (Zhang *et al.*, 2014).

The trade-off between effective tumor control and the risk of damage to surrounding tissues is evident, and SRS80 may not be the optimal choice for tumors located near critical structures. As the tumor volume increases as a result of the margin addition, with 2 mm and

SRS80 might provide effective tumor coverage, but might increase dose to surrounding healthy tissues significantly except at 0 mm where the brainstem recorded slightly higher dose at SRS50 and SRS55. The treatment time also increases, which might be uncomfortable for patient management.

The lower isodose levels, such as SRS50, are associated with better conformity and shorter treatment times, which can enhance patient outcomes. The lower doses delivered to critical structures at this margin suggest that SRS50 may be a safer option for patients, particularly those with tumors located near sensitive areas (Xu *et al.*, 2019).

When the margin is increased to 1mm, the exposure to surrounding healthy tissues begins to rise, although the increase is less pronounced compared to higher isodose levels (Badloe *et al.* 2021; Jhaveri *et al.*, 2019). The CI shows a slight reduction, but the GI remains stable. The treatment time increases slightly, which may be attributed to the need for more complex planning and delivery techniques.

Overall treatment time remains a critical factor in SRS procedures. Higher PIDLs lead to longer treatment sessions due to increased complexity in achieving precise dose distributions while maintaining safety margins for surrounding tissues but in this case the highest treatment time was found with margin increase of 2 mm. This was recorded with SRS 65% and 70% contrary to plans that used a 70-80% prescription isodose level according to a study by Hellerbach *et al.* (2022) (Hellerbach *et al.*, 2022). This might be due to different planning techniques and equipment used.

Shorter treatment times are essential for maximizing patient throughput in busy clinical settings. The selection of appropriate PIDLs that balance dose distribution with efficiency can help optimize scheduling and resource allocation (Ohtakara *et al.*, 2012) .

Therefore, in order to prevent significant dose variability, we advise 50-65% for targets with no PTV margin addition. According to this research, when a big margin like 1 or 2 mm is

employed, 70 and 80% prescription isodoses seem to be a good balance between GI, CI and the organs at risk especially the brain which may be linked to the risk of radio-necrosis. According to a study by Zhao *et al.* (2014) (Zhao *et al.*, 2014). It was discovered that the ideal PIDL for LINAC -based intracranial SRS fell between 50 and 75 percent. By contrast, 50% is often recommended for SRS based on Gamma Knife technology. The average PIDL for CyberKnife is 80%, although there is no indication that 80% is ideal. According to one other research, the ideal PIDL for CyberKnife is around 40%; however, this study was predicated on phantom experiments for extracranial intervention (Ding *et al.*, 2013). Many institutions employed PIDLs of 80-90% for LINAC -based SRS employing a dynamic conformal arc method, whereas a small number of centres used 70-80%. In a comparison of three widely used PIDLs, Ohtakara *et al.* (2012) (Ohtakara *et al.*, 2012), discovered that 70% performed better than 80 or 90%. The doses ranges from 5 to 9.4 cm³, whereas their study's target volumes varied from 7.4 to 25.9 cm³. Nevertheless, the tumor volume may also influence the best PIDL to choose. The ideal PIDL reduces when the tumor volume shrinks. The ideal PIDL for tumor sizes ranging from 1 to 7 cm³ was discovered to be 55%, a much smaller value than 70% and 80%. Five arcs that spread out at various couch angles are usually used in a dynamic conformal arc plan, and an isotropic dose fall-off is usually obtained around the target volume. The linear accelerator's physical properties, including the width of the leaves of the MLC, the beam quality and penumbra, the intra- and inter-leaf transmission, etc., set a limit on the GI. As shown above, adding more arcs than five only slightly improves GI (Ruggieri *et al.*, 2018).

An optimal PIDL helps achieve a balance between adequate tumor coverage and minimal exposure to normal tissues (Dimitriadis and Paddick, 2018). Understanding how PIDLs influence CI and GI can help clinicians minimize risks associated with LINAC -based SRS, particularly in sensitive areas like the brain.

4.3 Dosimetric Accuracy of LINAC -based SRS Plans Using the Newly Introduced Wireless Delta 4 Phantom+ Device.

4.3.1 Results

The analysis of all plans included the use of the three most suitable parameters: the dosimetric accuracy (with a limit of 2%), DTA (with a limit of 2 mm), and gamma pass rate. Table 13 summarises the results of gamma passing rate, distance to agreement and dose deviation of all plans with the different prescription isodose level. Overall, in all cases excellent agreement was seen between measured and calculated TPS doses. The minimum gamma passing rate was 99.6% and the maximum 100%. The gamma passing rate for all plans was higher than 95% using 2%/2 mm DD/ DTA. It can be observed that our criteria of 95% for the gamma index was met for all plans with all the different prescription isodose levels used. The correction factor was found to be 1.01. Figure 44 presents The Delta4 phantom+ software displaying the result. The absolute dosage is shown in two diode arrays in three dimensions on the top panel, with colour coding used to indicate the dose. Similarly, figure 45 also presents The Delta4 phantom+ software displaying three histograms: distance to agreement, dose deviation and gamma index.

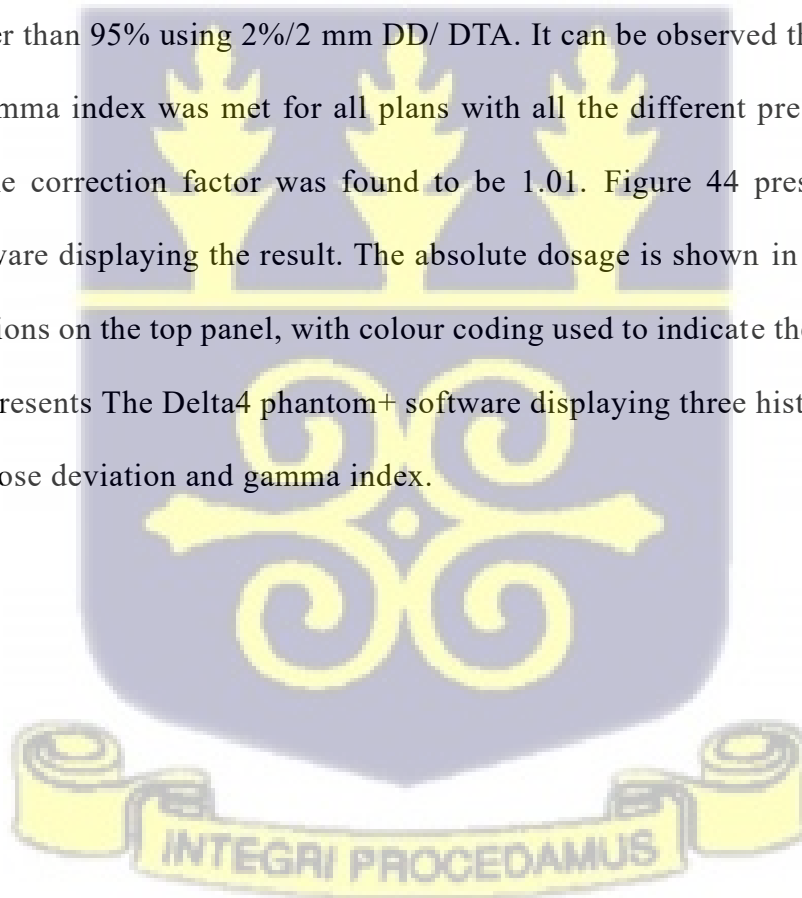


Table 13: Gamma index rate, distance to agreement and dose deviation of different prescription isodose.

ASSESSMENT PARAMETERS	MARGIN USED(mm)	PRESCRIPTION ISODOSE LEVEL					
		50%	55%	60%	65%	70%	80%
Gamma Index passing rate 2%/2mm	0	99.7	99.8	99.9	99.9	100	100
	1	99.6	99.7	99.9	99.7	99.8	100
	2	99.9	100	100	100	99.8	99.8
DoseDeviation (DD)	0	76.0	76.0	79.1	80.3	81.1	83.4
	1	76.1	76.1	79.5	80.7	81.5	83.7
	2	76.2	76.2	79.9	80.9	81.7	83.9
Dose to Time Agreement	0	100	100	100	100	100	100
	1	100	100	100	100	100	100
	2	100	100	100	100	100	100

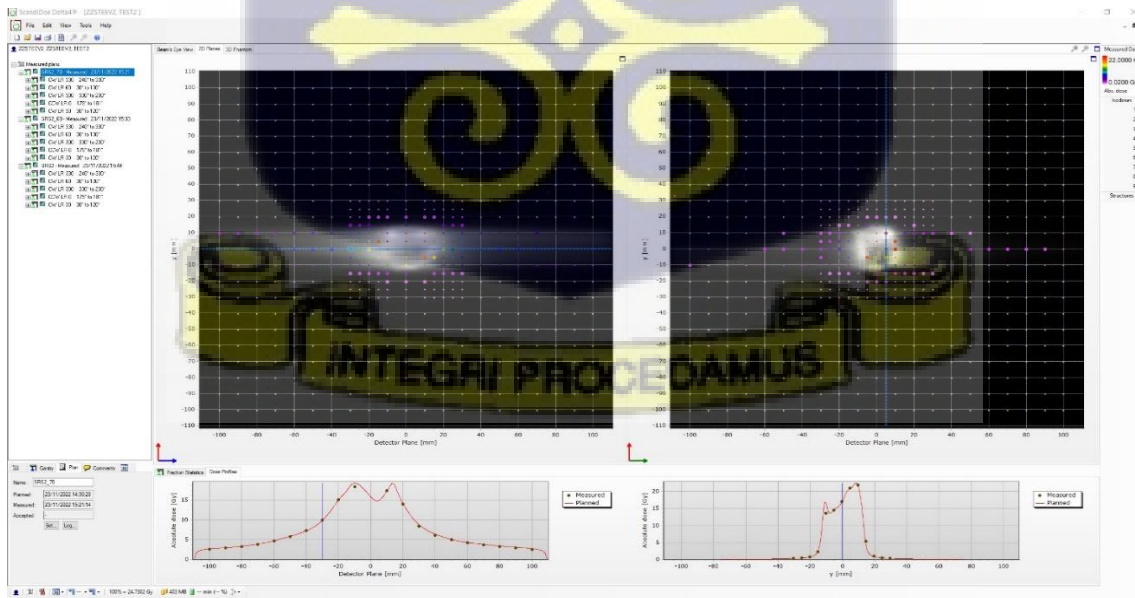


Figure 43: The Delta4 phantom+ software displaying the result. The absolute dosage is shown in two diode arrays in three dimensions on the top panel, with colour coding used to indicate the dose.

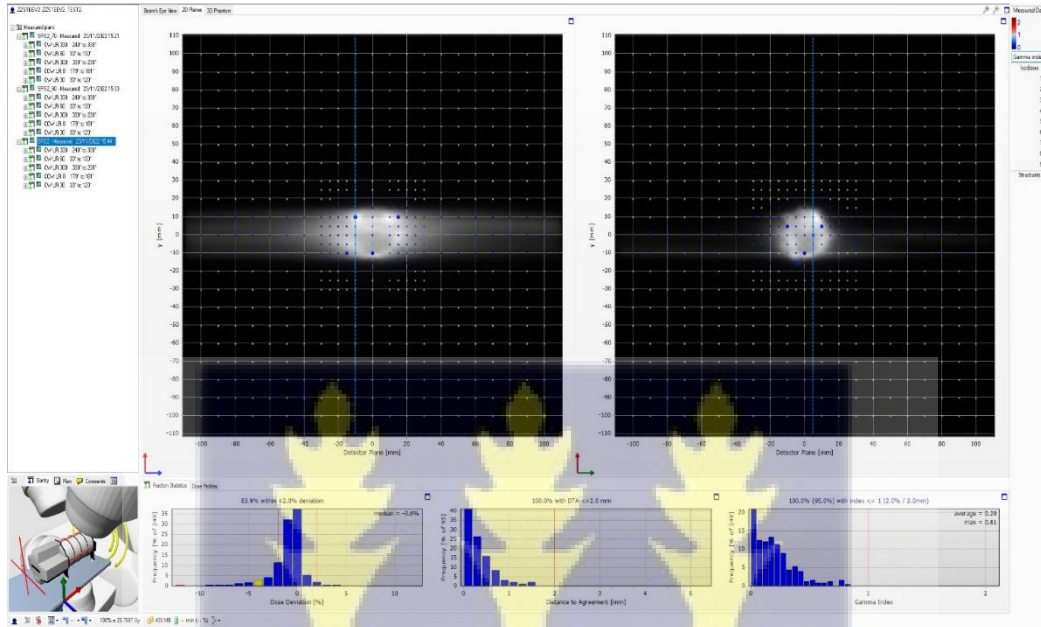


Figure 44: The Delta4 phantom+ software displaying three histograms: distance to agreement, dose deviation and gamma index.

4.3.2 Discussion

The use and suitability of the wireless Delta4+ Phantom was assessed for treatment verification of LINAC -based SRS plans made with different prescription isodose levels. We compared measurement made with phantom and treatment planning dose. We found the wireless Delta4 Phantom+ as an easily set-up device with minimal positional errors that provide consistent and comprehensive quality assurance suitable for SRS plans. Its functionality is identical to the plug-in Delta4 Phantom with a few exceptions (Srivastava and De Wagter, 2019). The wireless system, real-time results, its waterproof construction,

and ease of use make it well-suited to the measurement of small field and composite SRS plans.

To assure the accuracy of patient-specific QA testing, Delta4's first calibration and commissioning procedure must be completed with rigorous and precise measurements. It enables complete analysis of data and a quicker approach to conduct measurements without the need for additional QA systems. Measurements are taken on the phantom's two planes, and the software generate a 3D dose distribution using an interpolation approach (Delta4 Phantom+:The Fastest and most accurate 4D verification system, 2022).

There are documented evidence of the use of other detectors in SRS, such as ionization chambers, alanine pellets, plastic scintillators, Sun Nuclear Corporation (SNC) ArcCHECK , SNC SRS MapCHECK, IBA Matrixx Resolution, electronic portal imaging device (EPID) and IBA myQA SRS but their scope of operation varies (James *et al.*, 2023; Sasaki *et al.*, 2020).

The gamma index serves as a valuable tool in dosimetric verification analysis, allowing for a comparison between the TPS plan and the measurement (Figure 45). It provides a metric to assess the level of agreement in dose. It is commonly utilized for patient-specific quality assurance. The minimum gamma pass rate was 99.6% and the maximum 100%. The gamma passing rate was found to be above 95% for all plans. Dose goals were also achieved. Developing a centre-specific protocol is crucial, as the gamma index is influenced by the treatment planning and setup. Various factors can impact the final result, such as the type and sensitivity of the detector, algorithm of TPS, linear accelerator (LINAC) output and clinical judgement of dose tolerance level (Das *et al.*, 2022).

It is important to mention that the DTA and DD criteria utilised for gamma analysis are not entirely independent. They have a connection to the dose gradient factor. It is widely accepted that a passing rate of 90% with a 3 mm/3% clinical significance is commonly used for most

highly advanced treatment techniques (Li *et al.*, 2011). In this study a different gamma passing rate of 95 with a 2 mm/2% was used due to the sharp dose gradient in SRS. However, should our gamma index pass rate had been less than 95%, further verification would be necessary with any of the other's detectors such as gafchromic film. According to Nelms *et al.* (2011) Gamma passing rates using the criterion of (3%, 3 mm) are insensitive to clinically meaningful patient dose mistakes on a field by field basis (Nelms *et al.*, 2011).

Sadagopan *et al.* validated the accuracy and reproducibility of Delta4 device in comparing its results to measurement with film and an ion chamber (Sadagopan *et al.*, 2009). Similarly, Bedford *et al.* (2009) found that Delta4 demonstrated slightly stronger correlation between calculated and measured doses compared to the film. It is possible that this is due to the absolute nature of Delta4 measurements in contrast to the relative nature of film dosimetry (Bedford *et al.*, 2009).

Our measured pass rates were comparable with the rates of other detectors using the same pass criteria when used for treatment verification for VMAT Plans. The minimum gamma passing rate in our study was higher when compared to EBT-XD Film 96.70%, EPID 95.93%, SRSSMapCHECK 96.76%, and myQA SRS 97.91% using the same passing criteria 2%/2 mm (James *et al.*, 2023). Furthermore, in a study by Desai *et al.* (2021) the performance of the Delta4+ Phantom was evaluated by measuring 36 clinical cases using a ViewRay MRIdian LINAC. The findings were found to be identical to those obtained utilising a Sun Nuclear ArcCHECK. Both devices met the institution's 95% pass rate for a 3%/3mm gamma requirement but the use of 2%/2 mm gamma passing rates revealed subtle variances amongst the devices with the Delta4+ being a little superior in terms of the results (Desai *et al.*, 2021). The application of 2%/2 mm as a gamma parameter provided excellent sensitivity and minimum fluctuation. The detector's resolution allows for good visualization of the gamma

distribution graphically on the software. This is a very valuable visual tool for identifying regions of overdose and underdose (Woon *et al.*, 2018).

Our final measured gamma pass rates may be influenced by some factors such as the True Beam LINAC output variability, user configuration, and detector settings. However, it is challenging to separate these factors from the final findings. Moreover, the selection of a SRS quality assurance (QA) detector is contingent upon several elements that vary between institutions. These considerations include prior expertise, financial resources, user-friendliness, as well as the sensitivity and specificity requirements that align with the institution's unique SRS QA criteria (James *et al.*, 2023; Korreman *et al.*, 2009). Hence, it is important to interpret the gamma pass rates presented in this study as a validation of the Delta4 Phantom+ as suitable for SRS treatment verifications, rather than as a direct method for comparing it with the other detectors. Furthermore, although we recommend the use of 2%/2 mm because of the great degree of agreement our investigation was able to attain, other tight gamma parameters such 2%/1 mm or 1%/1 mm could be explored due to the high dosimetric accuracy of stereotactic treatments (Xia *et al.*, 2020).

4.4 Opinions of Some Planning Medical Physicists with Experience in SRS Treatment Planning on Margin Additions in the SRS Treatment of Single Brain Metastasis.

4.4.1 Results

The following is a summary of the responses to the five questions that were provided by 10 medical physicists who have expertise in planning SRS. These responses are shown in figures 46 and 47. The questions that were the most contentious and did not get a unanimous answer were those that concerned the incorporation of CTV expansion margin into the GTV and the utilization of CTV-PTV margins in SRS. The response rate for these questions was one hundred percent. The maximum and ideal margin expansions to be employed was 1 mm, and

this was suggested by five out of the ten, which represents fifty percent. The development of margins formulae specifically for SRS needs was supported by 80% of the respondent. The support of 80% of respondents for this initiative underscores the importance of addressing this issue in the field of radiation oncology. The only question with a high percentage of agreement was, should target contouring be compulsory in the treatment of brain metastasis with SRS. Also, there was no response favouring the use of 1.5 mm as an appropriate PTV margin in SRS treatment planning, as in Figure 46. As a consequence of the fact that it could be challenging to generate a PTV margin of 1.5 mm when using the LINAC -based treatment planning system.

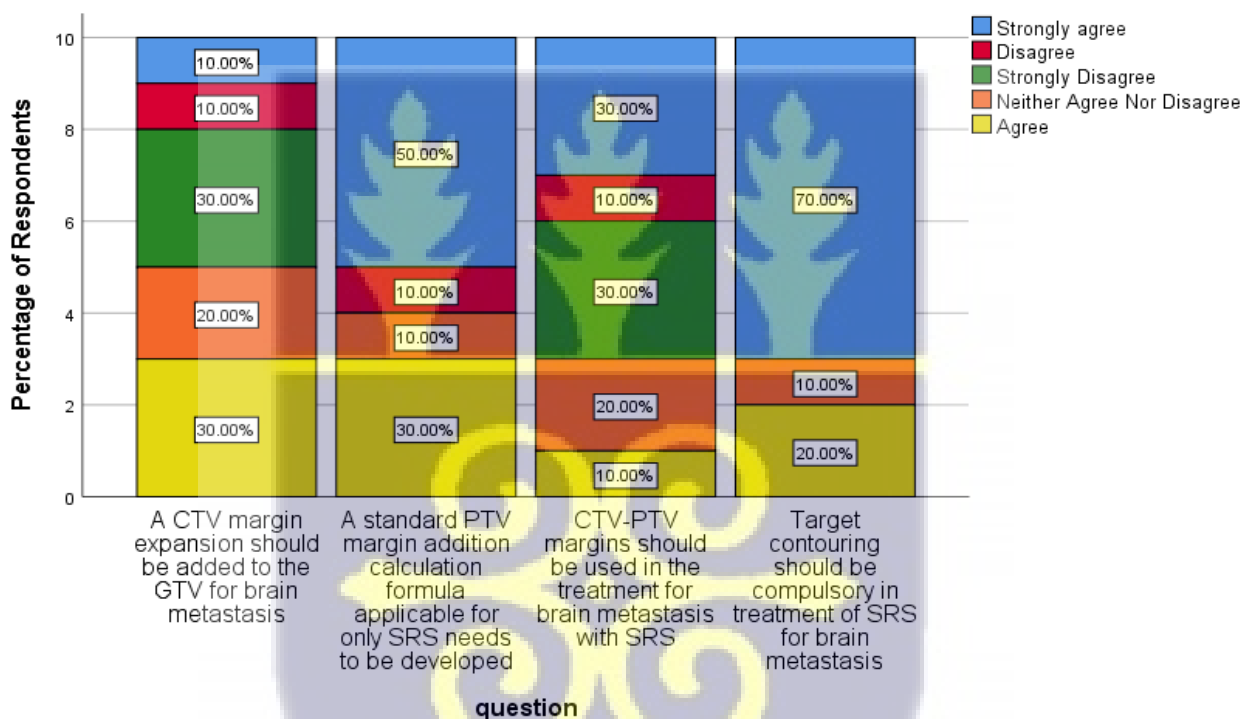


Figure 45: The graphical response of respondents for four of the questions

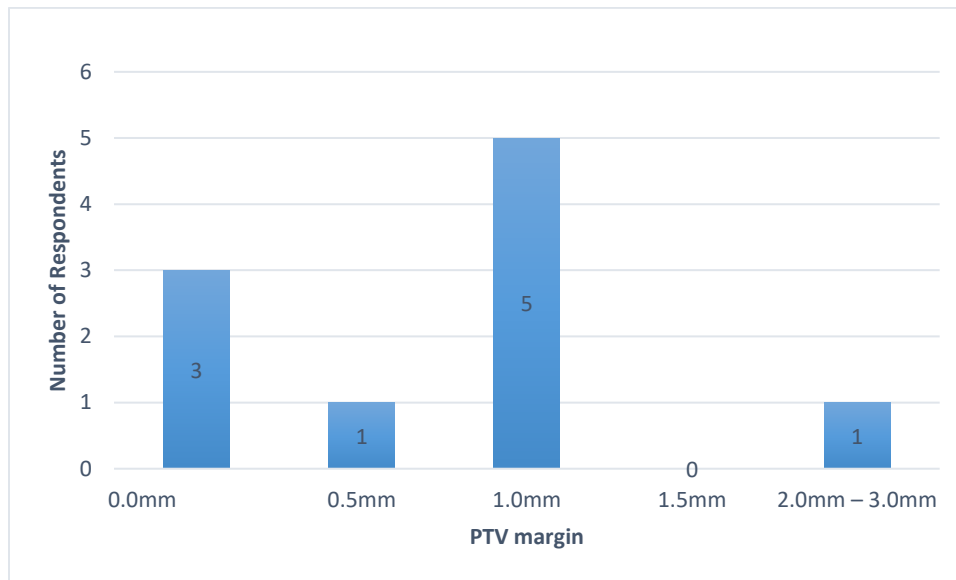
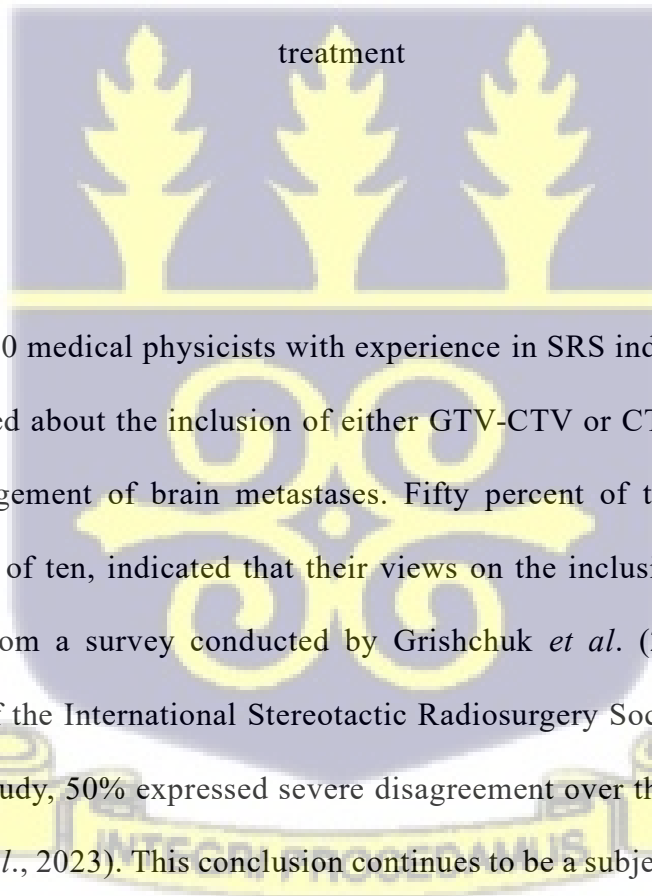


Figure 46: A bar graph distribution of respondents answer to the fifth question: what should be the maximum and optimal PTV Margin to be used accepted and applied in SRS



4.4.2 Discussion

The feedback from 10 medical physicists with experience in SRS indicates that a consensus has not been achieved about the inclusion of either GTV-CTV or CTV-PTV margins in the radio-surgical management of brain metastases. Fifty percent of the medical physicists, specifically five out of ten, indicated that their views on the inclusion of margins aligned with the findings from a survey conducted by Grishchuk *et al.* (2023), which included fourteen members of the International Stereotactic Radiosurgery Society (ISRS) guidelines committee. In this study, 50% expressed severe disagreement over the extension of CTV to GTV (Grishchuk *et al.*, 2023). This conclusion continues to be a subject of contention among the SRS community. A webinar by IOMP, titled "CTV-PTV Margins in Stereotactic Radiosurgery: Do We Need Them?", was presented in June 2021 by a senior physicist from the ICON Cancer Centre in Gold Coast, Queensland, Australia. The session revealed a lack

of consensus among participants, as indicated by a straightforward survey (Shakeshaft, 2021). According to Figure 46, 50% of respondents agreed that if margins are used, a maximum and ideal addition of 1 mm should be implemented. This aligns with a research by Minniti *et al.* (2020) which advocated for a 1 mm GTV-to-PTV margin while assessing thirty-one patients with a total of 204 brain metastases treated with the SIMT DCA SRS from October 2016 to September 2018 (Minniti *et al.*, 2020). Moreover, several SRS facilities in the United Kingdom use a maximum PTV margin of 1 mm (Diez *et al.*, 2022). This contradicted the 2 mm margin, which is the most often used by several SRS facilities in Australia and New Zealand (Pudsey *et al.*, 2022). The absence of agreement on this facet of SRS therapy for brain metastases presents an opportunity to formulate guidelines via clinical trials. When establishing the PTV margin, it is crucial to meticulously evaluate the need of the margin against the potential detrimental effects that an increased treated volume may impose on the patient. To mitigate the incidence of treatment problems associated with margin utilization, strategies such as adjusting the prescription dose or enhancing fractionation may be used (Kron, 2008). Numerous studies support the need for compulsory target contouring in SRS for brain metastasis. For instance, a study by Trifiletti *et al.* (2016) found that contouring can significantly reduce the risk of radiation necrosis, a serious complication of SRS (Trifiletti *et al.*, 2016). Contouring could improve local control of brain metastasis, further highlighting its importance (Mitchell *et al.*, 2022). Furthermore, a systematic review by Paddick and Lippitz, concluded that target contouring is a key factor in achieving optimal outcomes with SRS. They noted that contouring ensures the accurate delivery of radiation, reduces the risk of complications, and improves overall survival rates (Paddick and Lippitz, 2006). These findings provide strong evidence supporting the need for compulsory target contouring in the treatment of brain metastasis with SRS.

4.5 Geographical Distribution of Radiotherapy Systems for Brain Metastasis Treatment in Africa and Develop Guidelines for the Implementations of SRS Program in Africa.

4.5.1 Results

Current availability of radiotherapy facilities for the treatment of brain metastases in Africa

The literature search turned up two articles. Using the DIRAC database and this search, 239 radiotherapy centres in 33 countries were found. In Africa, there were two Gamma Knife machines, situated in Egypt and South Africa (Fezeu *et al.* 2014; GAMMA KNIFE SOUTH AFRICA, 2023). Three Cyberknife systems, two located in Egypt and one in Kenya (Elmore *et al.*, 2021) as presented in table 14. Furthermore, as of April 2023, there are 432 megavoltage machines in total, comprising 66 cobalt-60 units and 366 linear accelerators, primarily located in the Northern and Southern regions of the African continent. Radiotherapy utilizing the LINAC was observed in merely 29 nations across Africa. The total number of machines designated for the treatment of brain metastases was 437, with a mean of around 8. LINAC s represented the largest quantity of equipment accessible on the African continent for the treatment of brain metastases. Egypt and South Africa account for the largest quantity of machines 53.1% (232/437); however, only Egypt has all three machines necessary for the treatment of brain metastases patients.

The Gamma Knife emerged as the costliest among the available machines, priced between 5 and 7 million United States Dollars (USD) for acquisition and installation. It was succeeded by the Cyberknife, which ranges from 3 to 5 million USD, while the LINAC is the least expensive, costing between 2.4 and 2.8 million USD, with supplementary expenses for SRS capability. Comprehensive data on machine availability, GDP per capita, population, and cancer case numbers were accessible for 48 out of 54 nations, constituting 89.9%. Data on

GDP per capita was inaccessible for six nations: Equatorial Guinea, Eritrea, Sao Tome & Principe, Seychelles, Somalia, and Djibouti. According to the GLOBOCAN 2022 cancer statistics, Africa's population was about 1.4 billion, while the total number of cancer cases was 1,105,336. Cancer statistics for Seychelles are unavailable. Based on this data, the estimated number of brain metastases at a thirty percent assumption was 331,601. The average GDP per capita income was 8,067.77 USD.

Africa's most populous nation is Nigeria. It would have been believed that Nigeria accounted for the highest number of cancer cases and the estimated number of brain metastases but Egypt ended up accounting for 12.1% of all cancer cases (134,632/1,105,336) and 12.2% of all supposed brain metastases (40389.6/331,601.0), respectively. Figures 14 & 15 present the result of radiotherapy machines for brain metastasis treatment in Africa.

Table 14: Cost of purchase and installation of Radiotherapy Machines for Brain Metastasis Treatment

Radiotherapy Machines	Cost (USD million)
Cyber Knife	3 – 5 (Seung <i>et al.</i> , 2013)
Gamma Knife	5 – 7 (Saul, 2022.)
Linear Accelerator*	2.4 - 2.8* (Price of linear accelerators jumps 20%, 2022.)

*Extra cost for SRS Capability

When examining the DIRAC 2012 data and relevant literature, it was noted that there was only one Gamma Knife available in Africa for the treatment of brain metastasis, with no Cyberknife present. In contrast, there were 294 other megavoltage machines, which included 89 cobalt-60 units and 205 LINACs. A total of 161 new linear accelerators has been installed, while 23 cobalt-60 units have been decommissioned. This indicates a 78.5% increase in the

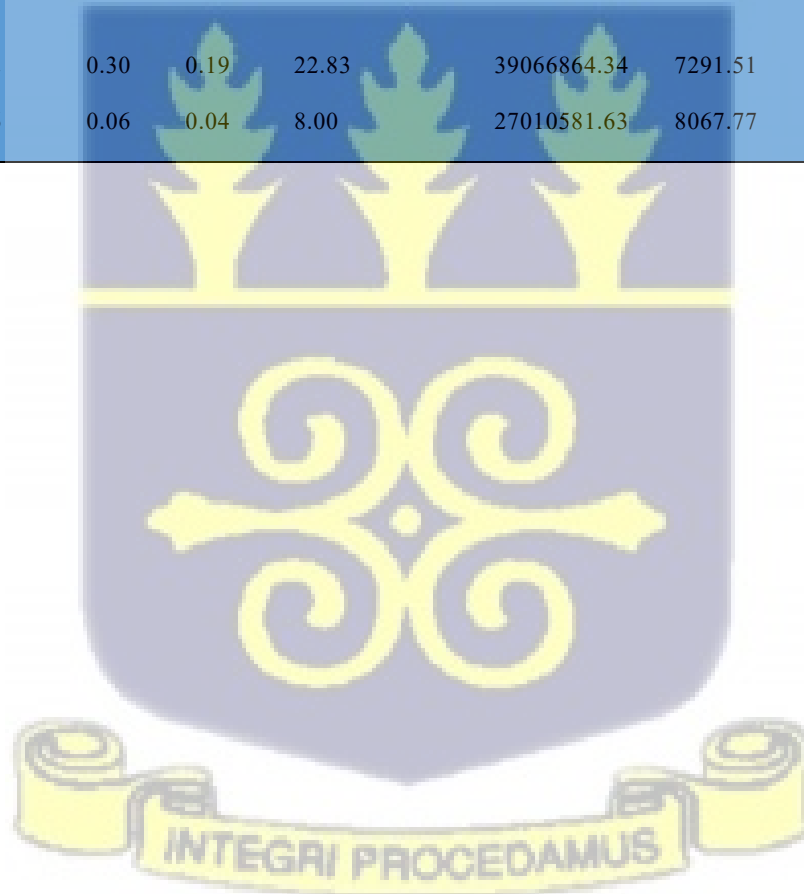
quantity of LINAC s installed and a 25.8% decrease in the number of cobalt-60 units since 2012. Radiotherapy LINAC s are currently accessible in 29 of the 54 countries, an increase from 23 in 2012 (Elmore *et al.*, 2021). It is important to highlight that among the 432 megavoltage machines installed in Africa, a significant portion is situated in lower middle-income countries, totalling 282 out of 432 as presented in table 15.

Table 15: An analysis of the different variables across the 54 nations in Africa

COUNTRIES	PROJECTED		NO. OF CYBER KNIFE	NO. OF GAMMA KNIFE	TOTAL NO. OF		GDP PER CAPITA/\$	TOTAL NO. OF MACHINES UNIT PER BRAIN METS	TOTAL NO. OF MACHINES	
	NO. OF CANCER CASES	NO. OF BRAIN METASTASIS			CO-60,	LINAC)				POPULATION
ALGERIA	58418	17525	0	0	2	35	45,606,480	12,997	0.002111221	37
ANGOLA	20327	6098	0	0	0	3	36,684,202	11,231	0.000491957	3
BENIN	6747	2024	0	0	0	0	13,712,828	5,329	0	0
BOTSWANA	2010	603	0	0	0	1	2,675,352	23,639	0.001658375	1
BURKINA FASO	12045	3614	0	0	0	0	23,251,485	3,352	0	0
BURUNDI	7929	2379	0	0	0	0	13,238,559	1,264	0	0
CAMEROON	20745	6224	0	0	2	1	28,647,293	5,379	0.000321363	2
CAPE VERDE	825	248	0	0	0	0	598,682	9,216	0	0
CENTRAL AFRICA REPUBLIC	2675	803	0	0	0	0	5,742,315	1,690	0	0
CHAD	8575	2573	0	0	0	0	18,278,568	2,529	0	0
COMOROS	609	183	0	0	0	0	852,075	4,089	0	0
CONGO (BRAZAVILLE)	2478	744	0	0	0	0	6,106,869	6,055	0	0
COTE D'IVOIRE	17300	5190	0	0	0	2	28,873,034	8,847	0.000385356	2
DJIBOUTI	765	230	0	0	0	0	1,136,455		0	0
DR CONGO	48839	14652	0	0	0	0	102,262,808	2,180	0	0

EGYPT	134632	40390	2	1	21	104	112,716,598	18,936	0.003094856	128
EQUATORIAL										
GUINEA	927	278	0	0	0	0	1,714,671		0	0
ERITREA	2408	722	0	0	0	0	3,748,901		0	0
ESWATINI	992	298	0	0	0	0	1,210,822	14,980	0	0
ETHIOPIA	77352	23206	0	0	1	2	126,527,060	3,690	0.000129279	3
GABON	1750	525	0	0	0	2	2,436,566	28,817	0.003809524	2
GAMBIA	1035	311	0	0	0	0	2,773,168	3,712	0	0
GHANA	24009	7203	0	0	2	3	34,121,985	8,940	0.000833021	5
GUINEA	7871	2361	0	0	0	0	14,190,612	4,503	0	0
GUINEA-										
BISSAU	1127	338	0	0	0	0	2,150,842	2,882	0	0
KENYA	42116	12635	1	0	2	15	55,100,586	6,930	0.00134549	18
LESOTHO	1876	563	0	0	0	0	2,330,318	3,807	0	0
LIBERIA	3552	1066	0	0	0	0	5,418,377	2,293	0	0
LIBYA	7661	2298	0	0	1	7	6,888,388	28,749	0.003480834	8
MADAGASCAR	20681	6204	0	0	2	1	30,325,732	2,604	0.000483536	3
MALAWI	17936	5381	0	0	0	0	20,931,751	2,112	0	0
MALI	14185	4256	0	0	0	1	23,293,698	4,226	0.00023499	1
MAURITANIA	3079	924	0	0	0	3	4,862,989	7,893	0.003247808	3
MAURITIUS	3050	915	0	0	2	1	1,300,557	27,147	0.003278689	3
MOROCCO	59370	17811	0	0	2	44	37,840,044	11,054	0.002582674	46
MOZAMBIQUE	25446	7634	0	0	0	1	33,897,354	1,901	0.000130996	1
NAMIBIA	3345	1004	0	0	1	1	2,604,172	12,898	0.001993024	2
NIGER	9787	2936	0	0	0	0	27,202,843	1,957	0	0
NIGERIA	124815	37445	0	0	2	7	223,804,632	9,333	0.000240356	9
RWANDA	8835	2651	0	0	0	2	14,094,683	3,390	0.000754575	2
SAO TOME										
AND PRINCIPE	151	45	0	0	0	0	231,856		0	0
SENEGAL	11317	3395	0	0	0	3	17,763,163	5,489	0.000883626	3
SEYCHELLES	0	0	0	0	0	0	107,660		0	0
SIERRA										
LEONE	4708	1412	0	0	0	0	8,791,092	2,956	0	0

SOMALIA	10134	3040	0	0	0	0	18,143,378	0	0	
SOUTH										
AFRICA	108168	32450	0	1	3	100	60,414,495	19,331	0.003174075	104
SOUTH SUDAN	6312	1894	0	0	0	0	11,088,796	7,089	0	0
SUDAN	27382	8215	0	0	6	4	48,109,006	7,089	0.000973876	10
TANZANIA	40464	12139	0	0	2	5	67,438,106	4,181	0.000659022	7
TOGO	5208	1562	0	0	0	1	9,053,799	3,209	0.000640041	1
TUNISIA	19446	5834	0	0	11	14	12,458,223	14,154	0.004456786	25
UGANDA	34008	10202	0	0	2	1	48,582,334	3,320	0.000294048	3
ZAMBIA	13831	4149	0	0	2	1	20,569,737	5,609	0.000723014	3
ZIMBABWE	16083	4825	0	0	0	1	16,665,409	4,275	0.000207258	1
					66	366				
TOTAL	1105336	331601.00	3	2	432		1,458,571,408	387253	0.042619669	437
STANDARD	30271.73									
DEVIATION		9081.52	0.30	0.19	22.83		39066864.34	7291.51	00121955870	23.21
MEAN	20469.19	6140.76	0.06	0.04	8.00		27010581.63	8067.77	0.0007892531	.09



Status of Radiation Therapy Equipment

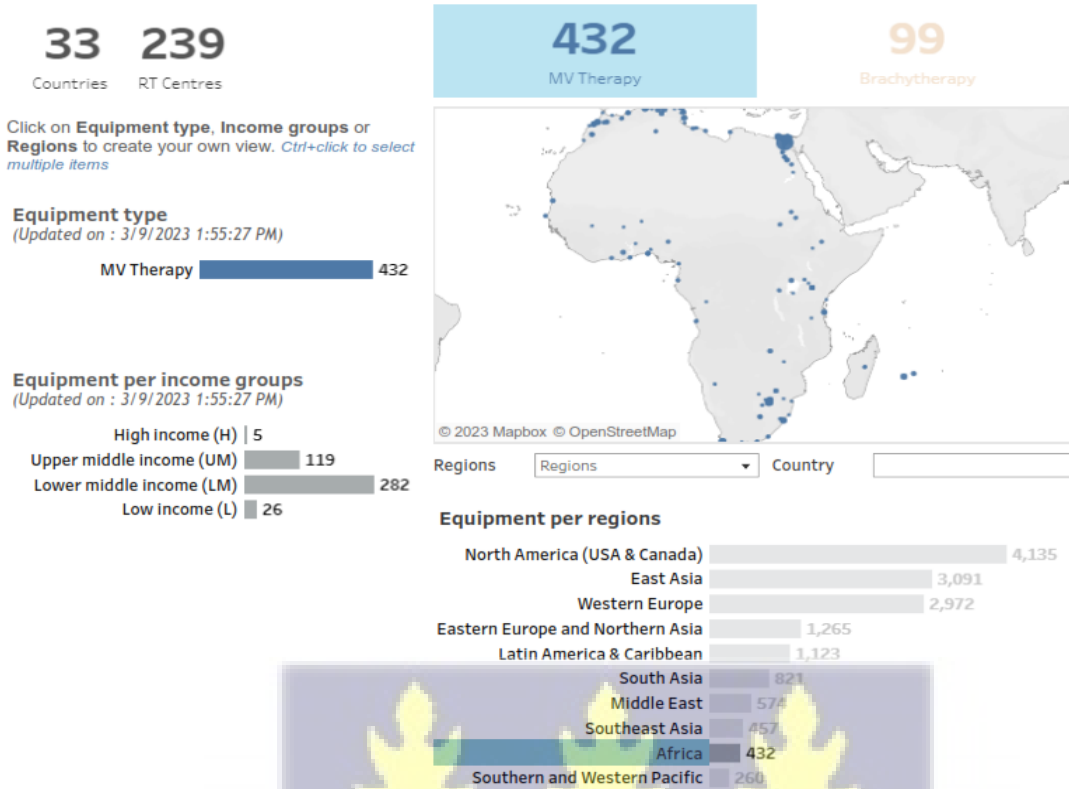
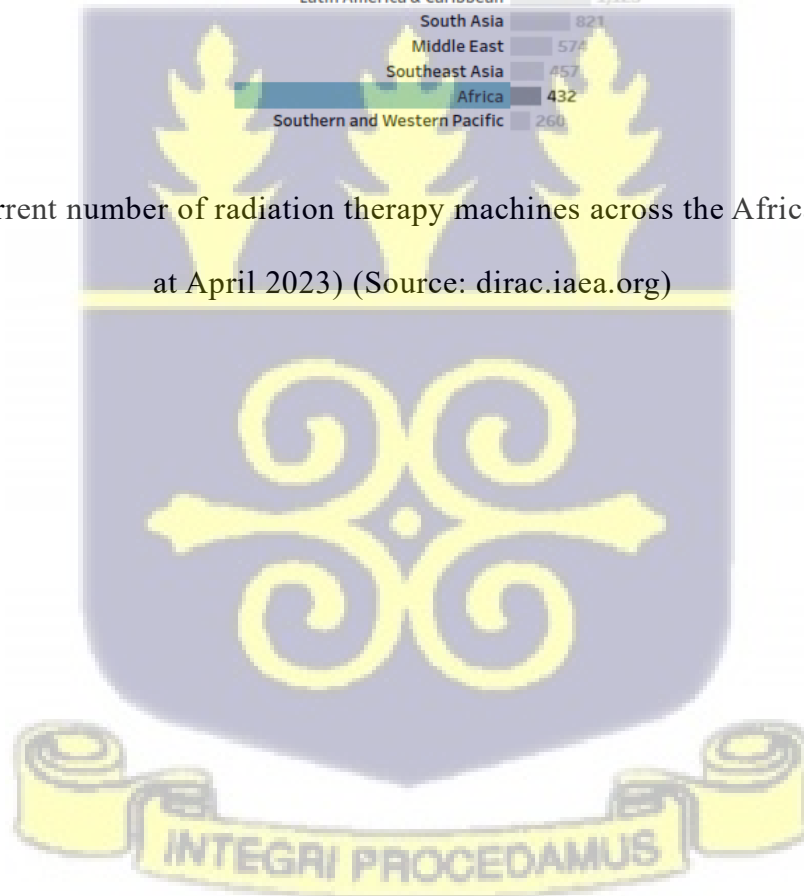


Figure 47: Current number of radiation therapy machines across the African continent (as at April 2023) (Source: dirac.iaea.org)



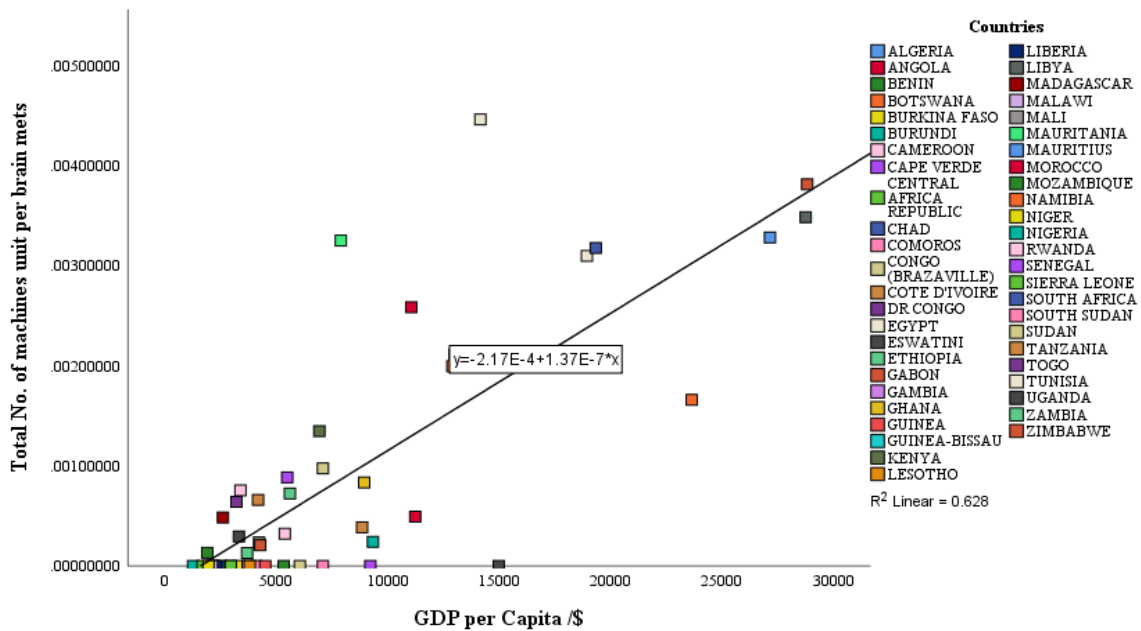


Figure 48: Scatter plot illustrating the total quantity of machines in relation to the anticipated number of brain metastases, categorized by GDP per capita (\$) across African nations.

The accessibility of these machines for treating brain metastasis patients was evaluated based on the GDP per capita of each nation. A significant difference in median income was detected between countries having radiotherapy capabilities and those without such facilities. The median GDP per capita for nations without radiotherapy capability was 3,352 USD (ranging from 1,690 USD to 14,980 USD), but for countries possessing at least one radiation therapy equipment, it was 7,893 USD (ranging from 1,901 USD to 28,817 USD). Despite Eswatini's elevated GDP per capita, it lacks installed radiotherapy machine, while Mozambique, with a lower GDP per capita, has one unit. Gabon had the highest GDP per capita; yet, the quantity of installed machines was inferior to that of Egypt, which has the greatest number of machines. The total number of machine units per brain metastasis cases shown a correlation with GDP per capita ($r^2=0.628$) as reported in figure 49. The linear regression model therefore reveals some variances.

This suggests that other reasons may account for the heterogeneity in the availability of these devices across different countries. These criteria may include the total incidence of cancer and brain metastasis cases in each nation, as well as the overall population.

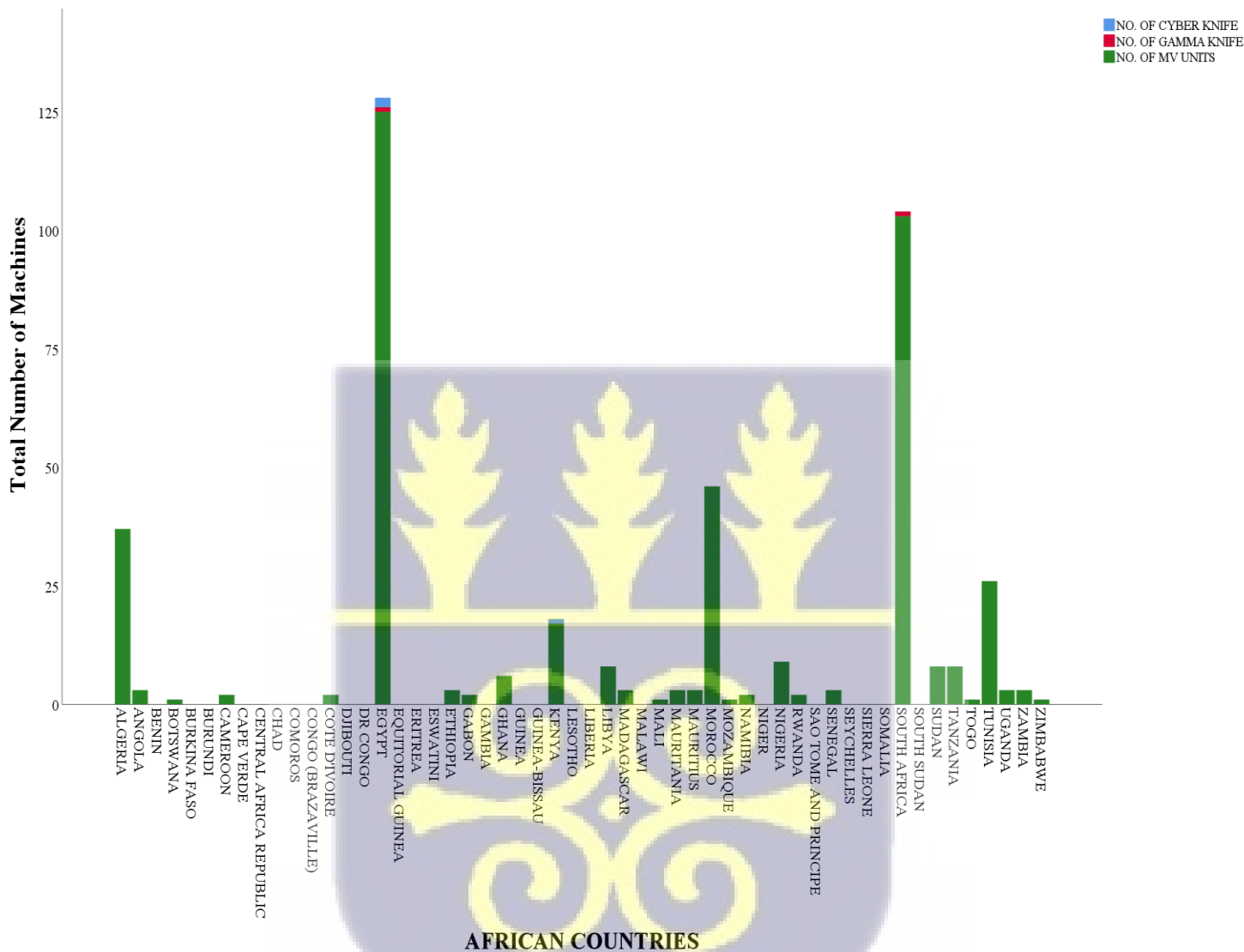


Figure 49: A bar graph showing the total number of machines per country in Africa

4.5.2 Discussion

This work examined the availability of accessible radiotherapy technology for treating brain metastases in Africa and offered practical instructions for establishing a stereotactic radiosurgery program. There is a rise in cancer cases, thereby leading to an increase in brain metastases. Radiotherapy is a principal therapeutic approach for cancer treatment (Ndlovu, 2019). and as such stereotactic radiosurgery plays a key role in the management of brain metastasis (Wagner *et al.*, 2020). When evaluating the current situation in Africa against the previous assessment from 2012 regarding machine distribution, we observed an enhancement in absolute radiotherapy capacity (Elmore *et al.*, 2021). Africa currently has two Gamma Knife units, three Cyber Knife units, 366 linear accelerators, and 66 cobalt-60 units. However, the rise in the quantity of these machines has not aligned with the demand for radiotherapy and the increasing incidence of cancer cases. In cases of brain metastasis and various other cancers where radiotherapy is a primary treatment option, this could result in a significant rise in mortality rates (Abdel-Wahab *et al.*, 2017; Cohen-Inbar and Sheehan, 2016; Thomson *et al.*, 2023).

The overall number of these machines in the United States and Europe exceeded four thousand and three thousand, respectively (IAEA, 2023). According to this analysis, LINACs comprised the largest proportion of the total machines available, totalling 83.8% (366/437). This growth may be attributed to the expansion efforts underway in several nations aimed at enhancing accessibility. The decrease in cobalt-60 units may result from the cessation of production, unavailability of replacement parts, suboptimal therapeutic results, and security apprehensions. In several industrialized and high-income nations, cobalt-60 teletherapy equipment are no longer used for treatment (Pomper *et al.*, 2016).

The restricted availability of Gamma Knife and Cyber Knife machines (2 Gamma Knife, 3 Cyber Knife) on the continent could be attributed to the significant expenses involved in

their acquisition and installation. In numerous African nations classified with lower GDP per capita, this indicates a diminished purchasing capacity for acquiring these machines (World Economics - The Global Authority on Geographic Investability, 2023). There may also be a lack of qualified specialists available, which is another factor to consider. It is possible that the absence of stereotactic radiosurgery (SRS) installations in Africa might be ascribed to the inadequate number of neurosurgeons, radiation oncologists, and physicists in this area. This shortage of professionals presents significant obstacles when it comes to resolving this problem. The aforementioned challenges are further complicated by the financial consequences that are involved with maintenance and repairs, which necessitates the establishment of expensive maintenance contracts with the manufacturers (Pahwa and Agrawal, 2023).

From this viewpoint, it is likely that a nation's economic conditions considerably contribute to this disparity because of the considerable costs connected with Gamma Knife and Cyber technologies. Numerous cases demonstrate that areas in the United States and Europe have budgets that surpass those of Africa and the Middle East by a factor of at least 10 (Fezeu *et al.*, 2014). The availability of equipment is closely linked to national income, indicating that financial resources play a crucial role in determining access. Given this situation, low-income countries lacking radiotherapy machines need to develop strategies to integrate this treatment into their national health care programs or collaborate with other organizations to address this need (CERN, 2017; Ige *et al.*, 2021). The International Atomic Energy Agency (IAEA) is one such organization. The IAEA provides several efforts aimed at assisting Low and Middle-Income Country (LMIC) member nations in securing access to radiation treatment. These programs include support in the decision-making process for selecting and acquiring radiotherapy equipment, in addition to aiding with machine installation and training (Barton *et al.*, 2017).

The Gamma Knife is the golden standard machine for stereotactic treatment for brain metastasis (Fezeu *et al.*, 2018; National Academies of Sciences 2021; Thomson *et al.*, 2023). The elevated installation costs have made it difficult for poor and middle-income nations, particularly in Africa to acquire radiotherapy machines. Despite a population above 1.4 billion, Africa lacks LINAC-based SRS installations (National Academies of Sciences, 2021). Compared to Gamma Knife and Cyberknife, LINAC -based SRS has the potential to be readily deployed as a specialised machine for brain metastasis patients since LINAC s may be described as being prominent on the continent according to this research. It is believed that half of the 366 LINAC may be improved into a LINAC-based SRS machines. This might lead to improved accessibility. A recent study by Dean *et al.* (2019) it was noted that there are around 428 specialized devices for SRS available in the United States (Dean *et al.*, 2019). Among these, LINAC-based systems emerged as the most widely utilized, representing 39%, while CyberKnife followed closely at 35%, and Gamma Knife accounted for 26%. Comparable trends have also been seen in Europe with regard to the greater use of LINAC -based stereotactic radiosurgery (SRS) systems in comparison to Gamma-based SRS systems (Pannullo *et al.*, 2019).

Linear accelerators tailored for stereotactic radiosurgery (SRS) have demonstrated clinical outcomes that are on par with those obtained through Gamma Knife radiosurgery. The comprehension of access to LINAC-based radiosurgery holds considerable promise for broader application in resource-limited environments. Furthermore, LINAC-based radiosurgery demonstrates enhanced adaptability, allowing for the delivery of different types of radiation treatments (Fezeu *et al.*, 2018). Furthermore, recent studies show that the expenses associated with Gamma Knife therapy per patient is significantly greater than that of LINAC-based treatment. This is applicable in situations where LINAC systems are

utilized extensively, as well as in cases where they are exclusively used for radiosurgery (Griffiths *et al.*, 2007; Hamilton and Dade Lunsford, 2016).

While certain nations in Africa are strategizing to obtain specialised machines for SRS, others are considering upgrading their current LINAC systems to function as LINAC-based SRS systems. For instance, Mauritius has progressed with its initiatives to obtain a CyberKnife machine as outlined in the Mauritian Government's National Cancer Control Programme for 2022-2025 (Mauritian Government National cancer control programme 2022-2025). Ghana is planning to enhance their linear accelerators to provide a linear accelerator-based stereotactic radiosurgery.

To reduce initial costs and enhance accessibility in resource-limited regions, ZAP Surgical Systems, Inc., based in San Carlos, California, has developed a self-shielded 2.7-MeV LINAC system specifically designed for SRS, marketed under the name Zap-X. This system is promoted as generally not needing a radiation bunker (National Academies of Sciences, 2021).

4.5.2.1 Guidelines for the Implementation of SRS Programs in Africa

The implementation of stereotactic radiosurgery (SRS) programs in Africa requires strategic planning that considers the continent's unique economic, technical, and infrastructural challenges. Advanced cancer care technologies, like SRS, can significantly improve patient outcomes, particularly for conditions like brain metastasis, which require precision and minimally invasive interventions. The following guidelines offer a comprehensive approach to establishing and expanding SRS programs in Africa, aimed at improving equity and access to life-saving treatments.

1. Strategic Partnerships and International Collaboration

International collaboration is crucial for overcoming the economic and technical challenges faced by African nations in adopting SRS technologies. Partnerships between African healthcare systems and international healthcare organizations, universities, or cancer institutes can help bridge gaps in knowledge, technology, and training. For example, partnerships like the one between the University of Cape Town in South Africa and European hospitals have demonstrated the value of international cooperation in providing access to specialized training and cutting-edge equipment. Through these collaborations, African healthcare workers can participate in fellowships, workshops, and hands-on training sessions, learning how to operate SRS systems like the Gamma Knife, CyberKnife, or LINAC-based platforms. Moreover, these partnerships can facilitate the donation or subsidized acquisition of SRS systems, making it financially viable for African countries to establish radiosurgery programs. International support can also provide the infrastructure needed for the installation and maintenance of SRS systems, which is critical given the limited technical resources available on the continent.

2. Training and Capacity Building

Training is a foundational element of any successful SRS program, as the technology requires highly specialized skills across multiple disciplines. African healthcare institutions must prioritize the training and education of radiation oncologists, neurosurgeons, medical physicists, and radiographers in the principles and practice of radiosurgery. A multidisciplinary approach to training is essential since SRS involves complex cases, such as brain metastases, that require collaboration between different specialists. International partnerships can offer access to fellowships, certification programs, and remote learning

opportunities that provide African healthcare workers with the skills needed to safely operate and maintain SRS systems. Furthermore, training programs should focus on building a critical mass of local expertise so that radiosurgery services can be expanded across hospitals and regions. As more healthcare professionals become proficient in the technology, the sustainability and reach of SRS programs will increase, ultimately improving patient outcomes (Fiagbedzi *et al.*, 2023).

3. Infrastructure Development

A successful SRS program requires significant investment in healthcare infrastructure. Governments, healthcare providers, and international donors must collaborate to ensure that hospitals and treatment centres are equipped with the necessary facilities to support advanced medical technologies like SRS. This includes stable power supplies an essential requirement given that SRS equipment is highly sensitive to power fluctuations as well as advanced imaging capabilities such as MRI and CT scanners, which are critical for accurate tumor targeting and treatment planning (Datta *et al.*, 2014). Additionally, robust quality assurance (QA) programs are vital to ensure that SRS procedures are performed safely and effectively. African governments should prioritize infrastructure development, particularly in regional hospitals and cancer centres, to expand access to advanced oncology care. Equipping more hospitals with modern radiotherapy and imaging equipment will decentralize access to SRS, reducing the need for patients to travel long distances for treatment.

4. Sustainable Funding Models

One of the greatest barriers to the widespread implementation of SRS in Africa is the high upfront cost of acquiring and maintaining radiosurgery systems. Sustainable funding models are essential to ensure the long-term viability of SRS programs. Governments should explore

public-private partnerships (PPPs), which can bring together public health systems and private investors to finance the acquisition of SRS equipment and its maintenance. International donors and development banks can also play a significant role in funding advanced cancer treatment technologies in Africa. Another approach is to establish multi-country partnerships that allow neighbouring nations to share the costs of SRS equipment and create regional cancer centres, thereby reducing the financial burden on individual countries. Furthermore, governments should allocate a portion of healthcare budgets specifically for advanced cancer treatments, ensuring that SRS programs are not underfunded. By developing sustainable financing mechanisms, African nations can build the capacity to treat more patients and maintain their SRS systems over the long term (Fiagbedzi *et al.*, 2023).

5. Equitable Access and Decentralization

To ensure that SRS programs benefit a broad range of patients, it is crucial to decentralize radiosurgery services beyond major urban centres. Most of Africa's existing SRS systems are concentrated in a few metropolitan hospitals, leaving rural and underserved populations without access to this advanced treatment. Establishing regional treatment centres that cater to multiple countries or regions would help address this disparity. These centres could serve as hubs for specialized cancer care, allowing patients from rural or neighbouring regions to access radiosurgery without the need for long-distance travel (Datta *et al.*, 2014). Additionally, telemedicine and mobile treatment units could be explored to extend SRS capabilities to more remote areas. These approaches would decentralize the provision of radiosurgery services and ensure that all patients, regardless of geographic location, have access to advanced cancer care.

6. Health Policy and Advocacy

Strong health policy advocacy is needed to place advanced cancer treatments, including SRS, on the agenda of African governments. National health policies should prioritize the development of cancer treatment infrastructure and integrate SRS into standard oncology care. This requires a shift in focus, as many African health policies have traditionally prioritized communicable diseases over non-communicable diseases like cancer. Advocates must work with policymakers to demonstrate the importance of advanced cancer care in reducing mortality rates and improving patient outcomes. Governments should allocate specific budgets for cancer treatment technologies, including radiosurgery, and create national cancer control programs that include the establishment of SRS services. Furthermore, efforts should be made to include SRS in national health insurance schemes or provide subsidies to ensure that these treatments are accessible to all economic groups, not just those who can afford private healthcare.



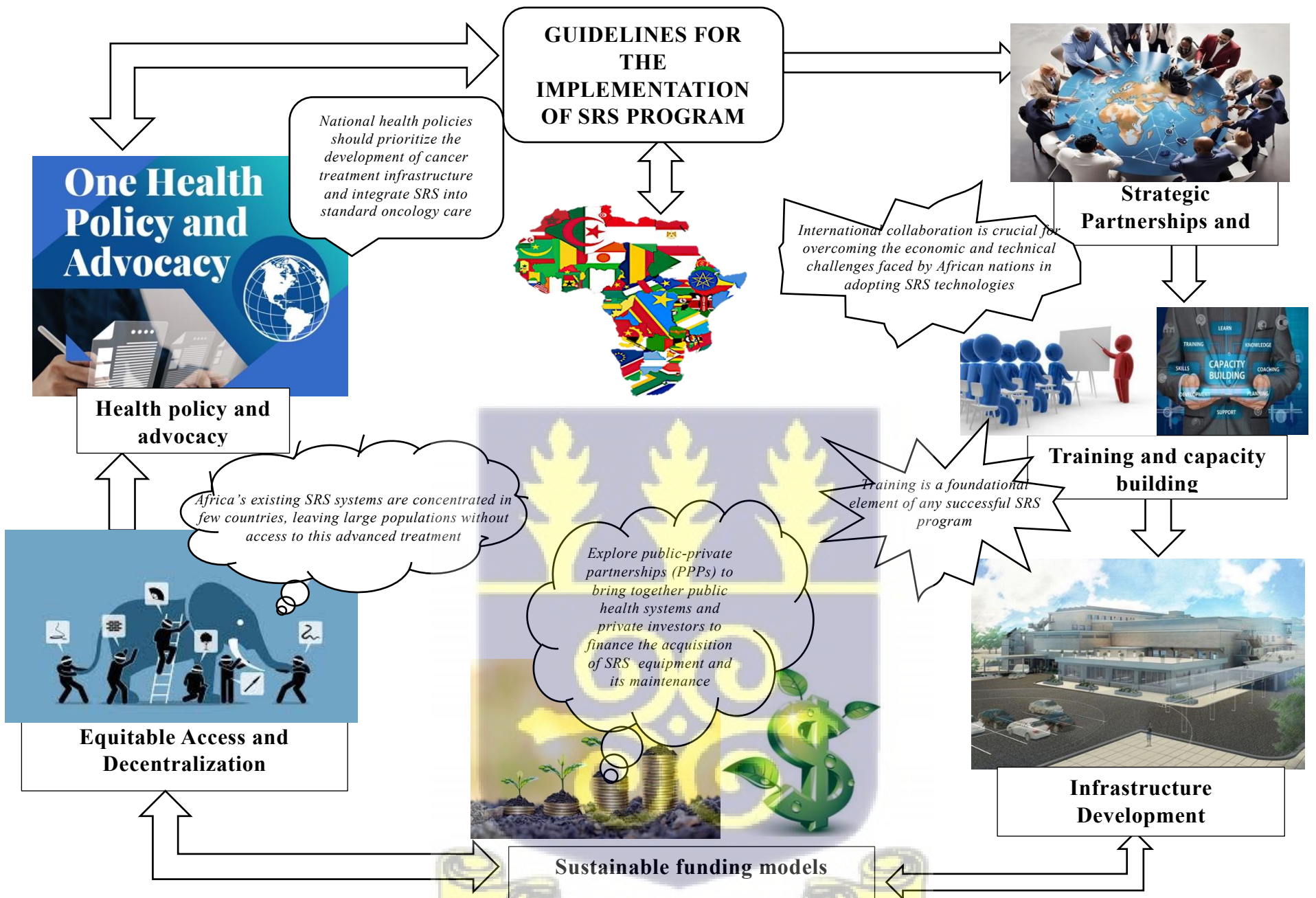


Figure 50: Model of guidelines for implementation of SRS

CHAPTER FIVE

CONCLUSION AND RECOMMENDATIONS

Introduction

This chapter contains the conclusion and recommendations sections. Based on the key findings, informed recommendations are provided together with potential avenues for further research or practical applications.

5.1 Conclusion

PTV margins is an important consideration in Gamma Knife radiosurgery for single brain metastasis and the expansion of this influence dosimetric parameters such as selectivity [S], gradient index [GI], V12, Paddicks conformal index [PCI] and treatment time [TI] and organs at risk. From a clinical perspective, the decision of what PTV margin and prescription isodose to use for SRS treatments for brain metastasis depends on the clinical goals established for the treatment type but in this case, increases in PTV margins target expansion for GK SRS though a relatively novel concept; should not go beyond 2 mm since this pose potential detrimental effects through the elevation of all dosimetric parameters.

For LINAC-SRS, the evaluation of prescription isodoses using the three margins (0, 1, and 2 mm) highlights the balance between effective tumor targeting and minimizing harm to adjacent healthy tissues. Lower isodoses like SRS50 and SRS55 are favoured for their precision and reduced risk to critical structures, such as the brain stem and optic nerves. In contrast, higher isodoses like SRS70 and SRS80, though potentially more effective, carry a higher risk of radiation exposure to surrounding healthy tissues, which may lead to

complications. Treatment planning should consider tumor location and patient anatomy, with smaller margins being ideal for accuracy, especially at lower isodose levels. Larger margins could typically be used to account for uncertainties related to patient movement, variations in tumor positioning, and potential anatomical changes over time. Hence, higher isodose levels can be ideal when a margin of 1 mm or 2 mm is used. This will ensure that the target area, including any microscopic disease surrounding the tumor, is fully covered by the prescribed radiation dose. This helps to ensure that all malignant cells receive an adequate dose, even if there are slight shifts or movements during treatment.

The evaluation of the wireless Delta4 Phantom+ provided robust verification of the LINAC-based stereotactic radiosurgery (SRS) plans. Across all prescription isodose levels and planning target volume (PTV) margins, the gamma index passing rate remained exceptionally high, ranging from 99.6% to 100%, well above the 95% acceptance threshold under the 2%/2 mm criteria. Dose deviation and distance-to-agreement analyses further confirmed excellent consistency between the treatment planning system (TPS) calculations and the phantom measurements, with a correction factor of 1.01, demonstrating strong dosimetric reliability. These findings underscore the Delta4 Phantom+ as a highly efficient tool for patient-specific quality assurance, offering rapid setup, accurate real-time measurement, and comprehensive three-dimensional dose analysis. Its ability to accurately capture the complex modulation patterns of VMAT SRS such as 1%/1 mm highlights its clinical utility, although future studies could expand by comparing its performance with other QA verification systems. Overall, the results affirm that the Delta4 Phantom+ ensures both accuracy and efficiency in plan verification, reinforcing confidence in the safe and precise delivery of stereotactic radiosurgery.

Regarding the opinion of the experienced medical physicist in SRS planning, no consensus was reached regarding margin use in SRS while some advocate that, if used, it should be applied with caution. This calls for further consultation among large groups of professionals directly involved with radiosurgery treatment for brain metastasis.

The adoption of SRS for brain metastasis treatment in Africa is currently limited though the number of cases keep increasing. There is a clear path forward for expanding access to this life-saving technology. By leveraging strategic partnerships, building local capacity through training, investing in infrastructure, and establishing sustainable funding models, African nations can overcome the challenges to implementing SRS programs. The decentralization of radiosurgery services, coupled with strong health policy advocacy, will ensure that these treatments become part of standard oncology care, benefiting a broader range of patients across the continent. Expanding access to SRS will have a significant impact on improving patient outcomes and reducing cancer-related mortality in Africa. Ultimately, the success of SRS programs will depend on the collective efforts of governments, international partners, and healthcare providers to make advanced cancer care both available and affordable.

5.2 Limitations

This research has many inherent limitations. The elusive nature of the investigation may explain some heterogeneity in the gathered data with the STEEV phantom and this was only focused on Gamma Knife and LINAC -based system homogeneity index evaluation was not used in this study. It is understood that in SRS/SRT, a considerable level of non-uniform dose distribution is permissible, hence the homogeneity index does not play a major role in the

assessment of the plan and is also end user dependent. There was a limitation of the Eclipse treatment planning system in computing dose for using margin sizes like 0.5 to 1.5 mm.

The comprehensiveness and trustworthiness of the DIRAC statistics are ambiguous due to the voluntary and self-reported nature of the database. Moreover, Africa presents a very dynamic landscape marked by frequent installations, yearly events, and systematic modifications or replacements of equipment. The precision of the GLOBOCAN 2022 estimates for current and anticipated brain metastasis cases may be undermined by the ongoing development of population-based cancer registries in Africa and the assumption of a 30 percent prevalence rate. The absence of comprehensive data for the specified six nations may hinder a thorough discussion of SRS in the African continent. The participation of medical physicists in the survey was limited.

5.3 Novel Contributions and Extension of this Thesis

5.3.1 Novel Contributions

This study has offered a direct, head-to-head analysis, providing evidence on the optimal planning target volume and prescription isodose to be used on either the Gamma Knife and LINAC -based System for single brain metastasis treatment. Such analysis is novel in its scope and detail, potentially guiding future protocols and improving treatment precision.

- ✓ By incorporating the newly introduced wireless Delta 4 Phantom+ phantom device to validate LINAC -based SRS plans, the field's understanding of the accuracy and reliability of modern dosimetric tools such as that have been validated. This validation offers clinical confidence in adopting such technologies for daily use and recommending

tighter gamma pass index criteria to be implemented, potentially leading to improved patient safety and more precise dose delivery in clinical practice.

- ✓ The study's investigation of the opinions of experienced medical physicists on the addition of PTV margins introduces a unique dimension. These insights will provide real-world perspectives on challenges, preferences, and decision-making processes in SRS planning that are not commonly covered in purely technical studies. This may lead to the development of more practical, evidence-based planning guidelines that bridge the gap between theory and practice.
- ✓ There is currently a significant knowledge gap in the accessibility and implementation of SRS in low-resource settings, particularly in Africa. By exploring the geographical distribution and usage of SRS systems across the continent, this study offers the first comprehensive examination of these disparities. The creation of implementation guidelines will not only expand access to advanced cancer treatment technologies in underserved regions but also contribute to the global body of knowledge on establishing sustainable SRS programs in developing countries.
- ✓ The detailed analysis of how varying prescription isodose levels affects treatment outcomes in LINAC -based systems, combined with common PTV margins, provide novel insights into the dosimetric planning strategies that yield the best balance between tumor control and healthy tissue sparing. This data is currently scarce in the field and could significantly influence clinical practice by refining treatment planning processes for brain metastasis, ultimately leading to better patient outcomes.

- ✓ The combined outcomes of this study will offer a new layer of evidence for refining SRS treatment protocols. By providing a detailed, quantitative comparison of treatment outcomes based on various planning parameters, this study contributes to the development of more standardized and optimal SRS protocols that can be adopted globally.

Overall, this study has advanced the field of SRS by providing a comprehensive, data-driven analysis of SRS planning parameters, validating cutting-edge dosimetric tools, offering practical expert insights, addressing geographical disparities in access to care, and potentially setting new standards for SRS treatment protocols worldwide. These contributions will support enhanced precision, safety, and accessibility in the treatment of brain metastases with SRS.

5.3.2 Extension of this Thesis

One factor in SRS practice is the method of treatment and the duration of treatments, both of which significantly influence the Biological Effective Dose (BED). Additional research is necessary in radiobiological experiments and modelling to comprehend how these factors influence treatment efficacy. Furthermore, as treatment practices achieve greater consistency, it may be possible to analyze patient data retrospectively not as a phantom study to identify correlations between BED and patient outcomes. The insights gained from these studies should subsequently be applied in the clinical setting to enhance the effectiveness of SRS treatments.

It would be essential to conduct longitudinal follow-up studies to assess the long-term effects of SRS on patient outcomes, including tumor control, survival rates, and potential late-onset complications. By tracking patients over an extended period, researchers can gain insights

into the durability of treatment effects and the incidence of adverse events, which are critical for evaluating the overall efficacy and safety of SRS.

Also, the use of other devices for patient specific QA for SRS for brain metastasis can be explored and compared with the Delta 4 Phantom+ phantom.

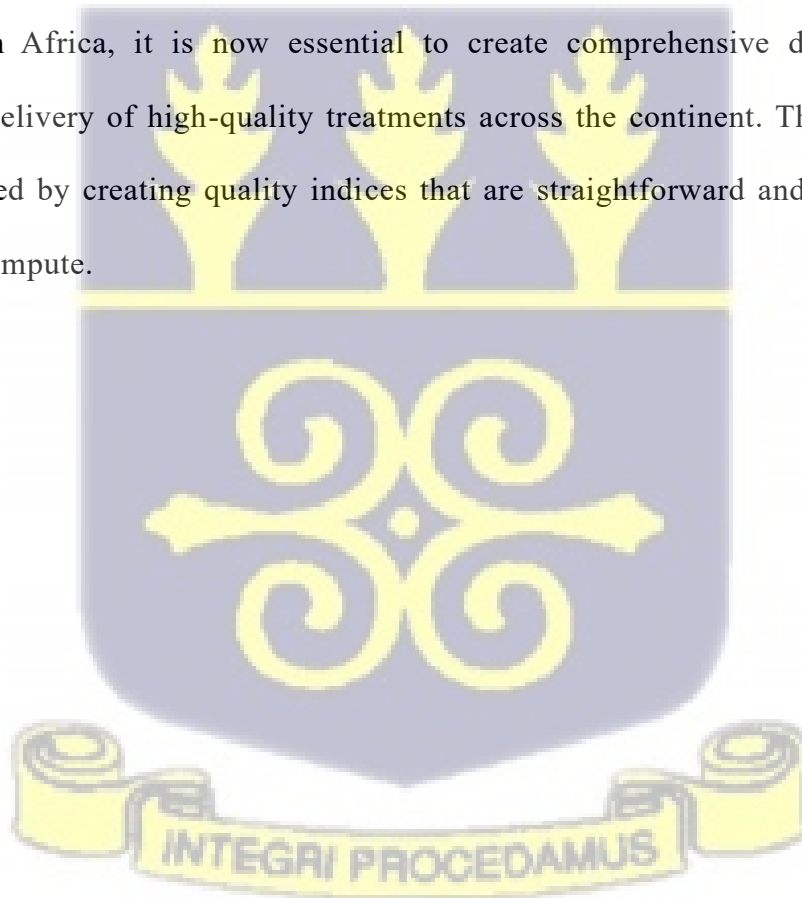
5.4 Recommendations

The Need for Standardization in SRS

The practice of SRS would greatly benefit from a standardized approach. The primary emphasis of this standardization should be directed towards the margins of the planning target volume and the prescription isodoses utilised, particularly in LINAC-based SRS. These require greater cohesion to enhance the execution of clinical trials, ensuring the generation of reliable data and enabling the assessment of treatment efficacy based on patient outcomes. In the effort to expand LINAC-based SRS centres in Africa, it is likely that variations will become more evident. Therefore, implementing standardisation initially within this group would be advantageous. An audit carried out in the UK has revealed instances of CyberKnife and LINAC centres adopting practices influenced by Gamma Knife methodologies. This suggests that other equipment subgroups recognize the importance of Gamma Knife planning practices. While certain centres utilising LINAC-based SRS apply a margin of 2mm with a prescription isodose exceeding 80%, others implement a 1mm margin at 40-80%. Following this, prescribed dosages may be adjusted to formulate guidelines for suitable clinical practices.

The quality of treatment plans is an aspect of SRS that could greatly improve with standardization. This is primarily evaluated through target conformity and dose gradient

beyond the target, both of which can be quantified using different indices. A variety of treatment planning parameters, such as the volume receiving 12 Gy, have demonstrated a correlation with patient complications and can serve as prognostic indicators or benchmarks for enhancing the quality of treatment plans. The application of non-coplanar and coplanar beams remains to be fully determined, although non-coplanar beams show advantages in conformity, gradient, and a decrease in the volume of 12 Gy in LINAC-based SRS. Consequently, a suitable measure for standardization would involve limiting the application of coplanar SRS. At present, there are no specific guidelines in the UK and Africa that outline the minimum acceptable quality for plans related to SRS. In light of the recent push for more SRS centres in Africa, it is now essential to create comprehensive documentation to guarantee the delivery of high-quality treatments across the continent. This initiative will also be enhanced by creating quality indices that are straightforward and practical for all subgroups to compute.



REFERENCES

- Abdel-Wahab, M., Fidarova, E. and Polo, A. (2017). Global access to radiotherapy in low- and middle-income countries. *Clinical Oncology*, 29(2), 99–104.
- Agazaryan, N., Tenn, S., Lee, C., Steinberg, M., Hegde, J., Chin, R., Pouratian, N., Yang, I., Kim, W., & Kaprealian, T. (2021). Simultaneous radiosurgery for multiple brain metastases: technical overview of the UCLA experience. *Radiation Oncology*, 16(1), 1–9. <https://doi.org/10.1186/s13014-021-01944-w>
- Alongi, F., Fiorentino, A., Mancosu, P., Navarra, P., Giaj Levra, N., Mazzola, R., & Scorsetti, M. (2016). Stereotactic radiosurgery for intracranial metastases: Linac-based and gamma-dedicated unit approach. In *Expert Review of Anticancer Therapy* (Vol. 16, Issue 7). <https://doi.org/10.1080/14737140.2016.1190648>
- Anand, U., Dey, A., Chandel, A. K. S., Sanyal, R., Mishra, A., Pandey, D. K., De Falco, V., Upadhyay, A., Kandimalla, R., Chaudhary, A., Dhanjal, J. K., Dewanjee, S., Vallamkondu, J., & Pérez de la Lastra, J. M. (2023). Cancer chemotherapy and beyond: Current status, drug candidates, associated risks and progress in targeted therapeutics. *Genes & Diseases*, 10(4), 1367–1401. <https://doi.org/10.1016/j.gendis.2022.02.007>
- Anthropomorphic STEEV phantom underpins independent auditing of SRS programmes*. (2022). <https://physicsworld.com/a/anthropomorphic-steev-phantom-underpins-independent-auditing-of-srs-programmes/>
- Antolak, J. A., & Rosen, I. I. (1999). Planning target volumes for radiotherapy: How much margin is needed? *International Journal of Radiation Oncology Biology Physics*, 44(5). [https://doi.org/10.1016/S0360-3016\(99\)00117-0](https://doi.org/10.1016/S0360-3016(99)00117-0)

- Arnaout, M. M., Hoz, S., Lee, A., & Taha, M. (2024). Management of patients with multiple brain metastases. *Egyptian Journal of Neurosurgery*, 39(1), 64. <https://doi.org/10.1186/s41984-024-00321-5>
- Arvold, N. D., Lee, E. Q., Mehta, M. P., Margolin, K., Alexander, B. M., Lin, N. U., Anders, C. K., Soffiatti, R., Camidge, D. R., Vogelbaum, M. A., Dunn, I. F., & Wen, P. Y. (2016). Updates in the management of brain metastases. *Neuro-Oncology*, 18(8), 1043–1065. <https://doi.org/10.1093/neuonc/nov127>
- Avanzo, M., Trianni, A., Botta, F., Talamonti, C., Stasi, M., & Iori, M. (2021). Artificial intelligence and the medical physicist: Welcome to the machine. *Applied Sciences (Switzerland)*, 11(4), 1–17. <https://doi.org/10.3390/app11041691>
- Ba, S. N., Regine, W. F., & Mehta, M. (2016). Stereotactic radiosurgery for treatment of brain metastases. *Journal of Oncology Practice*, 12(8), 703–712. <https://doi.org/10.1200/JOP.2016.012922>
- Badiyan, S. N., Regine, W. F., & Mehta, M. (2016). Stereotactic radiosurgery for treatment of brain metastases. *Journal of Oncology Practice*, 12(8), 703–712. <https://doi.org/10.1200/JOP.2016.012922>
- Badloe, J., Mast, M., Petoukhova, A., Franssen, J. H., Ghariq, E., van der Voort van Zijp, N., & Wiggeraad, R. (2021). Impact of PTV margin reduction (2 mm to 0 mm) on pseudoprogression in stereotactic radiotherapy of solitary brain metastases. *Technical Innovations and Patient Support in Radiation Oncology*, 17, 40–47. <https://doi.org/10.1016/j.tipsro.2021.02.008>
- Barton, M. B., Zubizarreta, E., & Gospodarowicz, M. (2017). Radiotherapy in Low- and Middle-income Countries. What Can We Do Differently? *Clinical Oncology*, 29(2),

69–71. <https://doi.org/10.1016/j.clon.2016.11.009>

Bayman, E., Ataman, Ö. U., Kinay, M., & Akman, F. (2010). How to determine margins for planning target volume (PTV): From 2D to 3D planning in radiotherapy for head and neck cancer? Portal imaging assessment for set-up errors. *Turk Onkoloji Dergisi*, 25(3), 104–110.

Beaton, L., Bandula, S., Gaze, M. N., & Sharma, R. A. (2019). How rapid advances in imaging are defining the future of precision radiation oncology. In *British Journal of Cancer* (Vol. 120, Issue 8). <https://doi.org/10.1038/s41416-019-0412-y>

Bedford, J. L., Lee, Y. K., Wai, P., South, C. P., & Warrington, A. P. (2009). Evaluation of the Delta 4 phantom for IMRT and VMAT verification. *Physics in Medicine and Biology*, 54(9), 167–176. <https://doi.org/10.1088/0031-9155/54/9/N04>

Bel, A., Van Herk, M., & Lebesque, J. V. (1996). Target margins for random geometrical treatment uncertainties in conformal radiotherapy. *Medical Physics*, 23(9). <https://doi.org/10.1118/1.597745>

Belcher, A. H., Liu, X., Chmura, S., Yenice, K., & Wiersma, R. D. (2017). Towards frameless maskless SRS through real-time 6DoF robotic motion compensation. *Physics in Medicine and Biology*, 62(23), 9054–9066. <https://doi.org/10.1088/1361-6560/aa93d2>

Bernstein, D., Taylor, A., Nill, S., & Oelfke, U. (2021). New target volume delineation and PTV strategies to further personalise radiotherapy. *Physics in Medicine and Biology*, 66(5). <https://doi.org/10.1088/1361-6560/abe029>

Biasi, G., Petasecca, M., Guatelli, S., Hardcastle, N., Carolan, M., Perevertaylo, V., Kron, T., & Rosenfeld, A. B. (2018). A novel high-resolution 2D silicon array detector for

small field dosimetry with FFF photon beams. *Physica Medica*, 45.

<https://doi.org/10.1016/j.ejmp.2017.12.010>

Boire, A., Brastianos, P. K., Garzia, L., & Valiente, M. (2020). Brain metastasis. *Nature Reviews Cancer*, 20(1), 4–11. <https://doi.org/10.1038/s41568-019-0220-y>

Bolten, J.-H., Dunst, J., & Siebert, F.-A. (2023). Geometric accuracy in patient positioning for stereotactic radiotherapy of intracranial tumors. *Physics and Imaging in Radiation Oncology*, 27, 100461. <https://doi.org/10.1016/j.phro.2023.100461>

Brain Tumor Facts. (2022). <https://braintumor.org/brain-tumors/about-brain-tumors/brain-tumor-facts/>

Brook, O. R., Thornton, E., Mendiratta-Lala, M., Mahadevan, A., Raptopoulos, V., Brook, A., Najarian, R., Sheiman, R., & Siewert, B. (2015). CT Imaging Findings after Stereotactic Radiotherapy for Liver Tumors. *Gastroenterology Research and Practice*, 2015(126245), 8. <https://doi.org/10.1155/2015/126245>

Brown, M. H., Marcrom, S. R., Patel, M. P., Popple, R. A., Travis, R. L., McDonald, A. M., Riley, K. O., Markert, J. M., Willey, C. D., Bredel, M., Fiveash, J. B., & Thomas, E. M. (2023). Understanding the Effect of Prescription Isodose in Single-Fraction Stereotactic Radiosurgery on Plan Quality and Clinical Outcomes for Solid Brain Metastases. *Neurosurgery*, 93(6), 1313–1318. <https://doi.org/10.1227/neu.0000000000002585>

Buatti, J. M., Friedman, W. A., Meeks, S. L., & Bova, F. J. (2000). RTOG 90-05: the real conclusion. *International Journal of Radiation Oncology*Biophysics*, 47(2), 269–271. [https://doi.org/10.1016/S0360-3016\(99\)00506-4](https://doi.org/10.1016/S0360-3016(99)00506-4)

Cagney, D. N., Martin, A. M., Catalano, P. J., Redig, A. J., Lin, N. U., Lee, E. Q., Wen, P.

- Y., Dunn, I. F., Bi, W. L., Weiss, S. E., Haas-Kogan, D. A., Alexander, B. M., & Aizer, A. A. (2017). Incidence and prognosis of patients with brain metastases at diagnosis of systemic malignancy: A population-based study. *Neuro-Oncology*, *19*(11), 1511–1521. <https://doi.org/10.1093/neuonc/nox077>
- Callens, D., Benazzouz, C., Stessens, L., Piot, W., Nulens, A., Lambrecht, M., Berkovic, P., & Daisne, J. F. (2024). A prospective randomized study comparing two frameless immobilization systems for cranial stereotactic radiotherapy. *Technical Innovations and Patient Support in Radiation Oncology*, *30*.
<https://doi.org/10.1016/j.tipsro.2024.100249>
- CERN. (2017). Developing medical linacs for challenging regions. *CERN Courier*, 31–34.
- Chambrelant, I., Jarnet, D., Bou-Gharios, J., Le Fèvre, C., Kuntz, L., Antoni, D., Jenny, C., & Noël, G. (2023). Stereotactic Radiation Therapy of Single Brain Metastases: A Literature Review of Dosimetric Studies. In *Cancers* (Vol. 15, Issue 15).
<https://doi.org/10.3390/cancers15153937>
- Chan, M., Wong, M., Leung, R., Cheung, S., & Blanck, O. (2018). Optimizing the prescription isodose level in stereotactic volumetric-modulated arc radiotherapy of lung lesions as a potential for dose de-escalation. *Radiation Oncology*, *13*(1).
<https://doi.org/10.1186/s13014-018-0965-6>
- Chao, S. T., De Salles, A., Hayashi, M., Levivier, M., Ma, L., Martinez, R., Paddick, I., Régis, J., Ryu, S., Slotman, B. J., & Sahgal, A. (2018). Stereotactic radiosurgery in the management of limited (1-4) brain metastases: Systematic review and International Stereotactic Radiosurgery Society practice guideline. *Clinical Neurosurgery*, *83*(3), 345–353. <https://doi.org/10.1093/neuros/nyx522>

- Cheok, S. K., Yu, C., Feng, J. J., Briggs, R. G., Chow, F., Hwang, L., Ye, J. C., Attenello, F. J., Tran, D., Chang, E., & Zada, G. (2023). Comparison of preoperative versus postoperative treatment dosimetry plans of single-fraction stereotactic radiosurgery for surgically resected brain metastases. *Neurosurgical Focus*, *55*(2).
<https://doi.org/10.3171/2023.5.FOCUS23209>
- Choi, C. Y. H., Chang, S. D., Gibbs, I. C., Adler, J. R., Harsh IV, G. R., Lieberson, R. E., & Soltys, S. G. (2012). Stereotactic radiosurgery of the postoperative resection cavity for brain metastases: Prospective evaluation of target margin on tumor control. *International Journal of Radiation Oncology Biology Physics*, *84*(2), 336–342.
<https://doi.org/10.1016/j.ijrobp.2011.12.009>
- Cilla, S., Cellini, F., Romano, C., Macchia, G., Pezzulla, D., Viola, P., Buwenge, M., Indovina, L., Valentini, V., Morganti, A. G., & Deodato, F. (2022). Personalized Automation of Treatment Planning for Linac-Based Stereotactic Body Radiotherapy of Spine Cancer. *Frontiers in Oncology*, *12*. <https://doi.org/10.3389/fonc.2022.824532>
- Clark, G. M., Popple, R. A., Prendergast, B. M., Spencer, S. A., Thomas, E. M., Stewart, J. G., Guthrie, B. L., Markert, J. M., & Fiveash, J. B. (2012). Plan quality and treatment planning technique for single isocenter cranial radiosurgery with volumetric modulated arc therapy. *Practical Radiation Oncology*, *2*(4), 306–313.
<https://doi.org/10.1016/j.prro.2011.12.003>
- Cohen-Inbar, O., & Sheehan, J. P. (2016). The role of stereotactic radiosurgery and whole brain radiation therapy as primary treatment in the treatment of patients with brain oligometastases - A systematic review. *Journal of Radiosurgery and SBRT*, *4*(2), 79–88.

<http://www.ncbi.nlm.nih.gov/pubmed/29296432>
<http://www.pubmedcentral.nih.gov/articlerender.fcgi?artid=PMC5658879>

- Combs, S. E., Baumert, B. G., Bendszus, M., Bozzao, A., Brada, M., Fariselli, L., Fiorentino, A., Ganswindt, U., Grosu, A. L., Lagerwaard, F. L., Niyazi, M., Nyholm, T., Paddick, I., Weber, D. C., Belka, C., & Minniti, G. (2021). ESTRO ACROP guideline for target volume delineation of skull base tumors. *Radiotherapy and Oncology*, *156*, 80–94. <https://doi.org/10.1016/j.radonc.2020.11.014>
- Dai, Z., Ma, L., Cao, T., Zhu, L., Zhao, M., & Li, N. (2021). Dosimetric and radiobiological comparison of treatment plan between CyberKnife and EDGE in stereotactic body radiotherapy for pancreatic cancer. *Scientific Reports*, *11*(1), 4065. <https://doi.org/10.1038/s41598-021-83648-5>
- Das, I. J., Dawes, S. L., Dominello, M. M., Kavanagh, B., Miyamoto, C. T., Pawlicki, T., Santanam, L., Vinogradskiy, Y., & Yeung, A. R. (2022). Quality and Safety Considerations in Stereotactic Radiosurgery and Stereotactic Body Radiation Therapy: An ASTRO Safety White Paper Update. *Practical Radiation Oncology*, *12*(4). <https://doi.org/10.1016/j.prro.2022.03.001>
- Das, S., Kharade, V., Pandey, V., KV, A., Pasricha, R. K., & Gupta, M. (2022). Gamma Index Analysis as a Patient-Specific Quality Assurance Tool for High-Precision Radiotherapy: A Clinical Perspective of Single Institute Experience. *Cureus*, *14*(Dd). <https://doi.org/10.7759/cureus.30885>
- Datta, N. R., Samiei, M., & Bodis, S. (2014). Radiation therapy infrastructure and human resources in low- and middle-income countries: Present status and projections for 2020. *International Journal of Radiation Oncology Biology Physics*, *89*(3).

<https://doi.org/10.1016/j.ijrobp.2014.03.002>

de Crevoisier, R., Lafond, C., Mervoyer, A., Hulot, C., Jaksic, N., Bessières, I., & Delpon, G. (2022). Image-guided radiotherapy. *Cancer/Radiotherapie*, 26(1–2).

<https://doi.org/10.1016/j.canrad.2021.08.002>

Dean, M. K., Ahmed, A. A., Johnson, P., & Elsayyad, N. (2019). Distribution of dedicated stereotactic radiosurgery systems in the United States. *Applied Radiation Oncology*, 8(1), 26–30. <https://appliedradiationoncology.com/articles/distribution-of-dedicated-stereotactic-radiosurgery-systems-in-the-united-states>

Delta4 Phantom+ : The Fastest and most accurate 4D verification system. (2020.) Retrieved February 25, 2024, from <https://delta4family.com/wp-content/uploads/2022/04/brochure-D017-03-001-04-Delta4-PhantomPlus.pdf>

Desai, V., Bayouth, J., Smilowitz, J., & Yadav, P. (2021). A clinical validation of the MR-compatible Delta4 QA system in a 0.35 tesla MR linear accelerator. *Journal of Applied Clinical Medical Physics*, 22(4), 82–91. <https://doi.org/10.1002/acm2.13216>

Diez, P., Hanna, G. G., Aitken, K. L., van As, N., Carver, A., Colaco, R. J., Conibear, J., Dunne, E. M., Eaton, D. J., Franks, K. N., Good, J. S., Harrow, S., Hatfield, P., Hawkins, M. A., Jain, S., McDonald, F., Patel, R., Rackley, T., Sanghera, P., ... Murray, L. (2022). UK 2022 Consensus on Normal Tissue Dose-Volume Constraints for Oligometastatic, Primary Lung and Hepatocellular Carcinoma Stereotactic Ablative Radiotherapy. *Clinical Oncology*, 34(5), 288–300. <https://doi.org/10.1016/j.clon.2022.02.010>

Dileep, P. K., Hartmann, S., Javadi, M., Palkowski, H., Fischer, T., & Ziegmann, G. (2023). Uncertainty estimation using Gaussian error propagation in metal forming

- process simulation. *PAMM*, 23(1). <https://doi.org/10.1002/pamm.202200073>
- Dimitriadis, A., & Paddick, I. (2018). A novel index for assessing treatment plan quality in stereotactic radiosurgery. *Journal of Neurosurgery*, 129(December), 118–124. <https://doi.org/10.3171/2018.7.GKS18694>
- Dimitriadis, A., Palmer, A. L., Thomas, R. A. S., Nisbet, A., & Clark, C. H. (2017). Adaptation and validation of a commercial head phantom for cranial radiosurgery dosimetry end-to-end audit. *British Journal of Radiology*, 90(1074), 1–9. <https://doi.org/10.1259/bjr.20170053>
- Ding, C., Solberg, T. D., Hrycushko, B., Xing, L., Heinzerling, J., & Timmerman, R. D. (2013). Optimization of normalized prescription isodose selection for stereotactic body radiation therapy: Conventional vs robotic linac. *Medical Physics*, 40(5). <https://doi.org/10.1118/1.4798944>
- Dou, Z., Wu, J., Wu, H., Yu, Q., Yan, F., Jiang, B., Li, B., Xu, J., Xie, Q., Li, C., Sun, C., & Chen, G. (2021). The infratentorial localization of brain metastases may correlate with specific clinical characteristics and portend worse outcomes based on voxel-wise mapping. *Cancers*, 13(2), 1–16. <https://doi.org/10.3390/cancers13020324>
- Duan, X., Giles, W., Kirkpatrick, J. P., & Yin, F. F. (2019). The effect of setup uncertainty on optimal dosimetric margin in LINAC-based stereotactic radiosurgery with dynamic conformal arc technique. *Journal of Radiosurgery and SBRT*, 6(1).
- Duggar, W. N., Morris, B., He, R., & Yang, C. (2022a). Total workflow uncertainty of frameless radiosurgery with the Gamma Knife Icon cone-beam computed tomography. *Journal of Applied Clinical Medical Physics*, 23(5), 1–10. <https://doi.org/10.1002/acm2.13564>

- Duggar, W. N., Morris, B., He, R., & Yang, C. C. (2022b). Ramifications of Setup Margin Use During Frameless Stereotactic Radiosurgery/Therapy With Gamma Knife Icon Cone-Beam Computed Tomography (CBCT): A Dosimetric Study. *Cureus*, *14*(2), 1–11. <https://doi.org/10.7759/cureus.21996>
- Eaton, D. J., Lee, J., Patel, R., Millin, A. E., Paddick, I., & Walker, C. (2018). Stereotactic radiosurgery for benign brain tumors: Results of multicenter benchmark planning studies. *Practical Radiation Oncology*, *8*(5), e295–e304. <https://doi.org/10.1016/j.prro.2018.02.006>
- Ebner, D., Rava, P., Gorovets, D., Cielo, D., & Hepel, J. T. (2015). Stereotactic radiosurgery for large brain metastases. *Journal of Clinical Neuroscience*, *22*(10), 1650–1654. <https://doi.org/10.1016/j.jocn.2015.05.019>
- Ekpene, U., Ametefe, M., Akoto, H., Bankah, P., Totimeh, T., Wepeba, G., & Dakurah, T. (2018). Pattern of intracranial tumours in a tertiary hospital in Ghana. *Ghana Medical Journal*, *52*(2), 79–83. <https://doi.org/10.4314/gmj.v52i2.3>
- El Shafie, R. A., Celik, A., Weber, D., Schmitt, D., Lang, K., König, L., Bernhardt, D., Höne, S., Forster, T., von Nettelblatt, B., Adeberg, S., Debus, J., & Rieken, S. (2020a). A matched-pair analysis comparing stereotactic radiosurgery with whole-brain radiotherapy for patients with multiple brain metastases. *Journal of Neuro-Oncology*, *147*(3), 607–618. <https://doi.org/10.1007/s11060-020-03447-2>
- El Shafie, R. A., Celik, A., Weber, D., Schmitt, D., Lang, K., König, L., Bernhardt, D., Höne, S., Forster, T., von Nettelblatt, B., Adeberg, S., Debus, J., & Rieken, S. (2020). A matched-pair analysis comparing stereotactic radiosurgery with whole-brain radiotherapy for patients with multiple brain metastases. *Journal of Neuro-Oncology*,

147(3), 607–618. <https://doi.org/10.1007/s11060-020-03447-2>

Elbanna, M., Chowdhury, N. N., Rhome, R., & Fishel, M. L. (2021). Clinical and Preclinical Outcomes of Combining Targeted Therapy With Radiotherapy. In *Frontiers in Oncology* (Vol. 11). <https://doi.org/10.3389/fonc.2021.749496>

Elmore, S. N. C., Polo, A., Bourque, J. M., Pynda, Y., van der Merwe, D., Grover, S., Hopkins, K., Zubizarreta, E., & Abdel-Wahab, M. (2021). Radiotherapy resources in Africa: an International Atomic Energy Agency update and analysis of projected needs. *The Lancet Oncology*, 22(9), e391–e399. [https://doi.org/10.1016/S1470-2045\(21\)00351-X](https://doi.org/10.1016/S1470-2045(21)00351-X)

Enrique, G.-V., Irving, S.-R., Ricardo, B.-I., Jesus, F.-L., Alan, R.-M., Inigo, V. A. A., Luis, B.-L., Allan, H. C., Graciela, P.-M. A., Liliana, N.-R., & Roque, E.-R. (2019). Diagnosis and management of brain metastases: an updated review from a radiation oncology perspective. *Journal of Cancer Metastasis and Treatment*, 5(54). <https://doi.org/10.20517/2394-4722.2019.20>

Fallows, P., Wright, G., & Bownes, P. (2019). A standardised method for use of the Leksell GammaPlan Inverse Planning module for metastases. *Journal of Radiosurgery and SBRT*, 6(3), 227–233.

Faruqi, S., Ruschin, M., Soliman, H., Myrehaug, S., Zeng, K. L., Husain, Z., Atenafu, E., Tseng, C. L., Das, S., Perry, J., Maralani, P., Heyn, C., Mainprize, T., & Sahgal, A. (2020). Adverse Radiation Effect After Hypofractionated Stereotactic Radiosurgery in 5 Daily Fractions for Surgical Cavities and Intact Brain Metastases. *International Journal of Radiation Oncology Biology Physics*, 106(4). <https://doi.org/10.1016/j.ijrobp.2019.12.002>

- Fecci, P. E., Champion, C. D., Hoj, J., McKernan, C. M., Rory Goodwin, C., Kirkpatrick, J. P., Anders, C. K., Pendergast, A. M., & Sampson, J. H. (2019). The evolving modern management of brain metastasis. *Clinical Cancer Research*, 25(22), 6570–6580. <https://doi.org/10.1158/1078-0432.CCR-18-1624>
- Fezeu, F., Awad, A. J., Przybylowski, C. J., Starke, R. M., Grober, Y., Schlesinger, D., Lee, C., Xu, Z., & Sheehan, J. (2014). Access to Stereotactic radiosurgery : Identification of Existing Disparities and a Modest Proposal to Reduce Them. *Cureus*, 6(1), 1–6. <https://doi.org/10.7759/cureus.157>
- Fezeu, F., Ramesh, A., Melmer, P. D., Moosa, S., Larson, P. S., & Henderson, F. (2018). Challenges and Solutions for Functional Neurosurgery in Developing Countries. *Cureus*, 10(9), 8–12. <https://doi.org/10.7759/cureus.3314>
- Fiagbedzi, E., Hasford, F., & Tagoe, S. N. (2024). Impact of Planning Target Volume Margins in Stereotactic Radiosurgery for Brain Metastasis: A Review. *Progress in Medical Physics*, 35(1), 1–9. <https://doi.org/10.14316/pmp.2024.35.1.1>
- Fiagbedzi, E., Hasford, F., Tagoe, S. N., & Nisbet, A. (2023). Radiotherapy infrastructure for brain metastasis treatment in Africa: practical guidelines for implementation of a stereotactic radiosurgery (SRS) program. In *Health and Technology* (Vol. 13, Issue 6). <https://doi.org/10.1007/s12553-023-00799-3>
- Frederick, A., Quirk, S., Grendarova, P., van Dyke, L., Meyer, T., Wepler, S., & Roumeliotis, M. (2022). An updated approach for deriving PTV margins using image guidance and deformable dose accumulation. *Physics in Medicine & Biology*, 67(7), 075004. <https://doi.org/10.1088/1361-6560/ac5ce5>
- GAMMA KNIFE SOUTH AFRICA*. (2023). Retrieved April 30, 2023, from

<https://eurolab.co.za/innovation-technology/gamma-knife-sa/>

Garcia, M. A., Anwar, M., Yu, Y., Duriseti, S., Merritt, B., Nakamura, J., Hess, C.,

Theodosopoulos, P. V, McDermott, M., Sneed, P. K., & Braunstein, S. E. (2018).

Brain metastasis growth on preradiosurgical magnetic resonance imaging. *Practical*

Radiation Oncology, 8(6). <https://doi.org/10.1016/j.prro.2018.06.004>

Gevaert, T., Pellegrini, L., Engels, B., Christian, N., Mitine, C., & De Ridder, M. (2017).

Evaluation of a dedicated brain metastases treatment planning optimization for radiosurgery: A new treatment paradigm? *Physica Medica*, 44.

<https://doi.org/10.1016/j.ejmp.2017.10.040>

Gilbo, P., Zhang, I., & Knisely, J. (2017). Stereotactic radiosurgery of the brain: A review of common indications. *Chinese Clinical Oncology*, 6(Suppl 2), 1–16.

<https://doi.org/10.21037/cco.2017.06.07>

Gill, S. K., Reddy, K., Campbell, N., Chen, C., & Pearson, D. (2015). Determination of optimal PTV margin for patients receiving CBCT-guided prostate IMRT: Comparative analysis based on CBCT dose calculation with four different margins. *Journal of Applied Clinical Medical Physics*, 16(6), 252–262.

<https://doi.org/10.1120/jacmp.v16i6.5691>

Goldberg, N., Langer, M., & Shtern, S. (2024). Robust radiotherapy planning with spatially-based uncertainty sets. *IISE Transactions*.

<https://doi.org/10.1080/24725854.2024.2363316>

Goncalves, P. H., Montezuma-Rusca, J. M., Yarchoan, R., & Uldrick, T. S. (2016). Cancer prevention in HIV-infected populations. *Seminars in Oncology*, 43(1), 173–188.

<https://doi.org/10.1053/j.seminoncol.2015.09.011>

- Gondi, V., Bauman, G., Bradfield, L., Burri, S. H., Cabrera, A. R., Cunningham, D. A., Eaton, B. R., Hattangadi-Gluth, J. A., Kim, M. M., Kotecha, R., Kraemer, L., Li, J., Nagpal, S., Rusthoven, C. G., Suh, J. H., Tomé, W. A., Wang, T. J. C., Zimmer, A. S., Ziu, M., & Brown, P. D. (2022). Radiation Therapy for Brain Metastases: An ASTRO Clinical Practice Guideline. *Practical Radiation Oncology*, *12*(4), 265–282. <https://doi.org/10.1016/j.prro.2022.02.003>
- Grierson, E., Wilkinson, D., Causer, L., & de Leon, J. (2023). Evaluating the geometric and dosimetric impact of applying anisotropic CTV to PTV margins in image-guided post-prostatectomy radiation therapy. *Journal of Medical Imaging and Radiation Oncology*, *67*(7). <https://doi.org/10.1111/1754-9485.13563>
- Griffiths, A., Marinovich, L., Barton, M. B., & Lord, S. J. (2007). Cost analysis of Gamma Knife stereotactic radiosurgery. *International Journal of Technology Assessment in Health Care*, *23*(4), 488–494. <https://doi.org/10.1017/S0266462307070584>
- Grishchuk, D., Dimitriadis, A., Sahgal, A., De Salles, A., Fariselli, L., Kotecha, R., Levivier, M., Ma, L., Pollock, B. E., Regis, J., Sheehan, J., Suh, J., Yomo, S., & Paddick, I. (2023). ISRS Technical Guidelines for Stereotactic Radiosurgery: Treatment of Small Brain Metastases (≤ 1 cm in Diameter). *Practical Radiation Oncology*, *13*(3), 183–194. <https://doi.org/10.1016/j.prro.2022.10.013>
- Guckenberger, M., Baus, W. W., Blanck, O., Combs, S. E., Debus, J., Engenhart-Cabillic, R., Gauer, T., Grosu, A. L., Schmitt, D., Tanadini-Lang, S., & Moustakis, C. (2020). Definition and quality requirements for stereotactic radiotherapy: consensus statement from the DEGRO/DGMP Working Group Stereotactic Radiotherapy and Radiosurgery. In *Strahlentherapie und Onkologie* (Vol. 196, Issue 5).

<https://doi.org/10.1007/s00066-020-01603-1>

Guo, F. (2018). 3-D treatment planning system—Leksell Gamma Knife treatment planning system. *Medical Dosimetry*, 43(2), 177–183.

<https://doi.org/10.1016/j.meddos.2018.03.001>

Gupta, T., Upasani, M., Master, Z., Patil, A., Phurailatpam, R., Nojin, S., Kannan, S., Godasastri, J., & Jalali, R. (2014). Assessment of three-dimensional set-up errors using megavoltage computed tomography (MVCT) during image-guided intensity-modulated radiation therapy (IMRT) for craniospinal irradiation (CSI) on helical tomotherapy (HT). *Technology in Cancer Research and Treatment*, 14(1).

<https://doi.org/10.7785/tcrt.2012.500391>

Gutschenritter, T., Venur, V. A., Combs, S. E., Vellayappan, B., Patel, A. P., Foote, M., Redmond, K. J., Wang, T. J. C., Sahgal, A., Chao, S. T., Suh, J. H., Chang, E. L., Ellenbogen, R. G., & Lo, S. S. (2021). The judicious use of stereotactic radiosurgery and hypofractionated stereotactic radiotherapy in the management of large brain metastases. *Cancers*, 13(1), 1–15. <https://doi.org/10.3390/cancers13010070>

Gutzmer, R., Vordermark, D., Hassel, J. C., Krex, D., Wendl, C., Schadendorf, D., Sickmann, T., Rieken, S., Pukrop, T., Höller, C., Eigentler, T. K., & Meier, F. (2020). Melanoma brain metastases – Interdisciplinary management recommendations 2020. In *Cancer Treatment Reviews* (Vol. 89, Issue May, p. 102083). Elsevier.

<https://doi.org/10.1016/j.ctrv.2020.102083>

Habbous, S., Forster, K., Darling, G., Jerzak, K., Holloway, C. M. B., Sahgal, A., & Das, S. (2021). Incidence and real-world burden of brain metastases from solid tumors and hematologic malignancies in Ontario: A population-based study. *Neuro-Oncology*

Advances, 3(1), 1–14. <https://doi.org/10.1093/noajnl/vdaa178>

Hamada, N. (2023). Noncancer Effects of Ionizing Radiation Exposure on the Eye, the Circulatory System and beyond: Developments made since the 2011 ICRP Statement on Tissue Reactions. *Radiation Research*, 200(2). <https://doi.org/10.1667/RADE-23-00030.1>

Hamdi, Y., Abdeljaoued-Tej, I., Zatchi, A. A., Abdelhak, S., Boubaker, S., Brown, J. S., & Benkahla, A. (2021). Cancer in Africa: The Untold Story. *Frontiers in Oncology*, 11(April), 1–19. <https://doi.org/10.3389/fonc.2021.650117>

Hamilton, T., & Dade Lunsford, L. (2016). Worldwide variance in the potential utilization of Gamma Knife radiosurgery. *Journal of Neurosurgery*, 125(December), 160–165. <https://doi.org/10.3171/2016.7.gks161425>

Han, E. Y., Diagaradjane, P., Luo, D., Ding, Y., Kalaitzakis, G., Zoros, E., Zourari, K., Boursianis, T., Pappas, E., Wen, Z., Wang, J., & Briere, T. M. (2020). Validation of PTV margin for Gamma Knife Icon frameless treatment using a PseudoPatient® Prime anthropomorphic phantom. *Journal of Applied Clinical Medical Physics*, 21(9), 278–285. <https://doi.org/10.1002/acm2.12997>

Handeland, A. H., Indelicato, D. J., Fredrik Fjæra, L., Ytre-Hauge, K. S., Pettersen, H. E. S., Muren, L. P., Lassen-Ramshad, Y., & Stokkevåg, C. H. (2023). Linear energy transfer-inclusive models of brainstem necrosis following proton therapy of paediatric ependymoma. *Physics and Imaging in Radiation Oncology*, 27. <https://doi.org/10.1016/j.phro.2023.100466>

Hanna, S. A., Mancini, A., Dal Col, A. H., Asso, R. N., & Neves-Junior, W. F. P. (2019). Frameless Image-Guided Radiosurgery for Multiple Brain Metastasis Using VMAT: A

Review and an Institutional Experience. In *Frontiers in Oncology* (Vol. 9).

<https://doi.org/10.3389/fonc.2019.00703>

Hartgerink, D., Swinnen, A., Roberge, D., Nichol, A., Zygmanski, P., Yin, F. F., Deblois, F., Hurkmans, C., Ong, C. L., Bruynzeel, A., Aizer, A., Fiveash, J., Kirckpatrick, J., Guckenberger, M., Andratschke, N., de Ruyscher, D., Popple, R., & Zindler, J. (2019). LINAC based stereotactic radiosurgery for multiple brain metastases: guidance for clinical implementation. *Acta Oncologica*, *58*(9), 1275–1282.

<https://doi.org/10.1080/0284186X.2019.1633016>

Hasford, F., Ige, T. A., & Trauernicht, C. (2020). Safety measures in selected radiotherapy centres within Africa in the face of Covid-19. *Health and Technology*, *10*(6), 1391–1396. <https://doi.org/10.1007/s12553-020-00472-z>

Hellerbach, A., Eichner, M., Rueß, D., Luyken, K., Hoevels, M., Judge, M., Baues, C., Ruge, M., Kocher, M., & Treuer, H. (2022). Impact of prescription isodose level and collimator selection on dose homogeneity and plan quality in robotic radiosurgery. *Strahlentherapie Und Onkologie*, *198*(5), 484–496. <https://doi.org/10.1007/s00066-021-01872-4>

Herrmann, H., Seppenwoolde, Y., Georg, D., & Widder, J. (2019). Image guidance: past and future of radiotherapy. In *Radiologe* (Vol. 59). <https://doi.org/10.1007/s00117-019-0573-y>

Herschtal, A., Foroudi, F., Silva, L., Gill, S., & Kron, T. (2013). Calculating geometrical margins for hypofractionated radiotherapy. *Physics in Medicine and Biology*, *58*(2). <https://doi.org/10.1088/0031-9155/58/2/319>

Hotca, A., & Goodman, K. A. (2023). Radiation Therapy: Intensity-Modulated

- Radiotherapy, Cyberknife, Gamma Knife, and Proton Beam. In *Interventional Oncology*. https://doi.org/10.1007/978-3-030-51192-0_120-1
- Hurkmans, C. W., Remeijer, P., Lebesque, J. V., & Mijnheer, B. J. (2001). Set-up verification using portal imaging; review of current clinical practice. *Radiotherapy and Oncology*, 58(2). [https://doi.org/10.1016/S0167-8140\(00\)00260-7](https://doi.org/10.1016/S0167-8140(00)00260-7)
- Huynh, E., Hosny, A., Guthier, C., Bitterman, D. S., Petit, S. F., Haas-Kogan, D. A., Kann, B., Aerts, H. J. W. L., & Mak, R. H. (2020). Artificial intelligence in radiation oncology. *Nature Reviews Clinical Oncology*, 17(12), 771–781. <https://doi.org/10.1038/s41571-020-0417-8>
- IAEA. (2023). *DIRAC (Directory of Radiotherapy Centres)*. Retrieved April 20, 2023, from <https://dirac.iaea.org/Query/Countries>
- ICRU. (1999). International Commission On Radiation Units and Measurements (ICRU). In *The American journal of roentgenology, radium therapy, and nuclear medicine* (Vol. 109, Issue 2). <https://doi.org/10.1259/bjr.74.879.740294>
- Ige, T. A., Jenkins, A., Burt, G., Angal-Kalinin, D., McIntosh, P., Coleman, C. N., Pistenmaa, D. A., O'Brien, D., & Dosanjh, M. (2021). Surveying the Challenges to Improve Linear Accelerator-based Radiation Therapy in Africa: a Unique Collaborative Platform of All 28 African Countries Offering Such Treatment. *Clinical Oncology*, 33(12), e521–e529. <https://doi.org/10.1016/j.clon.2021.05.008>
- Jairam, V., Chiang, V. L. S., Yu, J. B., & Knisely, J. P. S. (2013). Role of stereotactic radiosurgery in patients with more than four brain metastases. In *CNS oncology* (Vol. 2, Issue 2, pp. 181–193). <https://doi.org/10.2217/cns.13.4>
- James, S., Al-Basheer, A., Elder, E., Huh, C., Ackerman, C., Barrett, J., Hamilton, R., &

- Mostafaei, F. (2023). Evaluation of commercial devices for patient specific QA of stereotactic radiotherapy plans. *Journal of Applied Clinical Medical Physics*, 24(8), 1–11. <https://doi.org/10.1002/acm2.14009>
- Jayaprakash, S., Pendse, A. M., & Deshpande, S. (2022). Significance of Dosimetric Parameters in Patients Undergoing Gamma Knife Radiosurgery for Vestibular Schwannoma. *Journal of Medical Physics*, 47(2), 206–211. https://doi.org/10.4103/jmp.jmp_5_22
- Jhaveri, J., Chowdhary, M., Zhang, X., Press, R. H., Switchenko, J. M., Ferris, M. J., Morgan, T. M., Roper, J., Dhabaan, A., Elder, E., Eaton, B. R., Olson, J. J., Curran, W. J., Shu, H. K. G., Crocker, I. R., & Patel, K. R. (2019). Does size matter? Investigating the optimal planning target volume margin for postoperative stereotactic radiosurgery to resected brain metastases. *Journal of Neurosurgery*, 130(3), 797–803. <https://doi.org/10.3171/2017.9.JNS171735>
- Jin, J., Gao, Y., Zhang, J., Wang, L., Wang, B., Cao, J., Shao, Z., & Wang, Z. (2018). Incidence, pattern and prognosis of brain metastases in patients with metastatic triple negative breast cancer. *BMC Cancer*, 18(1), 1–8. <https://doi.org/10.1186/s12885-018-4371-0>
- Juloori, A., Arshad, M., Wong, A. C., Farrey, K., Yenice, K., Collins, J., Aydogan, B., Usuki, K., Pitroda, S. P., Milano, M. T., & Chmura, S. J. (2023). The clinical relevance of margins in frameless stereotactic radiosurgery for intact brain metastases: A randomized trial of 0 vs 2 mm margins. *Journal of Clinical Oncology*, 41(16_suppl). https://doi.org/10.1200/jco.2023.41.16_suppl.tps2080
- Jung, J., Tailor, J., Dalton, E., Glancz, L. J., Roach, J., Zakaria, R., Lammy, S., Chari, A.,

- Budohoski, K. P., Livermore, L. J., Yu, K., Jenkinson, M. D., Brennan, P. M., Brazil, L., Bunce, C., Bourmpaki, E., Ashkan, K., & Vergani, F. (2020). Management evaluation of metastasis in the brain (MEMBRAIN) - A United Kingdom and Ireland prospective, multicenter observational study. *Neuro-Oncology Practice*, 7(3), 344–355. <https://doi.org/10.1093/nop/npz063>
- Khalsa, S. S. S., Chinn, M., Krucoff, M., & Sherman, J. H. (2013). The role of stereotactic radiosurgery for multiple brain metastases in stable systemic disease: A review of the literature. In *Acta Neurochirurgica* (Vol. 155, Issue 7, pp. 1321–1327). <https://doi.org/10.1007/s00701-013-1701-5>
- Kinaci-Tas, B., Alderliesten, T., Verbraak, F. D., & Rasch, C. R. N. (2023). Radiation-Induced Retinopathy and Optic Neuropathy after Radiation Therapy for Brain, Head, and Neck Tumors: A Systematic Review. In *Cancers* (Vol. 15, Issue 7). <https://doi.org/10.3390/cancers15071999>
- Kirkpatrick, J. P., Soltys, S. G., Lo, S. S., Beal, K., Shrieve, D. C., & Brown, P. D. (2017). The radiosurgery fractionation quandary: single fraction or hypofractionation? *Neuro-Oncology*, 19(2), ii38–ii49. <https://doi.org/10.1093/neuonc/now301>
- Kirkpatrick, J. P., Wang, Z., Sampson, J. H., McSherry, F., Herndon, J. E., Allen, K. J., Duffy, E., Hoang, J. K., Chang, Z., Yoo, D. S., Kelsey, C. R., & Yin, F. F. (2015). Defining the optimal planning target volume in image-guided stereotactic radiosurgery of brain metastases: Results of a randomized trial. *International Journal of Radiation Oncology Biology Physics*, 91(1), 100–108. <https://doi.org/10.1016/j.ijrobp.2014.09.004>
- Knisely, J. P. S., & Apuzzo, M. L. J. (2019). Historical Aspects of Stereotactic

Radiosurgery: Concepts, People, and Devices. *World Neurosurgery*, 130, 593–607.

<https://doi.org/10.1016/j.wneu.2019.04.030>

Kocher, M., Wittig, A., Piroth, M. D., Treuer, H., Seegenschmiedt, H., Ruge, M., Grosu, A.

L., & Guckenberger, M. (2014). Stereotactic radiosurgery for treatment of brain

metastases: A report of the DEGRO Working Group on Stereotactic Radiotherapy.

Strahlentherapie Und Onkologie, 190(6), 521–532. <https://doi.org/10.1007/s00066->

014-0648-7

Korreman, S., Medin, J., & Kjær-Kristoffersen, F. (2009). Dosimetric verification of

RapidArc treatment delivery. *Acta Oncologica*, 48(2), 185–191.

<https://doi.org/10.1080/02841860802287116>

Korytko, T., Radivoyevitch, T., Colussi, V., Wessels, B. W., Pillai, K., Maciunas, R. J., &

Einstein, D. B. (2006). 12 Gy gamma knife radiosurgical volume is a predictor for

radiation necrosis in non-AVM intracranial tumors. *International Journal of Radiation*

Oncology Biology Physics, 64(2), 419–424.

<https://doi.org/10.1016/j.ijrobp.2005.07.980>

Kraft, J., Zindler, J., Minniti, G., Guckenberger, M., & Andratschke, N. (2019).

Stereotactic Radiosurgery for Multiple Brain Metastases. In *Current Treatment*

Options in Neurology (Vol. 21, Issue 2). Current Treatment Options in Neurology.

<https://doi.org/10.1007/s11940-019-0548-3>

Kron, T. (2008). Reduction of margins in external beam radiotherapy. *Journal of Medical*

Physics, 33(2), 41–42. <https://doi.org/10.4103/0971-6203.41190>

Kuksis, M., Gao, Y., Tran, W., Hoey, C., Kiss, A., Komorowski, A. S., Dhaliwal, A. J.,

Sahgal, A., Das, S., Chan, K. K., & Jerzak, K. J. (2021). The incidence of brain

metastases among patients with metastatic breast cancer: a systematic review and meta-analysis. *Neuro-Oncology*, 23(6), 894–904.

<https://doi.org/10.1093/neuonc/noaa285>

Kutuk, T., Kotecha, R., Tolakanahalli, R., Wiczorek, D. J. J., Lee, Y. C., Ahluwalia, M. S., Hall, M. D., McDermott, M. W., Appel, H., Gutierrez, A. N., Mehta, M. P., & Tom, M. C. (2022). Zero Setup Margin Mask versus Frame Immobilization during Gamma Knife® Icon™ Stereotactic Radiosurgery for Brain Metastases. *Cancers*, 14(14). <https://doi.org/10.3390/cancers14143392>

Lauko, A., Rauf, Y., & Ahluwalia, M. S. (2020). Medical management of brain metastases. In *Neuro-Oncology Advances* (Vol. 2, Issue 1, pp. 1–14).

<https://doi.org/10.1093/noajnl/vdaa015>

Lawrence, Y. R., Li, X. A., Naqa, I., Hahn, C. A., Marks, L. B., Merchant, T. E., & Dicker, A. P. (2010). Radiation Dose-Volume Effects in the Brain. *International Journal of Radiation Oncology Biology Physics*, 76(3 SUPPL.), 20–27.

<https://doi.org/10.1016/j.ijrobp.2009.02.091>

Lee, H., Jeong, S. H., Jeong, B. H., Park, H. Y., Lee, K. J., Um, S. W., Jung Kwon, O., Kim, H., Barnholtz-Sloan, J. S., Sloan, A. E., Davis, F. G., Vigneau, F. D., Lai, P., Sawaya, R. E., Fecci, P. E., Champion, C. D., Hoj, J., McKernan, C. M., Rory Goodwin, C., ... Aizer, A. A. (2016). Current approaches to the management of brain metastases. *Neuro-Oncology*, 17(1), 6570–6580.

<https://doi.org/10.1093/neuonc/nou099>

Lee, Y. C., & Kim, Y. (2021). A patient-specific QA comparison between 2D and 3D diode arrays for single-lesion SRS and SBRT treatments. *Journal of Radiosurgery and*

SBRT, 7(4), 295–307. <http://www.ncbi.nlm.nih.gov/pubmed/34631231>

Leone, J. P., & Leone, B. A. (2015). Breast cancer brain metastases: The last frontier.

Experimental Hematology and Oncology, 4(1), 1–10. <https://doi.org/10.1186/s40164-015-0028-8>

Leszczyńska, P., Leszczyński, W., Wydmański, J., Kinga, D., Kaletka, A. N., Tukiendorf, A., & Hawrylewicz, L. (2017). Delineation of margins for the planning target volume (PTV) for image-guided radiotherapy (IGRT) of gastric cancer based on intrafraction motion. *Asian Pacific Journal of Cancer Prevention*, 18(1), 37–41.

<https://doi.org/10.22034/APJCP.2017.18.1.37>

Leybovich, L. B. (2002). An immobilization and localization technique for SRT and IMRT of intracranial tumors. *Journal of Applied Clinical Medical Physics*, 3(4), 317.

<https://doi.org/10.1120/1.1511401>

Li, H., Dong, L., Zhang, L., Yang, J. N., Gillin, M. T., & Zhu, X. R. (2011). Toward a better understanding of the gamma index: Investigation of parameters with a surface-based distance method. *Medical Physics*, 38(12), 6730–6741.

<https://doi.org/10.1118/1.3659707>

Lin, A. L., & Avila, E. K. (2017). Neurologic Emergencies in the Patients With Cancer.

Journal of Intensive Care Medicine, 32(2), 99–115.

<https://doi.org/10.1177/0885066615619582>

Lippitz, B., Lindquist, C., Paddick, I., Peterson, D., O'Neill, K., & Beaney, R. (2014).

Stereotactic radiosurgery in the treatment of brain metastases: The current evidence. In *Cancer Treatment Reviews* (Vol. 40, Issue 1, pp. 48–59). Elsevier Ltd.

<https://doi.org/10.1016/j.ctrv.2013.05.002>

- Liu, J. L., Walker, E. V., Paudel, Y. R., Davis, F. G., & Yuan, Y. (2022). Brain Metastases among Cancer Patients Diagnosed from 2010–2017 in Canada: Incidence Proportion at Diagnosis and Estimated Lifetime Incidence. *Current Oncology*, 29(3), 2091–2105. <https://doi.org/10.3390/currconcol29030169>
- Liu, Q., Tong, X., & Wang, J. (2019). Management of brain metastases: History and the present. In *Chinese Neurosurgical Journal* (Vol. 5, Issue 1, pp. 1–8). Chinese Neurosurgical Journal. <https://doi.org/10.1186/s41016-018-0149-0>
- Liu, Q., Zhang, H., Jiang, X., Qian, C., Liu, Z., & Luo, D. (2017). Factors involved in cancer metastasis: A better understanding to “seed and soil” hypothesis. *Molecular Cancer*, 16(1), 1–19. <https://doi.org/10.1186/s12943-017-0742-4>
- Low, D. A. (2010). Gamma dose distribution evaluation tool. *Journal of Physics: Conference Series*, 250, 349–359. <https://doi.org/10.1088/1742-6596/250/1/012071>
- Ludmir, E. B., Grosshans, D. R., & Woodhouse, K. D. (2018). Radiotherapy advances in pediatric neuro-oncology. In *Bioengineering* (Vol. 5, Issue 4). <https://doi.org/10.3390/bioengineering5040097>
- Lupattelli, M., Ali, E., Ingrosso, G., Saldi, S., Fulcheri, C., Borghesi, S., Tarducci, R., & Aristei, C. (2020). Stereotactic radiotherapy for brain metastases: Imaging tools and dosimetric predictive factors for radionecrosis. *Journal of Personalized Medicine*, 10(3), 1–13. <https://doi.org/10.3390/jpm10030059>
- Ma, L., Sahgal, A., Larson, D. A., Pinnaduwege, D., Fogh, S., Barani, I., Nakamura, J., McDermott, M., & Sneed, P. (2014). Impact of millimeter-level margins on peripheral normal brain sparing for gamma knife radiosurgery. *International Journal of Radiation Oncology Biology Physics*, 89(1), 206–213.

<https://doi.org/10.1016/j.ijrobp.2014.01.011>

Makris, D. N., Pappas, E. P., Zoros, E., Papanikolaou, N., Saenz, D. L., Kalaitzakis, G., Zourari, K., Efstathopoulos, E., Maris, T. G., & Pappas, E. (2019). Characterization of a novel 3D printed patient specific phantom for quality assurance in cranial stereotactic radiosurgery applications. *Physics in Medicine & Biology*, 64(10), 105009. <https://doi.org/10.1088/1361-6560/ab1758>

Manna, S. (2023). Evaluation of Patient-Specific Quality Assurance for RapidArc Treatment Delivery Using Dose Volume Histogram. *Journal of Polymer and Composites*. <https://doi.org/10.37591/jopc.v11i07.126106>

Mauritian Government National cancer control programme 2022-2025. (2019).

Mazzola, R., Corradini, S., Gregucci, F., Figlia, V., Fiorentino, A., & Alongi, F. (2019). Role of radiosurgery/stereotactic radiotherapy in oligometastatic disease: Brain oligometastases. In *Frontiers in Oncology* (Vol. 9, Issue APR, pp. 1–7). <https://doi.org/10.3389/fonc.2019.00206>

McDonald, B. A., Zachiu, C., Christodouleas, J., Naser, M. A., Ruschin, M., Sonke, J. J., Thorwarth, D., Létourneau, D., Tyagi, N., Tadic, T., Yang, J., Li, X. A., Bernchou, U., Hyer, D. E., Snyder, J. E., Bubula-Rehm, E., Fuller, C. D., & Brock, K. K. (2023). Dose accumulation for MR-guided adaptive radiotherapy: From practical considerations to state-of-the-art clinical implementation. In *Frontiers in Oncology* (Vol. 12). <https://doi.org/10.3389/fonc.2022.1086258>

McKenzie, A., Van Herk, M., & Mijnheer, B. (2002). Margins for geometric uncertainty around organs at risk in radiotherapy. *Radiotherapy and Oncology*, 62(3). [https://doi.org/10.1016/S0167-8140\(02\)00015-4](https://doi.org/10.1016/S0167-8140(02)00015-4)

- Meeks, S. L., Pukala, J., Ramakrishna, N., Willoughby, T. R., & Bova, F. J. (2011).
Radiosurgery technology development and use. *Journal of Radiosurgery and SBRT*,
1(1), 21–29.
<http://www.ncbi.nlm.nih.gov/pubmed/29296294><http://www.pubmedcentral.nih.gov/articlerender.fcgi?artid=PMC5658896>
- Mesko, S., Wang, H., Tung, S., Wang, C., Pasalic, D., Chapman, B. V., Moreno, A. C.,
Reddy, J. P., Garden, A. S., Rosenthal, D. I., Gunn, G. B., Frank, S. J., Fuller, C. D.,
Morrison, W., & Phan, J. (2020). Estimating PTV Margins in Head and Neck
Stereotactic Ablative Radiation Therapy (SABR) Through Target Site Analysis of
Positioning and Intrafractional Accuracy. *International Journal of Radiation Oncology
Biology Physics*, *106*(1), 185–193. <https://doi.org/10.1016/j.ijrobp.2019.09.010>
- Milano, M. T., Grimm, J., Niemierko, A., Soltys, S. G., Moiseenko, V., Redmond, K. J.,
Yorke, E., Sahgal, A., Xue, J., Mahadevan, A., Muacevic, A., Marks, L. B., &
Kleinberg, L. R. (2021). Single- and Multifraction Stereotactic Radiosurgery
Dose/Volume Tolerances of the Brain. *International Journal of Radiation Oncology
Biology Physics*, *110*(1). <https://doi.org/10.1016/j.ijrobp.2020.08.013>
- Minniti, G., Capone, L., Alongi, F., Figlia, V., Nardiello, B., El Gawhary, R., Scaringi, C.,
Bianciardi, F., Tolu, B., Gentile, P., & Paolini, S. (2020). Initial Experience With
Single-Isocenter Radiosurgery to Target Multiple Brain Metastases Using an
Automated Treatment Planning Software: Clinical Outcomes and Optimal Target
Volume Margins Strategy. *Advances in Radiation Oncology*, *5*(5), 856–864.
<https://doi.org/10.1016/j.adro.2020.06.008>
- Minniti, G., Niyazi, M., Alongi, F., Navarria, P., & Belka, C. (2021). Current status and

- recent advances in reirradiation of glioblastoma. In *Radiation Oncology* (Vol. 16, Issue 1). <https://doi.org/10.1186/s13014-021-01767-9>
- Minniti, G., Scaringi, C., Poggi, M., Rea, M. L. J., Trillò, G., Esposito, V., Bozzao, A., Enrici, M. M., Toscano, V., & Enrici, R. M. (2015). Fractionated stereotactic radiotherapy for large and invasive non-functioning pituitary adenomas: Long-term clinical outcomes and volumetric MRI assessment of tumor response. *European Journal of Endocrinology*, 172(4), 433–441. <https://doi.org/10.1530/EJE-14-0872>
- Mitchell, D. K., Kwon, H. J., Kubica, P. A., Huff, W. X., O'Regan, R., & Dey, M. (2022). Brain metastases: An update on the multi-disciplinary approach of clinical management. *Neurochirurgie*, 68(1), 69–85. <https://doi.org/10.1016/j.neuchi.2021.04.001>
- Miura, H., Kenjo, M., Doi, Y., Ueda, T., Nakao, M., Ozawa, S., & Nagata, Y. (2023). Effect of Target Changes on Target Coverage and Dose to the Normal Brain in Fractionated Stereotactic Radiation Therapy for Metastatic Brain Tumors. *Advances in Radiation Oncology*, 8(6). <https://doi.org/10.1016/j.adro.2023.101264>
- Mizuno, T., Takada, K., Hasegawa, T., Yoshida, T., Murotani, K., Kobayashi, H., Sakurai, T., Yamashita, Y., Akazawa, N., & Kojima, E. (2019). Comparison between stereotactic radiosurgery and whole-brain radiotherapy for 10-20 brain metastases from non-small cell lung cancer. *Molecular and Clinical Oncology*, 10(1), 560–566. <https://doi.org/10.3892/mco.2019.1830>
- Mukherji, A. (2018). Basics of Planning and Management of Patients during Radiation Therapy. In *Basics of Planning and Management of Patients during Radiation Therapy*. <https://doi.org/10.1007/978-981-10-6659-7>

- Murrell, D. H., Perera, F., Chambers, A. F., & Foster, P. J. (2016). Brain Metastasis: Basic Biology, Clinical Management, and Insight From Experimental Model Systems. In *Introduction to Cancer Metastasis* (Vol. 2, pp. 317–333). Elsevier Inc.
<https://doi.org/10.1016/B978-0-12-804003-4.00017-7>
- Nakazawa, H., Mori, Y., Komori, M., Tsugawa, T., Shibamoto, Y., Kobayashi, T., Hashizume, C., Uchiyama, Y., & Hagiwara, M. (2014). Simulational study of a dosimetric comparison between a Gamma Knife treatment plan and an intensity-modulated radiotherapy plan for skull base tumors. *Journal of Radiation Research*, *55*(3), 518–526. <https://doi.org/10.1093/jrr/rrt136>
- Nataf, F., Schlienger, M., Liu, Z., Foulquier, J. N., Grès, B., Orthuon, A., Vannetzel, J. M., Escudier, B., Meder, J. F., Roux, F. X., & Touboul, E. (2008). Radiosurgery With or Without A 2-mm Margin for 93 Single Brain Metastases. *International Journal of Radiation Oncology Biology Physics*, *70*(3), 766–772.
<https://doi.org/10.1016/j.ijrobp.2007.11.002>
- National Academies of Sciences, E. and M. (2021). *Radioactive Sources: Applications and Alternative Technologies* (Vol. 4). The National Academies Press.
<https://doi.org/10.17226/26121>
- Navarria, P., Clerici, E., Carta, G., Attuati, L., Picozzi, P., Franzese, C., D’Agostino, G. R., Tomatis, S., Mancosu, P., Cozzi, L., Reggiori, G., & Scorsetti, M. (2018). Randomized Phase III Trial Comparing Gamma Knife and Linac Based (EDGE) Approaches for Brain Metastases Radiosurgery: Results from the Gadget Trial. *International Journal of Radiation Oncology*Biology*Physics*, *102*(3).
<https://doi.org/10.1016/j.ijrobp.2018.06.349>

- Ndlovu, N. (2019). Radiotherapy treatment in cancer control and its important role in Africa. *Ecancermedicalscience*, *13*, 1–7. <https://doi.org/10.3332/ecancer.2019.942>
- Nelms, B. E., Zhen, H., & Tom, W. A. (2011). Per-beam, planar IMRT QA passing rates do not predict clinically relevant patient dose errors. *Medical Physics*, *38*(2), 1037–1044. <https://doi.org/10.1118/1.3544657>
- Niedermeyer, S., Schmutzer-Sondergeld, M., Weller, J., Katzendobler, S., Kirchleitner, S., Forbrig, R., Harter, P. N., Baumgarten, L. V., Schichor, C., Stoecklein, V., & Thon, N. (2024). Neurosurgical resection of multiple brain metastases: outcomes, complications, and survival rates in a retrospective analysis. *Journal of Neuro-Oncology*, *169*(2), 349–358. <https://doi.org/10.1007/s11060-024-04744-w>
- Noël, G., Simon, J. M., Valery, C. A., Cornu, P., Boisserie, G., Hasboun, D., Ledu, D., Tep, B., Delattre, J. Y., Marsault, C., Baillet, F., & Mazon, J. J. (2003). Radiosurgery for brain metastasis: Impact of CTV on local control. *Radiotherapy and Oncology*, *68*(1), 15–21. [https://doi.org/10.1016/S0167-8140\(03\)00207-X](https://doi.org/10.1016/S0167-8140(03)00207-X)
- Ohtakara, K., Hayashi, S., & Hoshi, H. (2012). Characterisation of dose distribution in linear accelerator-based intracranial stereotactic radiosurgery with the dynamic conformal arc technique: consideration of the optimal method for dose prescription and evaluation. *The British Journal of Radiology*, *85*(1009), 69–76. <https://doi.org/10.1259/bjr/20905396>
- Ohtakara, K., Hayashi, S., Tanaka, H., & Hoshi, H. (2012). Consideration of optimal isodose surface selection for target coverage in micro-multileaf collimator-based stereotactic radiotherapy for large cystic brain metastases: comparison of 90%, 80% and 70% isodose surface-based planning. *The British Journal of Radiology*, *85*(1017),

e640-6. <https://doi.org/10.1259/bjr/21015703>

- Omotoso, O., Teibo, J. O., Atiba, F. A., Oladimeji, T., Paimo, O. K., Ataya, F. S., Batiha, G. E. S., & Alexiou, A. (2023). Addressing cancer care inequities in sub-Saharan Africa: current challenges and proposed solutions. In *International Journal for Equity in Health* (Vol. 22, Issue 1). BioMed Central Ltd. <https://doi.org/10.1186/s12939-023-01962-y>
- Ormrod, D., Holm, K., Goa, K., & Spencer, C. (1999). Epirubicin: a review of its efficacy as adjuvant therapy and in the treatment of metastatic disease in breast cancer. *Drugs & Aging*, 15(5), 389–416. <https://doi.org/10.2165/00002512-199915050-00006>
- Pacelli, R., Caroprese, M., Palma, G., Oliviero, C., Clemente, S., Cella, L., & Conson, M. (2019). Technological evolution of radiation treatment: Implications for clinical applications. In *Seminars in Oncology* (Vol. 46, Issue 3). <https://doi.org/10.1053/j.seminoncol.2019.07.004>
- Paddick, I., & Lippitz, B. (2006). A simple dose gradient measurement tool to complement the conformity index. *Journal of Neurosurgery*, 105(Supplement), 194–201. <https://doi.org/10.3171/sup.2006.105.7.194>
- Pagett, C. J. H., Lilley, J., Lindsay, R., Short, S., & Murray, L. (2022). Optimising tumour coverage and organ at risk sparing for hypofractionated re-irradiation in glioblastoma. *Physics and Imaging in Radiation Oncology*, 21. <https://doi.org/10.1016/j.phro.2022.02.012>
- Pahwa, B., & Agrawal, D. (2023). Role of novel policy implementation for Gamma Knife (GK) procedures in improving access to neurosurgical care in lower middle income countries (LMICs) GK in LMICs. *World Neurosurgery: X*, 18(January), 100166.

<https://doi.org/10.1016/j.wnsx.2023.100166>

Palmisciano, P., Ferini, G., Khan, R., Bin-Alamer, O., Umana, G. E., Yu, K., Cohen-Gadol, A. A., El Ahmadieh, T. Y., & Haider, A. S. (2022). Neoadjuvant Stereotactic Radiotherapy for Brain Metastases: Systematic Review and Meta-Analysis of the Literature and Ongoing Clinical Trials. *Cancers*, *14*(17), 75–87.

<https://doi.org/10.3390/cancers14174328>

Palorini, F., Cavallo, A., Ferella, L., & Orlandi, E. (2019). Central Nervous System (Brain, Brainstem, Spinal Cord), Ears, Ocular Toxicity. In *Modelling Radiotherapy Side Effects*. <https://doi.org/10.1201/b21956-7>

Pannullo, S. C., Julie, D. A. R., Chidambaram, S., Balogun, O. D., Formenti, S. C., Apuzzo, M. L. J., & Knisely, J. P. S. (2019). Worldwide Access to Stereotactic Radiosurgery. *World Neurosurgery*, *130*, 608–614.

<https://doi.org/10.1016/j.wneu.2019.04.031>

Paoletti, L., Ceccarelli, C., Menichelli, C., Aristei, C., Borghesi, S., Tucci, E., Bastiani, P., & Cozzi, S. (2022). Special stereotactic radiotherapy techniques: procedures and equipment for treatment simulation and dose delivery. *Reports of Practical Oncology and Radiotherapy*, *27*(1), 1–9. <https://doi.org/10.5603/RPOR.a2021.0129>

Papadopoulou, A., Govina, O., Tsatsou, I., Mantzorou, M., Mantoudi, A., Tsiou, C., & Adamakidou, T. (2022). Quality of life, distress, anxiety and depression of ambulatory cancer patients receiving chemotherapy. *Medicine and Pharmacy Reports*, *95*(4), 418–429. <https://doi.org/10.15386/mpr-2458>

Park, S.-Y., Choi, N., & Jang, N. Y. (2021). Frameless immobilization system with roll correction for stereotactic radiosurgery of intracranial brain metastases. *Journal of*

Radiation Research, 62(6), 1015–1021. <https://doi.org/10.1093/jrr/rrab071>

Parker, B. C. (2002). PTV margin determination in conformal SRT of intracranial lesions.

Journal of Applied Clinical Medical Physics, 3(3), 176.

<https://doi.org/10.1120/1.1474308>

Patel, G., Mandal, A., Choudhary, S., Mishra, R., & Shende, R. (2020). Plan evaluation

indices: A journey of evolution. *Reports of Practical Oncology & Radiotherapy*,

25(3), 336–344. <https://doi.org/10.1016/j.rpor.2020.03.002>

Patel, T. R., McHugh, B. J., Bi, W. L., Minja, F. J., Knisely, J. P. S., & Chiang, V. L.

(2011). A comprehensive review of MR imaging changes following radiosurgery to

500 brain metastases. *American Journal of Neuroradiology*, 32(10), 1885–1892.

<https://doi.org/10.3174/ajnr.A2668>

Patro, K. C., Avinash, A., Pradhan, A., Boya, R. R., Kundu, C., Bhattacharyya, P. S.,

Pilaka, V. K. R., Muvvala, M., Prabu, A. C., Kumar, A. A., Aketi, S., Prasad, P.,

Priyasha, V. N., Avidi, V. S. P. K., Atchayalingam, M., & Karthikeyan, K. (2022).

Step-by-Step Stereotactic Radiotherapy Planning of Brain Metastasis: A Guide to

Radiation Oncologists—the ROSE Case (Radiation Oncology from Simulation to

Execution). *Journal of Current Oncology*, 5(2), 94–101.

<https://doi.org/10.1177/25898892221145226>

Phadke, M., Ozgun, A., Eroglu, Z., & Smalley, K. S. M. (2022). Melanoma brain

metastases: Biological basis and novel therapeutic strategies. In *Experimental*

Dermatology (Vol. 31, Issue 1, pp. 31–42). <https://doi.org/10.1111/exd.14286>

Phantom Patient for Stereotactic End-to-End Verification - CIRS. (2023). Retrieved

November 30, 2023, from <https://www.cirsinc.com/products/radiation->

therapy/phantom-patient-for-stereotactic-end-to-end-verification/

Piedade, P. A. (2019). Volume-dose indexes and dose prescription descriptive review of radiosurgery planning. *Brazilian Journal of Radiation Sciences*, 7(3B).

<https://doi.org/10.15392/bjrs.v7i3b.889>

Pomper, M. A., Dalnoki-Veress, F., & Moore, G. M. (2016). *Treatment, not terror*.

<https://stanleycenter.org/publications/report/TreatmentNotTerror212.pdf>

Price of linear accelerators jumps 20%. (2023). Retrieved June 30, 2023, from

<https://www.modernhealthcare.com/article/20130724/NEWS/307249943/price-of-linear-accelerators-jumps-20>

Pudsey, L., Haworth, A., White, P., Moutrie, Z., Jonker, B., Foote, M., & Poder, J. (2022).

Current status of intra-cranial stereotactic radiotherapy and stereotactic radiosurgery in Australia and New Zealand: key considerations from a workshop and surveys.

Physical and Engineering Sciences in Medicine, 45(1), 251–259.

<https://doi.org/10.1007/s13246-022-01108-4>

Putz, F., Mengling, V., Perrin, R., Masitho, S., Weissmann, T., Rösch, J., Bäuerle, T.,

Janka, R., Cavallaro, A., Uder, M., Amarteifio, P., Doussin, S., Schmidt, M. A.,

Dörfler, A., Semrau, S., Lettmaier, S., Fietkau, R., & Bert, C. (2020). Magnetic resonance imaging for brain stereotactic radiotherapy: A review of requirements and pitfalls. *Strahlentherapie Und Onkologie*, 196(5), 444–456.

<https://doi.org/10.1007/s00066-020-01604-0>

Rahman, R., Alexander, B. M., & Wen, P. Y. (2020). Neurologic Complications of Cranial

Radiation Therapy and Strategies to Prevent or Reduce Radiation Toxicity. In *Current Neurology and Neuroscience Reports* (Vol. 20, Issue 8).

<https://doi.org/10.1007/s11910-020-01051-5>

Rajput, S., Kumar Sharma, P., & Malviya, R. (2023). Fluid mechanics in circulating tumour cells: Role in metastasis and treatment strategies. *Medicine in Drug Discovery*, 18, 100158. <https://doi.org/10.1016/j.medidd.2023.100158>

Rattan, R., Kataria, T., Banerjee, S., Goyal, S., Gupta, D., Pandita, A., Bisht, S., Narang, K., & Mishra, S. R. (2019). Artificial intelligence in oncology, its scope and future prospects with specific reference to radiation oncology. *BJR|Open*, 1(1), 20180031. <https://doi.org/10.1259/bjro.20180031>

Robert, N., Sehgal, T., Singh, R., Oinam, A., Trivedi, G., Singh, B., Bahl, A., Madan, R., & Rai, B. (2023). Rotational set up uncertainly in non-6D couch and its effects in clinical target volume-planning target volume margin calculation for different sites. *Journal of Medical Physics*, 48(1). https://doi.org/10.4103/jmp.jmp_78_22

Rajo-Santiago, J., Habraken, S. J. M., Romero, A. M., Lathouwers, D., Wang, Y., Perkó, Z., & Hoogeman, M. S. (2023). Robustness analysis of CTV and OAR dose in clinical PBS-PT of neuro-oncological tumors: Prescription-dose calibration and inter-patient variation with the Dutch proton robustness evaluation protocol. *Physics in Medicine and Biology*, 68(17). <https://doi.org/10.1088/1361-6560/acead1>

Romanelli, P., & Beltramo, G. (2022). Image-Guided Stereotactic Radiosurgery for the Treatment of Spasticity and Pain: A Preliminary Experience. *Cureus*. <https://doi.org/10.7759/cureus.24021>

Romano, K. D., Trifiletti, D. M., Garda, A., Xu, Z., Schlesinger, D., Watkins, W. T., Neal, B., Larner, J. M., & Sheehan, J. P. (2017). Choosing a Prescription Isodose in Stereotactic Radiosurgery for Brain Metastases: Implications for Local Control. *World*

Neurosurgery, 98, 761-767.e1. <https://doi.org/10.1016/j.wneu.2016.11.038>

Ruggieri, R., Naccarato, S., Mazzola, R., Ricchetti, F., Corradini, S., Fiorentino, A., & Alongi, F. (2018). Linac-based VMAT radiosurgery for multiple brain lesions: Comparison between a conventional multi-isocenter approach and a new dedicated mono-isocenter technique. *Radiation Oncology*, 13(1), 1–9.
<https://doi.org/10.1186/s13014-018-0985-2>

Ruschin, M., Sahgal, A., Ma, L., Wang, L., Gete, E., & Nichol, A. (2020). General Techniques for Radiosurgery. In *Radiotherapy in Managing Brain Metastases*.
https://doi.org/10.1007/978-3-030-43740-4_16

SABR UK Consortium. (2015). *Stereotactic Ablative Body Radiation Therapy (SABR): A Resource Version 5.0. January*, 1–99.
http://www.academia.edu/7657886/Stereotactic_Ablative_Body_Radiation_Therapy_SABR_A_Resource%0Ahttp://www.actionradiotherapy.org/wp-content/uploads/2014/12/UKSABRConsortiumGuidelinesv5.pdf

Sadagopan, R., Bencomo, J. A., Martin, R. L., Nilsson, G., Matzen, T., & Balter, P. A. (2009). Characterization and clinical evaluation of a novel IMRT quality assurance system. *Journal of Applied Clinical Medical Physics*, 10(2), 104–119.
<https://doi.org/10.1120/jacmp.v10i2.2928>

Sadeghi, S., Siavashpour, Z., Sadr, A. V., Farzin, M., Sharp, R., & Gholami, S. (2021). A rapid review of influential factors and appraised solutions on organ delineation uncertainties reduction in radiotherapy. In *Biomedical Physics and Engineering Express* (Vol. 7, Issue 5). <https://doi.org/10.1088/2057-1976/ac14d0>

Sadowski, B. M., Fillmann, M., Szałkowski, D., & Kukołowicz, P. (2022). Evaluation of

- SRS MapCHECK with StereoPHAN phantom as a new pre-treatment system verification for SBRT plans. *Polish Journal of Medical Physics and Engineering*, 28(2), 84–89. <https://doi.org/10.2478/pjmpe-2022-0010>
- Saenz, D., Papanikolaou, N., Zoros, E., Pappas, E., Reiner, M., Chew, L. T., Lim, H. Y., Hancock, S., Nevelsky, A., Njeh, C., & Anagnostopoulos, G. (2020). *Robustness of single-isocenter multiple-metastasis stereotactic radiosurgery end-to-end testing across institutions*. 1–23. <https://doi.org/10.21203/rs.3.rs-15983/v1>
- Safain, M. G., Rahal, J. P., Raval, A., Rivard, M. J., Mignano, J. E., Wu, J. K., & Malek, A. M. (2014). Use of cone-beam computed tomography angiography in planning for gamma knife radiosurgery for arteriovenous malformations: A case series and early report. *Neurosurgery*, 74(6). <https://doi.org/10.1227/NEU.0000000000000331>
- Sahgal, A., Ruschin, M., Ma, L., Verbakel, W., Larson, D., & Brown, P. D. (2017). Stereotactic radiosurgery alone for multiple brain metastases? A review of clinical and technical issues. *Neuro-Oncology*, 19, ii2–ii15. <https://doi.org/10.1093/neuonc/nox001>
- Sasaki, M., Sugimoto, W., & Ikushima, H. (2020). Simplification of head and neck volumetric modulated arc therapy patient-specific quality assurance, using a Delta4 PT. *Reports of Practical Oncology and Radiotherapy*, 25(5), 793–800. <https://doi.org/10.1016/j.rpor.2020.07.004>
- Saul, S. (2023). *Geography Has Role in Medicare Cancer Coverage*. Retrieved May 1, 2023, from [https://www.nytimes.com/2008/12/17/health/policy/17knife.html#:~:text=authorized it for use throughout,and%2C increasingly%2C prostate cancer](https://www.nytimes.com/2008/12/17/health/policy/17knife.html#:~:text=authorized%20it%20for%20use%20throughout,and%2C%20increasingly%2C%20prostate%20cancer)
- Saw, C. B., Gillette, C., Peters, C. A., & Koutcher, L. (2018). Clinical implementation of

- radiosurgery using the Helical TomoTherapy unit. *Medical Dosimetry*, 43(3), 284–290. <https://doi.org/10.1016/j.meddos.2017.10.004>
- Saw, C. B., Li, S., Battin, F., McKeague, J., & Peters, C. A. (2018). External beam planning module of Eclipse for external beam radiation therapy. *Medical Dosimetry*, 43(2), 195–204. <https://doi.org/10.1016/j.meddos.2018.03.003>
- Scaringi, C., Agolli, L., & Minniti, G. (2018). Technical advances in radiation therapy for brain tumors. In *Anticancer Research* (Vol. 38, Issue 11). <https://doi.org/10.21873/anticancer.12954>
- Schell, M. C., Bova, F. J., Larson, D. a, Leavitt, D. D., Lutz, W. R., Podgorsak, E. B., & Wu, A. (1995). *Stereotactic Radiosurgery Report of Task Group 42 Radiation Therapy Committee for the American Association for Physicists in Medicine* (Issue 5).
- Schmitt, D., Blanck, O., Gauer, T., Fix, M. K., Brunner, T. B., Fleckenstein, J., Loutfi-Krauss, B., Manser, P., Werner, R., Wilhelm, M. L., Baus, W. W., & Moustakis, C. (2020). Technological quality requirements for stereotactic radiotherapy: Expert review group consensus from the DGMP Working Group for Physics and Technology in Stereotactic Radiotherapy. *Strahlentherapie Und Onkologie*, 196(5), 421–443. <https://doi.org/10.1007/s00066-020-01583-2>
- Scobioala, S., Kittel, C., Elsayad, K., Kroeger, K., Oertel, M., Samhuri, L., Haverkamp, U., & Eich, H. T. (2019). A treatment planning study comparing IMRT techniques and cyber knife for stereotactic body radiotherapy of low-risk prostate carcinoma. *Radiation Oncology*, 14(1), 1–10. <https://doi.org/10.1186/s13014-019-1353-6>
- Seravalli, E., Van Haaren, P. M. A., Van Der Toorn, P. P., & Hurkmans, C. W. (2015). A comprehensive evaluation of treatment accuracy, including end-to-end tests and

clinical data, applied to intracranial stereotactic radiotherapy. *Radiotherapy and Oncology*, 116(1). <https://doi.org/10.1016/j.radonc.2015.06.004>

Seung, S. K., Larson, D. A., Galvin, J. M., Mehta, M. P., Potters, L., Schultz, C. J., Yajnik, S. V., Hartford, A. C., & Rosenthal, S. A. (2013). American college of radiology (ACR) and american society for radiation oncology (ASTRO) practice guideline for the performance of stereotactic radiosurgery (SRS). In *American Journal of Clinical Oncology: Cancer Clinical Trials* (Vol. 36, Issue 3, pp. 310–315). <https://doi.org/10.1097/COC.0b013e31826e053d>

Shakeshaft, J. (2021). *IOMP webinar: CTV-PTV Margins in Stereotactic Radiosurgery: Do we need them?* IOMP. <https://doi.org/https://www.youtube.com/watch?v=b0DBzK6qq9c>

Shibamoto, Y., & Iwata, H. (2020). The Quest for Optimal Fractionation Schedules in Stereotactic Radiotherapy. *Cureus*, 12(1), 1–10. <https://doi.org/10.7759/cureus.6777>

Shirato, H. (2023). Biomedical advances and future prospects of high-precision threedimensional radiotherapy and four-dimensional radiotherapy. In *Proceedings of the Japan Academy Series B: Physical and Biological Sciences* (Vol. 99, Issue 9). <https://doi.org/10.2183/pjab.99.024>

Shiue, K., Barnett, G. H., Suh, J. H., Vogelbaum, M. A., Reddy, C. A., Weil, R. J., Angelov, L., Neyman, G., & Chao, S. T. (2014). Using higher isodose lines for gamma knife treatment of 1 to 3 brain metastases is safe and effective. *Neurosurgery*, 74(4). <https://doi.org/10.1227/NEU.0000000000000289>

Sikdar, D., Krishnan, A. S., RS, N., Chakravarty, A., Gupta, D., Gupta, S., Kumar, A., Joseph, D., & Gupta, M. (2024). MV CBCT based assessment of setup uncertainties

- and planning target volume margin in head and neck cancer. *Reports of Practical Oncology and Radiotherapy*, 29(2), 141–147. <https://doi.org/10.5603/rpor.99361>
- Simon, M., Papp, J., Csiki, E., & Kovács, Á. (2022). Plan Quality Assessment of Fractionated Stereotactic Radiotherapy Treatment Plans in Patients With Brain Metastases. *Frontiers in Oncology*, 12(March), 1–8. <https://doi.org/10.3389/fonc.2022.846609>
- Simpson, J. R., Drzymala, R. E., & Rich, K. M. (2006). Stereotactic Radiosurgery and Radiotherapy. In *Technical Basis of Radiation Therapy* (pp. 233–253). https://doi.org/10.1007/3-540-35665-7_11
- Skourou, C., Hickey, D., Rock, L., Houston, P., Sturt, P., O’ Sullivan, S., Faul, C., & Paddick, I. (2021). Treatment of multiple intracranial metastases in radiation oncology: a contemporary review of available technologies. *BJR Open*, 3(1), 20210035. <https://doi.org/10.1259/bjro.20210035>
- Solberg, T. D., Medin, P. M., Mullins, J., & Li, S. (2008). Quality Assurance of Immobilization and Target Localization Systems for Frameless Stereotactic Cranial and Extracranial Hypofractionated Radiotherapy. *International Journal of Radiation Oncology Biology Physics*, 71(1 SUPPL.), 131–135. <https://doi.org/10.1016/j.ijrobp.2007.05.097>
- Soliman, H., Das, S., Larson, D. A., & Sahgal, A. (2016). Stereotactic radiosurgery (SRS) in the modern management of patients with brain metastases. *Oncotarget*, 7(11), 12318–12330. <https://doi.org/10.18632/oncotarget.7131>
- Soltys, S. G., Grimm, J., Milano, M. T., Xue, J., Sahgal, A., Yorke, E., Yamada, Y., Ding, G. X., Li, X. A., Lovelock, D. M., Jackson, A., Ma, L., El Naqa, I., Gibbs, I. C.,

- Marks, L. B., & Benedict, S. (2021). Stereotactic Body Radiation Therapy for Spinal Metastases: Tumor Control Probability Analyses and Recommended Reporting Standards. *International Journal of Radiation Oncology Biology Physics*, *110*(1). <https://doi.org/10.1016/j.ijrobp.2020.11.021>
- Song, J. H., Kim, M. J., Park, S. H., Lee, S. R., Lee, M. Y., Lee, D. S., & Suh, T. S. (2015). Gamma analysis dependence on specified low-dose thresholds for VMAT QA. *Journal of Applied Clinical Medical Physics*, *16*(6), 263–272. <https://doi.org/10.1120/jacmp.v16i6.5696>
- Srivastava, R. P., & De Wagter, C. (2019). Clinical experience using Delta 4 phantom for pretreatment patient-specific quality assurance in modern radiotherapy. *Journal of Radiotherapy in Practice*, *18*(2), 210–214. <https://doi.org/10.1017/S1460396918000572>
- Stojkovski, I., Krstevska, V., & Smichkoska, S. (2017). Impact on radiation dose and volume V57 Gy of the brain on recurrence and survival of patients with glioblastoma multiformae. *Radiology and Oncology*, *51*(4). <https://doi.org/10.1515/raon-2017-0041>
- Suh, J. H., Kotecha, R., Chao, S. T., Ahluwalia, M. S., Sahgal, A., & Chang, E. L. (2020). Current approaches to the management of brain metastases. In *Nature Reviews Clinical Oncology* (Vol. 17, Issue 5, pp. 279–299). Springer US. <https://doi.org/10.1038/s41571-019-0320-3>
- Sung, K. H., & Choi, Y. E. (2018). Dose gradient curve: A new tool for evaluating dose gradient. *PLoS ONE*, *13*(4). <https://doi.org/10.1371/journal.pone.0196664>
- Tabouret, E., Chinot, O., Metellus, P., Tallet, A., Viens, P., & Gonçalves, A. (2012). Recent trends in epidemiology of brain metastases: An overview. In *Anticancer*

Research (Vol. 32, Issue 11, pp. 4655–4662).

Tanaka, Y., Oita, M., Inomata, S., Fuse, T., Akino, Y., & Shimomura, K. (2020). Impact of patient positioning uncertainty in noncoplanar intracranial stereotactic radiotherapy.

Journal of Applied Clinical Medical Physics, 21(2), 89–97.

<https://doi.org/10.1002/acm2.12820>

Tham, B. Z., Aleman, D., Nordström, H., Nygren, N., & Coolens, C. (2023). Plan

Assessment Metrics for Dose Painting in Stereotactic Radiosurgery. *Advances in*

Radiation Oncology, 8(6), 101281. <https://doi.org/10.1016/j.adro.2023.101281>

The Delta4 Phantom+ wireless Phantom. (n.d.). Retrieved February 26, 2024, from

https://images10.newegg.com/UploadFilesForNewegg/itemintelligence/NZXT/D017_2003_20001_2001_20Delta4_20Phantom_20The_20wireless_20phantom1448638537616.pdf

The Royal Australian and New Zealand College of Radiologists. (2022). Quality

Guidelines for Volume Delineation in Radiation Oncology. *Ranzcr*, 2.1, 1–18.

The ZAP-X® Gyroscopic Radiosurgery System. (n.d.). Retrieved May 28, 2024, from

<https://miamineurosciencecenter.com/en/services/zap-x-radiosurgery-system/>

Thompson, J. F., Soong, S. J., Balch, C. M., Gershenwald, J. E., Ding, S., Coit, D. G.,

Flaherty, K. T., Gimotty, P. A., Johnson, T., Johnson, M. M., Leong, S. P., Ross, M.

I., Byrd, D. R., Cascinelli, N., Cochran, A. J., Eggermont, A. M., McMasters, K. M.,

Mihm, M. C., Morton, D. L., & Sondak, V. K. (2011). Prognostic significance of

mitotic rate in localized primary cutaneous melanoma: An analysis of patients in the

multi-institutional american joint committee on cancer melanoma staging database.

Journal of Clinical Oncology, 29(16), 2199–2205.

<https://doi.org/10.1200/JCO.2010.31.5812>

Thomson, H. M., Fortin Ensign, S. P., Edmonds, V. S., Sharma, A., Butterfield, R. J., Schild, S. E., Ashman, J. B., Zimmerman, R. S., Patel, N. P., Bryce, A. H., Vora, S. A., Sio, T. T., & Porter, A. B. (2023). Clinical Outcomes of Stereotactic Radiosurgery-Related Radiation Necrosis in Patients with Intracranial Metastasis from Melanoma. *Clinical Medicine Insights: Oncology*, 17, 1–11.

<https://doi.org/10.1177/11795549231161878>

Topkan, E., Kucuk, A., Senyurek, S., Sezen, D., Durankus, N. K., Akdemir, E. Y., Saglam, Y., Bolukbasi, Y., Pehlivan, B., & Selek, U. (2021). Stereotactic Radiosurgery Techniques and Quality Assurance for Brain Metastases. In *Highlights on Medicine and Medical Research Vol. 2*. <https://doi.org/10.9734/bpi/hmmr/v2/2346e>

Torrens, M., Chung, C., Chung, H. T., Hanssens, P., Jaffray, D., Kemeny, A., Larson, D., Levivier, M., Lindquist, C., Lippitz, B., Novotny, J., Paddick, I., Prasad, D., & Yu, C. P. in. (2014). Standardization of terminology in stereotactic radiosurgery: Report from the Standardization Committee of the International Leksell Gamma Knife Society: special topic. *Journal of Neurosurgery*, 121(December), 2–15.

<https://doi.org/10.3171/2014.7.gks141199>

Traylor, J. I., Habib, A., Patel, R., Muir, M., Gadot, R., Briere, T., Yeboa, D. N., Li, J., & Rao, G. (2019). Fractionated stereotactic radiotherapy for local control of resected brain metastases. *Journal of Neuro-Oncology*, 144(2), 343–350.

<https://doi.org/10.1007/s11060-019-03233-9>

Trifiletti, D. M., Lee, C. C., Kano, H., Cohen, J., Janopaul-Naylor, J., Alonso-Basanta, M., Lee, J. Y. K., Simonova, G., Liscak, R., Wolf, A., Kvint, S., Grills, I. S., Johnson, M.,

- Liu, K. Du, Lin, C. J., Mathieu, D., Héroux, F., Silva, D., Sharma, M., ... Sheehan, J. P. (2016). Stereotactic Radiosurgery for Brainstem Metastases: An International Cooperative Study to Define Response and Toxicity. *International Journal of Radiation Oncology Biology Physics*, 96(2), 280–288.
<https://doi.org/10.1016/j.ijrobp.2016.06.009>
- Trifiletti, D. M., Redmond, K. J., Kim, M. M., Soltys, S. G., Milano, M. T., & Hattangadi-Gluth, J. A. (2023). Novel Applications of Stereotactic Radiosurgery Beyond Oncology: Prospective Trials in Functional Radiosurgery. In *International Journal of Radiation Oncology Biology Physics* (Vol. 115, Issue 1).
<https://doi.org/10.1016/j.ijrobp.2022.06.077>
- Trifiletti, D. M., Sheehan, J. P., Grover, S., Dutta, S. W., Rusthoven, C. G., Kavanagh, B. D., Sahgal, A., & Showalter, T. N. (2017). National trends in radiotherapy for brain metastases at time of diagnosis of non-small cell lung cancer. In *Journal of Clinical Neuroscience* (Vol. 45). <https://doi.org/10.1016/j.jocn.2017.08.028>
- TrueBeam. (2024). Retrieved February 20, 2024, from <https://www.varian.com/products/radiotherapy/treatment-delivery/truebeam>
- Tsz, W., & Li, Y. (2014). *Determining Rational Planning Target Volume Margins for Intracranial Stereotactic Radiotherapy*.
- Uchinami, Y., Katoh, N., Abo, D., Taguchi, H., Yasuda, K., Nishioka, K., Soyama, T., Morita, R., Miyamoto, N., Suzuki, R., Sho, T., Nakai, M., Ogawa, K., Kakisaka, T., Orimo, T., Kamiyama, T., Shimizu, S., & Aoyama, H. (2021). Treatment outcomes of stereotactic body radiation therapy using a real-time tumor-tracking radiotherapy system for hepatocellular carcinomas. *Hepatology Research*, 51(8).

<https://doi.org/10.1111/hepr.13649>

Ueda, Y., Ohira, S., Yamazaki, H., Mabuchi, N., Higashinaka, N., Miyazaki, M., &

Teshima, T. (2019). Dosimetric performance of two linear accelerator-based radiosurgery systems to treat single and multiple brain metastases. *British Journal of Radiology*, 92(1100), 20190004. <https://doi.org/10.1259/bjr.20190004>

Valerie Cruz Ordinario, M., Trinconi Trinconi Cunha, M., Rafiqul Islam, M., Mathai, S.,

Adetola Tolani, M., poojary, shamali, Suleimenova, A., Ben Abdallah, I., Karmacharya Badgami, R., Bardakhchyan, S., Gauraiya Chinchalker, G., Gössling, G., Radmilo Djordjevic, F., Gueye, C., Ndumbalo, J., Patil, R., Shilpakar, R., Shrestha, A., Nathan Tan, H. C., & Luke, S. (2024). *Global perspective of barriers in research among oncologists from low-middle income countries*.

Valiente, M., Ahluwalia, M. S., Boire, A., Brastianos, P. K., Goldberg, S. B., Lee, E. Q.,

Le Rhun, E., Preusser, M., Winkler, F., & Soffiatti, R. (2018). The Evolving Landscape of Brain Metastasis. *Trends in Cancer*, 4(3), 176–196.

<https://doi.org/10.1016/j.trecan.2018.01.003>

van Heerden, J., Lisa Christine, I., Downing, J., Davidson, A., Hessissen, L., Schoeman, J.,

Ladas, E. J., Abdelhafeez, H., Georgia Odongo Arao, S., Fentie, A. M., Kamal, S., Parkes, J., Naiker, T., Ludick, A., Balagadde-Kambugu, J., & Geel, J. (2023). Current status of African pediatric oncology education efforts aligned with the Global Initiative for Childhood Cancer. In *Pediatric Hematology and Oncology* (Vol. 40, Issue 3). <https://doi.org/10.1080/08880018.2022.2117882>

Van Herk, M., Remeijer, P., Rasch, C., & Lebesque, J. V. (2000). The probability of

correct target dosage: Dose-population histograms for deriving treatment margins in

- radiotherapy. *International Journal of Radiation Oncology Biology Physics*, 47(4).
[https://doi.org/10.1016/S0360-3016\(00\)00518-6](https://doi.org/10.1016/S0360-3016(00)00518-6)
- van Reenen, C. J., Trauernicht, C. J., & Bojecho, C. (2023). The application of gradient dose segmented analysis of in-vivo EPID images for patients undergoing VMAT in a resource-constrained environment. *Journal of Applied Clinical Medical Physics*, 24(8).
<https://doi.org/10.1002/acm2.13985>
- Van Schelt, J. (2021). Lens dose to standing patients treated with electrons to the hand. *Medical Dosimetry*, 46(4). <https://doi.org/10.1016/j.meddos.2021.04.005>
- Velten, C., Kabarriti, R., Garg, M., & Tomé, W. A. (2021). Single isocenter treatment planning techniques for stereotactic radiosurgery of multiple cranial metastases. *Physics and Imaging in Radiation Oncology*, 17(December 2020), 47–52.
<https://doi.org/10.1016/j.phro.2021.01.002>
- Vergalasova, I., Liu, H., Alonso-Basanta, M., Dong, L., Li, J., Nie, K., Shi, W., Teo, B. K. K., Yu, Y., Yue, N. J., Zou, W., & Li, T. (2019a). Multi-institutional dosimetric evaluation of modern day stereotactic radiosurgery (SRS) treatment options for multiple brain metastases. *Frontiers in Oncology*, 9(JUN), 1–12.
<https://doi.org/10.3389/fonc.2019.00483>
- Vogelbaum, M. A., Brown, P. D., Messersmith, H., Brastianos, P. K., Burri, S., Cahill, D., Dunn, I. F., Gaspar, L. E., Gatson, N. T. N., Gondi, V., Jordan, J. T., Lassman, A. B., Maues, J., Mohile, N., Redjal, N., Stevens, G., Sulman, E., van den Bent, M., Wallace, H. J., ... Schiff, D. (2022). Treatment for Brain Metastases: ASCO-SNO-ASTRO Guideline. *Journal of Clinical Oncology*, 40(5), 492–516.
<https://doi.org/10.1200/JCO.21.02314>

- Wagner, S., Lanfermann, H., Wohlgemuth, W. A., & Gufler, H. (2020). Effects of effective stereotactic radiosurgery for brain metastases on the adjacent brain parenchyma. *British Journal of Cancer*, *123*(1), 54–60. <https://doi.org/10.1038/s41416-020-0853-3>
- Wang, Y., & Feng, W. (2022). Cancer-related psychosocial challenges. *General Psychiatry*, *35*(5), e100871. <https://doi.org/10.1136/gpsych-2022-100871>
- Wang, Y., Fu, J., Zhou, H., Li, H., Xu, Q., & Wei, S. (2023). Clinical characteristics of radiation-induced optic neuropathy: A single-center retrospective study. *Advances in Ophthalmology Practice and Research*, *3*(3). <https://doi.org/10.1016/j.aopr.2023.05.003>
- Wilson, B. (2013). *Development of Trajectory-Based Techniques for the Stereotactic Volumetric Modulated Arc Therapy of Cranial Lesions*.
- Wolden, S. L., Barker, C. A., Kushner, B. H., Bodduluri, H., Della-Biancia, C., Kramer, K., Modak, S., & Cheung, N. K. V. (2008). Brain-sparing radiotherapy for neuroblastoma skull metastases. *Pediatric Blood and Cancer*, *50*(6). <https://doi.org/10.1002/pbc.21384>
- Woon, W., Ravindran, P. B., Ekanayake, P., Vikraman, S., Lim, Y. Y. F., & Khalid, J. (2018). A study on the effect of detector resolution on gamma index passing rate for VMAT and IMRT QA. *Journal of Applied Clinical Medical Physics*, *19*(2), 230–248. <https://doi.org/10.1002/acm2.12285>
- World Economics - The Global Authority on Geographic Investability*. (2024). Retrieved February 1, 2024, from <https://www.worldeconomics.com/GDP-Per-Capita/>
- Xia, Y., Adamson, J., Zlateva, Y., & Giles, W. (2020). Physics investigation Application of TG-218 action limits to SRS and SBRT pre-treatment patient specific QA. *Journal of*

Radiosurgery and SBRT, 7, 135–147.

- Xu, Q., Kubicek, G., Mulvihill, D., Goldman, W., Eastwick, G., Turtz, A., Fan, J., & Luo, D. (2021). Evaluating the impact of prescription isodose line on plan quality using Gamma Knife inverse planning. *Journal of Applied Clinical Medical Physics*, 22(9), 289–297. <https://doi.org/10.1002/acm2.13388>
- Xu, Y., Ma, P., Xu, Y., & Dai, J. (2019). Selection of prescription isodose line for brain metastases treated with volumetric modulated arc radiotherapy. *Journal of Applied Clinical Medical Physics*, 20(12), 63–69. <https://doi.org/10.1002/acm2.12761>
- Xuyao, Y., Zhiyong, Y., Yuwen, W., Hui, Y., Yongchun, S., Yang, D., LuJun, Z., & Ping, W. (2020). Improving stereotactic radiotherapy (SRT) planning process for brain metastases by Cyberknife system: reducing dose distribution in healthy tissues. *Journal of Cancer*, 11(14), 4166–4172. <https://doi.org/10.7150/jca.41102>
- Yakar, M., & Etiz, D. (2021). Artificial intelligence in radiation oncology. *Artificial Intelligence in Medical Imaging*, 2(2), 13–31. <https://doi.org/10.35711/aimi.v2.i2.13>
- Yamamoto, M., Serizawa, T., Shuto, T., Akabane, A., Higuchi, Y., Kawagishi, J., Yamanaka, K., Sato, Y., Jokura, H., Yomo, S., Nagano, O., Kenai, H., Moriki, A., Suzuki, S., Kida, Y., Iwai, Y., Hayashi, M., Onishi, H., Gondo, M., ... Tsuchiya, K. (2014). Stereotactic radiosurgery for patients with multiple brain metastases (JLGK0901): A multi-institutional prospective observational study. *The Lancet Oncology*, 15(4), 387–395. [https://doi.org/10.1016/S1470-2045\(14\)70061-0](https://doi.org/10.1016/S1470-2045(14)70061-0)
- Yoda, K. (2017). A Radiotherapy Treatment Margin Formula When Systematic Positioning Errors are Relatively Small Compared to Random Positioning Errors: A First-Order Approximation. *International Journal of Medical Physics, Clinical Engineering and*

Radiation Oncology, 06(02). <https://doi.org/10.4236/ijmpcero.2017.62017>

Youssoufi, M. A., Bougtib, M., Douama, S., Ait Erraïsse, M., Abboud, F. Z., Hassouni, K., & Bentayeb, F. (2021). Evaluation of PTV margins in IMRT for head and neck cancer and prostate cancer. *Journal of Radiotherapy in Practice*, 20(1).

<https://doi.org/10.1017/S1460396919000931>

Zeng, J., Chen, J., Zhang, D., Meng, M., Zhang, B., Qu, P., Pang, Q., & Wang, P. (2020). Assessing cumulative dose distributions in combined external beam radiotherapy and intracavitary brachytherapy for cervical cancer by treatment planning based on deformable image registration. *Translational Cancer Research*, 9(10).

<https://doi.org/10.21037/tcr-20-1196>

Zhang, J., Wang, L., Xu, B., Huang, M., Chen, Y., & Li, X. (2021). Influence of Using a Contrast-Enhanced CT Image as the Primary Image on CyberKnife Brain Radiosurgery Treatment Plans. *Frontiers in Oncology*, 11(September), 1–10.

<https://doi.org/10.3389/fonc.2021.705905>

Zhang, M., Zhang, Q., Gan, H., Li, S., & Zhou, S. min. (2016). Setup uncertainties in linear accelerator based stereotactic radiosurgery and a derivation of the corresponding setup margin for treatment planning. *Physica Medica*, 32(2), 379–385.

<https://doi.org/10.1016/j.ejmp.2016.02.002>

Zhang, Q., Zheng, D., Lei, Y., Morgan, B., Driewer, J., Zhang, M., Li, S., Zhou, S., Zhen, W., Thompson, R., Wahl, A., Lin, C., & Enke, C. (2014). A new variable for SRS plan quality evaluation based on normal tissue sparing: the effect of prescription isodose levels. *The British Journal of Radiology*, 87(1043), 20140362.

<https://doi.org/10.1259/bjr.20140362>

Zhao, B., Jin, J.-Y., Wen, N., Huang, Y., Siddiqui, M. S., Chetty, I. J., & Ryu, S. (2014).

Prescription to 50-75% isodose line may be optimum for linear accelerator based radiosurgery of cranial lesions. *Journal of Radiosurgery and SBRT*, 3(2).

Zou, W., Dong, L., & Kevin Teo, B. K. (2018). Current State of Image Guidance in Radiation Oncology: Implications for PTV Margin Expansion and Adaptive Therapy. In *Seminars in Radiation Oncology* (Vol. 28, Issue 3).

<https://doi.org/10.1016/j.semradonc.2018.02.008>



APPENDICES

Appendix I

Clinical Practice in Stereotactic Radiosurgery (SRS) for Brain Metastasis

This questionnaire is designed to gather your expert opinion on the treatment of brain metastasis using Stereotactic Radiosurgery (SRS). Your responses will provide valuable insights into the use of contouring, margin expansion, and margin calculation in SRS. Your participation is voluntary, and all responses will be kept confidential. For each statement, select the option that best reflects your opinion.

1. Target contouring should be compulsory in the treatment of SRS for brain metastasis.

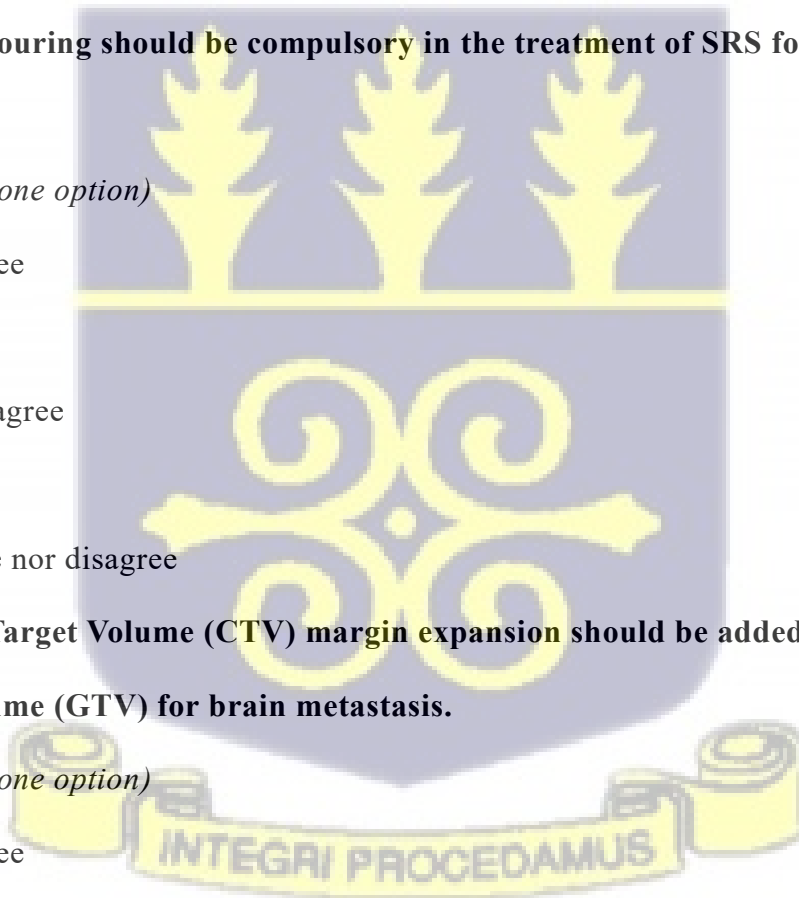
(Please choose one option)

- a) Strongly Agree
- b) Agree
- c) Strongly Disagree
- d) Disagree
- e) Neither agree nor disagree

2. A Clinical Target Volume (CTV) margin expansion should be added to the Gross Tumor Volume (GTV) for brain metastasis.

(Please choose one option)

- a) Strongly Agree
- b) Agree
- c) Strongly Disagree



d) Disagree

e) Neither agree nor disagree

3. What should be the maximum and optimal Planning Target Volume (PTV) margin to be accepted and applied in SRS treatment?

(Please choose one option)

a) 0.0 mm

b) 0.5 mm

c) 1.0 mm

d) 1.5 mm

e) 2.0 mm - 3.0 mm

4. CTV-PTV margins should be used in the treatment for brain metastasis with SRS.

(Please choose one option)

a) Strongly Agree

b) Agree

c) Strongly Disagree

d) Disagree

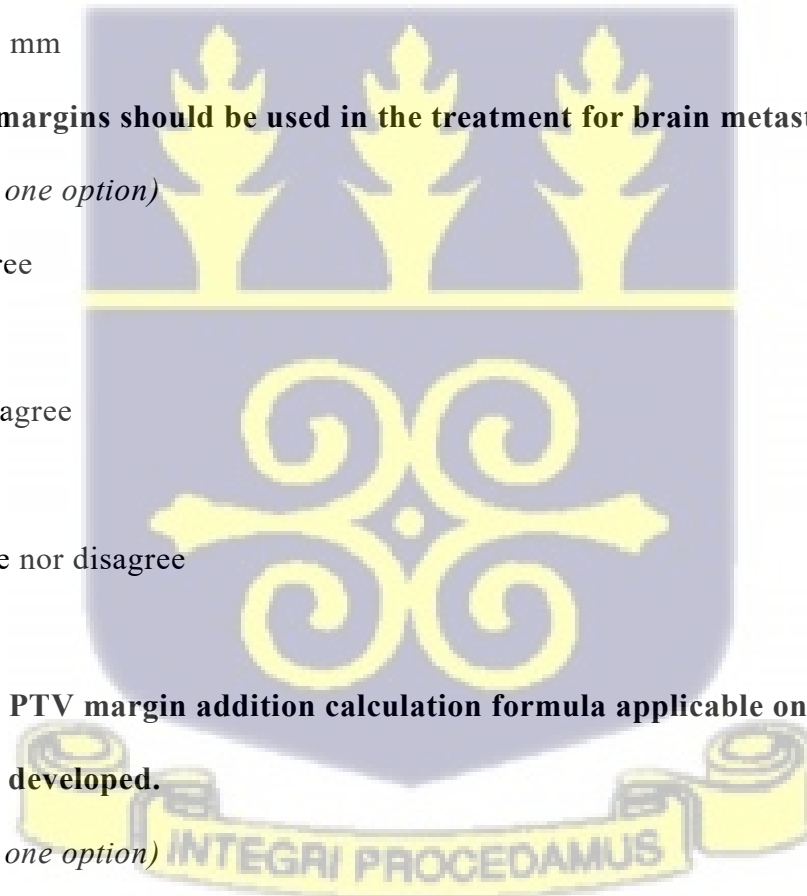
e) Neither agree nor disagree

5. A standard PTV margin addition calculation formula applicable only for SRS needs to be developed.

(Please choose one option)

a) Strongly Agree

b) Agree



- c) Strongly Disagree
- d) Disagree
- e) Neither agree nor disagree

Link to the questionnaire as a participant.

[https://docs.google.com/forms/d/e/1FAIpQLSdk5EA4v7Fk4MoNvsbLPdWAoPn-PXA_uMv633yrz0hO-1xThQ/viewform?usp=sf link](https://docs.google.com/forms/d/e/1FAIpQLSdk5EA4v7Fk4MoNvsbLPdWAoPn-PXA_uMv633yrz0hO-1xThQ/viewform?usp=sf_link)



Appendix II (Ethics approval letters)



UNIVERSITY OF GHANA
ETHICS COMMITTEE FOR BASIC AND APPLIED SCIENCES (ECBAS)

P. O. Box LG 1195, Legon, Accra, Ghana

Ref. No: ECBAS 077/20-21

23rd December, 2021.

Ms. Emmanuel Fiagbedzi
Department of Medical Physics
University of Ghana
Legon, Accra

Dear Mr. Fiagbedzi,

ECBAS 077/20-21: DOSIMETRIC ANALYSIS OF PLANNING TARGET VOLUME MARGINS ON THE TREATMENT PLANNING OF STEREOTACTIC RADIOSURGERY TREATMENT FOR METASTATIC INTRACRANIAL TUMORS

This is to inform you that the above referenced study has been presented to the Ethics Committee for Basic and Applied Sciences for a full board review and the following actions taken subject to the conditions and explanation provided below:

Expiry Date: 14/12/2022
On Agenda for: Initial Submission
Date of Submission: 15/11/2021
ECBAS Action: Approved
Reporting: Annually

Please accept my congratulations.

Yours sincerely,

Professor Daniel Bruce Sarpong
ECBAS Chairperson





University College London Hospitals

NHS Foundation Trust

Private and Confidential

Mr Emmanuel Fiagbedzi
40 Brookstreet, Luton
Luton
IU31DS
United Kingdom

Honorary Contract Team
2nd Floor West
250 Euston Road
London
NW1 2PG

Direct line:
Email: uclh.honorarycontracts@nhs.net
27th Feb. 2022

Dear Emmanuel,

TERMS OF PLACEMENT AS HONORARY APPOINTEE

Mr Emmanuel Fiagbedzi
40 Brookstreet, Luton
Luton
IU31DS
United Kingdom

Placement Title: Honorary Research RT physicist

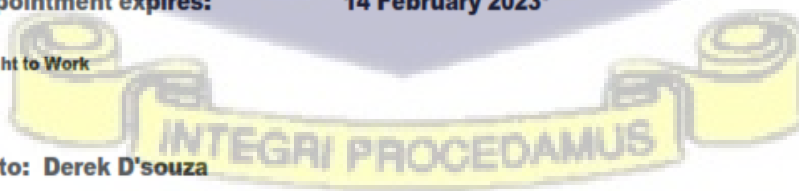
Place of Work or Main Base: University College London Hospital

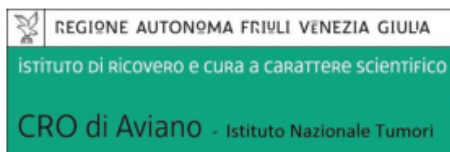
Starting Date of Honorary Appointment: 8-Mar-2022

Honorary Appointment expires: 14 February 2023*

*Expiration of Right to Work

Responsible to: Derek D'souza





MO_01.01_SPPA_01 Rev_01

SECTION A

**REQUEST FOR FREQUENCY AUTHORIZATION
IN THE PREMISES OF CRO**

At the care of the applicant

To the Health Management Office (dirsan@cro.it)

The undersigned
Surname, Name: FIAGBEDZI, EMMANUEL WORLALI K. Date of birth 16/03/1987
Educational qualifications: MASTER OF MEDICAL PHYSICS
Fiscal Code: FGB MNL 87C16 Z318F
City of residence: LONDON Province: LUTON CAP: _____
Address: 40 BROOK STREET, LUTON
Domicile (if different from residence): GHANA
Telephone number or mobile phone: +447448708019
E-mail: emmanuel2q4@gmail.com

ASKS

To be admitted/to (department-division/service)
DEPARTMENT OF MEDICAL PHYSICS
as: PhD STUDENT (trainee, PhD student, speciality student (post graduation), volunteer, student, senior visiting scientist etc.) to perform the following activity (tick only one of the three options): SRS TREATMENT PLANNING & DELIVERY

Observation activities and direct actions in NON-health areas as technical offices, administrative offices, libraries, etc.

N.B. The request to carry out these activities must be sent at least 2 months before the potential start date of frequency

To this end declares, under its own responsibility, to be in possession of (tick the box):

- Vaccine documentation (tetanus) *
- Certification proving the General Formation of Workers (4 hours) According to the State-Region Agreement of 21 December 2011 (see Italian law) **

* required ONLY for those who plan to operate as a maintenance technician, warehouseman, workshop worker.

** in the absence of the requested certificate, CRO will inform the applicant of the specific risks to which he may be exposed at the premises of the Company.

Appendix III (PUBLICATIONS FROM THE THESIS)

Health and Technology
<https://doi.org/10.1007/s12553-023-00799-3>

REVIEW PAPER



Radiotherapy infrastructure for brain metastasis treatment in Africa: practical guidelines for implementation of a stereotactic radiosurgery (SRS) program

Emmanuel Flagbedzi^{1,2,3} · Francis Hasford² · Samuel Nii Tagoe² · Andrew Nisbet³

Received: 31 August 2023 / Accepted: 7 November 2023

© The Author(s) under exclusive licence to International Union for Physical and Engineering Sciences in Medicine (IUPESM) 2023

Abstract

Purpose Radiosurgery with the Gamma Knife is the golden standard for the treatment of brain metastasis cases but its accessibility however in many countries is limited. Modern radiotherapy has made this treatment possible using other equipment such as linear accelerator and Cyberknife. The objective of this study was to explore the distribution of available radiotherapy equipment for brain metastasis treatment in Africa and provide practical guidelines to the establishment of a Stereotactic Radiosurgery (SRS) Program.

Materials and methods The International Atomic Energy Agency (IAEA)'s Division of Human Health's Directory for Radiotherapy Centres (DIRAC), served as the primary source for the distribution of radiotherapy equipment throughout Africa and worldwide. Data on megavoltage radiotherapy equipment for the 54 African countries were extracted from this database. Cancer incidence and brain metastasis assumption were made using data from the GLOBOCAN 2020 database and country's income was assessed using the Gross Domestic Product (GDP) per capita on the world economics database. Further literature search was also carried out in PubMed on the price and availability of dedicated equipment for brain metastasis management in Africa. All these searches were done in April, 2023.

Results There was increase in the number of brain metastasis cases. There were only two Gamma Knife machines in Africa. Three Cyberknife; two in Egypt and one in Kenya and 432 other megavoltage units (66 Cobalt-60s, 366 Linacs) distributed across the continent. The cost of a Gamma Knife machine could be up to 7 million United States Dollars (USD) compared to that of Linac between 2.4 and 2.8 million USD and Cyberknife between 3 and 5 million USD. A country's (GDP) per capita was a vital determinant of the number of these machines in countries which did not have any machines to ones which have at least one machine.

Conclusion Access to radiosurgery treatment for brain metastasis with the Gamma Knife or Cyberknife is limited due to the low number of these equipment. With the increase in radiotherapy expansion with linear accelerators, it is likely that the continent will be able to increase its stereotactic radiosurgery treatment centers by implementing Linac-based SRS following suitable guidelines. This will help provide comprehensive care to patients and promote quality of life.

Keywords Stereotactic radiosurgery · Gamma knife · Cyberknife · Linac · Brain Metastasis

✉ Emmanuel Flagbedzi
 emmanuel2g4@gmail.com; emmanuel.flagbedzi@ucc.edu.gh

Francis Hasford
 haspee@yahoo.co.uk

Samuel Nii Tagoe
 samniitagoe@yahoo.co.uk

Andrew Nisbet
 andrew.nisbet@ucl.ac.uk

¹ College of Health and Allied Sciences, Department of Medical Imaging Technology and Sonography, University of Cape Coast, Cape Coast, Ghana

² Department of Medical Physics, University of Ghana, Accra, Ghana

³ Department of Medical Physics, University College London, London, UK

Published online: 17 November 2023

Springer



Impact of Planning Target Volume Margins in Stereotactic Radiosurgery for Brain Metastasis: A Review

Emmanuel Fiagbedzi^{1,2}, Francis Hasford¹, Samuel Nii Tagoe¹

¹Department of Medical Physics, University of Ghana, Accra, ²Department of Medical Imaging Technology and Sonography, College of Health and Allied Sciences, University of Cape Coast, Cape Coast, Ghana

Received 4 January 2024

Revised 1 March 2024

Accepted 5 March 2024

Corresponding author

Emmanuel Fiagbedzi
(emmanuel2g4@gmail.com)
Tel: 233-205022825
Fax: 233-209218921

Margin inclusion or exclusion remains the most critical and controversial aspect of stereotactic radiosurgery (SRS) for metastatic brain tumors. This review aimed to examine the available literature on the impact of margins in SRS of brain metastasis and to assess the response of some medical physicists on the use of these margins. The Preferred Reporting Items for Systematic Reviews and Meta-Analyses method was used to review articles published in PubMed, Embase, and Science Direct databases from January 2012 to December 2022 using the following keywords: planning target volume, brain metastasis, margin, and stereotactic radiosurgery. A simple survey consisting of five questions was completed by ten medical physicists with experience in SRS treatment planning. The results were analyzed using IBM SPSS Statistics version 26.0. Of the 1,445 articles identified, only 38 articles were chosen. Of these, eight papers were deemed relevant to the focus of this review. These papers showed an increase in the risk of radionecrosis, whereas differences in local control were variable as the margin increased. In the survey, the response rate to whether or not to use margins in SRS, a critical question, was 50%. Margin addition increases the risk of radio-necrosis. The local control rate varies among treatment modalities and cannot be generalized. From the survey, no consensus was reached regarding the use of these margins. This calls for further deliberations among professionals directly involved in SRS.

Keywords: Planning target volume, Stereotactic radiosurgery, Margins, Brain metastasis



Original Research Article

Dose Verification for LINAC-Based Stereotactic Radiosurgery Planned at Different Prescription Isodose Levels Using Delta4 Phantom+

Emmanuel Fiagbedzi*, Francis Hasford and Samuel Nii Tagoe

Department of Medical Physics, University of Ghana, Ghana

* Corresponding author: emmanuel2g4@gmail.com

ABSTRACT

Background: Linear accelerator (LINAC)-based stereotactic radiosurgery (SRS) plans and their treatment are complex techniques that require a comprehensive quality assurance program before they are clinically implemented. To cope with this intricacy, clinics must comprehensively validate treatment plans to deliver precise doses and assure patients. The study aimed to verify the treatment planning dose to the dose delivered at the LINAC during the SRS treatment planned at different prescription isodoses with the new wireless Delta4 Phantom+.

Materials and Methods: Clinically accepted volumetric modulated arc therapy (VMAT) SRS plans made with the Stereotactic End-to-End Verification (STEEV) anthropomorphic phantom were created with six different prescription isodose level using 6 MV flattening filter free (FFF) beam. All these VMAT SRS plans were replicated on the Delta4 Phantom+ and delivered with Varian Truebeam LINAC. The planned and delivered dose showed excellent correlation, and this was evaluated using distance to agreement (2 mm), dose deviation (2%), and gamma-index passing rate.

Results: The results showed that the calculated treatment planning system (TPS) dose and the measurement with the Delta4 Phantom+ were in excellent accord. The minimum gamma pass rate was 99.6% and the maximum 100%. The gamma passing rate above 95% for all plans and dose goals were achieved.

Conclusion: The verification with the Delta4 Phantom+ measurement depicted an excellent correlation with the dose of the SRS treatment plans for the different prescription isodose levels. The wireless Delta4 Phantom+ device is precise and consistent. It is a quickly set-up device, suitable for SRS treatment verification and allows for real-time measurement. However, we do recommend a stricter passing rate for VMAT SRS Plans.

Keywords – Stereotactic radiosurgery, prescription isodose, treatment plans, Delta4 Phantom+, Gamma-index.

Copyright © 2024. This is an open-access article distributed under the terms of the Creative Commons Attribution License (CC BY): *Creative Commons - Attribution 4.0 International - CC BY 4.0*. The use, distribution or reproduction in other forums is permitted, provided the original author(s) and the copyright owner(s) are credited and that the original publication in this journal is cited, in accordance with accepted academic practice. No use, distribution or reproduction is permitted which does not comply with these terms.

INTEGRI PROCEDAMUS

Original Article

Cite this article: Fiagbedzi E, Tagoe SNA, Hasford F, and Nisbet A. (2025) Influence of planning target volume margins using various prescription isodoses in gamma knife radiosurgery for single brain metastasis: a phantom study. *Journal of Radiotherapy in Practice*. 24(e4), 1–8. doi: [10.1017/S1460396925000019](https://doi.org/10.1017/S1460396925000019)

Received: 29 August 2024
Revised: 18 November 2024
Accepted: 23 December 2024

Keywords:

Gamma knife; margin; parameters; planning target volume; prescription isodose

Corresponding author:

Emmanuel Fiagbedzi;
Email: emmanuel2g4@gmail.com

The article has been updated since publication. A notice detailing the change has been published at <https://doi.org/10.1017/S1460396925000159>.

Influence of planning target volume margins using various prescription isodoses in gamma knife radiosurgery for single brain metastasis: a phantom study

Emmanuel Fiagbedzi^{1,2} , Samuel Nii Adu Tagoe¹, Francis Hasford¹ and Andrew Nisbet³

¹Department of Medical Physics, University of Ghana, Accra, Ghana; ²Department of Medical Imaging Technology and Sonography, University of Cape Coast, Cape Coast, Ghana and ³Department of Medical Physics, University College London, London, UK

Abstract

Objective: The study seeks to evaluate the influence of planning target volume (PTV) margins on plan parameters during inverse planning of brain metastases with the Gamma Knife treatment unit, considering various prescription isodose levels (PIL).

Material & Method: CT scan images of a STEEV anthropomorphic phantom were transferred into the GAMMA PLAN Treatment Planning System. A target measuring a volume of 4.9cc was centrally contoured. Plans with a 0 mm volume margin at five prescription isodose levels from 50% to 70% at 5% increment were created. With 0.5 mm, 1 mm, 1.5 mm and 2 mm PTV margins, identical plans were regenerated. Adjustments were made to each plan when necessary to achieve same target coverage. One-way ANOVA test was used to analyse the influence of PTV margins on parameters including Selectivity[S], Gradient index [GI], V12, Paddick's conformal index [PCI] and Treatment time [TI].

Results: Margin addition resulted in PTV volume increase. The findings indicated that the PTV margin of 2.0 mm exhibited the highest mean selectivity of (0.93 ± 0.00) , PCI (0.92 ± 0.01) , GI (2.50 ± 0.04) , V12 (16.17 ± 0.38) and treatment time $(118.32 \pm 2.91 \text{ min})$. The 0.0 mm PTV margin had the lowest mean value for all the parameters except for the treatment time $(105.58 \pm 3.48 \text{ min})$ which was slightly higher compared to the 0.5 mm PTV margin $(M = 86.36 \pm 4.13 \text{ min})$.

Conclusion: Incremental increases in PTV margins for Gamma knife radiosurgery though a relatively controversial concept influence all dosimetric parameters, which may pose potential detrimental effects and thus need to be carefully evaluated for brain metastasis treatment.

Introduction

Brain metastases develop in 10–40% of cancer patients.¹ The treatment modalities available include stereotactic radiosurgery (SRS), surgical resection and whole-brain radiotherapy.^{2–4} Among these, stereotactic radiosurgery has been found to be very effective with good prognosis.⁵ SRS relies on highly accurate positioning, immobilization and treatment planning to deliver high doses of radiation to brain targets.⁶ The primary goal of any treatment planning in radiotherapy is to deliver the highest achievable dose of radiation to the target volume while respecting the critical structures surrounding the target.⁷ It is common practice in conventional radiotherapy to place a margin around the clinical target volume (CTV) to form a planning target volume (PTV). The PTV compensates for the inaccuracies intrinsic to the process of radiotherapy, including patient alignment, geometrical setup uncertainties and patient intra-treatment motion.⁸ Defining an excessive amount of volume as part of PTV can lead to higher chances of injury to the surrounding critical organs receiving collateral high doses.^{9–11}

A Gamma Knife (GK) radiosurgery system is manufactured by Elekta AB, a Swedish company that specializes in advanced radiation oncology and neurosurgery systems. The Gamma Knife system uses small arcs of cobalt-60 sources to deliver high-dose precision local radiation. It is equipped with a treatment planning system (TPS).^{3,12} It is an uncommon practice in planning Gamma Knife radiosurgery to place additional planning margin around the target volume to compensate for treatment uncertainties from patient head motion during treatment, beam collimation uncertainties or both. Some studies suggest that planning target volume (PTV) margins can vary significantly for small targets and fractionated treatment compared to conventional fractionated treatments.^{13,14} The Leksell stereotactic coordinate system, which revolutionized radiosurgery delivery capabilities through multiple platforms, has raised the need to redefine margin addition.¹⁵

© The Author(s), 2025. Published by Cambridge University Press. This is an Open Access article, distributed under the terms of the Creative Commons Attribution licence (<https://creativecommons.org/licenses/by/4.0/>), which permits unrestricted re-use, distribution and reproduction, provided the original article is properly cited.



Appendix IV Supplementary LINAC Data

v= 5.0cm³

0 margin	Prescription Isodose						
		SRS 80	SRS 50	SRS 55	SRS 60	SRS 65	SRS 70
	Brain	10.62	12.14	11.59	10.99	10.82	10.58
	Brain stem	422.00	488.19	468.26	420.97	445.19	421.17
	GI	0.42	0.48	0.46	0.44	0.43	0.42
	Left lens	15.31	28.77	17.95	18.79	15.46	15.92
	Left ON	164.88	159.19	158.66	155.93	193.93	180.95
	Right lens	13.64	12.05	14.15	14.91	17.99	16.96
	Right ON	99.2	61.33	63.19	84.65	90.58	99.41
	Conformity Index	1.14	1.23	1.18	1.15	1.16	1.14
Time (Min.)	5.31	4.29	4.64	4.90	4.98	5.09	

V = 7.7cm³

Margin 1mm	Prescription Isodose						
		SRS 80	SRS50	SRS55	SRS 60	SRS65	SRS70
	Brain	14.76	15.97	15.35	14.84	14.66	14.76
	Brain stem	578.60	523.50	530.11	530.54	536.15	578.60
	GI	0.45	0.48	0.47	0.46	0.44	0.45
	Left lens	19.22	22.33	25.42	21.75	19.61	19.22
	Left ON	162.98	170.99	247.78	231.18	181.18	162.98
	Right lens	22.77	29.27	20.51	29.98	22.54	22.77
	Right ON	102.46	85.00	80.41	87.88	96.06	102.46
	Conformity Index	1.08	1.15	1.10	1.09	1.09	1.08
Time (Min.)	7.03	5.40	5.90	6.58	6.75	7.03	

V = 9.4cm³

Margin 2mm	Prescription Isodose						
		SRS80	SRS50	SRS 55	SRS60	SRS 65	SRS 70
	Brain	18.03	18.03	17.39	17.40	17.46	17.44
	Brain stem	706.67	534.81	555.46	565.33	584.89	606.37
	GI	0.47	0.49	0.47	0.47	0.46	0.46
	Left lens	26.51	38.16	27.75	29.06	29.13	28.40
	Left ON	209.55	178.40	178.80	215.60	220.69	145.47
	Right lens	27.84	30.90	29.49	28.18	27.33	30.17
	Right ON	99.33	93.44	95.08	77.62	76.65	82.69
	Conformity Index	1.11	1.09	1.06	1.07	1.09	1.08
Time (Min.)	7.4	6.29	7.06	7.77	8.22	7.83	

